

Aus dem Institut für Physiologie der Ludwig-Maximilians-Universität München

Abteilung für Physiologische Genomik

Direktorin: Prof. Dr. Magdalena Götz

**Regeneration of neurons after brain injury: Role of the STAT  
signaling pathway in the inhibition of neurogenesis of reactive  
astrocytes**

Dissertation

zum Erwerb des Doktorgrades der Medizin

an der Medizinischen Fakultät der

Ludwig-Maximilians-Universität zu München

vorgelegt von

Steffen Tiedt

aus

Rostock

2015

Mit Genehmigung der Medizinischen Fakultät  
der Ludwig-Maximilians-Universität München

Berichterstatterin: Prof. Dr. Magdalena Götz

Mitberichterstatter: Priv.-Doz. Dr. Florence Bareyre  
Priv.-Doz. Dr. Regina Fluhrer  
Priv.-Doz. Dr. Harald J. Schneider

Mitbetreuung durch den  
promovierten Mitarbeiter: Dr. Christophe Heinrich

Dekan: Prof. Dr. med. Dr. h.c. M. Reiser, FACR, FRCR

Tag der mündlichen Prüfung: 23.07.2015





Meiner Familie



## Table of Contents

<b>1.</b>	<b>Introduction.....</b>	<b>1</b>
1.1.	Overview	1
1.2.	Cortical development	2
1.2.1.	Neural stem / progenitor cells	3
1.2.2.	Embryonic neurogenesis	5
1.2.3.	Embryonic gliogenesis	6
1.2.4.	Time course of cortical development	7
1.3.	Adult neurogenesis	8
1.3.1.	Subventricular zone	9
1.3.2.	Dentate gyrus	11
1.4.	Neurological disorders and reactive gliosis	13
1.4.1.	Stroke	13
1.4.1.1.	Risk factors	14
1.4.1.2.	Pathophysiology	14
1.4.1.3.	Clinical findings	16
1.4.2.	Reactive gliosis and reactive astrocytes	17
1.4.2.1.	Stem cell-like properties of reactive astrocytes?	19
1.4.2.2.	Role of astrogliosis	19
1.4.2.3.	Regulation of astrogliosis	20
1.5.	New avenues toward neuronal repair	21
1.5.1.	Physiological neuronal repair: potential role of adult neurogenesis?	21
1.5.1.1.	Striatum	21
1.5.1.2.	Cerebral cortex	23
1.5.2.	Possible forms of therapy by delivering external factors / cells	24
1.5.2.1.	Delivery of factors improving the endogenous repair	24
1.5.2.2.	Cellular transplantation	24
1.5.3.	Neuronal reprogramming	26
1.5.3.1.	Reprogramming of postnatal cortical astrocytes in vitro	27
1.5.3.2.	Reprogramming of reactive astrocytes in vitro	28
1.5.3.3.	Reprogramming of reactive astrocytes in vivo	29

---

1.5.3.4.	Neuronal reprogramming from different somatic cell types	30
1.6.	JAK/STAT signaling	31
1.6.1.	Structure of the STAT molecules	32
1.6.2.	JAK/STAT pathway	34
1.6.2.1.	Canonical STAT signaling cascade	35
1.6.2.2.	Non-canonical STAT signaling	37
1.6.3.	Expression and functions	38
1.6.3.1.	Organism	38
1.6.3.2.	CNS	39
1.7.	Questions and goal of dissertation	43
<b>2.</b>	<b>Methods and Materials .....</b>	<b>45</b>
2.1.	Materials	45
2.1.1.	Equipment	45
2.1.2.	Consumables	46
2.1.3.	Chemicals	47
2.1.4.	Buffers and solutions	49
2.1.4.1.	Western blot	49
2.1.4.2.	Tissue Preparation for Immunohistochemistry	53
2.1.4.3.	Immunohistochemistry/-cytochemistry	54
2.1.4.4.	Molecular cloning	55
2.1.5.	Cell culture	56
2.1.5.1.	Media and components	56
2.1.5.2.	Solutions	56
2.1.6.	Oligonucleotides	58
2.1.6.1.	miRNAs	58
2.1.7.	Plasmids	59
2.1.7.1.	Established plasmids	59
2.1.7.2.	Newly designed plasmids	60
2.2.	Methods	62
2.2.1.	Animals	62
2.2.1.1.	Mouse strains	62
2.2.1.2.	Doxycyclin administration	62



---

2.2.1.3.	Anesthesia	63
2.2.1.4.	Surgical stab wound of adult animals	63
2.2.1.5.	Experimental focal cerebral ischemia of adult animals	63
2.2.2.	Western blot	64
2.2.2.1.	Tissue collection and lysis	64
2.2.2.2.	Protein quantification and sample preparation	65
2.2.2.3.	Gel preparation	66
2.2.2.4.	Protein electrophoresis	66
2.2.2.5.	Transfer	66
2.2.2.6.	Signal detection	67
2.2.2.7.	Membrane stripping	67
2.2.2.8.	Quantitative analysis of immunoblotting	68
2.2.3.	Histological procedures	68
2.2.3.1.	Perfusion, brain sectioning, storage of sections	68
2.2.3.2.	Immunohistochemistry	68
2.2.3.3.	Microscopic analysis	69
2.2.3.4.	Cell counts and statistical analysis	70
2.2.4.	Cell culture	70
2.2.4.1.	Cell strains and primary cultures	70
2.2.4.2.	Transfection	71
2.2.4.3.	Immunocytochemistry	71
2.2.4.4.	Western blot	72
2.2.4.5.	Neurosphere assay	73
2.2.5.	Molecular cloning	73
2.2.5.1.	Restriction digestion of DNA	73
2.2.5.2.	Analysis of DNA fragments	74
2.2.5.3.	Ligation	74
2.2.5.4.	Preparation of bacterial agar plates	75
2.2.5.5.	Transformation of chemo-competent E.coli	75
2.2.5.6.	Bacterial liquid cultures	75
2.2.5.7.	Small scale DNA preparation (MiniPrep)	75
2.2.5.8.	Large scale DNA preparation (MaxiPrep)	76

---

2.2.5.9.	Sequencing of DNA	76
2.2.5.10.	Design of miRNAs against STAT3 and STAT1	76
2.2.5.11.	Virus production	76
<b>3.</b>	<b>Results .....</b>	<b>77</b>
3.1.	Expression of STAT3 and activation of STAT3 signaling in the injured cerebral cortex	77
3.1.1.	Expression analysis of GFAP and STAT3 over a time course of seven days after stab wound injury	78
3.1.2.	Analysis of STAT3 expression and activation after stab wound using subcellular fractionated cortical extracts	79
3.1.2.1.	Protocol for subcellular fractionation	79
3.1.2.2.	Expression pattern of STAT3 after stab wound	79
3.1.2.3.	Analysis of STAT3 signaling activation after stab wound by studying the phosphorylation status of STAT3 at Tyr705	82
3.1.3.	Expression and activation pattern of STAT3 after MCAo	84
3.1.4.	Expression analysis of STAT1 and STAT5	86
3.2.	Which cell types express and activate STAT3 signaling in the injured cerebral cortex?	87
3.2.1.	Cellular localization of STAT3 at three days after stab wound	87
3.2.2.	Activation pattern of STAT3 signaling after stab wound by investigating STAT3 phosphorylation status	91
3.2.3.	Activation pattern of STAT3 signaling after MCAo by studying STAT3 phosphorylation status	95
3.2.4.	Activation pattern of STAT3 signaling in non-invasive injury models like APP/PS1 and CKp25	97
3.2.4.1.	Mouse model of amyloidosis: the APP/PS1 mouse	98
3.2.4.2.	Mouse model of non-invasive neuronal death: the CK/p25 mouse	98
3.2.4.3.	Activation of STAT3 signaling in mouse models of non-invasive brain injury	99
3.2.5.	Activation of STAT3 signaling in the adult neurogenic niches – SVZ and SGZ	101

---

3.2.6.	Cellular localization and activation pattern of STAT1 and STAT5 following stab wound injury	102
3.3.	Does STAT3 signaling inhibit reprogramming of reactive and postnatal astrocytes into neurons?	104
3.3.1.	Molecular cloning of constructs containing miRNAs against STAT3 and STAT1	105
3.3.1.1.	Design of effective miRNAs against STAT3 and STAT1	106
3.3.1.2.	Cloning of constructs containing several miRNAs against STAT3 and STAT1	108
3.3.1.3.	Cloning of the miRNAs against STAT3 and STAT1 into retroviral vectors	111
3.3.2.	Expression analysis of STAT3 and pSTAT3 in postnatal astrocytes	113
3.3.3.	Effects of STAT3 signaling activation on neuronal reprogramming of postnatal astrocytes	115
3.3.4.	Effects of STAT3 level reduction on reprogramming of postnatal astrocytes into neurons	119
3.4.	Do reactive astrocytes acquire stem cell properties after acute invasive injury?	122
<b>4.</b>	<b>Discussion .....</b>	<b>125</b>
4.1.	Comprehensive summary of the results	125
4.2.	Expression and activation of STAT3 in the adult injured cerebral cortex	127
4.2.1.	Expression of STAT3 and pSTAT3 within the different subcellular compartments	127
4.2.2.	Upregulation and activation of STAT3 signaling over time after stab wound	128
4.2.3.	Upregulation and activation of STAT3 signaling after MCAo	130
4.2.4.	Upregulation and activation of STAT3 signaling in mouse models of non-invasive brain injury	133
4.3.	STAT5 and STAT1 signaling in the injured cerebral cortex	134
4.3.1.	Expression of STAT5a after stab wound	134
4.3.2.	Activation of STAT1 after stab wound	135

4.4.	Impact of STAT3 signaling on reprogramming of postnatal astrocytes into neurons	136
4.4.1.	Expression and activation of STAT3 in postnatal astrocytes	137
4.4.2.	Inhibition of STAT signaling: several possible approaches	137
4.4.3.	Impact of STAT3 signaling on reprogramming of postnatal astrocytes into neurons	140
4.5.	Acquisition of stem cell properties by reactive astrocytes after brain injury	142
4.6.	Effect of STAT signaling on reprogramming of reactive astrocytes into neurons in the adult injured brain	143
<b>5.</b>	<b>Summary.....</b>	<b>146</b>
<b>6.</b>	<b>Zusammenfassung.....</b>	<b>148</b>
<b>7.</b>	<b>References .....</b>	<b>150</b>
<b>8.</b>	<b>List of Abbreviations.....</b>	<b>175</b>
<b>9.</b>	<b>List of Figures .....</b>	<b>180</b>
<b>10.</b>	<b>Acknowledgements/Danksagung.....</b>	<b>183</b>
<b>11.</b>	<b>Publications .....</b>	<b>184</b>
<b>12.</b>	<b>Curriculum Vitae .....</b>	<b>186</b>

# 1. Introduction

## 1.1. Overview

Since Cajal and Golgi “founded” modern brain research it has been thought for a very long time that once the generation of neurons during development has been completed, a process called developmental neurogenesis, no more neurons can be generated throughout the whole life. Cajal was the first who declared this dogma (Cajal, 1913-14). But in the early nineties a group led by Reynolds and Weiss discovered that Cajal’s hypothesis was wrong (Reynolds and Weiss, 1992) by showing that cells from the adult mouse striatum are able to divide and differentiate into neurons and astrocytes *in vitro*. Later, other groups found two regions in the adult mammalian brain where generation of neurons, now called adult neurogenesis, is still ongoing: the subgranular zone (SGZ) in the hippocampus and the subependymal zone (SEZ), also referred to as subventricular zone (SVZ), near the lateral ventricles in the forebrain (Gould and Cameron, 1996, Lois and Alvarez-Buylla, 1994).

Currently, we are not able to treat many neurological conditions, e.g. stroke and Alzheimer’s disease, in a curative manner as the neuronal loss cannot be substituted. Could the process of adult neurogenesis help to substitute these lost neurons after brain injury and help to repair the brain? Studies in different injury models over many years have revealed that although proliferation and neurogenesis in these two adult neurogenic niches increase after injury, the survival and functional integration of newly generated neurons into existing neuronal circuits in the damaged area remains very low if at all present. Therefore other approaches to replace the neuronal loss need to be found.

In addition to cellular transplantation, which has major ethical and immunological obstacles, a new concept has been invented by the laboratory of Magdalena Götz: endogenous glial cells that proliferate in the vicinity of virtually all CNS lesions could be reprogrammed into functional neurons by forced expression of neurogenic fate determinants. Indeed the lab was able to show that reactive astrocytes can be reprogrammed into functional subtype specific neurons in a highly sufficient manner *in vitro* (Heinrich et al., 2010). Recently, it was even demonstrated that this reprogramming process can be triggered *in vivo* (Guo et al., 2014).

Unfortunately, long-term survival and functional circuitry integration of these newly generated neurons remain very limited so far.

As a consequence, a better understanding of the biological process is needed to identify reasons for these limitations. For example a prudent way would be to determine pathways that inhibit neuronal reprogramming. In particular the STAT signaling pathway is known to promote gliogenesis and inhibit neurogenesis during embryonic development (Bonni et al., 1997). Could the activation of this pathway in reactive astrocytes explain the low efficiency of reprogramming by maintaining these cells in their glial lineage?

By decreasing gliogenic pathways it may be possible to elicit neurogenesis in the adult injured cerebral cortex. Here we studied STAT expression after brain lesion and investigated the potential role of STAT signaling in impairing reprogramming of reactive astrocytes into neurons in the adult injured cortex.

## **1.2. Cortical development**

The mammalian nervous system consists of two very distinct cell types: neurons and glia. In the adult brain a multitude of subtypes exists for each one of them. Together they have to fulfill remarkable tasks such as ensuring cognitive function, sensory perception and consciousness amongst others. A complex, highly-organized formation is needed. Therefore, during pre- and postnatal development of the nervous system, an essential diversification and integration has to take place.

Rudolf Virchow, well-known for the Virchow's triad (hypercoagulability, endothelial dysfunction and hemodynamic changes as contributors to thrombosis) was the first who referred to supportive cells (from now on called "glia") in the central nervous system (CNS) in 1846 (Kriegstein and Alvarez-Buylla, 2009). Wilhelm His, Sr., father of Wilhelm His, Jr. who discovered the bundle of His in the heart, continued this work four decades later. First he added the hypothesis that neurons and glia were produced from two distinct progenitor pools (reviewed in (Kriegstein and Alvarez-Buylla, 2009)) and he also discovered that the development of the mammalian neocortex depends on the proliferation of cells lining the ventricle of the neural tube (reviewed in (Bentivoglio and Mazzarello, 1999)). The concept of two different progenitor pools for neurons and glia became very popular throughout the

majority of the last century for many experts and is still a dogma for many not working in the field. But substantial progress in research in the last three decades influenced experts to no longer fully agree with this hypothesis. Evidence now suggests that cells considered to be part of the glial lineage – radial glia (RG) and a subpopulation of astrocytes – are in fact the neural stem cells (NSC) that give rise to differentiated neurons and glial cells throughout development and in the postnatal brain (Kriegstein and Alvarez-Buylla, 2009).

I will use the term glia to refer to both, differentiated macroglia (astrocytes, oligodendrocytes and ependymal cells) and glial cells that maintain stem cell properties (RG) but not to microglia as they are derived from the mesoderm.

### **1.2.1. Neural stem / progenitor cells**

Both neurons and glia originate from the neuroectoderm via a pseudostratified neuroepithelium (reviewed in (Bonfanti and Peretto, 2007, Kriegstein and Alvarez-Buylla, 2009)). These neuroepithelial cells are columnar, touch ventricular and pial surface (Temple, 2001) and increase in cell number by symmetric division (Fig. 1). In addition, they generate some early neurons, called Cajal-Retzius cells, which settle in the marginal zone (MZ) (Fig. 1). Approximately around onset of cortical neurogenesis, embryonic day 9 (E9) – E10 in the mouse, they begin to transform into RG (Fig. 1) by acquisition of glial properties – a transition more fluent than sudden (reviewed in (Gotz and Huttner, 2005)). It is characterized by morphological changes (lengthening of the radial processes due to ongoing thickening of the cortex), presence of glycogen storage granules and upcoming expression of astroglial markers like glutamate aspartate transporter (GLAST), brain lipid-binding protein (BLBP), Tenascin C (TN-C) (reviewed in (Campbell and Gotz, 2002)) and intermediate filament proteins like nestin, vimentin and “radial cell form” (RC1) (Edwards et al., 1990) and RC2 epitopes as well as glial fibrillary acidic protein (GFAP) (Benjelloun-Touimi et al., 1985, Choi and Lapham, 1978, Choi, 1988, Eng, 1985, Levitt and Rakic, 1980, Kriegstein and Alvarez-Buylla, 2009), latter not in rodents and chicken (Onteniente et al., 1983, Bignami and Dahl, 1974).

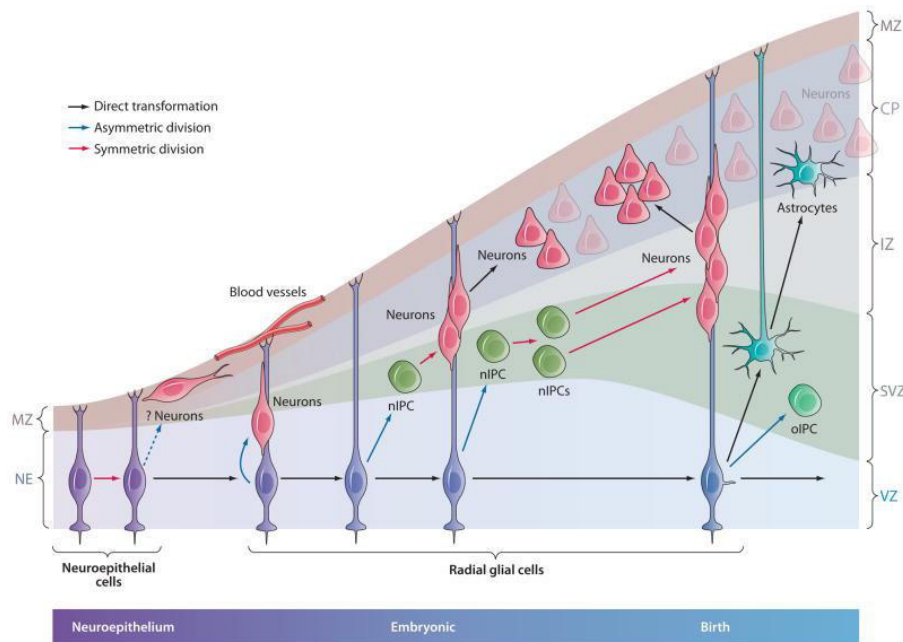


**Fig. 1: Cortical development**

Neurons can be generated in different ways: 1. directly from RG via asymmetric cell division 2. indirectly via neuronal intermediate progenitor cells (nIPCs) and one round of amplification 3. again indirectly via nIPCs but two rounds of amplification; Figure from Kriegstein and Alvarez-Buylla, 2009.

RG remain in contact with pial and ventricular surface with their cell bodies in the ventricular zone (VZ), a region next to the ventricles. It can be subdivided into a septal part, a cortical part, the lateral ganglionic eminence (LGE) and the medial ganglionic eminence (MGE).

In contrast to the historic opinion that RG will only serve as guidance for neuronal migration to the cortical plate (CP), many studies in the last three decades supported the finding that RG also act as main neural progenitor cells. In fact, this idea was invented by the lab of Magdalena Götz (Malatesta et al., 2000, Hartfuss et al., 2001) and later confirmed by others (Noctor et al., 2001, Anthony et al., 2004). Shortly after these initial findings the importance of the transcription factor Paired box protein 6 (Pax6) for the neurogenic potential of RG was identified by the lab of Magdalena Götz (Heins et al., 2002, Campbell and Gotz, 2002). RG acquired this status because they perform asymmetric cell division to self-renew and to produce either a nIPC, also referred to as basal progenitor cell or transit amplifying cell, or a neuron (Noctor et al., 2004, Haubensak et al., 2004). NIPCs are more restricted than RG and are already committed to the neuronal lineage as they express neuronal markers (reviewed in (Guillemot, 2005)). However, it is not the VZ that is thought to be the major site of neurogenesis but the SVZ (Fig. 1). Studies (Noctor et al., 2004, Miyata et al., 2004) revealed that SVZ cells are derived from RG and subsequently divide into neurons and that it is indeed



the nIPCs which populate the SVZ (Fig. 1) (Kriegstein and Alvarez-Buylla, 2009). That does not exclude the existence of nIPCs in the VZ at earlier time points (Noctor et al., 2007). As described above (Fig. 1), nIPCs will undergo symmetric cell division to produce either two neurons or two additional nIPCs (Noctor et al., 2007, Noctor et al., 2004, Haubensak et al., 2004, Miyata et al., 2004, Kriegstein and Alvarez-Buylla, 2009). With the subsequent growth of CP and SVZ the VZ shrinks more and more until birth (Bonfanti and Peretto, 2007).

### 1.2.2. Embryonic neurogenesis

The existence of a multitude of neuronal subtypes in the adult brain requires a high diversity of neural progenitor cells (reviewed in (Kriegstein and Alvarez-Buylla, 2009)). As all cell decisions, the subtype specification can also be regulated via cell-intrinsic and -extrinsic signals. Long it was thought that extrinsic information would largely regulate the cell fate but nowadays studies suggest that it is mainly determined via intrinsic cellular mechanisms. The two main classes of cortical neurons are interneurons, which make local connections and projection neurons, whose axons reach intracortical, subcortical and subcerebral targets. The latter are excitatory glutamatergic neurons with a typical pyramidal morphology (Molyneaux et al., 2007). They are generated from progenitors of the germinal zone of the dorsal telencephalon (pallium) (Guillemot, 2005, Anderson et al., 2002), a process directed by Pax6 and Neurogenin (Neurog) 2 (Fode et al., 2000, Guillemot, 2007) and sequentially reach the different cortical layers by radial migration. They settle in an inside-out fashion, i.e. later-born neurons make up the upper layers, therefore passing earlier born neurons, which display deeper layers. On the contrary, interneurons are inhibitory, contain  $\gamma$ -aminobutyric acid (GABA) and are produced by progenitors from the ventral telencephalon (subpallium), e.g. from the LGE, the caudal ganglionic eminence (CGE), the MGE and the septal part of the VZ, (Molyneaux et al., 2007) before migrating tangentially to their final locations. Their generation is governed by the proneural proteins mammalian achaete-scute homolog 1 (Mash1) (Casarosa et al., 1999, Parras et al., 2002) and distal-less homeobox 1/2 (Dlx1/2) (Petryniak et al., 2007). In addition to these major spatial differences, each subdivision generates again a multitude of neuronal subtypes differing in molecular profile, morphology and connectivity (reviewed in (Campbell, 2005, Guillemot, 2005)). Another factor for variation is for example the temporal pattern (Desai and McConnell, 2000). So far studies suggest the coexistence of

single multipotential progenitor cells (He et al., 2001, Parnavelas et al., 1991, Yung et al., 2002), which are intrinsically capable to generate many neuronal and glial subtypes, and fate-restricted progenitor cells (Battiste et al., 2007, Anthony et al., 2004), suggesting heterogeneity of RG populations (Kriegstein and Alvarez-Buylla, 2009). Recently it has been shown that from all early cortical progenitors, most exclusively generate neurons, few produce neurons before becoming glia-restricted progenitors and that there are no glia-restricted early cortical progenitors (Hartfuss et al., 2001).

The developmental processes underlying the difference between the small and non-folded (lissencephalic) neocortex of the rodent and the larger and higher-folded (gyrencephalic) neocortex of the human are subject of current research. An explanation could be the separation of the SVZ in an outer subventricular zone (OSVZ) and an inner subventricular zone (ISVZ) by a thin layer (Smart et al., 2002) with the existence of additional RG in the OSVZ (then called oRG) and more rounds of amplification by nIPCs to increase overall resulting neuron number in the CP (Lui et al., 2011).

### **1.2.3. Embryonic gliogenesis**

RG cell bodies stay in the VZ throughout the whole period of cortical development to cope with their two jobs: generation of IPCs and neurons as well as guidance for newly born neurons to the CP. At the end of this period RG lose their ventricular attachment and migrate toward the CP via somal translocation. In mammals most RG transform via morphological changes (bipolar -> unipolar -> multipolar) into astrocytes (Kriegstein and Alvarez-Buylla, 2009, Takahashi et al., 1990). In addition to the generation of astrocytes from RG from the VZ and subsequently progenitors from the SVZ, an old idea about the contribution of differentiated astrocytes in the postnatal cortex by local proliferation (Hajos et al., 1981) was recently shown to be true (Ge et al., 2012). Some RG also transform into ependymal cells (Spassky et al., 2005).

The onset of cortical embryonic gliogenesis, which follows neurogenesis, is regulated by a variety of factors, which will be reviewed in detail later (see chapter 1.6.3.2.), but are summarized shortly at this point: when important neurogenic factors like Neurog1 are downregulated at the end of neurogenesis, the signal transducer and activator of transcription (STAT) 3 can bind to its glial promoters, e.g. GFAP. Factors like the bone morphogenetic

protein (BMP) and Notch help to regulate this process via their downstream targets Smad and Hes.

Oligodendrocytes also arise from RG during development (Fogarty et al., 2005). They originate from multiple locations in three big waves: 1. from the MGE 2. from the LGE and CGE and 3. from the dorsal cortex itself. Interestingly, most of early-generated oligodendrocytes (first and second wave) disappear after birth so that their adult population basically comprises the third wave production (Kessaris et al., 2006). Oligodendrocyte progenitor cells (OPCs) are neuronal antigen 2 (NG2) expressing proliferating cells which exist throughout the whole brain (Rivers et al., 2008). OPCs are likely to correspond to oIPCs, however, compared to the actively proliferating IPCs in VZ and SVZ, NG2 expressing OPCs are found in grey and white matter and are usually quiescent, only proliferating symmetrically in response to local signals (reviewed in (Kriegstein and Alvarez-Buylla, 2009)).

#### 1.2.4. Time course of cortical development

For a better understanding of the different timelines and overlaps of neuronal, astrocytic and oligodendrocytic production, I will here shortly review the time points for the rat brain (Fig. 2): VZ neurogenesis commences at E12, peaks at E14 and recedes at E17 (Parnavelas, 1999). The SVZ emerges at E14 dorsally from the VZ. From late embryonic days (rat E17) to postnatal day 14 (P14) cells originating from the SVZ are essentially destined for glial lineages ((Sauvageot and Stiles, 2002). The peak of astrocyte generation occurs between P0 and P2 (Fig. 2) while oligodendrocyte formation has its climax at P14 (Parnavelas, 1999, Levison et al., 1993, Zerlin et al., 1995).

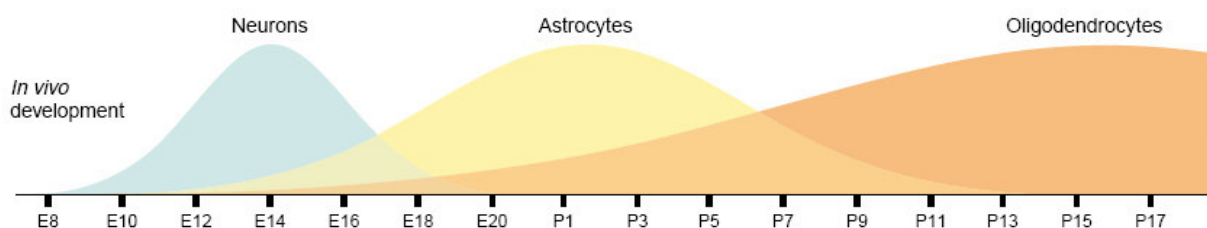


**Fig. 2: Temporal pattern of generation of neurons, astrocytes and oligodendrocytes in rats**

Generation of cells of the CNS occurs with a temporal distinct yet overlapping pattern. Neuron production peaks at E14, astrocytes highest increase is around P1 and oligodendrocytes have their production climax at P14. Figure from Sauvageot and Stiles, 2002.

### 1.3. Adult neurogenesis

*“Once development was ended, the fonts of growth and regeneration of the axons and dendrites dried up irrevocably. In adult centers, the nerve paths are something fixed and immutable: everything may die, nothing may be regenerated. It is for the science of the future to change, if possible, this harsh decree.”*

Santiago Ramon y Cajal (Cajal, 1913-14)

This long-lasting dogma that after brain development neuronal loss could not be substituted was for a very long time believed to be entirely true. Although Joseph Altman and colleagues reported in the early sixties about cells in the dentate gyrus that incorporate radioactive thymidine, a sign for cell division, (Altman, 1962) and Michel Kaplan showed via electron microscopy that these cells are indeed neurons (Kaplan and Hinds, 1977), leading neurobiologists still strongly disagreed with these findings at the emblematic conference “Hope for a New Neurology” in 1984 (Colucci-D'Amato et al., 2006). Positions changed when Fernando Nottebohm used neuronal markers and 5-bromo-2'-deoxyuridine (BrdU) for detection of proliferating cells in adult birds (Nottebohm, 1985). Finally, after isolating stem-like cells from the adult brain (Reynolds and Weiss, 1992, Lois and Alvarez-Buylla, 1993), a new chapter of neuroscience started. While in most other CNS regions the germinal layers disappear soon after birth, leaving only an ependymal monolayer, two principal neurogenic niches in the adult brain have been identified since then (Fig. 3): the SGZ, corresponding to the inner layer of the dentate gyrus in the hippocampus (Gould and Cameron, 1996, Kempermann et al., 1997) and the SVZ in the lateral wall of the lateral ventricles (Lois and Alvarez-Buylla, 1994). For these two regions Cajal's statement is now proven to be wrong. It still remains controversial if other brain regions also enable adult neurogenesis under physiological conditions *in vivo*, e.g. the subcallosal zone (SCZ) (Seri et al., 2006).

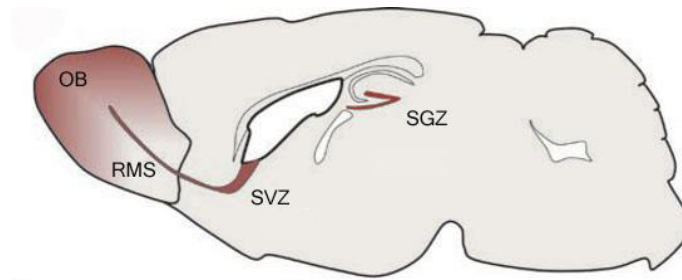


**Fig. 3: Neurogenic niches in the adult mammalian brain: SVZ and SGZ**

This schematic illustration displays the SVZ in the lateral wall of the lateral ventricles and the SGZ in the dentate gyrus of the hippocampal formation. The former generates neuroblasts which migrate via the rostral migratory stream (RMS) to the olfactory bulb (OB). Figure modified from Ma et al., 2009.

### 1.3.1. Subventricular zone

At the end of developmental neurogenesis most RG transform into parenchymal astrocytes (Alves et al., 2002, Voigt, 1989) while a subset gives rise to ependymal cells (Spassky et al., 2005) or astroglial stem cells in the adult SVZ (Merkle et al., 2007). Due to their expression of astroglial markers as GFAP, GLAST and others (Doetsch et al., 1997, Colak et al., 2008, Ma et al., 2009a) they are frequently called SVZ astrocytes. Furthermore they retain embryonic RG properties: a specific cell morphology with a cell body located under the ependymal cell layer, an apical process with endings on the ventricle as well as a long basal process with endings on blood vessels (Mirzadeh et al., 2008) and expression of Nestin and (Sex determining region Y)-box 2 (Sox2). For a long time the original nature of the adult NSCs in the SVZ was debated. While it was shown that they are derived from RG (Merkle et al., 2004), it was not entirely clear if they are the SVZ astrocytes (Doetsch et al., 1999) or ependymal cells (Johansson et al., 1999). In the following years it was reported that ependymal cells become postmitotic after development (Spassky et al., 2005) and only regulate quiescence and self-renewal of adult NSCs (Ramirez-Castillejo et al., 2006) but could be activated after a stroke to generate neuroblasts and glia (Carlen et al., 2009, Ma et al., 2009a). Eventually our lab showed that it is indeed the SVZ astrocytes that comprise the adult NSCs (Beckervordersandforth et al., 2010). They are relatively quiescent and widely known as Type B cells (Fig. 4). Recently they were shown to build up a pinwheel organization in the SVZ: the apical endings of B cells as core and two different types of ependymal cells in its periphery and thereby expressing their original epithelial properties (Mirzadeh et al., 2008). After generation of actively proliferating Type C cells (IPC or transit amplifying progenitors) (Doetsch et al., 1999) these will then subsequently

give rise to Type A cells (immature neuroblasts) which migrate in chains via the RMS to the OB (Fig. 3 and 4) (Lois and Alvarez-Buylla, 1994). This highly diversified structure is built by two different layers, the granule cell layer and the glomerular layer. Their basic neuron addition by adult neurogenesis is different: while the glomerular layer shows a constant net addition of a third of the total neuronal population within nine months, only a minor fraction is added to the granule cell layer (Ninkovic et al., 2007). In addition to the location of the progenitor cells in the postnatal SVZ (Merkle et al., 2004), the expression of different transcription factors in the SVZ or RMS plays the largest role in leading to a heterogenous population of neuroblasts and subsequently different types of the mainly GABAergic interneurons in the different neuronal cell layers of the OB (Carleton et al., 2003, Hack et al., 2005). For example Pax6 and Dlx2 together are essential for the generation of dopaminergic periglomerular neurons and a subpopulation of superficial granule cells (Brill et al., 2008). Other work showed that the role of Pax6 can be opposed by Olig2 which promotes a transit-amplifying precursor state (Hack et al., 2005). A recent study by our lab extended the knowledge about Pax6 even more: it regulates the survival of dopaminergic neurons of the OB by regulating crystalline  $\alpha$ A, which subsequently blocks apoptosis by inhibiting the activation of procaspase-3 (Ninkovic et al., 2010). In addition to the mainly GABAergic interneurons of the OB, a lineage of glutamatergic juxtglomerular interneurons was recently identified, characterized by the expression of Neurog2, T-box brain protein (Tbr) 1 and 2. Additionally, this lineage was also recruited to the cerebral cortex after induction of a lesion (see description of Macklis model in subchapter 1.5.1.2.), therefore possibly displaying a source for regeneration after injury (Brill et al., 2009). Whether neurogenesis and migration of neuroblasts to the OB continue in adult humans is part of an ongoing debate (Curtis et al., 2007, Sanai et al., 2007, Kriegstein and Alvarez-Buylla, 2009) but recent work shifted evidence strongly toward the idea that adult neurogenesis in the human OB occurs at a very low level or not even at all (Bergmann et al., 2012). In agreement it was reported that while the young human brain still contains solid chain migration of immature neurons via the RMS, this process appears to be distinctly decreased in older children and adults (Sanai et al., 2011).

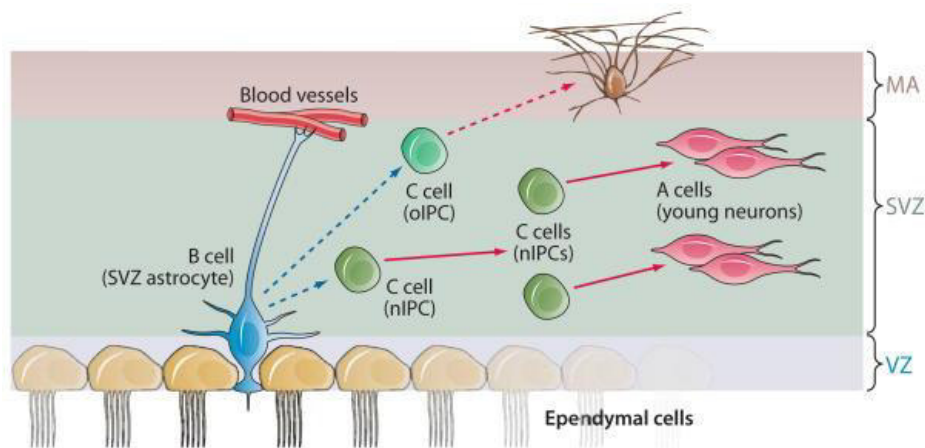


**Fig. 4: Scheme of progenitor cells in the adult brain SVZ**

SVZ astrocytes with two processes (blue), leading either to the ventricle or blood vessels, give rise to Type C cells (olIPCs or nIPCs, green). NIPCs generate Type A cells (red). Blue dashes represent asymmetric cell divisions, red dashes stand for symmetric cell divisions. Figure from Kriegstein and Alvarez-Buylla, 2009.

The role of OB neurogenesis in olfaction is well described (Lazarini and Lledo, 2011). Adult OB neurogenesis is a necessity for olfactory fear-conditioning (Valley et al., 2009) and olfactory perceptual learning (Moreno et al., 2009). In contrast, the adult generation of bulbar neurons is not required for odorant detection, discrimination or associative olfactory learning (Imayoshi et al., 2008, Sultan et al., 2010, Lazarini and Lledo, 2011). On the other hand OB neurogenesis is regulated by environmental factors: it increases for example during olfactory behaviour (Rocheffort et al., 2002, Magavi et al., 2005). In contrast, long-term sensory deprivation diminishes the survival of adult-born granule cells (Mandairon et al., 2006).

### 1.3.2. Dentate gyrus

The second main neurogenic region in the adult mammalian brain is the inner layer of the dentate gyrus in the hippocampal formation – the SGZ (Fig. 5). A link between SGZ stem cells and developmental RG has not yet been provided by experimental evidence (reviewed in (Kriegstein and Alvarez-Buylla, 2009)). Nevertheless, anatomical studies led to the idea that RG in the dentate neuroepithelium (Altman and Bayer, 1990) transform upon others into radial astrocytes (Eckenhoff and Rakic, 1984), which are the precursors for new neurons in the hippocampus (Seri et al., 2001, Fukuda et al., 2003, Kempermann et al., 2003). In addition, both embryonic SGZ progenitors and adult SGZ radial astrocytes present with the primary

cilium, the apical process described above for SVZ astrocytes (Breunig et al., 2008, Kriegstein and Alvarez-Buylla, 2009).

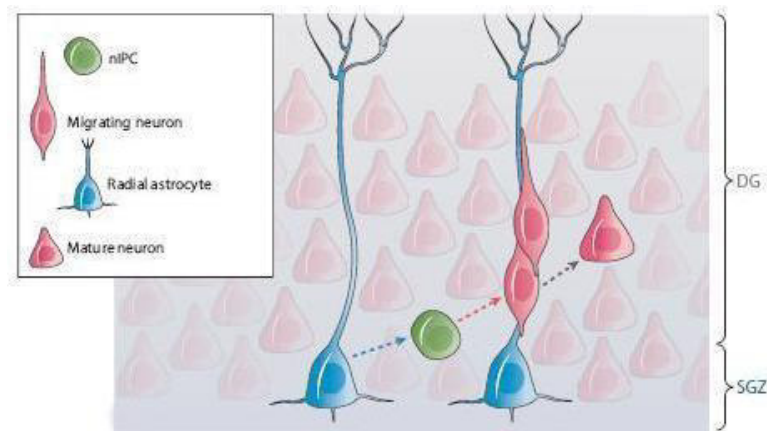


**Fig. 5: Scheme of progenitor cells in the adult brain SGZ**

Radial astrocytes, subsiding in the SGZ, have a long process that reaches through the granule cell layer to the deep molecular layer. They give rise to nIPCs (Type D cells, Type II progenitors) that in turn generate young neurons. After some time of attachment to the radial process of the radial astrocytes they differentiate into granule cells. The dashed arrows stand for asymmetric (blue), symmetric (red) division and transformation (black). Figure modified from Kriegstein and Alvaret-Buylla, 2009.

Radial astrocytes, also referred to as Type I progenitors, express GFAP and Nestin (in contrast to other SGZ astrocytes which express only GFAP) and give rise to Type II progenitors (also called Type D cells, see Fig. 5), which correspond to nIPCs (small basophilic cells) (Filippov et al., 2003). Type D cells are subdivided into D1-4 cells with D1 being more immature and D2-4 having already more neuronal properties. The latter express e.g. the Poly-sialated neural cell adhesion molecule (PSA-NCAM), doublecortin, neurogenic differentiation (NeuroD) as well as the neuronal nuclear antigen (NeuN) (Fukuda et al., 2003, Seri et al., 2004, Seki and Arai, 1993) and increasingly acquire electrophysiological properties of new neurons (Song et al., 2002). Unlike the NSCs in the adult SVZ, radial astrocytes in the SGZ mainly generate glutamatergic excitatory dentate granule cells (Ma et al., 2009a). In addition to their neurogenic function, radial astrocytes also exhibit the classical astrocyte character of supporting neuronal and synaptic activity (Fukuda et al., 2003) as well as the function to guide new born neurons during their migration.

Studies suggest that adult neurogenesis in the hippocampus potentially has implications on learning and memory (especially the dorsal part of the hippocampus, due to connectivity with the septo-temporal axis) as well as affective behaviour (particularly the ventral part) (Zhao et al., 2008). The role in spatial learning and memory remains elusive as one study showed that



ablated SGZ neurogenesis leads to impaired spatial learning and memory in a maze test (Raber et al., 2004) but others did not see defects (Meshi et al., 2006). Misguided neurogenesis can also lead to depression (Dranovsky and Hen, 2006) or epilepsy (Parent et al., 2006). Vice versa is true as well: hippocampal neurogenesis is regulated by different environmental cues (Kempermann et al., 1997). The survival of newborn neurons in the adult SGZ was positively influenced by hippocampus-dependent learning tasks (Leuner et al., 2006). Moreover studies report that chronic stressors decrease SGZ cell proliferation (Mirescu and Gould, 2006) while antidepressants increase SGZ neurogenesis (Warner-Schmidt and Duman, 2006). Activity seems to be important for the SGZ and SVZ (Ma et al., 2009b). Adult neurogenesis has also been shown to be regulated by a variety of signals. The most relevant seem to be Wnt (name origins from hybrid of Int and Wingless (Wg) in *Drosophila*) (Lie et al., 2005), Sonic Hedgehog (Shh) (Ahn and Joyner, 2005), Notch signaling (Androutsellis-Theotokis et al., 2006), BMP antagonists (Bonaguidi et al., 2008) and several cytokines (Bauer, 2009, Muller et al., 2009) – all known to promote progenitor proliferation and maintenance (Ma et al., 2009a).

#### **1.4. Neurological disorders and reactive gliosis**

Common acute (such as stroke and head trauma) and degenerative neurological disorders (such as Parkinson's disease and Alzheimer's disease) are caused and/or accompanied by a major and irreversible loss of neurons (Ma et al., 2009a). A growing number of scientists has therefore focused on the question of how to substitute this loss and thereby repair the brain. Could the process of adult neurogenesis described beforehand be helpful in this regard? Interestingly, virtually all neurological disorders associated with neuronal loss are accompanied by a reactive gliosis. Can this process lead us to repair the brain? Here I will first introduce stroke, one of the most prevalent neurological disorders. Next I will focus on reactive gliosis and especially on reactive astrocytes.

##### **1.4.1. Stroke**

Worldwide, fifteen million people annually have a stroke. Forty percent of them or six million per year die and another thirty percent or 4.5 million per year become permanently disabled (Mathers C, 2008). It is the second most common cause of death and the major cause of permanent disability. The costs for stroke were 73.7 billion dollars in 2010 (USA) (Lloyd-Jones

et al., 2010) and are estimated to be 2.21 trillion dollars until 2050 (from 2005 on, USA) (Roger et al., 2011). Actually, the Russian Federation and China are estimated to have five to ten times higher death rates than the USA - stroke spares no ethnic or racial group, it is considered to be a global problem (Moskowitz et al., 2010). To get a better understanding of this disorder it is essential to review risk factors, pathophysiology and clinical findings as well as current forms of therapy.

#### **1.4.1.1. Risk factors**

Stroke has a multitude of risk factors. Some of them like age, male sex, family history of cerebrovascular diseases and race are unmodifiable (Allen and Bayraktutan, 2008, Hankey, 2006). However, 60% - 80% of stroke risk is accounted to risk factors that are modifiable. Most of them affect the heart or structure and function of blood vessels. Causal relations have been found for conditions like hypertension (Lawes et al., 2004a), diabetes (Lawes et al., 2004b), hypercholesterolemia (Amarenco et al., 2006), cigarette smoking (Bonita et al., 1999), atrial fibrillation (Hart et al., 1999), valvular heart disease (Kizer et al., 2005), ischemic cardiomyopathy (Loh et al., 1997) and carotid stenosis (Rothwell et al., 2003) (reviewed in (Moskowitz et al., 2010)).

#### **1.4.1.2. Pathophysiology**

In over 85%, stroke is caused by the occlusion of a cerebral artery (local thrombosis or embolus; following explanations will refer to this cause). The remaining 15% can be explained with hemorrhage or cardiac arrest (Moskowitz et al., 2010). Especially the brain is vulnerable to ischemia because of its high consumption of glucose and oxygen due to intrinsic metabolic activity and large concentrations of the excitatory neurotransmitter glutamate (Choi, 1992, Moskowitz et al., 2010). The tissue distal to an occluded blood vessel can be roughly separated in two regions (Fig. 6). First, the infarct core, which consists of irreversibly damaged tissue with < 20% of baseline blood flow level. Here, ATP levels are depleted and energy metabolism is irrevocably stopped. This inner part of affected tissue is surrounded by a region "at risk", the ischemic penumbra or peri-infarct zone (Astrup et al., 1981). In this region, the significantly decreased blood flow levels can hardly provide basal ATP levels and oxygen metabolism. It is

functionally impaired but potentially recoverable (Fig. 6). The described separation and its course over time are important to explain an inconsistency at first sight: head imaging of a stroke patient shows an ischemic lesion increasing over time but his initial symptoms improve (Fig. 6, (Dirnagl et al., 1999)).

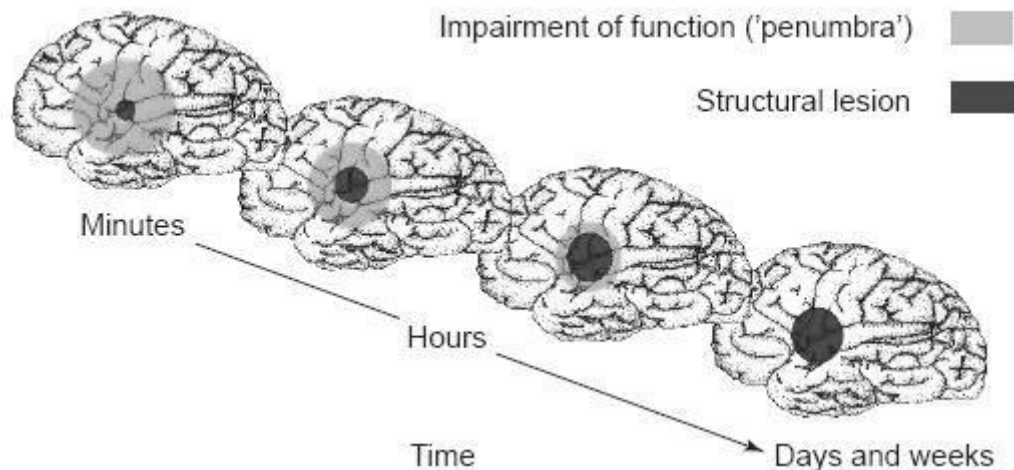


**Fig. 6: Regression of functional neurological deficit while structural lesion grows**

Early time points after stroke show a small lesion and do not reflect functional impairment. With time parts of the penumbra recover and other do not – the structural lesion grows while symptoms regress. Figure from Dirnagl et al., 1999.

Four major processes contribute to the pathophysiology of stroke: excitotoxicity, cortical spreading depolarizations (CSD), inflammation and apoptosis (Fig. 7). At first sight excitotoxicity develops as glutamate accumulates in the extracellular space due to energy and consecutive failure of ion pumps as well as reuptake mechanisms (Choi and Rothman, 1990). Subsequently, glutamate activates its receptors (2-amino-3-(5-methyl-3-oxo-1, 2-oxazol-4-yl)propanoic acid (AMPA) and N-Methyl-D-aspartate (NMDA)), which leads to influx of calcium, sodium, chloride and water into neurons. The ensuing edema can negatively influence the tissue perfusion (reviewed in (Dirnagl et al., 1999)). Intracellular calcium, which is also increased by release from mitochondria, activates proteases, lipases and nucleases (Ankarcrona et al., 1995). Additionally, reactive oxygen species (ROS) are produced, which lead to oxidative and nitrosative stress.

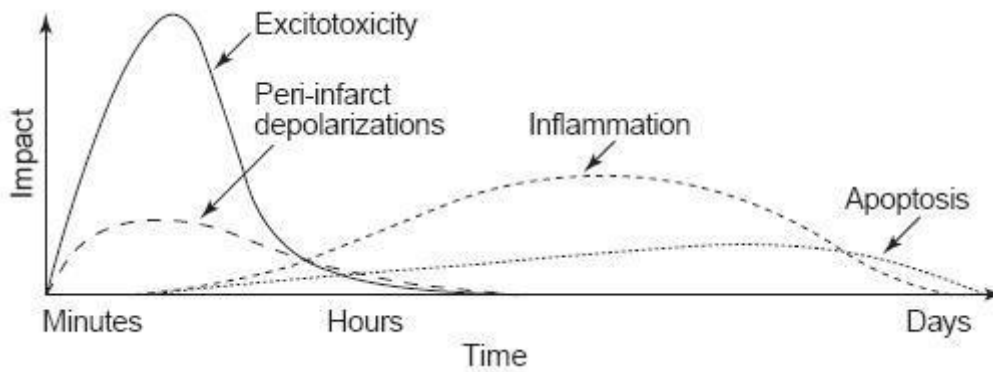


**Fig. 7: Detrimental cascade of pathophysiologic events in focal cerebral ischemia**

While excitotoxicity and peri-infarct depolarizations occur minutes after focal ischemia, inflammation and apoptosis are processes that have a later onset and whose impact decrease in the range of days. X-axis displays course of time after onset of cerebral ischemia. Y-axis shows impact of particular process on final outcome. Figure from Dirnagl et al., 1999.

CSDs (Moskowitz et al., 2010), also referred to as peri-infarct depolarizations, occur when ischemic cells depolarize as a consequence of low energy supply and the release of potassium and glutamate. Whilst in the core region, cells can undergo anoxic depolarization and never repolarize, penumbral cells can repolarize but at the expense of further energy consumption (Dirnagl et al., 1999). The frequency of depolarizations counts several per hour with a correlation to growth of infarct size (Mies et al., 1993).

The increase in calcium, oxygen free radicals and hypoxia itself trigger the expression of a number of proinflammatory genes resulting in activation of microglia and astrocytes (a process called reactive gliosis (Robel et al., 2011) which I will refer to in the next subchapter) as well as hematogenous cells, e.g. macrophages and neutrophils, that cross the disrupted blood brain barrier (Dirnagl et al., 1999).

Necrosis and apoptosis are the principal mechanisms of cell death, also after ischemic injury. Which one occurs depends on intensity of stimulus, type of cell and life-cycle stage. Necrosis is predominant after acute permanent vascular occlusion while milder injury is more often followed by apoptosis (Moskowitz et al., 2010).

#### 1.4.1.3. Clinical findings

Patients with stroke can suffer from a plethora of possible symptoms. Depending on the occluded artery and the affected tissue behind it, patients can, amongst others, suffer from motor or sensory impairments, loss of vision or aphasia. If we focus on the cerebral cortex and

its blood flow providing vessels anterior, middle and posterior cerebral artery as well as both vertebral arteries, possible symptoms include: contralateral hemiparesis or -plegia (motor cortex in frontal lobe), contralateral numbness (sensory cortex in parietal lobe), aphasia (most often involvement of Broca's or Wernicke's area), hemineglect (if parietal lobe is affected) and vision loss (e.g. if visual cortex in occipital lobe is involved) amongst others. Affection of the cerebellum can lead to vertigo as well as altered coordination and gait. Symptoms related to deficits of the cranial nerves will often occur if the brainstem is involved and comprise e.g. altered smell, vision, eye movements, facial sensation and muscle strength, hearing, taste, swallowing and tongue movement. So far only one medical drug for reestablishment of flow and subsequent salvaging of brain tissue in the acute setting was approved by the US agency for Food and Drug Administration (FDA): Tissue plasminogen activator (tPA) administration since 1996. Due to several contraindications and a narrow time window of four and a half hours (Hacke et al., 2008) after supposable occlusion only less than 10% of patients are treated this way (Zivin, 2009).

To investigate stroke in an experimental way the model of focal transient cerebral ischemia in adult mice is widely used and established (Hata et al., 1998). After a defined time of occlusion of the middle cerebral artery (MCAo) by a filament, the brain tissue will subsequently be perfused again and examined at later time points. It was especially valuable for us as our collaborators were greatly experienced with this model (Plesnila et al., 2004, Vosko et al., 2006). It is explained in detail in subchapter 2.2.1.6.

#### **1.4.2. Reactive gliosis and reactive astrocytes**

The reaction of glial cells to CNS insults is called reactive gliosis. Microglia as well as macroglia are part of this process. While microglia (Hanisch and Kettenmann, 2007) and NG2 cells (Kang et al., 2010) are the cells activated during the early stage, astrocytes react later by multiple changes regarding their morphology and gene expression, a process also referred to as astrogliosis (Robel et al., 2011, Sofroniew, 2009). Not only occurs astrogliosis after stroke but after all forms of CNS injuries like trauma, neurodegenerative diseases or infection. Sofroniew suggested a definition of astrogliosis by bringing up four key features: first it is a spectrum of changes in astrocytes responding to all forms and severities of CNS injuries (like described above); second these changes vary with form and severity of insult along a graduated

continuum of progressive alterations in molecular expression, cellular hypertrophy, proliferation and scar formation (Fig. 8); third the changes are regulated by specific signaling events; fourth the changes have the potential to alter astrocyte activities potentially affecting surrounding neural tissue beneficially or detrimentally (Fig. 9) (Sofroniew, 2009).

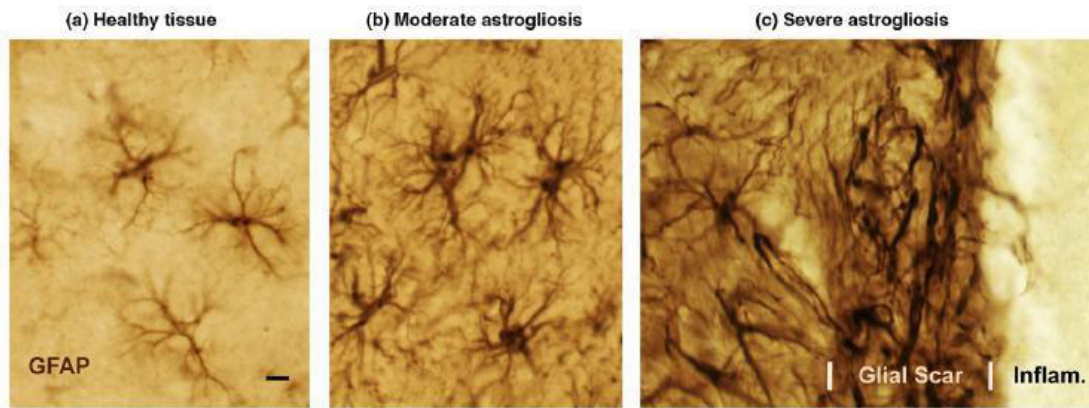


**Fig. 8: Progressive alterations of reactive astrogliosis after tissue insults**

Immunohistochemical staining with GFAP of the cerebral cortex of adult mice reveals non-overlapping processes of astrocytes in healthy tissue (a), moderate hypertrophy of astrocytes without overlapping processes after tissue insult (b) and severe hypertrophy and glial scar formation with overlapping of astrocytic processes (c). Figure from Sofroniew, 2009.

Sofroniew's second feature can be further described by introducing different gradations of cellular hypertrophy. While mild reactive astrogliosis displays hypertrophy of cell bodies and processes but preservation of non-overlapping domains of individual astrocytes (Wilhelmsson et al., 2006), an extreme activation includes scar formation, overlapping astrocytic processes and newly proliferating cells (Fig. 8) (Bush et al., 1999, Faulkner et al., 2004, Sofroniew, 2009).

Our lab was able to show that it is mature protoplasmic astrocytes from the grey matter and not cells arising from endogenous glial progenitors that seem to be the major source for these proliferating cells (Buffo et al., 2008). With fate mapping of quiescent astrocytes using the tamoxifen inducible recombination in the GLAST locus (GFP expression is specifically induced in astrocytes and kept in their progeny) and injection of lentiviral vectors into the grey matter as well as the use of BrdU as proliferation marker, our lab was able to show that these mature astrocytes re-enter cell cycle during scar formation (Buffo et al., 2008). Other potential origins like NG2-glia (Tatsumi et al., 2008) or ependymal cells (Carlen et al., 2009) from the forebrain are discussed (Robel et al., 2011). Furthermore, reactive astrocytes were shown to alter their expression of molecules involved in cell structure (upregulation of GFAP, Vimentin and Nestin (Eddleston and Mucke, 1993, Robel et al., 2011)), energy metabolism (BLBP (Pekny and Nilsson,

2005), lactate (Pellerin et al., 2007)), intracellular signaling (e.g. STAT 3 (Herrmann et al., 2008) (discussed in details in subchapter 1.6.3.2.), nuclear factor  $\kappa$ B (NF $\kappa$ B) (Brambilla et al., 2005)) and membrane transporters (e.g. glutamate transporter (Rothstein et al., 1996)) among others (Sofroniew, 2009).

#### **1.4.2.1. Stem cell-like properties of reactive astrocytes?**

As shown by the upregulation of Vimentin, Nestin, BLBP and also the dermatan-sulfate-dependent epitope 1 (DSD1) proteoglycan, cluster of differentiation (CD) 15 and in some cases Musashi, reactive astrocytes share hallmarks with NSCs and developmental radial glia (Robel et al., 2011). Unfortunately, it was not possible so far to observe these reactive astrocytes giving rise to any neurons without stimulus *in vivo*. In contrast, our lab and others were able to show that *in vitro* these cells acquire the potential to generate neurospheres (i.e. spherical, floating cellular aggregates) (Buffo et al., 2008, Lang et al., 2004), an indicator of multipotency and self-renewal. Using this neurosphere assay, cells, dissociated from brain tissue, can be propagated under specific culture conditions with mitogens to proliferate and later serum to differentiate. Our laboratory was able to show that a clone from a single reactive astrocyte could give rise to neurons, astrocytes and oligodendrocytes, demonstrating multipotency of at least the initial cell (Buffo et al., 2008).

#### **1.4.2.2. Role of astrogliosis**

The role of reactive astrogliosis can be both, beneficial and detrimental. For over 100 years glial scar formation was only seen as an inhibitor of axon regeneration (Fig. 9) establishing a negative view of this process per se (Sofroniew, 2009). Analysis of axon regeneration was performed extensively and supported this hypothesis (Silver and Miller, 2004). But in addition, the last decades have also shown that reactive astrogliosis exhibits a plethora of beneficial effects. Experiments with ablation of reactive astrocytes led to disrupted scar formation in turn resulting in increased spread of inflammatory cells (Fig. 9), failure to repair blood-brain barrier (BBB), increased lesion size and neuronal loss as well as impaired recovery of function (Sofroniew, 2005, Bush et al., 1999, Faulkner et al., 2004, Voskuhl et al., 2009, Myer et al., 2006, Sofroniew, 2009). The hypothesis that scar-forming astrocytes are highly valuable for

neural protection and repair was further supported by studies showing for example that reactive astrocytes reduce vasogenic edema after stroke (Zador et al., 2009) and take up potentially excitotoxic glutamate (Rothstein et al., 1996). The evolving concept now is that reactive astrogliosis is needed in early stages after injury to limit tissue damage and inflammation but persistent scar formation can be harmful (Robel et al., 2011).



**Fig. 9: Different roles of the glial scar**

Whereas during early stages after injury the glial scar prevents further expansion of inflammatory cells to healthy tissue and thereby further tissue damage, at later stages the glial scar barrier hinders axon growth and possible regeneration. Figure modified from Sofroniew, 2009.

#### 1.4.2.3. Regulation of astrogliosis

After CNS insults many different cells like glial cells, neurons or inflammatory cells, can release molecules that influence astrocytes in various ways. Amongst others, cytokines like interleukins, leukemia inhibitory factor (LIF) and ciliary neurotrophic factor (CNTF) (John et al., 2003), neurotransmitters like glutamate and noradrenalin (Bekar et al., 2008) or other small molecules like adenosine triphosphate (ATP) (Neary et al., 2003) and nitric oxide (NO) (Swanson et al., 2004) are known to stimulate this complex process (Sofroniew, 2009). Important intracellular signals include e.g. STAT3 (Herrmann et al., 2008, Robel et al., 2011), NFκB (Brambilla et al., 2005) and cytoplasmic polyadenylation element-binding protein 1 (CPEB1) (Jones et al., 2008). Particularly STAT3 is seen as a key regulator of glial scar formation as knockout studies suggested limited migration of reactive astrocytes after spinal cord injury (SCI) (Okada et al., 2006). However, expression patterns after cerebral ischemia seem to be contradictory but will be discussed in details in subchapter 1.6.3.2. Other factors that were shown to exhibit specific functions regarding astrogliosis include e.g. glycoprotein (gp) 130 (limiting infection) (Drogemuller et al., 2008), nuclear factor (erythroid-derived 2)-like 2 (Nrf2) (neuroprotection via increase of glutathione and less oxidative stress) (Shih et al., 2003) and CPEB1 (increased astrocyte migration) (Jones et al., 2008).



## **1.5. New avenues toward neuronal repair**

As extensively described above virtually all neurological disorders, especially the highly prevalent stroke, are caused or at least accompanied by neuronal loss. How can we substitute these neurons and repair the brain? Can adult endogenous neurogenesis be stimulated after injury to reproduce the lost neurons? Or can we substitute these neurons by either producing them *in vitro* and transplanting them subsequently or converting another cell type into neurons *in vivo*? Along this line reactive astrocytes may represent an interesting population as described above. Here I will first discuss if physiological endogenous neuronal repair can occur after injury. I will then concentrate on possibilities of cell transplantation while this chapter will close with a broad introduction to neuronal reprogramming, the subject of the present work.

### **1.5.1. Physiological neuronal repair: potential role of adult neurogenesis?**

As described in subchapter 1.3. adult neurogenesis is restricted to two neurogenic niches - the SVZ lining the ventricles and the SGZ in the hippocampus. Virtually no neurogenesis to repair lost neurons occurs outside of them, which is especially true for the striatum and the cerebral cortex.

#### **1.5.1.1. Striatum**

It was shown that neuroblasts from the adult neurogenic niches reroute along the vasculature (Ohab et al., 2006, Massouh and Saghatelian, 2010, Thored et al., 2007) toward damaged tissue (Parent et al., 2002, Lindvall and Kokaia, 2006, Kokaia and Lindvall, 2003). Lindvall's group also reported about increased cell proliferation in the SVZ following MCAo. In addition, their experiments revealed that neurons generated after the stroke and possibly neuroblasts generated before the insult migrated into the damaged striatum and expressed markers of developing and mature medium-sized spiny striatal neurons (Fig. 10). They also described a density gradient of new born neurons in the striatum with the highest being closest to the SVZ (Arvidsson et al., 2002). However, only 20% of the newly generated neurons survived longer than six weeks with only half of them being positive for mature neuronal markers (Fig. 10). The resulting population displayed only 0.2% of the originally lost striatal neurons.

Experiments about function and integration into neuronal circuits were missed (Lie et al., 2004). Nonetheless, ablation of these neuroblasts leads to increased lesion size and impaired behavioral deficits (Jin et al., 2010).

Another group reported migration of endogenous progenitors from the SVZ after transient forebrain ischemia into the affected hippocampal CA1 region to regenerate new pyramidal neurons (without endogenous neurogenesis in CA1 per se) - a response that was greatly enhanced by the intraventricular administration of growth factors (Nakatomi et al., 2002). 28 days after ischemia they observed a substitution of up to 40% with up to 20% still surviving at six months. Additionally, they could show that these newly generated neurons participated in reconstruction of the intrahippocampal connection although synapses remained morphologically immature with altered electrophysiological properties at three months (Nakatomi et al., 2002).

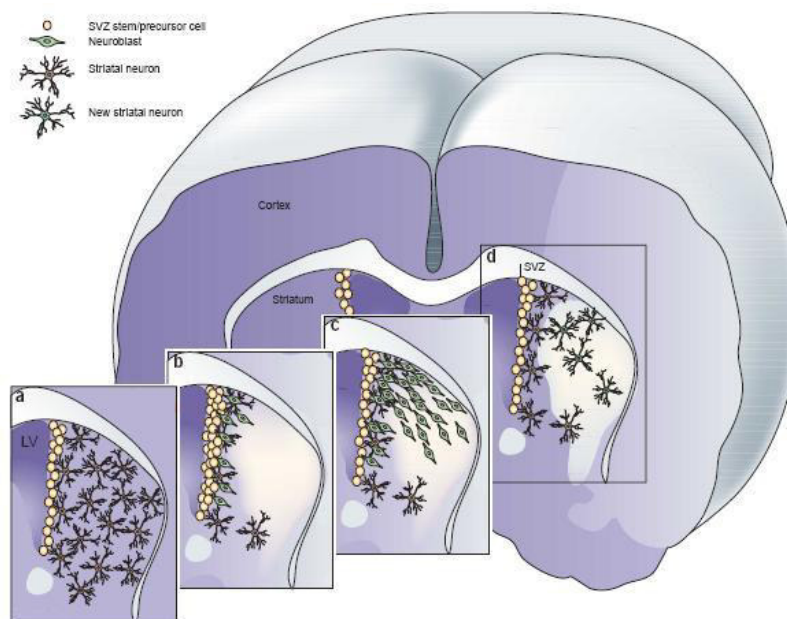


**Fig. 10: Generation of striatal neurons from SVZ stem cells after stroke**

(a) NSCs in the SVZ next to the striatum. (b) MCAo leads to death of striatal neurons (white area) and increased proliferation of SVZ precursors. (c) Newly generated neurons migrate into the damaged striatum. (d) After six weeks only few neurons survive and mature. Figure from Lindvall et al., 2004.

Similarly, an increase in cell proliferation and neurogenesis in the SGZ was observed after focal ischemia (Jin et al., 2001, Arvidsson et al., 2001), global ischemia (Takagi et al., 1999, Liu et al., 1998) and other insults like seizures (Parent et al., 1997).

### 1.5.1.2. Cerebral cortex

Cortical neurogenesis after insults was often reported not to occur (Arvidsson et al., 2002, Parent et al., 2002) or at very low levels (Magavi et al., 2000) (Lindvall et al., 2004). In particular the work of Sanjay Magavi and Jeffrey Macklis needs to be more emphasized as they used a methodically very different approach to induce cell death - a model also referred to as the Macklis model (also used in the earlier mentioned (Brill et al., 2009)). Cortical pyramidal projecting neurons were targeted by retrograde callosal transfer of beforehand in the contralateral motorcortex injected latex nanospheres that contained chlorine e6, a nontoxic chromophore. Laser illumination at 670nm was used to activate the chlorin e6 to produce cytotoxic singlet oxygen (Madison and Macklis, 1993). Overall this method constitutes a highly selective, precise and restricted way to induce apoptotic neuronal cell. Although Magavi et al. suggest cortical endogenous neural precursors to be the major source of the newly generated cortical neurons their work does not exclude the possibility that SVZ precursor cells proliferated after migration into these regions, leaving the origin of these neurons still unknown. In contrast, a recent study referred to cortical layer 1 neuronal progenitor cells as a source of adult neurogenesis after ischemia that mostly produced layer 4 neurons (Ohira et al., 2010). Unfortunately, they reported survival only for few weeks, could not exclude the possibility of migration of SVZ precursor cells and did not show electrophysiological characteristics of these cells as well as proof of functional integration. Studies on behavioral recovery were also not performed. As this single study was not supported by others so far the observed effects may at least partially be due to the mild ischemic condition (global forebrain ischemia) that was used.

The underlying mechanism of substitution of neuronal loss has been mostly studied in ischemic or the Macklis model as described above. Fewer groups have used mechanical brain injury, e.g. stab wound injury, to examine neurogenesis after the insult. In particular our lab has shown that no long-time surviving neurons at all are regenerated after stab wound injury (Simon et al., 2011, Buffo et al., 2005). The latter reference will be discussed in detail in subchapter 1.5.3.2.

Overall it seems evident that after brain injury, proliferation and neurogenesis in the adult neurogenic niches are increased and migration of neuronal precursors to the injury site occurs

to a certain extent. However, long-term survival and functional integration into existing neuronal circuits of these newly generated neurons in the damaged areas remain very low.

### **1.5.2. Possible forms of therapy by delivering external factors / cells**

Essentially, two ideas on how to externally drive substitution of neuronal loss after brain insults exist. The indirect way is to infuse factors into the brain, which are believed to improve endogenous physiological brain repair, the direct way implies cell transplantation.

#### **1.5.2.1. Delivery of factors improving the endogenous repair**

Several factors have been reported to increase neurogenesis in SVZ or SGZ by improving survival of new neurons after injury, e.g. fibroblast growth factor 2 (FGF-2) (Yoshimura et al., 2001), epidermal growth factor (EGF) (Teramoto et al., 2003), stem cell factor (Jin et al., 2002), erythropoietin (EPO) (Shingo et al., 2001), brain-derived neurotrophic factor (BDNF) (Gustafsson et al., 2003), caspase inhibitors (Ekdahl et al., 2002) and anti-inflammatory drugs (Monje et al., 2003, Lindvall et al., 2004). Unfortunately, only one study provided evidence that neurons are indeed functionally replaced (Nakatomi et al., 2002). However, it cannot be excluded that the functional improvement was due to other effects of these growth factors and not to newly generated neurons (Lindvall et al., 2004). A limiting feature for some factors could be also their relatively high molecular weight that can make it impossible to pass the BBB. Alternatives include smaller peptides, transnasal delivery to bypass the BBB (Fletcher et al., 2009) or compounds that can upregulate endogenous trophic factor production (Zhang et al., 1998, Moskowitz et al., 2010).

#### **1.5.2.2. Cellular transplantation**

Cell transplantation has been investigated intensively in many neurological disorders (Lindvall and Kokaia, 2006), but so far the FDA has not approved a single therapy. In the following section I will shortly introduce different cell types and potential reasons why cell transplantation could improve functional recovery. A plethora of human cell types has been analyzed for transplantation after stroke, most of them displaying heterogenous populations:

(1) neural stem/progenitor cells (including the derivation from induced pluripotent stem cells (iPS cells)); (2) immortalized cell lines; and (3) hematopoietic/endothelial progenitors and stromal cells isolated from bone marrow, umbilical cord, peripheral blood or adipose tissue (Bliss et al., 2007, Lindvall and Kokaia, 2006). Usually these cells have been either grafted into the lesion site or delivered intravenously. The finding that both ways showed cells surrounding the lesion suggests that targeted migration takes place (Bliss et al., 2007). Another population of cells has been in the focus of biomedical research very lately: neurons that were reprogrammed from somatic cells would also need to be transplanted (described in detail in subchapter 1.5.3.4.).

NPCs used for transplantation derived either from human embryonic stem (hES) cells or fetal tissue. HES cells can be differentiated into NPCs with various methods (Koch et al., 2009). For fetal tissue derived NPCs the first clinical trial was completed (Phase I) for Batten disease (CNS lysosomal storage disease) (Taupin, 2006, Bliss et al., 2010). Advantages for ES cells are their pluripotency, immortality *in vitro* and high expansion possibilities. Disadvantages are ethical issues (accompanied by political restrictions), insufficient availability and their tumorigenic potential (Banerjee et al., 2011). However, as it was recently shown how to generate iPS cells, whereby somatic cells as fibroblasts were reprogrammed to ES-like cells with three or four critical factors (Takahashi et al., 2007, Park et al., 2008), the first two disadvantages may be overcome.

The widely used immortalized cell line NTera-2 (NT2) derived from human teratocarcinoma over 20 years ago. The advantage of potentially unlimited expansion in culture is balanced by the risk of malignant transformation (Bliss et al., 2010). Despite showing survival after transplantation their effects on functional recovery remain not clear yet (Bliss et al., 2006) (Borlongan et al., 1998).

Until recently, most cell transplantation studies after brain injury used non-neural cell. Human bone marrow cells (HBMC), human umbilical cord blood cells (HUCBC), peripheral blood progenitor cells and adipose tissue mesenchymal progenitor cells have been shown to migrate to the brain and differentiate into neuronal marker-expressing cells (Banerjee et al., 2011). Unfortunately, only very few transplanted cells are found in the brain with even less cells expressing neuronal markers. Advantages are avoidance of ethical issues and immunological reactions at least for HBMC and peripheral blood stem cells as autologous and allogeneic

transplantation would be possible (paragraph reviewed in (Bliss et al., 2007)). Also, mesenchymal stem cells (MSCs) do not initiate T cell priming or antibody production and are therefore even with xenografts hypoimmunogenic (Li et al., 2002, Bliss et al., 2010). Except for neural stem/progenitor cell transplantation all mentioned cell types are currently under investigation in clinical trials.

Many reasons for better functional recovery in animal studies with cell transplantation after neurological disorders are discussed. Unfortunately, evidence for the desirable integration into host brain circuitries is very limited and most likely not a major player (Song et al., 2002). Neuroprotection seems to be more contributing to functional recovery, as acute cell delivery often reduces lesion size (Hicks and Jolkkonen, 2009). Different cell types are believed to secrete trophic factors like the vascular endothelial growth factor (VEGF), glial cell-derived neurotrophic factor (GDNF), FGF and BDNF. Additionally, post-injury inflammation is attenuated after cell transplantation, which seems to be mediated by downregulation of inflammatory and immune response genes and suppression of T cell proliferation (Bliss et al., 2010). Another process that is suggested to contribute to functional recovery is enhancement of endogenous repair processes, consisting of vascular regeneration, induction of host brain plasticity and recruitment of endogenous progenitors. Overall it is more the trophic factors, released by transplanted cells, than integration of the cells which lead to functional recovery (Bliss et al., 2010).

Despite all progress made in the last years many issues for translation to the bedside like choice of cell type, cell numbers to be given, optimum timing of treatment and optimum route of cell delivery remain unsolved (Banerjee et al., 2011).

### **1.5.3. Neuronal reprogramming**

Compared to the aforementioned possibilities the idea to recruit *in vivo* endogenous cells to repair the brain appears to be unique and innovative as it would overcome many of the major obstacles associated with cellular transplantation. Particularly the lab of Magdalena Götz has examined the potential of reactive astrocytes at the injury site being converted into functional neurons (Heins et al., 2002, Buffo et al., 2005, Berninger et al., 2007). As described above in subchapter 1.2.1., 1.3.1. and 1.3.2. neural stem/progenitor cells, i.e. RGs during development

and adult SVZ astrocytes as well as SGZ radial astrocytes, have properties of glial cells, which supports this idea strongly. That is why our lab has explored the question if even non-neurogenic astrocytes from non-neurogenic regions (as described above, e.g. the cerebral cortex) could be reprogrammed into functional neurons (i.e. typifying neuronal lineage reprogramming or cell-fate conversion (Vierbuchen and Wernig, 2011)) when supporting this process by overexpressing transcription factors known to instruct NSC neurogenesis. In the following paragraphs I will first focus on the conversion of postnatal cortical astrocytes *in vitro* into functional neurons, then describe recent findings on how to reprogram glial cells from the adult cerebral cortex after injury *in vitro* into functional neurons, explore the question if conversion of glial cells into functional neurons can occur *in vivo* in the injured adult cortex and finally discuss a topic that has been in the focus of biomedical research very lately - neurons that were reprogrammed from somatic cells.

#### **1.5.3.1. Reprogramming of postnatal cortical astrocytes in vitro**

Earlier work suggested that the low grade of spontaneous neurogenesis of postnatal astrocytes declines to zero during the second postnatal week (Laywell et al., 2000). Epigenetic silencing could be at least partially the reason for the loss of neurogenic capacity as *Neurog1* and *Neurog2* loci are repressed by the polycomb group complex (Hirabayashi et al., 2009). When investigating which neurogenic fate determinants could direct these astrocytes into functional, subtype-specific neurons our lab has provided some of the leading work. First it was reported that *Pax6* is necessary for the generation of glutamatergic neurons from cortical radial glia (Heins et al., 2002). A next study, also by our group, showed that forced expression of *Pax6* can also reprogram postnatal astroglial cells to action potential firing cells (in agreement to the former study that while being present in the developing cortex its expression levels decrease in postnatal astrocytes). Additionally, the same effect can be achieved by the proneural proteins *Neurog2* and *Mash1*. Of note, *Neurog2*, but neither *Pax6* or *Mash1*, could direct these cells toward a glutamatergic lineage, indicated by induction of the expression of *Tbr1* (Berninger et al., 2007).

One of our most recent work (Heinrich et al., 2010) showed that non-neurogenic astroglia could be reprogrammed into glutamatergic synapse-forming neurons by overexpression of a single transcription factor. Using primary cultures of adherent GFAP-positive astrocytes

isolated from the cerebral cortex of postnatal mice (P5-7) and retroviral vectors encoding high levels of Neurog2 expression we showed that ~70% of Neurog2-infected astrocytes were reprogrammed into neurons (indicated by immunohistochemistry with the neuronal markers  $\beta$ III-tubulin and Microtubule-associated protein 2 (MAP2) and repetitive action potential firing in electrophysiological patch clamp recordings) while control retrovirus-transduced glial cells remained in their glial lineage. Furthermore, we showed that after 2-3 weeks 60% of these astrocyte-derived neurons matured into synapse-forming glutamatergic neurons which was proven by perforated patch-clamp recordings. To ascertain that it was indeed astrocytes that gave rise to neurons, the described experiments were repeated with GLAST<sup>CreERT2</sup>GFP mice (as described in subchapter 1.4.2., (Mori et al., 2006)). Furthermore, this study provided evidence that forced expression of Dlx2, a transcription factor important for the generation of GABAergic neurons during embryonic development and adult neurogenesis (Brill et al., 2008, Petryniak et al., 2007), could lead to generation of functional GABAergic neurons from the same postnatal cortical astroglia (Heinrich et al., 2010, Berninger, 2010). Again, these astrocyte-derived neurons exhibited  $\beta$ III-tubulin and MAP2 expression as well as action potential firing. This conversion could be greatly enhanced by co-expression with Mash1 (from 35% to 95% of infected cells) (whole paragraph refers to (Heinrich et al., 2010)). This study has provided the first evidence that mature neurons can be generated by direct conversion across cell lineages by forced expression of a single neurogenic transcription factor (Neurog2 induces astrocytes to switch their phenotype toward glutamatergic neurons while Dlx2 converts astrocytes into GABAergic neurons).

#### **1.5.3.2. Reprogramming of reactive astrocytes in vitro**

In contrast to astroglial stem cells residing in the adult neurogenic niches, mature parenchymal astroglia are largely postmitotic (Buffo et al., 2008). So far no group reported about effects of forced expression of neurogenic fate determinants on mature quiescent astrocytes (Berninger, 2010). But as described above after CNS lesion astrocytes become reactive. Some of them can even proliferate depending on the severity of the lesion.

Within the same study cited above (Heinrich et al., 2010) we were able to show that reactive astrocytes that were isolated from the injured adult cerebral cortex could also be reprogrammed into neurons *in vitro*. To show that, we first applied a mechanical stab wound



injury in the cortex of adult mice and subsequently cultured reactive astrocytes under non-adherent conditions. We observed partial dedifferentiation and expansion as neurospheres (see subchapter 1.4.2.1. for description) supporting the hypothesis that these previously quiescent astrocytes proliferate and dedifferentiate after injury as well as exhibit stem cell-like properties *in vitro*. These neurosphere cells underwent the same experiments as described in 1.5.3.1. with transduction of a retroviral vector expressing Neurog2 or forced expression of Dlx2 showing that functional glutamatergic and GABAergic neurons, respectively, could be generated, indicating that neuronal reprogramming is not restricted to immature postnatal astrocytes (as described in subchapter 1.5.3.1.) but can also be accomplished from differentiated astrocytes from the adult cerebral cortex following reactivation after injury (Heinrich et al., 2010).

### **1.5.3.3. Reprogramming of reactive astrocytes in vivo**

A major challenge remains the translation of these *in vitro* findings into the enormously more complex setting of the injured brain *in vivo*. How can this be done?

It was shown that after stab wound or MCAo many cells, some of them being positive for the astroglial marker S100 calcium binding protein  $\beta$  (S100 $\beta$ ), upregulate the oligodendrocyte transcription factor 2 (Olig2) (Buffo et al., 2005). As it was known that Olig2 is expressed in precursor cells during development (e.g. motoneuron precursor cells (Mizuguchi et al., 2001)) and typically decreased in mature cell types (e.g. neurons (Hack et al., 2005)), it has been suggested that Olig2 is required for some cells to maintain an undifferentiated state. An experiment to repress Olig2 via retroviral expression of a Olig2VP16 fusion protein to let cells differentiate, led indeed to some transduced doublecortin (DCX, marker for young neurons)-positive cells. Interestingly, Pax6 expression was observed in some Olig2VP16-infected cells. Taking also into account that the majority of these Pax6-positive cells expressed DCX, it has been suggested that Pax6 may act as an intermediate toward the neuronal lineage. Unfortunately, these neurons could not be shown to survive for several weeks, mature or differentiate and therefore cannot be taken as an example of complete reprogramming (Buffo et al., 2005).

Several years later, this pioneer work has now been repeated with other neurogenic fate determinants (reviewed in (Arlotta and Berninger, 2014)). Using a transgenic mouse model and a triple combination of neurogenic fate determinants (Mash1, brain-2 (Brn2) and myelin transcription factor-like 1 (Myt1l)) Torper and colleagues demonstrated the conversion of striatal astrocytes into neurons *in vivo* (Torper et al., 2013). This work was supported by a study from Andrew Grande et al. showing that the combination of Ngn2, different growth factors and injury induced neurogenesis (Grande et al., 2013). While the latter did not report about the identity of the originating cells, both studies did not investigate the functional properties of newly generated neurons. In a landmark study Guo et al. investigated the effect of retroviral expression of NeuroD1, a downstream target of Ngn2, on the reprogramming of reactive astrocytes and NG2 cells in a stab wound model. Over 80% of infected cells were neurons, which were also shown to be capable of firing action potentials and receive synaptic input (Guo et al., 2014). Regrettably, less than 20 % survived longer than three weeks.

Considering the difficulty to reprogram reactive astrocytes into long-term surviving functional neurons *in vivo* so far, pathways impairing neurogenesis in the injured cortex need to be examined. It is most likely that these pathways keep reactive astrocytes within their glial lineage. One of them could be the STAT signaling pathway which was shown to be important for embryonic gliogenesis (mentioned in subchapter 1.2.3. and will be described in detail in subchapter 1.6.3.2.). Ultimately, one strategy may therefore be to block these gliogenic pathways.

#### **1.5.3.4. Neuronal reprogramming from different somatic cell types**

For a long time it was thought that somatic cells are irreversibly committed to their fate. Mainly Sir John B. Gurdon and Shinya Yamanaka, 2012's winners of the Nobel Prize in Medicine or Physiology, changed this misbelief and discovered that mature cells can be reprogrammed to become pluripotent (Takahashi and Yamanaka, 2006, Gurdon, 1962). The aforementioned work of the Götz lab discovering that mouse postnatal astrocytes can be reprogrammed into GABAergic and glutamatergic neurons *in vitro* (Heinrich et al., 2010) was published in the same year as a report about reprogramming of mouse embryonic fibroblasts into glutamatergic neurons *in vitro* (Vierbuchen et al., 2010). The world wide interest in direct conversion toward the neuronal lineage became even clearer in 2011 when these two

challenging studies were followed by many others in high-impact journals (for review see (Vierbuchen and Wernig, 2011)). Using defined sets of transcription factors, interestingly virtually always including Mash1, functional glutamatergic, GABAergic, dopaminergic and motoneurons were generated by reprogramming of mouse and human postnatal and adult fibroblasts (Ambasudhan et al., 2011, Pfisterer et al., 2011, Caiazzo et al., 2011, Pang et al., 2011, Kim et al., 2011, Qiang et al., 2011), lately also hepatocytes (Marro et al., 2011) and human cortical pericytes (Karow et al., 2012). Of note is particularly the work of Caiazzo et al. and Qiang et al., who cultured human fibroblasts from patients with Parkinson's disease or Alzheimer's disease, respectively and reprogrammed them into dopaminergic or glutamatergic neurons, respectively.

To transfer these *in vitro* findings in the vastly more complex living brain, Torper and colleagues engineered human fibroblasts and astrocytes to express inducible forms of neurogenic fate determinants and were able to demonstrate that these cells, after transplantation, converted into neurons upon activation of these reprogramming genes (Torper et al., 2013).

Unfortunately, all within this subchapter described studies are confronted with the critical step that cellular transplantation (see subchapter 1.5.2.2.) would need to be clinically implemented.

## **1.6. JAK/STAT signaling**

As already mentioned in subchapter 1.5.3.3. some pathways impairing neuronal reprogramming in the injured cortex by keeping reactive astrocytes within their glial lineage may exist. The JAK/STAT signaling, a well-known intracellular pathway that transmits information of extracellular cytokines to the nucleus and subsequently activates the transcription of definite genes, is known to promote the onset of astroglialogenesis during development (see subchapter 1.2.3., (Bonni et al., 1997)) and to be activated after specific CNS lesions (see subchapter 1.4.2.3., (Okada et al., 2006)). Consequently, this pathway needs to be investigated regarding its possible block of neuronal conversion of glial cells. Here I will introduce structure of the molecules, signaling cascade as well as expression and function in the organism and specifically the CNS, always with the focus on STAT3.

### 1.6.1. Structure of the STAT molecules

The term STAT originates from Shuai et al., who found that a single phosphotyrosine was needed to turn on interferon (IFN)- $\gamma$  mediated gene activation (Shuai et al., 1993). So far seven STAT proteins have been identified in mammals (STAT1, 2, 3, 4, 5a, 5b, 6) with a size ranging from 750 to 850 amino acids (aa) and a molecular weight from 84 to 113 kilo Dalton (kDa). Their chromosomal locations (STAT1 and 4 on chromosome 1, STAT2 and 6 on 10 and STAT3 and 5 on 11) led to the hypothesis that they arose from a single primordial gene. Six domains of the protein have yet been found, which are the amino-terminal domain, the coiled-coil domain, the deoxyribonucleic acid (DNA) binding domain, the linker domain, the SH2/tyrosine activation domain and the carboxy-terminal transcriptional activation domain (Fig. 11) (Kisseleva et al., 2002).

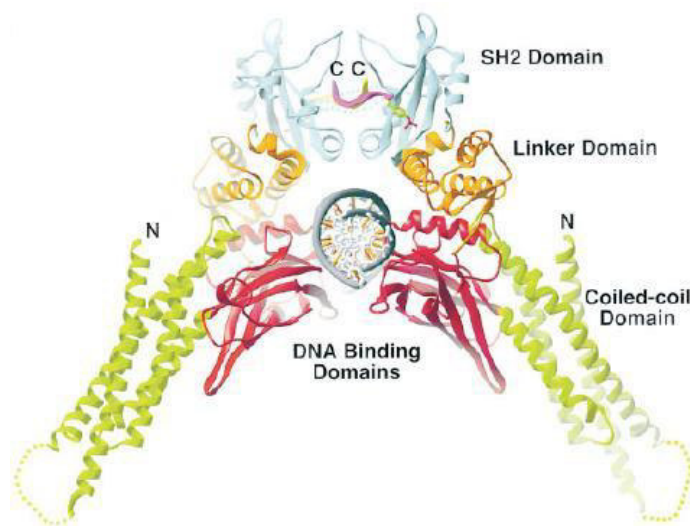


**Fig. 11: Crystal structure of STAT1 molecule**

STAT molecules share structurally and functionally conserved domains: the amino-terminal domain, the coiled-coil domain (green), the deoxyribonucleic acid (DNA) binding domain (red), the linker domain (orange) and the SH2/tyrosine activation domain (blue). In contrast, the transcriptional activation domain, located at the carboxy-terminus, is rather divergent and contributes to STAT specificity. The N-terminal domain is not displayed. The DNA backbone is colored in grey. Figure from Chen et al., 1998.

The N-terminal domain consists of approximately 130 amino acids and is believed to regulate e.g. the interaction with the transcriptional coactivator cAMP responsive element-binding (CREB)-binding protein (CBP)/p300 (Horvath et al., 1996) and the nuclear translocation of the whole molecule (Strehlow and Schindler, 1998). Adjacent to the coiled-coil domain, which comprises four  $\alpha$ -helices (approximately aa 315-350) (Chen et al., 1998). Studies have suggested implications in receptor binding, tyrosine phosphorylation and nuclear export

(Zhang et al., 2000, Begitt et al., 2000). The DNA binding domain (approx. aa 320-480) is located carboxy-terminally to the coiled-coil domain (Fig. 11) and contains several  $\beta$ -sheets, followed by the proverbial Linker domain (aa 465-585 for STAT3). An important role in regulating the signaling plays the src homology 2 (SH2) domain with its competence to bind to specific phosphotyrosine motifs. Consistent with that it is the most highly conserved STAT domain (Kisseleva et al., 2002). It is composed of the residues 580-680 which build up a pocket by an anti-parallel  $\beta$ -sheet and two flanking  $\alpha$ -helices (Fig. 11). The recognition of phosphotyrosine motifs is important for recruitment to the cytokine receptor, association with the activating JAKs as well as STAT homo (except STAT2)- or heterodimerization (Gupta et al., 1996). Latter is an interaction between the SH2 domain of one STAT monomer and the tyrosine phosphorylated tail segment around residue 700 (705 for STAT3, 701 for STAT1) of the other monomer (Kisseleva et al., 2002, Levy and Darnell, 2002). The last domain is not visible in Fig. 11 as it is the least conserved STAT domain. Whereas it structurally displays the carboxy-terminus it functionally represents the transcriptional activation domain. Literally, it displays high influence on transcriptional activity and binds transcriptional coactivators (like the IFN regulatory factor 9 (IRF9)), too. An important regulator of the latter seems to be serine phosphorylation (residue 727 in STAT1 and 3) (Decker and Kovarik, 2000).

Highly influential regulations can be achieved via modifications of the STAT molecules. Phosphorylation of the tyrosine residue around 700 is important for dimerization (Shuai et al., 1993) and subsequent DNA binding (Shuai et al., 1994). An additional tyrosine phosphorylation at 657 was reported to be the binding site for phosphoinositide 3-kinase (PI3K), whose relevance has not been determined yet (Pfeffer et al., 1997, Heinrich et al., 2003). The above described serine phosphorylation seems to be important for full transcriptional activation (e.g. by mitogen-activated protein kinases (MAPKs) (Decker and Kovarik, 2000). STAT methylation of an arginine residue and acetylation are possibly related to increased transcriptional effectiveness (Mowen et al., 2001, Shankaranarayanan et al., 2001, Yuan et al., 2005). Also carboxy-terminal truncated isoforms can be found (except for STAT2). They are referred to as  $\beta$ -isoforms (for STAT3: 79 kDa; normal length molecules:  $\alpha$ -isoform, 86 kDa) and have been shown to function as dominant negative forms (Caldenhoven et al., 1996). It is widely accepted that balanced STAT transcriptional activity requires the participation of negative regulators (Levy and Darnell, 2002, Kisseleva et al., 2002). Nonetheless, also positive regulatory roles for these forms have been reported (Schaefer et al., 1997). The half-lives of

STAT proteins, relevant e.g. for loss-of-function experiments, differ greatly (STAT3 $\alpha$ : 8,5 h; STAT3 $\beta$ : 4,5h; STAT1: 16h) (Heinrich et al., 2003).

### 1.6.2. JAK/STAT pathway

STATs conduct information for approximately 50 cytokines. These include the highly conserved families of hematopoietic cytokines and their corresponding receptors like the IFN family (IFN- $\alpha/\beta$ , IFN- $\gamma$ , interleukin (IL)-10, IL-19, IL-20, IL-22), the gp130 family (IL-6, IL-11, oncostatin M (OSM), LIF, cardiotrophin-1 (CT-1), granulocyte colony-stimulating factor (G-CSF), IL-12, IL-23, Leptin, CNTF, novel neurotrophin-1 (NNT-1)/B cell-stimulating factor-3 (BSF-3)), the  $\gamma$ C family (IL-2, IL-4, IL-7, IL-9, IL-15, IL-21) and the single chain family (Epo, growth hormone (GH), prolactin (PRL), thyroid peroxidase (Tpo)) of receptors (Schindler and Strehlow, 2000, Kisseleva et al., 2002). Their receptors usually consist of two transmembrane signal transducing subunits (often gp130 and LIF-receptor (LIFR)) with or without a specificity providing third ligand binding  $\alpha$  component (Fig. 12) (Heinrich et al., 2003). STAT signaling can also be activated via non-cytokine receptors like receptor-tyrosine kinases (RTKs, e.g. EGF or platelet derived growth factor (PDGF)), G-protein-coupled receptors (e.g. Angiotensin II receptor (AT<sub>1</sub>)) (Schindler and Strehlow, 2000), radicals and excitatory neurotransmitters (Dziennis and Alkayed, 2008).

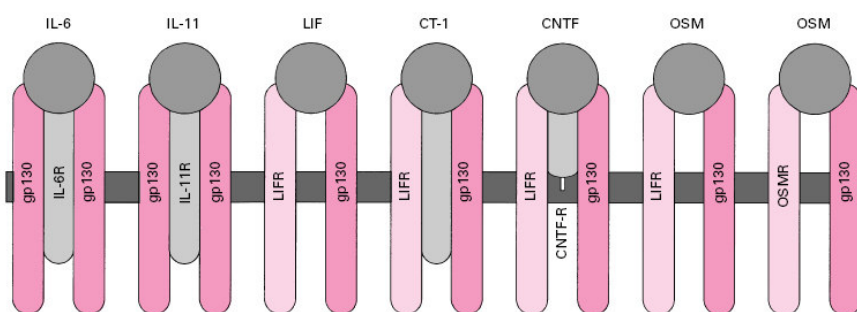


**Fig. 12: Receptor composition for cytokines from the gp130 family**

The grey horizontal bar symbols the cell membrane. Reddish vertical bars represent transmembrane signal transducing subunits. Cytokines appear as grey circles. Receptors comprise a gp130 subunit plus again gp130, LIFR or Oncostatin M-receptor (OSMR). Third ligand binding  $\alpha$  components exist for the receptors of IL-6, IL-11, CT-1 and CNTF. Figure from Heinrich et al., 1998.

### 1.6.2.1. Canonical STAT signaling cascade

After binding of the specific cytokine to its corresponding receptor, the receptor subunits dimerize into their active conformation (Fig. 13). JAKs, a family comprising four members in mammals (JAK1, JAK2 and Tyrosine Kinase 2 [TYK2] as well as JAK3, which is mainly expressed in hematopoietic cells) (Heinrich et al., 1998), bind to a membrane-proximal region of the cytokine receptor, which contains box1 and box2 motifs (Heinrich et al., 2003) and subsequently carry out a characteristic series of three tyrosine phosphorylations (Fig. 13). First they transphosphorylate themselves followed by the phosphorylation of tyrosine residues in the cytoplasmic tail of the receptors, which in turn function as docking sites for SH2 domains of latent cytoplasmic monomeric STAT proteins (mainly accepted hypothesis, although reports about preassociated STAT factors prior to stimulation exist (Stancato et al., 1996, Ndubuisi et al., 1999)). Consecutively and at last, JAKs phosphorylate also the STAT molecules at the important carboxy-terminal tyrosine residue around 700. In turn, STAT molecules dissociate from the receptor and are now able to homo (except STAT2)- or heterodimerize as described above (Fig. 13).

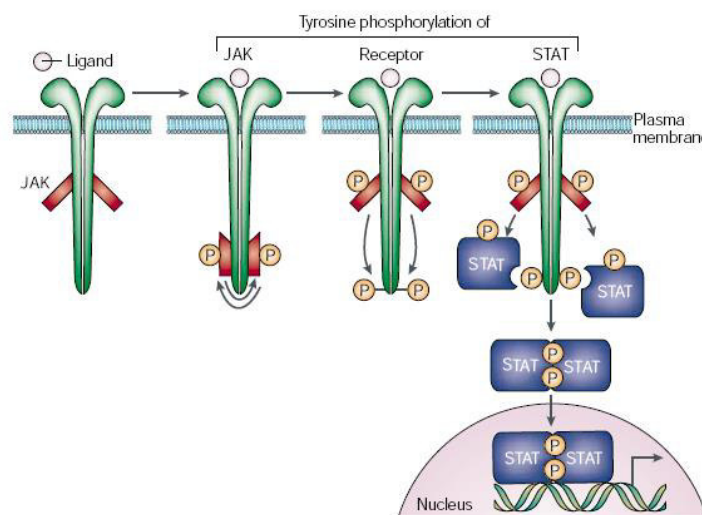


**Fig. 13: Canonical JAK/STAT pathway**

After cytokine binding to a specific receptor, JAKs bind to a membrane-proximal region of the receptor. First they transphosphorylate themselves, second they phosphorylate the receptor subunits and third they phosphorylate STAT proteins, which could associate to the receptor as the phosphorylated receptors subunits serve as docking sites for their SH2 domains. The STAT molecules then dimerize and translocate to the nucleus where they bind to the DNA. Figure from Levy et al., 2002.

Nuclear translocation requires dimerization in response to tyrosine phosphorylation but the phosphorylation itself is not an absolute necessity as also artificially dimerized not

phosphorylated STATs were found in the nucleus (Bromberg et al., 1999). Like all molecules larger than 60 kDa, STATs are transported across the nuclear pore complex (NPC) in an active bidirectional process that is energy and activation dependent (Kisseleva et al., 2002). After transfer to the nucleus they bind to specific DNA elements (Fig. 13, except for STAT2: that is why it also cannot form homodimers) and activate transcription of specific genes (Levy and Darnell, 2002, Aaronson and Horvath, 2002, Li, 2008). CBP and p300 then help to bridge the STAT dimer to the ribonucleic acid (RNA) Polymerase II (Zhang et al., 1996). STAT dimers usually bind to an 8-10-base pair consensus DNA sequence also referred to as  $\gamma$ -interferon activation site (GAS). STAT-DNA interaction at adjacent sites can be strengthened by tetramer formation (Vinkemeier et al., 1996, Levy and Darnell, 2002) and binding to transcriptional coactivators (like the IRF9) using the serine phosphorylation site (residue 727 for STAT1 and STAT3) (Decker and Kovarik, 2000). STAT binding sites were found in the promoter regions of GFAP, STAT1, STAT3 and JAK1 amongst others (He et al., 2005). Transcribed genes also encode for cell-survival factors like the B-cell lymphoma 2 (Bcl-2) family of proteins, factors involved in proliferation, e.g. cyclin D1 and myc, VEGF as an example for relation to angiogenesis and metastasis (Bromberg, 2002) and acute phase protein genes such as C-reactive protein,  $\alpha_1$ -antichymotrypsin and  $\alpha_2$ -macroglobulin (Heinrich et al., 1998). In contrast, STATs have also been reported to be associated with transcriptional repression (Ivanov et al., 2001). After dephosphorylation STATs will leave the nucleus (Begitt et al., 2000, Haspel and Darnell, 1999). Overall the STAT signaling expresses a large heterogeneity due to the possible combinations of the many different STAT and JAK molecules.

JAK/STAT signaling pathways do not work autonomously, they are rather regulated in a multitude of ways (Fig. 14). In addition to the beforehand described posttranscriptional modifications like tyrosine and serine phosphorylation that activate the pathway, many inhibitory molecules exist. Unspecific regulation as receptor internalization is accompanied by e.g. SH2-domain-containing tyrosine phosphatases (SHP2), which are able to dephosphorylate the receptor complex as well as JAKs and STAT dimers (Fig. 14), which consecutively recycle from the nucleus to the cytoplasm (Haspel et al., 1996, Lehmann et al., 2003). Suppressor of cytokine signaling (SOCS) bind directly to JAKs and inactivate them (Krebs and Hilton, 2001). Interestingly, SOCS genes are activated by the same cytokines that activate STAT, providing a classical feedback loop (Fig. 14) (Aaronson and Horvath, 2002). DNA recognition by STAT dimers can be prevented by protein inhibitors of activated STAT (PIAS) (Fig. 14) (Shuai, 2000).



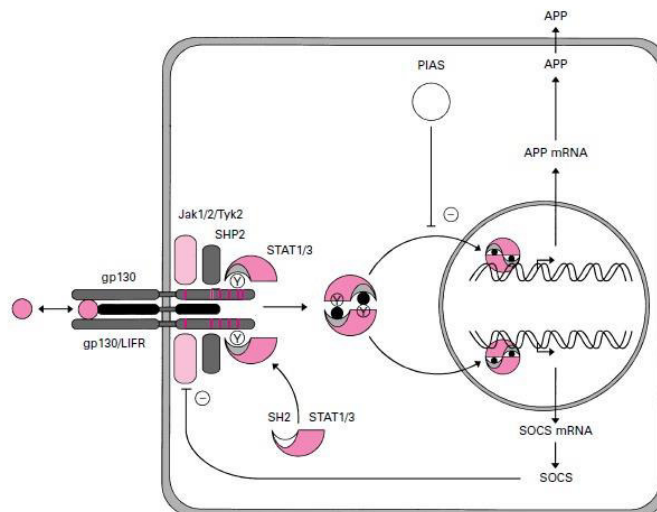


**Fig. 14: Inhibitory regulators of STAT signaling**

Suppressor of cytokine signaling (SOCS) by direct JAK inhibition, protein inhibitors of activated STAT (PIAS) by impairment of DNA recognition of STAT dimers and SH2-domain-containing tyrosine phosphatases (SHP2) by dephosphorylation of multiple sites lead to inhibition of the STAT signaling cascade and therefore the transcription of DNA regions encoding acute phase proteins (APP). Figure modified from Heinrich et al., 1998.

### 1.6.2.2. Non-canonical STAT signaling

While the pathway described so far is referred to as canonical mode, some recent research found STAT signaling events, e.g. in *Drosophila*, not fitting into this pathway and therefore representing the “non-canonical” mode (Li, 2008). First it was reported that JAK overactivation leads to global disruption of heterochromatin and therefore subsequent expression of genes, usually not regulated by STAT (Shi et al., 2006, Betz and Darnell, 2006). Further investigation of the underlying mechanism revealed that the *Drosophila* STAT equivalent STAT92E is also localized in the nucleus of unstimulated cells in an unphosphorylated form and here stabilizes the heterochromatin protein 1 (HP1). Phosphorylation of STAT92E would lead to dissociation from heterochromatin, subsequent HP1 displacement and eventually heterochromatin destruction independent of transcription (Shi et al., 2008, Li, 2008). Consistent with these studies, it has also been shown that unphosphorylated mammalian STAT3 and STAT5a localize partially in a nuclear manner. Furthermore, it was proposed that unphosphorylated STATs constantly shuttle between nucleus and cytoplasm (Reich and Liu, 2006, Vinkemeier, 2004, Liu et al., 2005) and use distinct methods to induce gene transcription (Yang et al., 2007, Yang and Stark, 2008). The described non-canonical pathway is not counteracting the canonical

pathway but rather conducive to the latter as heterochromatin disruption is necessary for activation of transcription by the canonical mode.

### **1.6.3. Expression and functions**

Here, I refer to STAT expression as the expression of the functional gene product - the specific STAT protein.

STAT proteins exert a multitude of functions and are expressed throughout the whole organism. Therefore I will focus here on STAT3, the main object of the present work. In addition, the most important aspects for other STATs will be mentioned. The main section about STAT expression and function in the CNS, separated in parts about development, the adult CNS and the adult CNS after injury, is preceded by a small introduction of the pattern of expression and functions of STAT proteins in the whole organism.

#### **1.6.3.1. Organism**

Originally, STAT3 was identified in hepatocytes as an acute-phase response factor, stimulated by IL-6 (Akira et al., 1994). Later it was found to be expressed in most tissues (Kisseleva et al., 2002). Consistent with this, STAT3 gene disruption leads to early embryonic death at around E7.5 in mice (Takeda et al., 1997). However, the genetically engineered „floxed“ STAT3 allele has enabled the generation of tissue-specific knockouts. Highlighting its role in cell survival and proliferation, STAT3 has also been determined to be active in a number of murine and human tumors (Kisseleva et al., 2002, Bowman and Jove, 1999). A recently published example punctuated this by showing correlation between the tyrosine phosphorylation of STAT3 and lower cancer survival of patients (Birner et al., 2010). Going along with that, STAT3 has been shown to activate genes like c-myc, Bcl-X<sub>L</sub> and Fas, which were found to regulate cell transformation. By experimental mutation, STAT3 can be converted into an oncogene (Bromberg et al., 1999). Furthermore, STAT3 was reported to regulate cyclical mammary gland involution as STAT3 null mammary gland mice exhibited a significant delay in programmed cell death (Chapman et al., 1999). In addition, it has an important role for the integrity of skin and hair (Sano et al., 1999), cell migration and wound healing (Levy and Lee, 2002) as well as in

the immune system, e.g. for the thymic epithelium, in T lymphocytes, monocytes and granulocytes (Takeda et al., 1998, Takeda et al., 1999, Lee et al., 2002).

STAT5 (STAT5a) was first described as a prolactin-induced transcription factor (Burdon et al., 1994). Further screening revealed that two distinct proteins exist, STAT5a and STAT5b (Azam et al., 1995), which share 96% identity and are only distinct at their carboxy terminals (Mui et al., 1995). Both proteins are expressed in all tissues. Although *in vitro* studies with dominant negative STAT5 mutants showed functional redundancy for the two proteins, single knockout studies revealed remarkably distinct phenotypes and in addition suggested that STAT5b could partially compensate for the loss of STAT5a (Teglund et al., 1998). As being prolactin-induced transcription factors, both have roles in development of the mammary gland as well. Primarily STAT5b appears to transduce information for GH and is therefore strongly suggested to exhibit the same functions as GH does (Teglund et al., 1998). Many biochemical studies have implicated important roles for STAT5 in hematopoiesis, particularly for lymphoid and myeloid lineages (Kisseleva et al., 2002).

Whereas STAT1 was determined to be important in susceptibility to tumors, growth control and responses to interferons, STAT2 is more involved in transduction of IFN signals (Levy and Darnell, 2002). Expression of STAT4 is restricted to NK cells, dendritic cells and T lymphocytes. STAT6, which is expressed in all tissues, and 4 are relevant for Th1 cell differentiation (Levy and Darnell, 2002).

### **1.6.3.2. CNS**

#### **Physiological conditions**

As STAT3 was shown to be a highly influential factor in the regulation of the onset of gliogenesis (Bonni et al., 1997), the following part will describe in detail the different molecular mechanisms of the temporal switch between neurogenesis and gliogenesis.

As described above, neurogenesis and astroglialogenesis in the developing rodent brain occur within a two-week perinatal period in a temporally distinct yet overlapping pattern with the birth marking the end point for neurogenesis. It is important to understand which factors regulate both processes as well as the change between them. Neurog2 in the dorsal

telencephalon for generation of glutamatergic neurons and Mash 1 in the ventral telencephalon for production of GABAergic and cholinergic neurons were identified as relevant factors for neurogenesis (Casarosa et al., 1999, Fode et al., 2000) but it was not clear which factors would regulate astroglialogenesis. In 1997 Michael Greenberg's group at Harvard found the first evidence that JAK/STAT signaling could be a highly influential factor in the regulation of astroglialogenesis. They reported that in E14/17 rat embryos CNTF would lead cortical precursors via STAT3 to the astroglial lineage. Besides, a STAT binding site in the rat and human GFAP promoter was found to have a critical role (Bonni et al., 1997). An additional synergistic functioning pattern of two factors, namely LIF and BMP, was identified to promote astroglialogenesis. In detail, their downstream signaling molecules STAT3 and Smad (mainly Smad1, others are Smad5 and 8) were found to be closely attached in a complex bridged by p300 (Nakashima et al., 1999). BMP was known to act sequentially: first, complex formation with Neurog to promote neurogenesis and later with STAT to promote astroglialogenesis (Li et al., 1998, Gross et al., 1996). Two years after Nakashima's findings one mechanism potentially guiding the change from neurogenesis to astroglialogenesis was identified: Neurog1, which is high during cortical neurogenesis and low during gliogenesis, sequesters the CBP/p300/Smad1/STAT3 complex away from glial promoters and directly suppresses JAK/STAT signaling (Fig. 15) (Sun et al., 2001).

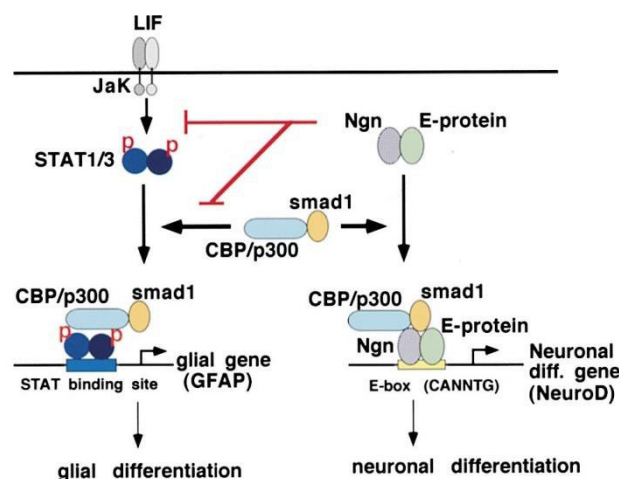


**Fig. 15: Mechanism of the molecular switch from neurogenesis to astroglialogenesis**

During early embryonic days Ngn (Neurogenin, mainly Neurog1) dimerizes with an E-protein (E12 or E47) and with the help of the CBP/p300/Smad1 complex activates transcription of genes encoding proneuronal proteins like NeuroD. When levels of Ngn drop at later time points, the CBP/p300/Smad1 complex can bind to STAT3 (here shown in a heterodimer with STAT1) and subsequently activate glial promoters. Figure from Sun et al., 2001.

Reports that STAT3 is present and active from E7.5 on (time of neurogenesis when no astroglialogenesis occurs) are consistent with that (Foshay and Gallicano, 2008). STAT3 is already present at times of neurogenesis but cannot act on glial promoters as Neurog1 sequesters away the complex that is needed for transcriptional activation (Fig. 15). As binding sites for Neurog and STAT3 on CBP overlap, both factors compete for CBP binding (Sun et al., 2001). When levels for Neurog would drop, STAT3 could associate to the complex and activate glial promoters (Fig. 15). Moreover, it was reported that the STAT3 recognition sequence in the GFAP promoter is highly methylated in NSCs during the time of neurogenesis, making it impossible for STAT3 to bind (Asano et al., 2009). Additional work with E17/18 rat embryos supported this as suppression of STAT3 at this gliogenic stage was found to promote neurogenesis and to inhibit astroglialogenesis (Gu et al., 2005). Next to STAT and BMP a third player in astroglial cell fate decision and its crosstalk to JAK/STAT was identified: Notch. During neurogenesis it inhibits neuronal differentiation and promotes morphological differentiation typical for radial glia, while later it promotes astrocytic differentiation and induction of GFAP. The crosstalk between Notch and STAT3 is suggested to be mediated by Hes, a downstream target of Notch, which associates with Jak2 and STAT3, facilitates complex formation between them and therefore promotes STAT3 phosphorylation and activation (Kamakura et al., 2004). Supporting the major role of STAT during astroglialogenesis, a positive autoregulatory loop and a direct effect of STAT on astroglial genes during astroglialogenesis was postulated when binding sites for STAT1 and 3 were detected in the promoters of STAT1, STAT3, gp130, Jak1, GFAP and S100 $\beta$  (He et al., 2005). Further roles for STAT proteins have been described e.g. in proliferation of embryonic CNS cells (Cattaneo et al., 1996), for the maintenance of NSCs in an undifferentiated state (Yoshimatsu et al., 2006) and in neuronal pathfinding (Conway, 2006).

As described above, STAT3 expression is already present during neurogenesis and still increases postnatally at times of gliogenesis. But from P21 on STAT3 activity is shown to decrease except in hypothalamic leptin-responsive neurons (Stromberg et al., 2000) suggesting that STAT3 is required for maintenance of the hypothalamic neuroendocrine axis in the adult (Dziennis and Alkayed, 2008). In contrast, pSTAT3 is not upregulated in the SVZ (Bauer and Patterson, 2006). Whereas STAT3 decreases in the aging rodent brain from three months to 26 months, STAT1 remains unchanged in cortex, striatum and hippocampus (De-Fraja et al., 2000). Moreover, the STAT proteins also differ functionally. While STAT3 and 5

promote neuronal survival by inducing neuroprotective genes, STAT1 promotes neurodegeneration by inducing apoptotic and other cell death promoting genes (Dziennis and Alkayed, 2008).

### **CNS injury**

The role of STAT proteins in acute CNS injuries has mainly been investigated after SCI so far. For example Okada et al. suggested STAT3 as a key regulator of reactive astrocytes in the healing process (Okada et al., 2006). They found phosphorylated STAT (pSTAT) 3 being upregulated from twelve hours until two weeks after SCI with nuclear translocation mainly occurring in reactive astrocytes. Further evaluation via conditional STAT3 knockout showed limited migration of reactive astrocytes, widespread infiltration of inflammatory cells, neural disruption and demyelination. A possible link was provided by the decrease of E-cadherin, a cell adhesion molecule, due to STAT3 activation (Okada et al., 2006). Another study using a conditional STAT3 knockout confirmed the results that reactive astrocytes did not longer built a highly aligned border but were found randomly in the vicinity of the lesion after SCI (Herrmann et al., 2008). As astrocyte scar formation is believed to restrict inflammation, limit lesion size and preserve function (Voskuhl et al., 2009), STAT3 is suggested as a key regulator of scar formation. Another detailed expression analysis of pSTAT3 after SCI revealed that pSTAT3 is upregulated already from 6h after SCI on, peaks at 12h and decreases thereafter. Immunohistochemical studies after SCI showed pSTAT3 being present in neurons at acute stages and in reactive astrocytes and microglia more during chronic stages (Yamauchi et al., 2006). Compared to STAT3, STAT1 has only insufficiently been examined after SCI. Herrmann and colleagues reported an activation of STAT1 signaling at three days after SCI (Herrmann et al., 2008). Experiments with entorhinal cortex lesion (by electrocoagulation of unilateral entorhinal afferents to the fascia dentata) showed pSTAT3 induction in reactive astrocytes of the fascia dentata. Expression was detected at one and three days after lesion, but not anymore at seven days. A similar time course was seen in sprouting neurons (Xia et al., 2002).

Consistent with its clinical relevance some studies have been conducted on STAT expression after ischemia. The resulting pattern seems to be at least partially contradictory. Planas et al. reported about STAT3 being activated several days after transient focal cerebral ischemia mainly in microglia with control level expression in neurons and other glial cells (Planas et al.,

1996). In contrast even the same group reported four years later that STAT3 is highly activated after ischemia in pyramidal neurons of layer V, astrocytes and microglia (Justicia et al., 2000). For STAT1 and STAT5 nearly the same conflict can be found. While Takagi et al. found STAT1 to be phosphorylated within hours and translocated into neuronal nuclei after MCAo (Takagi et al., 2002), another group reported about STAT1 not being expressed after several hours after MCAo, but after four days (Planas et al., 1997). Phosphorylation of STAT5 was found in Cornu ammonis area 1 (CA1) of the rat hippocampus at one and three hours, but not anymore at six and 24 hours after transient global ischemia (Zhang et al., 2007), whereas another group found STAT5 gene expression (in addition to STAT2 and 6) upregulated after 24 hours (Sun et al., 2007). Data for STAT expression after a stab wound injury to the adult cerebral cortex are entirely lacking so far. The characteristics of STAT expression after experimental stroke and acute lesion in the cerebral cortex as well as the functions of STAT signaling in these settings are therefore still unclear and need further evaluation.

Compared to acute injuries even less has been investigated so far regarding the role of STAT proteins in neurodegenerative diseases like AD. While Zambrano et al. proposed a neuroprotective role via IL-3 (Zambrano et al., 2010), Hashioka et al. suggested a neurotoxic role of astrocytes mediated by IFN- $\gamma$  and subsequently the JAK/STAT pathway (Hashioka et al., 2009), supported by the finding that IFN- $\gamma$  is apparently involved in the stimulation of beta-secretase and beta-amyloid production (Hong et al., 2003). Additionally, it has been found that IL-6 could be contributing to the tau hyperphosphorylation pattern (Orellana et al., 2005). Unfortunately, we were not able to identify studies that specifically investigated the role of STAT proteins in the mouse models APP/PS1 and CK/p25.

## **1.7. Questions and goal of dissertation**

As reviewed in subchapter 1.5.3. cellular reprogramming into neurons displays an innovative approach of cell-based therapy for many neurological disorders. Compared to transplantation of exogenous cells the idea to recruit *in vivo* endogenous glial cells, which proliferate after injury, to repair the brain appears to be unique and innovative as it would overcome many of the major obstacles associated with cellular transplantation. Whilst so far it was not possible to reprogram reactive astrocytes *in vivo* in a highly sufficient manner into long-term surviving neurons (by forced expression of neurogenic fate determinants) it is decisive to search not

only for factors that enhance neurogenesis but also to study inhibiting factors as especially STAT3 was suggested. Along this line, the expression pattern of STAT after stroke is not fully understood yet and for stab wound, CK/p25 and APP/PS1 is still completely unknown.

The aim of this present project is to investigate if i) the STAT signaling cascade is activated in reactive astrocytes after injury of the cerebral cortex and ii) these STAT-mediated pathways could hamper the neuronal reprogramming of these astrocytes.

In particular, it should be examined which STAT molecules (i.e. STAT1, STAT3, STAT5) are expressed and at which time points after an insult in the adult cerebral cortex. Moreover, it should be studied if the respective STAT signaling is activated by investigating the phosphorylation status of these STAT molecules. For this, two different mouse models will mainly be used: one mimicking a stroke (MCAo) and the second one mimicking an acute mechanical injury (i.e. the stab wound model). To increase the significance of our potential findings, it should be investigated whether STAT signaling is altered in the cerebral cortex of mouse models representing features of Alzheimer's disease (i.e. the CK/p25 and APP/PS1 models). To answer these questions, the expression pattern of STAT will be assessed in a semi-quantitative manner and over time following the injury using western blot. Additionally, immunohistochemistry will help us to determine which different cell types (e.g. neurons and astrocytes) express and activate STAT after injury as well as to study the spatial distribution of STAT activation, e.g. how distant from the insult the expression can be detected.

Next, based on these findings obtained with western blot and immunohistochemistry, it should be investigated if the activation of STAT signaling in reactive astrocytes impairs the glia-to-neuron conversion. For this aim, the well established neuronal reprogramming of postnatal astrocytes *in vitro* (see subchapter 1.5.3.1.) will be used. In particular, it should be tested whether gain-/loss-of-function of STAT1 and STAT3 signaling in cultured postnatal astrocytes may impair/promote their reprogramming toward the neuronal lineage.



## 2. Methods and Materials

### 2.1. Materials

#### 2.1.1. Equipment

Centrifuge 5810R	Co. Eppendorf (Hamburg, D)
Centrifuge Mikro 22R	Co. Hettich (Tuttlingen, D)
Centrifuge Qualitron® Microcentrifuges	Co. Krackeler Scientific (Albany, NY, USA)
Centrifuge Sorvall Evolution RC	Co. Thermo Sc. (Waltham, MA, USA)
Centrifuge Universal 320R	Co. Hettich (Tuttlingen, D)
Electrophoresis power supply LKB GPS 200/400	Co. Pharmacia (not existent anymore)
Electrophoresis power supply PowerPac 200	Co. BIO-RAD (Hercules, CA, USA)
Electrophoresis system Mini-PROTEAN Tetra	Co. BIO-RAD (Hercules, CA, USA)
Fluorescent table	Co. Renner (Dannstadt, D)
Forceps	Co. Fine Science Tools (Heidelberg, D)
Freezer (-20°C)	Co. AEG (Frankfurt am Main, D)
Freezer (-20°C)	Co. Liebherr (Bulle, CH)
Freezer (-80°C)	Co. Thermo Sc. (Waltham, MA, USA)
Freezer (-80°C)	Co. GFL (Burgwedel, D)
Gel imaging system Gel Doc™ XR	Co. BIO-RAD (Hercules, CA, USA)
Gel system GeneMate	Co. BioExpress (Kaysville, UT, USA)
Gel system PerfectBlue	Co. PEQLAB (Erlangen, D)
Hand drill	Co. Foredom (Bethel, CT, USA)
Ice machine	Co. Scotsman (Vernon Hills, IL, USA)
Incubator	Co. Memmert (Schwabach, D)
Incubator	Co. Binder (Bohemia, NY, USA)
Incubator Galaxy 170R	Co. New Brunswick (Enfield, CT, USA)
Kryostat CM 3050S	Co. Leica (Wetzlar, D)
Laboratory balances	Co. Mettler Toledo (Giessen, D)
Laminar flow	Co. Bdk (Sonnenbühl-Genkingen, D)

Magnetic stirrer IKA COMBIMAG RET	Co. IKA Jahnke und Kunkel (Staufen, D)
Microscope Axiovert 40CFL	Co. Zeiss (Oberkochen, D)
Light source HXP-120	Co. Visitron Systems (Puchheim, D)
Microscope Fluo BX61	Co. Olympus (Tokio, J)
Microscope Leica MZ6	Co. Leica (Wetzlar, D)
Microscope LSM 710	Co. Zeiss (Oberkochen, D)
Microwave	Co. Privileg (Stuttgart, D)
Mouse cages	Co. Tecniplast (Buguggiate, I)
pH-meter pH720	Co. WTW inoLab (Weilheim, D)
Pipette controller accu-jet <sup>®</sup> pro	Co. Brand (Wertheim, D)
Pipettes (10µl, 20µl, 100µl, 200µl, 1000µl)	Co. Eppendorf (Hamburg, D)
Pipettes (2µl, 20µl, 100µl, 200µl, 1000µl)	Co. Gilson (Middleton, WI, USA)
Refrigerator	Co. Privileg (Stuttgart, D)
Refrigerator	Co. Liebherr (Bulle, CH)
Shaker Duomax 1030	Co. Heidolph (Schwabach, D)
Shaker IKA-Vibrax VXR	Co. IKA Jahnke und Kunkel (Staufen, D)
Shaker Thermoshake	Co. C. Gerhardt (Königswinter, D)
Spectrophotometer Nano-Drop ND-1000	Co. Thermo Sc. (Waltham, MA, USA)
Spectrophotometer Prim Advanced	Co. Secomam (Alès, F)
Stereotactic mouse adaptor	Co. Stoelting (Wood Dale, IL, USA)
Thermomixer comfort	Co. Eppendorf (Hamburg, D)
Tissue grinder	Co. Wheaton (Millville, NJ, USA)
Trans-Blot SD Semi-Dry Transfer Cell	Co. BIO-RAD (Hercules, CA, USA)
Vortex-Genie 2	Co. Bender & Hobein (Bruchsal, D)
Water bath	Co. Memmert (Schwabach, D)
Water bath GFL 1083	Co. GFL (Burgwedel, D)
Water bath Haake D1/L	Co. Haake (Karlsruhe, D)

### 2.1.2. Consumables

Cell culture flasks CELLSTAR <sup>®</sup> (T25, T75, T175)	Co. Greiner Bio-One (Kremsmünster, A)
Cell strainer	Co. BD Biosc. (Franklin Lakes, NJ, USA)

---

Coverslips	Co. Carl Roth (Karlsruhe, D)
Eye and nose ointment	Co. Bepanthen (Leverkusen, D)
Filaments (Vicryl)	Co. Ethicon (Norderstedt, D)
Filter paper	Co. BIO-RAD (Hercules, CA, USA)
Filter tips Biosphere	Co. Sarstedt (Nürnbrecht, D)
Glass slides	Co. ThermoScientific (Waltham, MA, USA)
Gloves	Co. Diana Bar. v. Schaezler (Augsburg, D)
Gloves	Co. Ansell (Brüssel, B)
Insulin needles (U-100, 1ml)	Co. BD Biosc. (Franklin Lakes, NJ, USA)
Microscope slides	Co. Carl Roth (Karlsruhe, D)
Microscope slides	Co. Thermo Sc. (Waltham, MA, USA)
Pasteur pipettes	Co. VWR International (Darmstadt, D)
Parafilm	Co. Peckiney Plastic P. (Chicago, IL, USA)
PVDF membrane	Co. Merck Millipore (Billerica, MA, USA)
Reaction tubes (0,5ml; 1ml; 2ml)	Co. Brand (Wertheim, D)
Reaction tubes safelock (1,5ml; 2ml)	Co. Eppendorf (Hamburg, D)
Reaction tubes (15ml; 50ml)	Co. Greiner Bio-One (Kremsmünster, A)
Scalpel blades	Co. Fine Science Tools (Heidelberg, D)
Serological pipettes (5ml; 10ml; 25ml)	Co. Sarstedt (Nürnbrecht, D)
V-Lance™ Knife (19 Gauge)	Co. Alcon (Hünenberg, CH)
Well plates (24/6)	Co. Orange Scientific (Braine-l'Alleud, B)

### 2.1.3. Chemicals

Aceton	Co. Carl Roth (Karlsruhe, D)
Acetic acid	Co. Carl Roth (Karlsruhe, D)
Acrylamid (30%)	Co. BIO-RAD (Hercules, CA, USA)
Agarose	Co. Serva (Heidelberg, D)
Ammonium persulfate (APS)	Co. BIO-RAD (Hercules, CA, USA)
Ampicillin	Co. Life Technologies (Carlsbad, CA, USA)
Aprotinin	Co. Biomol (Hamburg, D)
Bacto-Agar	Co. Carl Roth (Karlsruhe, D)

---

Bacto-Tryptone	Co. BD (Franklin Lakes, NJ, USA)
BCA assay reagent A/B	Co. Interchim (Montlucon, F)
BrdU	Co. Sigma-Aldrich (St. Louis, MO, USA)
Bromphenol blue	Co. Sigma-Aldrich (St. Louis, MO, USA)
Corn oil	Co. Sigma-Aldrich (St. Louis, MO, USA)
Deoxycholic acid	Co. Sigma-Aldrich (St. Louis, MO, USA)
4',6-diamidino-2-phenylindole dilactate (DAPI)	Co. Life Technologies (Carlsbad, CA, USA)
Doxycyclin	Co. Sigma-Aldrich (St. Louis, MO, USA)
ECL Western Blotting Detection	Co. Chemicon
Edetate disodium	Co. Sigma-Aldrich (St. Louis, MO, USA)
Ethanol (>99,8%)	Co. Carl Roth (Karlsruhe, D)
Ethanol (70%)	Co. Carl Roth (Karlsruhe, D)
Ethidium bromide	Co. Carl Roth (Karlsruhe, D)
Ethylenediamine-tetraacetic acid (EDTA)	Co. Sigma-Aldrich (St. Louis, MO, USA)
Ethylene glycol	Co. Sigma-Aldrich (St. Louis, MO, USA)
Glycerol	Co. Sigma-Aldrich (St. Louis, MO, USA)
Glycine	Co. Sigma-Aldrich (St. Louis, MO, USA)
Goat serum	Co. Life Technologies (Carlsbad, CA, USA)
Hydrogen chloride (5N)	Co. Sigma-Aldrich (St. Louis, MO, USA)
Imidazole	Co. Sigma-Aldrich (St. Louis, MO, USA)
Isopropanol	Co. Carl Roth (Karlsruhe, D)
Kanamycin	Co. Life Technologies (Carlsbad, CA, USA)
Ketaminhydrochlorid (Ketavet, 100 mg/ml)	Co. Pfizer (New York City, NY, USA)
Leukemia Inhibitory Factor	Co. Sigma-Aldrich (St. Louis, MO, USA)
Leupeptin	Co. Biomol (Hamburg, D)
Methanol	Co. Merck (Darmstadt, D)
2-Mercaptoethanol	Co. Sigma-Aldrich (St. Louis, MO, USA)
Mounting solution (AquaPolymount)	Co. Polysciences (Warrington, PA, USA)
NaCl solution (Saline, 0,9 %)	Co. B. Braun (Melsungen, D)
Non fat dry milk blocker	Co. BIO-RAD (Hercules, CA, USA)
NP-40	Co. Sigma-Aldrich (St. Louis, MO, USA)
Paraformaldehyd (PFA)	Co. Sigma-Aldrich (St. Louis, MO, USA)

Pefabloc	Co. Biomol (Hamburg, D)
Pepstatin	Co. Biomol (Hamburg, D)
Monopotassium dihydrogen phosphate	Co. Merck (Darmstadt, D)
Potassium chloride (KCl)	Co. Sigma-Aldrich (St. Louis, MO, USA)
2-Propanol	Co. Carl Roth (Karlsruhe, D)
Proteinase K	Co. Carl Roth (Karlsruhe, D)
Sodium chloride	Co. Sigma-Aldrich (St. Louis, MO, USA)
Sodium citrate	Co. Sigma-Aldrich (St. Louis, MO, USA)
Sodium dodecyl sulfate (SDS)	Co. Sigma-Aldrich (St. Louis, MO, USA)
Sodium dihydrogen phosphate	Co. Merck (Darmstadt, D)
di-Sodium hydrogen phosphate	Co. Sigma-Aldrich (St. Louis, MO, USA)
di-Sodium hydrogen phosphate dihydrate	Co. Merck (Darmstadt, D)
Sodium hydroxide	Co. Sigma-Aldrich (St. Louis, MO, USA)
Sodium pyrophosphate	Co. Sigma-Aldrich (St. Louis, MO, USA)
Spectinomycin	Co. Life Technologies (Carlsbad, CA, USA)
Sucrose	Co. Merck (Darmstadt, D)
TEMED (Tetramethylethylenediamine)	Co. BIO-RAD (Hercules, CA, USA)
Triton X-100	Co. Sigma-Aldrich (St. Louis, MO, USA)
TRISbase	Co. Sigma-Aldrich (St. Louis, MO, USA)
TRISHCl	Co. Sigma-Aldrich (St. Louis, MO, USA)
Tween 20	Co. Sigma-Aldrich (St. Louis, MO, USA)
Vanadate	Co. New England BioLabs (Ipswich, USA)
Xylacinhydrochlorid (Rompun, 2 Vol %)	Co. Bayer (Leverkusen, D)
Xyelene cyanol solution	Co. Sigma-Aldrich (St. Louis, MO, USA)
Yeast extract	Co. BD (Franklin Lakes, NJ, USA)

#### **2.1.4. Buffers and solutions**

##### **2.1.4.1. Western blot**

###### Whole cell lysis buffer:

50 mM TRISHCl

0,15 mM	Saline		
1 %	Triton X-100		
10 %	Glycerol		
5 mM	EDTA		
Protease inhibitors (for 5 ml lysis buffer):		Phosphatase inhibitors (for 5 ml lysis buffer):	
10 µg	Leupeptin	100 µMol	Sodium pyrophosphate
5 µg	Aprotinin	200 mMol	Imidazol
20 µg	Pepstatin	20 µMol	Vanadate
2 mg	Pefabloc		

Subcellular fractioning lysis buffer:

Low salt buffer (LSB; 5 ml):		High salt buffer (HSB):	
50 µl	Hepes pH 8,0	1 ml	LSB
50 µl	1 M KCl	80 µl	NaCl 5M
4,9 ml	H <sub>2</sub> Odd		

+ same inhibitors as for the whole cell lysis buffer

20 Vol % Tween:

50 ml	Tween 20
200 ml	H <sub>2</sub> Odd

TBS buffer (10x):

12,1 g	TRISbase
87,8 g	Sodium Chloride
ad 1 l H <sub>2</sub> Odd; pH 8,0 with HCl (5N); autoclave	

TBS-T (0,1 Vol %; 1x):

100 ml	TBS 10x
5 ml	20 Vol % Tween 20
ad 1 l H <sub>2</sub> Odd	

Electrophoresis buffer (10x):

30,3 g      TRISbase  
144 g      Glycine  
10 g      SDS  
ad 1 l H<sub>2</sub>Odd; pH 8,45

APS (10 % (w/v)):

100 mg      Ammonium persulfate  
ad 1 ml H<sub>2</sub>Odd

SDS (20 % (w/v)):

2 g      SDS  
ad 10 ml H<sub>2</sub>Odd

Stacking gel buffer (TRIS 0,5M; pH 6,8):

30,28 g      TRISbase  
ad 500 ml H<sub>2</sub>Odd; pH 6,8 with HCl (5N)

Running gel buffer (TRIS 1,5M; pH 8,8):

90,85 g      TRISbase  
ad 500 ml H<sub>2</sub>Odd; pH 8,8 with HCl (5N)

Stacking gel solution (5 % Acrylamid; for two 1 mm thick gels):

5,7 ml      H<sub>2</sub>Odd  
1,7 ml      Acrylamid (30 %)  
2,5 ml      Stacking gel buffer  
50 µl      SDS (20 %)  
50 µl      APS (10 %)  
10 µl      TEMED

Running gel solution (10 % Acrylamid; for two 1 mm thick gels):

4,1 ml      H<sub>2</sub>Odd

3,3 ml	Acrylamid (30 %)
2,5 ml	Running gel buffer
50 µl	SDS (20 %)
50 µl	APS (10 %)
5 µl	TEMED

Transfer buffer:

100 ml	TBS 10x
200 ml	Methanol
	ad 1 l H <sub>2</sub> O

Loading dye (4x):

2 ml	1 M TRISHCl pH 8,5
8 ml	20 % SDS
5 ml	Glycerol
1,6 ml	2-Mercaptoethanol
50 mg	Bromphenol blue
3,4 ml	H <sub>2</sub> O

Stripping buffer:

380 µl	2-Mercaptoethanol
10 ml	10 % (w/v) SDS
6,25 ml	TRISHCl (pH 6,8)

Blocking solution for western blot (5 % (w/v) milk powder):

2 g	Milk powder
	ad 40 ml TBS-T (1x)

Antibody solution for western blot (5 % (w/v) BSA):

0,5 g	BSA
	ad 10ml TBS-T (1x)



**2.1.4.2. Tissue Preparation for Immunohistochemistry**Doxycyclin drinking water (100 ml):

50 mg          Doxycyclin  
1,5 g          Sucrose  
                 ad 100 ml H<sub>2</sub>O

BrdU drinking water (100 ml):

100 mg        BrdU  
1 g            Sucrose  
                 ad 100 ml H<sub>2</sub>O

Anesthesia solution:

2,5 ml        Saline  
1 ml          Ketavet  
0,25 ml      Rompun

Paraformaldehyd stock (PFA; 20 % (w/v)):

134 g        di-Sodium hydrogen phosphate dihydrate in 800 ml H<sub>2</sub>Odd  
400 g        Paraformaldehyd  
ca. 10 ml    Sodium hydroxide  
                 pass through paper filters; ad 2 l H<sub>2</sub>Odd; pH 7,4

Paraformaldehyd (4 %):

100 ml       PFA 20 %  
400 ml       H<sub>2</sub>Odd

Sucrose solution (30 % (w/v)) for cryoprotection:

15 g          Sucrose  
                 ad 50 ml PBS 1x

PO<sub>4</sub>-buffer (10x; pH 7,2 - 7,4):

65 g	Sodium dihydrogen phosphate
15 g	Sodium hydroxide
2 ml	HCl (5N)
	ad 400 ml H <sub>2</sub> O

Storing solution for free floating brain tissue sections:

150 ml	Glycerol
150 ml	Ethylene glycol
50 ml	PO <sub>4</sub> -buffer (10x)
150 ml	H <sub>2</sub> O

**2.1.4.3. Immunohistochemistry/-cytochemistry**Phosphate buffer saline (PBS; 10x):

58,75 g	di-Sodium hydrogen phosphate
10 g	Monopotassium dihydrogen phosphate
400 g	Sodium chloride
10 g	Potassium chloride
	ad 5 l H <sub>2</sub> O; pH 7,4

Blocking solution for brain tissue sections (2 % (w/v) BSA):

0,2 g	BSA
	ad 10 ml PBS 1x

Blocking solution for cells:

0,2 g	BSA
50 µl	Triton X-100
	ad 10 ml PBS 1x

Sodium citrate buffer (0,1 M):

29,41 g	Sodium citrate
---------	----------------

ad 1 l H<sub>2</sub>Odd; pH 6,0

#### **2.1.4.4. Molecular cloning**

##### TAE (50x):

242 g        TRISbase  
57,1 ml      Acetic Acid  
37,2 g        Edetate disodium  
ad 1 l H<sub>2</sub>Odd

##### TAE (1x):

20 ml        TAE 50x  
980 ml       H<sub>2</sub>Odd

##### Ethidium bromide

100 mg       Ethidium bromide  
2 ml         H<sub>2</sub>Odd

##### DNA sample buffer:

20 ml        Glycerol  
1 ml         50x TAE  
200 µl       Bromphenol blue  
500 µl       Xylene cyanol solution  
ad 50 ml H<sub>2</sub>Odd

##### LB (lysogeny broth):

0,5 % (w/v)    NaCl  
1 % (w/v)      Bacto-Tryptone  
0,5 % (w/v)    yeast extract  
20 mM          TRISHCl (pH 7,4)  
ad 500 ml H<sub>2</sub>Odd; pH = 7,0 with NaOH

### 2.1.5. Cell culture

#### 2.1.5.1. Media and components

B27	Co. Life Technologies (Carlsbad, CA, USA)
Basic fibroblast growth factor (FGF)	Co. Life Technologies (Carlsbad, CA, USA)
Bovine serum albumin (BSA)	Co. Sigma-Aldrich (St. Louis, MO, USA)
DMEM/F12 + GlutaMAX™	Co. Life Technologies (Carlsbad, CA, USA)
DMEM/F12	Co. Life Technologies (Carlsbad, CA, USA)
D-Glucose (45 %)	Co. Sigma-Aldrich (St. Louis, MO, USA)
Earle's Balanced Salt Solution (EBSS)	Co. Life Technologies (Carlsbad, CA, USA)
Fetal calf serum	Co. Life Technologies (Carlsbad, CA, USA)
Hank's Balanced Salt Solution (HBSS)	Co. Life Technologies (Carlsbad, CA, USA)
Hepes (1 M)	Co. Life Technologies (Carlsbad, CA, USA)
Horse serum	Co. Life Technologies (Carlsbad, CA, USA)
Human epidermal growth factor (EGF)	Co. Life Technologies (Carlsbad, CA, USA)
Hyaluronidase	Co. Sigma-Aldrich (St. Louis, MO, USA)
Lipofectamine 2000	Co. Invitrogen (Carlsbad, CA, USA)
Optimem	Co. Invitrogen (Carlsbad, CA, USA)
Penicillin/Streptomycin (100x)	Co. Life Technologies (Carlsbad, CA, USA)
Poly-D-Lysine (PDL)	Co. Sigma-Aldrich (St. Louis, MO, USA)
Trypsin/EDTA (0,05 %)	Co. Life Technologies (Carlsbad, CA, USA)
Trypsin	Co. Sigma-Aldrich (St. Louis, MO, USA)

#### 2.1.5.2. Solutions

##### Basic astrocytes medium:

5 ml	Penicillin/Streptomycin (100x)
5 ml	Glucose (45 %)
490 ml	DMEM-F12

Astrocytes proliferation medium:

10 ml	Fetal calf serum
5 ml	Horse serum
2 ml	B27
100 µl	EGF (10 ng/ml)
100 µl	FGF (10 ng/ml)
1 ml	Glutamax
81,8 ml	Basic astrocytes medium

Astrocytes differentiation medium:

2 ml	B27
1 ml	Glutamax
97 ml	Basic astrocytes medium

RIPA buffer with 0,1 % (w/v) SDS:

6,06 g	TRISHCl pH 8,0
17,6 g	Sodium chloride
0,5 g	Deoxycholic acid
0,5 ml	NP-40
50 µg	SDS

add protease/phosphatase inhibitors (see above for whole cell lysis buffer)  
ad 50 ml H<sub>2</sub>O

HEK medium:

2 ml	Fetal calf serum
200 µl	Penicillin/Streptomycin
17,8 ml	DMEM

Solution 1 (HBSS-Glucose):

50 ml	HBSS 10x
9 ml	Glucose (300 mg/ml)
7,5 ml	Hepes 1 M

ad 500 ml H<sub>2</sub>O<sub>dd</sub>

Solution 2 (Sucrose-HBSS):

25 ml HBSS 10x  
 154 g Sucrose  
 ad 500 ml H<sub>2</sub>O<sub>dd</sub>

Solution 3 (BSA-EBSS-Hepes):

20 g BSA  
 10 ml Hepes 1M  
 ad 500 ml EBSS

Neurosphere medium:

47 ml DMEM/F12  
 1 ml B27  
 0,5 ml Penicillin/Streptomycin  
 0,4 ml Hepes 1 M  
 50 µl FGF (20 µg/ml)  
 100 µl EGF (10 µg/ml)

Dissociation medium:

7,0 mg Hyaluronidase  
 13,3 mg Trypsin  
 10 ml Solution 1

**2.1.6. Oligonucleotides**

**2.1.6.1. miRNAs**

The following microRNAs (miRNAs) were obtained from Life Technologies (Carlsbad, CA, USA):

---

Against STAT3:	Sequence (5' → 3') Top Strand	(Position)
----------------	-------------------------------	------------

---

miRNA-STAT3-1	TTTCCATTTCAGATCCTGCATG	(719)
miRNA-STAT3-2	TTTCGTGGTAAACTGGACACC	(1191)
miRNA-STAT3-3	TGCAGAATTTAGCCCATGTGA	(1798)

**Table 1: Designed miRNAs against STAT3**

Shown sequences display only mature miR RNAi sequence of the Top Strand.

Against STAT1:	Sequence (5' → 3') Top Strand	(Position)
miRNA-STAT1-1	TTATATGCCAGTTGCATGCGC	(231)
miRNA-STAT1-2	TTATCCTGGAGATTACGCTTG	(608)
miRNA-STAT1-3	TGACGTTGGAGATCACCCACGA	(1714)
miRNA-STAT1-4	TGATGAAGCCCATAAATGCACC	(2077)

**Table 2: Designed miRNAs against STAT1**

Shown sequences display only mature miR RNAi sequence of the Top Strand.

## 2.1.7. Plasmids

### 2.1.7.1. Established plasmids

Plasmid	Source
pcDNA <sup>TM</sup> 6.2-GW/EmGFP-miR	Co. Life technologies (Carlsbad, CA, USA)
STAT3-C Flag pRc/CMV	Addgene plasmid 8722 (Cambridge, MA, USA)
OE STAT3 (IRAVp968E059D)	Co. Source BioScience (Nottingham, UK)
OE STAT1 (IRAVp968D078D)	Co. Source BioScience (Nottingham, UK)
pDONR <sup>TM</sup> 221	Co. Life Technologies (Carlsbad, CA, USA)
pCAG-IRES-GFP Destination	Our laboratory
pCAG Destination	Our laboratory
pCMV-GFP	Our laboratory
pCAG-Mash1-IRES-DsRed	Our laboratory
pCAG-IRES-DsRed	Our laboratory

**Table 3: Available plasmids**

Displayed are name of plasmid and corresponding source.

**2.1.7.2. Newly designed plasmids**

During the work on this doctoral thesis several new plasmids were designed (pCAG-EmGFP-2miRNA-STAT3, pCAG-EmGFP-2miRNA-STAT1, pCAG-EmGFP-2miRNA-STAT1/3, pCAG-STAT3-IRES-GFP and pCAG-STAT1-IRES-GFP). In order to control our molecular cloning and to show that pCAG-EmGFP-2miRNA-STAT3, pCAG-EmGFP-2miRNA-STAT1 and pCAG-EmGFP-2miRNA-STAT1/3 indeed comprise the respective miRNA sequence we sequenced the appropriate part of them (for sequencing method see section 2.2.5.9.). Sequences of interest are marked in bold (respective miRNA sequence surrounded by an additional linker (TGCTG; before), a subsequent loop sequence (19 nucleotides from miR-155) and nucleotides 1-8 and 11-21 of the sense target sequence).

pCAG-EmGFP-2miRNA-STAT3:

ACCGTCGATCGTTTAAGGGAGGTAGTGAGTCGACCAGTGGATCCTGGAGGCTTGCTGAAGGCTGTA  
**TGCTGTTTCCATT**CAGATCCTGCATGGTTTTGGCCACTGACTGACCATGCAGGCTGAATGGAAACAG  
 GACACAAGGCCTGTTACTAGCACTCACATGGAACAAATGGCCCAGATCCTGGAGGCTTGCTGAAGGC  
 TGTAT**TGCTGTTTCCATT**CAGATCCTGCATGGTTTTGGCCACTGACTGACCATGCAGGCTGAATGGAA  
**ACAGGACACAAGGCCTGTTACTAGCACTCACATGGAACAAATGGCCCAGATCTGGCCGCACTCGAG**  
 ATATCTAGACCCAGCTTCTTGTACAAAGTGGTTGATGGCCGCGTCGACAATCAACCTCTGGATTACA  
 AAATTTGTGAAAGATTGACTGGTATTCTTAACTATGTTGCTCCTTTTACGCTATGTGGATACGCTGCTT  
 TAATGCCTTTGTATCATGCTATTGCTTCCCGTATGGCTTTCATTTTCTCCTCCTTGTATAAATCCTGGTT  
 GCTGTCTCTTTATGAGGAGTTGTGGCCCGTTGTCAGGCAACGTGGCGTGGTGTGCACTGTGTTTGCT  
 GACGCAACCCCCACTGGTTGGGGCATTGCCACCACCTGTCAGCTCCTTCCGGGACTTTCGCTTTCCC  
 CCTCCCTATTGCCACGGCGGAACTCATCGCCGCTGCCTTGGCCGCTGCTGGACAGGGGCTCGGCTG  
 TTGGGCACTGACAATCCGTGGTGTGTCGGGGAAAGCTGACGTCCTTTCATGGCTGCTCGCCTGTG  
 TTGCCACCTGGATTCTGCGCGGGACGTCCTTCTGCTACGTCCTTCCGGCCCTCAATCCAGCGGACCTT  
 CCTTCCCGCGGCCTGCTGCCGGCTCTGCGGCCTTCCGCGTCTTCGCTTCGCCCTCAGACGAGTCG  
 GATCTCCCTTTGGGCCGCTCCCCGCTGGATT



pCAG-EmGFP-2miRNA-STAT1:

ACGTCGATCGTTTAAGGGAGGTAGTGAGTCGACCAGTGGATCCTGGAGGCTTGCTGAAGGCTGTAT  
**GCTGTTATATGCCAGTTGCATGCGCGTTTTGGCCACTGACTGACGCGCATGCCTGGCATATAACAG**  
GACACAAGGCCTGTTACTAGCACTCACATGGAACAAATGGCCCAGATCCTGGAGGCTTGCTGAAGGC  
TGTATGCTGTGACGTTGGAGATCACCACGAGTTTTGGCCACTGACTGACTCGTGGTGCTCCAACGTC  
**ACAGGACACAAGGCCTGTTACTAGCACTCACATGGAACAAATGGCCCAGATCTGGCCGCACTCGAG**  
ATATCTAGACCCAGCTTCTTGTACAAAGTGGTTGATGGCCGCGTCGACAATCAACCTCTGGATTACA  
AAATTTGTGAAAGATTGACTGGTATTCTTAACTATGTTGCTCCTTTTACGCTATGTGGATACGCTGCTT  
TAATGCCTTTGTATCATGCTATTGCTTCCCGTATGGCTTTCATTTTCTCCTCCTTGATAAAATCCTGGTT  
GCTGTCTCTTATGAGGAGTTGTGGCCGTTGTCAGGCAACGTGGCGTGGTGTGCACTGTGTTTGCT  
GACGCAACCCCCACTGGTTGGGGCATTGCCACCACCTGTCAGCTCCTTCCGGGACTTTCGCTTCCC  
CCTCCCTATTGCCACGGCGGAACCTCATCGCCGCTGCCTTGGCCGCTGCTGGACAGGGGCTCGGCTG  
TTGGGCACTGACAATTCCGTGGTGTGTCGGGGAAAGCTGACGTCCTTCCATGGCTGCTCGCCTGTG  
TTGCCACCTGGATTCTGCGCGGGACGTCCTTCTGCTACGTCCTTCCGGCCCTCAATCCAGCGGACCTT  
CCTTCCCGCGGCCTGCTGCCGGCTCTGCGGCCTTCCGCGTCTTCGCCTTCGCCCTCAGACGAGTCG  
G

pCAG-EmGFP-2miRNA-STAT1/3:

CCGTCGATCGTTTAAGGGAGGTAGTGAGTCGACCAGTGGATCCTGGAGGCTTGCTGAAGGCTGTAT  
**GCTGTTTCCATTCAGATCCTGCATGGTTTTGGCCACTGACTGACCATGCAGGCTGAATGGAAACAG**  
GACACAAGGCCTGTTACTAGCACTCACATGGAACAAATGGCCCAGATCCTGGAGGCTTGCTGAAGGC  
TGTATGCTGTTTCCATTCAGATCCTGCATGGTTTTGGCCACTGACTGACCATGCAGGCTGAATGGAA  
**ACAGGACACAAGGCCTGTTACTAGCACTCACATGGAACAAATGGCCCAGATCCTGGAGGCTTGCTGA**  
**AGGCTGTATGCTGTTATATGCCAGTTGCATGCGCGTTTTGGCCACTGACTGACGCGCATGCCTGGCA**  
**TATAACAGGACACAAGGCCTGTTACTAGCACTCACATGGAACAAATGGCCCAGATCCTGGAGGCTTG**  
CTGAAGGCTGTATGCTGTGACGTTGGAGATCACCACGAGTTTTGGCCACTGACTGACTCGTGGTGC  
**TCCAACGTCACAGGACACAAGGCCTGTTACTAGCACTCACATGGAACAAATGGCCCAGATCTGGCCG**  
CACTCGAGATATCTAGACCCAGCTTCTTGTACAAAGTGGTTGATGGCCGCGTCGACAATCAACCTCT  
GGATTACAAAATTTGTGAAAGATTTGACTGGTATTCTTAACTATGTTGCTCCTTTTACGCTATGTGGAT  
ACGCTGCTTTAATGCCTTTGTATCATGCTATTGCTTCCCGTAT

## **2.2. Methods**

### **2.2.1. Animals**

#### **2.2.1.1. Mouse strains**

All animal procedures were carried out in accordance with the policies of the use of Animals and Humans in Neuroscience Research, revised and approved by the Society of Neuroscience and the state of Bavaria under licence number 55.2-1-54-2531-144/07. All efforts were made to minimize animal suffering and to reduce the number of animals used. Most experiments were conducted on C57BL/6J mice, a common inbred strain of laboratory mice, which was used at different ages (adult: of 8-10 weeks of age (20-25 g), postnatal days 1 and 5-7). Additionally the following mouse lines were used for experiments:

- APP/PS1: this line carries the Swedish double mutation KM670/671NL of the amyloid precursor protein (APP) as well as the mutation L166P of presenilin 1 (PS1), both controlled by the neuronal promoter Thy1.
- CK/p25: this line overexpresses an inducible form (TetOFF) of the p25-GFP fusion protein under the control of the neuronal promoter CAMKII (CK).

Both strains were used and analyzed in collaboration with Dr. Gwendolyn Behrendt.

#### **2.2.1.2. Doxycyclin administration**

Ck/p25 mice received Doxycyclin drinking water prenatally via the mother and until six weeks of age. As Doxycycline is light sensitive it was applied in bottles impervious for light and was exchanged every second day. Mice were kept for another five weeks to allow p25 overexpression.

### **2.2.1.3. Anesthesia**

In order to anesthetize mice prior to perfusion we used anesthesia solution. 5  $\mu$ l per 1 g body weight were injected intraperitoneally via insulin needle. Animal reflexes (e.g. eye blink reflex and the reflex after pinching the hindpaw) were checked until they disappeared. In case of sustained appearance additional anesthesia of 20  $\mu$ l was given.

### **2.2.1.4. Surgical stab wound of adult animals**

After anesthesia mice were placed in a stereotactic mouse adaptor in a flat skull position. To get access to the brain the skin above the skull was cut with a razor blade and trepanated with a hand drill between bregma and lambda. Subsequently, a stab wound was made by a sharp and thin scalpel (Ophthalmic Corneal V-lance knife) in the right cerebral sensorimotor cortex at the following coordinates: anteroposterior (AP) = from -1,6 to -2,4, mediolateral (ML) = -1,5, dorsoventral (DV) = -0,5 mm with Bregma as reference. Touching of the white matter was avoided. To lower infection rate and inflammation the bone was replaced and the skin incision was sutured with vicryl filament. Consecutively, mice were housed in individual Plexiglas cages with food and water *ad libitum* and kept in a 12 h light-dark cycle (room temperature = 22  $\pm$  1°C).

### **2.2.1.5. Experimental focal cerebral ischemia of adult animals**

These experiments were performed in the lab of Prof. Martin Dichgans at the Institute of Stroke and Dementia research (ISD) with the help of Rebekka Fischer, Christof Haffner, Jan Burk and Veronika Lellek.

Adult C57BL/6J mice underwent occlusion of the medial cerebral artery (MCA) as described previously (Vosko et al., 2006). Briefly, mice were anesthetized with isoflurane inhalation (initiation by 5 % isoflurane (< 1 min) and maintenance by 2 % isoflurane in a mixture of 70 %/30 % of N<sub>2</sub>O/O<sub>2</sub>). Body temperature was maintained between 37 °C and 38 °C with a DC temperature regulation system (FHA, Bowdoin, USA). After anesthesia a fiberoptic probe (Perimed, Järfäla, SE) was placed over the MCA territory (+ 2 mm posterior and + 6 mm lateral to bregma). The regional cerebral blood flow (rCBF) was recorded in all animals by laser

Doppler flowmetry (Perimed, Järfäla, SE). Focal cerebral ischemia was induced by occlusion of the MCA using an intraluminal filament technique. After ventral midline neck incision, the left common and external carotid arteries were ligated. The internal carotid artery (ICA) was temporarily clipped with a microvascular clip (Aesculap, D). A silicon-coated 8-0 nylon monofilament (Ethicon, Johnson & Johnson, Norderstedt, D) was gently advanced into the ICA until resistance was felt. Successful occlusion of the MCA reduced the rCBF baseline by > 70%. After induction of ischemia, laser Doppler probes were removed and the mice were returned to their cages and allowed to wake up. During the 1 to 2 hours of ischemia cages were placed in an incubator (Babytherm 4200, Drägerwerk AG Lübeck, Germany) to keep the body temperature stable. After one to two hours animals were again anesthetized and the filament was removed. Animals were kept for three to four days. Between the different animal subsets that underwent either one or two hours of ischemia and were kept for three or four days I did not recognize significant difference and therefore pulled them together for analysis.

Animal care and all experimental procedures were performed in strict accordance to the German and National Institutes of Health animal legislation guidelines and were approved by the local animal care and use committees.

### **2.2.2. Western blot**

#### **2.2.2.1. Tissue collection and lysis**

Dissection of brain tissue was conducted in HBSS medium. After careful removal of the meninges the brain was cut coronally in 3-4 slices. Hind- and forebrain were discarded. By putting the slices in a plane view in the dish we were able to dissect the grey matter without any contact to the white matter. Tissue pieces from both hemispheres (ipsi- and contralateral to the lesion) were then collected in defined 1,5 ml eppendorf tubes and immediately frozen in liquid nitrogen followed by storage at -80 °C.

For whole cell lysis cortical tissue pieces were defrosted to 4 °C and 200 µl of whole cell lysis buffer was added. After transfer to a dounce tissue grinder the tight pestle was repeatedly moved up and down (10-15 times) to homogenize the tissue. After repeated sonication with a sonotrode (10 s, 20 s, 20 s) at 10 % intensity the samples were left on ice for 15 minutes to

be subsequently centrifuged on 14000 g for 15 minutes at 4 °C. The supernatant was collected and kept at -80 °C until further processing.

For subcellular fractionation a protocol by Na et al. (Na et al., 2007) was adopted. Therefore tissue pieces were also defrosted to 4 °C and 200 µl of LSB was added. After transfer to a dounce tissue grinder and douncing for 20 times 1 % of NP-40 was added. After keeping the samples for 15 minutes on ice they were again dounced for 20 times. After another 15 minutes on ice they were centrifuged for 3500 RPM for 5 minutes at 4 °C. From the resulting suspension the upper 150 µl were taken as preliminary cytosolic fraction, the next 40 µl were discarded and the pellet was treated as preliminary nuclear fraction. The final cytosolic fraction evolved from the supernatant of the preliminary cytosolic fraction after centrifuging it at 14000 RPM for 1 hour at 4 °C (separation of membrane pellet and cytosolic fraction) and was kept at -80 °C until further processing. The preliminary nuclear fraction was processed the following: adding 200 µl LSB, resuspension, centrifuging at 3500 RPM for 5 minutes at 4 °C, discarding the upper 180 µl, adding 200 µl to the pellet, resuspension, centrifuging at 3500 RPM for 5 minutes at 4 °C and discarding as much as possible without touching the pellet. 50 µl of HSB and 1 % NP-40 were added to the pellet, resuspended and kept on ice for 45 minutes. After another centrifugation step of 14000 RPM at 4 °C for 5 minutes the supernatant of the resulting solution built up the final nuclear fraction which was kept at -80 °C until further processing.

#### **2.2.2.2. Protein quantification and sample preparation**

Protein quantification was conducted with the BCA (bicinchoninic acid) assay. Shortly, this biochemical method displays a colorimetric assay measuring the protein concentration via absorption (wavelength 562 nm) of bicinchoninic acid chelating with a  $\text{Cu}^+$  ion which evolved by reduction of  $\text{Cu}^{2+}$  by peptide bonds under alkaline conditions (also called Biuret reaction). Therefore the color range from green to purple correlates with the quantity of peptide bonds.

According to the manufacturer's protocol reagents B and A from the BC assay kit were mixed 1:50 and 5 µl lysate was added to 1 ml reagent mix. After incubation at 37 °C for 30 minutes samples were analyzed using a spectrophotometer. Different BSA concentrations were used as protein standard. According to the measured protein concentrations probes were adjusted

to 10 µg. Thereby we ensured the loading of equal amounts of protein. After adding 4x loading dye, probes were heated at 95 °C for 5 minutes and subsequently cooled on ice for another five minutes.

#### **2.2.2.3. Gel preparation**

Running and stacking gel solutions were mixed using the above described protocol and chemicals. First, glass plates were filled with the running gel solution at a level of 75 %. Water diluted isopropanol was used to remove bubbles and was washed away again after polymerization of the running gel solution (approx. 30 minutes). Stacking gel solution and a ridge were added on top and left for another 30 minutes for polymerization. Finally glass plates containing the SDS-polyacrylamide gel were transferred to the electrophoresis chamber.

#### **2.2.2.4. Protein electrophoresis**

Protein samples were loaded in the SDS-polyacrylamide gel and run with SDS-PAGE running buffer (electrophoresis buffer 1x) at a voltage of 80 – 120 V. Under these conditions sampled proteins get surrounded by negatively charged SDS according to their size. Smaller proteins migrate faster than larger proteins to the positively charged electrode, which allows separation of proteins by molecular weight.

#### **2.2.2.5. Transfer**

To make proteins accessible to antibodies they have to be transferred from the gel to a PVDF-membrane. For preparation, the membrane needs to be incubated in methanol followed by incubation in transfer buffer. Also filter papers were shortly incubated in transfer buffer. Eventually, the Trans-Blot SD Semi-Dry Transfer Cell system was used to transfer proteins at a voltage of 15 V for 42 minutes. From anode to cathode a defined order was applied (anode -> filter paper -> membrane -> gel -> filter paper -> cathode).

### 2.2.2.6. Signal detection

Chemiluminescent detection was used to analyze proteins of interest. Therefore, membranes were first blocked with 5 % (w/v) milk powder and afterwards incubated with the specific primary antibody (in 5 % (w/v) BSA) at 4 °C overnight. Used antibodies include:

- Anti-STAT3 (rabbit, 1:1000, Cell Signaling, Beverly, MA, USA)
- Anti-pSTAT3 (rabbit, 1:1000, Cell Signaling, Beverly, MA, USA)
- Anti-STAT5 (rabbit, 1:500, Santa Cruz Biotechnology, CA, USA)
- Anti-pSTAT5 (rabbit, 1:500, Cell Signaling, Beverly, MA, USA)
- Anti-STAT5a (rabbit, 1:500, Santa Cruz Biotechnology, CA, USA)
- Anti-pSTAT1 (rabbit, 1:1000, Cell Signaling, Beverly, MA, USA)
- Anti-GFAP (rabbit, 1:2000, Sigma-Aldrich, St. Louis, MO, USA)
- Anti-Nucleoporin (mouse, 1:1000, BD, Franklin Lakes, NJ, USA)
- Anti-Enolase (goat, 1:200, Santa Cruz Biotechnology, CA, USA)
- Anti-GAPDH (mouse, 1:7500, Abcam, Cambridge, UK)

Anti-Glyceraldehyd 3-phosphate dehydrogenase (GAPDH) was used as loading control for whole cell lysates. Anti-Enolase and anti-Nucleoporin were used as cytosolic and nuclear loading control, respectively, in subcellular fractionated samples. After washing steps with TBS-T, horseradish peroxidase labeled secondary antibodies (1:10000, GE Healthcare, Wixom, WI, USA; in 5 % (w/v) milk powder) were applied. These were detected by ECL Western Blotting Detection (Merck Millipore, Billerica, MA, USA). The abundance of the band was quantified using Image J 1.42q (National Institute of Health, USA) software after background correction. Protein amounts were normalized to loading controls.

### 2.2.2.7. Membrane stripping

For reprobing membranes, primary and secondary antibodies were removed. Therefore, membranes were kept in stripping buffer for 30 minutes at approx. 60 °C in a water bath. Extensive washing with TBS-T was followed by control signal detection.

### **2.2.2.8. Quantitative analysis of immunoblotting**

First, western blot membranes were scanned. Then by using Image J 1.42q the grey pixel value of the respective band was quantified (by rectangular selections) and expressed as an arbitrary unit. The ipsilateral fraction was calculated in relation to the contralateral fraction, which was set as 100 %. Consequently, the results are displayed as “relative densities”. For each quantification, values are given as mean  $\pm$  SEM. For detection of statistical significance, data were subjected to a 2-tailed t-test for independent samples with assumed same variances using SPSS 21 (IBM Corp., Armonk, NY, USA). Differences were considered statistically significant when the probability value was  $< 0.05$ .

### **2.2.3. Histological procedures**

#### **2.2.3.1. Perfusion, brain sectioning, storage of sections**

Adult animals were deeply anesthetized according to our anesthesia protocol (see 2.2.1.5.). Subsequently, they were transcardially perfused with PBS 1x followed by 4 % PFA (100 ml/animal). Brains were postfixed in the same fixative for at least 2 h to maximal overnight at 4 °C. Brains were cryoprotected by saturation in 30 % sucrose followed by washing in PBS and cut at a Cryostat (Kryostat CM 3050S) with a thickness of 30  $\mu$ m. Sections were stored at -20 °C in storing solution until further processing.

#### **2.2.3.2. Immunohistochemistry**

Sections were first pretreated in 0,25 % Triton X-100 in PBS for 30 min, followed by incubation in blocking solution (2 % (w/v) BSA in PBS) for 60 min. Primary antibodies were incubated on specimen overnight at 4 °C in 2 % BSA, 0,1 % Triton X-100 in PBS. The following primary antibodies were used:

- Anti-pSTAT3 (rabbit, 1:333, Cell Signaling, Beverly, MA, USA)
- Anti-STAT3 (rabbit, 1:200, Cell Signaling, Beverly, MA, USA)
- Anti-GFAP (mouse IgG1, 1:500, Sigma-Aldrich, St. Louis, MO, USA)
- Anti-NeuN (mouse IgG1, 1:100, Merck Millipore, Billerica, MA, USA)



- Anti-pSTAT1 (rabbit, 1:333, Cell Signaling, Beverly, MA, USA)
- Anti-STAT5 (rabbit, 1:100, Santa Cruz Biotechnology, CA, USA)
- Anti-pSTAT5 (rabbit, 1:100, Cell Signaling, Beverly, MA, USA)
- Anti-STAT5a (rabbit, 1:100, Santa Cruz Biotechnology, CA, USA).

After extensive washing in PBS, sections were incubated with appropriate species- or subclass-specific secondary antibodies conjugated to:

- Cy<sup>TM</sup>3 (1:500, Dianova, Hamburg, D)
- Cy<sup>TM</sup>5 (1:500, Dianova, Hamburg, D)
- Alexa Fluor 488 (1:500, Life technologies, Carlsbad, CA, USA)
- FITC (fluorescein isothiocyanate, 1:500, Dianova, Hamburg, D)
- TRITC (tetramethyl rhodamine isothiocyanate, 1:500, Dianova, Hamburg, D)
- DyLight 649 (1:500, Dianova, Hamburg, D)

for 2 h in the dark at room temperature. After extensive washing in PBS and incubation with DAPI (1:1000, 5 minutes) sections were mounted on glass slides and embedded in Aqua-Polymount and covered by a glass coverslip. Specific labeling was checked by omitting the primary antibody.

For pSTAT3, STAT3, STAT5, STAT5a, pSTAT5 and pSTAT1 staining, pretreatment was needed to better access nuclear proteins. Therefore, sections were incubated in sodium citrate buffer at 95 °C in a water bath for 20 minutes. Afterwards, specimens were carefully rinsed before incubation with the primary antibody. Rinsing in TBS instead of PBS as diluent was used for pSTAT3, pSTAT1 and pSTAT5 to avoid staining interactions with phosphate molecules from PBS. Double-labelling was conducted by first, staining of no-treatment-necessary antibodies followed by 7 minutes of post-fixation with 4 % PFA followed by pretreatment for the second primary antibody.

### **2.2.3.3. Microscopic analysis**

Stainings were first evaluated with an epifluorescence microscope (BX61, Olympus) equipped with the appropriate filter sets and then analysed in detail with a laser-scanning confocal microscope (LSM710, Carl Zeiss) using the same settings for equivalent stainings. Z-stacks of digital images were taken using the ZEN software (Carl Zeiss). Subsequently, single confocal

images were selected from the Z-stacks. Alternatively, the Z-stacks were merged in one picture using the maximum intensity projection function provided by the above mentioned software.

#### **2.2.3.4. Cell counts and statistical analysis**

Cell counts and representative pictures for figures were performed by taking pictures of several randomly selected views per cover slip analyzed by means of a Zeiss LSM 710 confocal microscope using a 10X, 25X or 40X objective. Subsequently, cells were quantified using Image J 1.42q (National Institute of Health, USA) software. For each quantification, values are given as mean  $\pm$  SEM. Cell counting data were subjected to a 2-tailed t-test for independent samples with assumed same variances for statistical significance using SPSS 21 (IBM Corp., Armonk, NY, USA). Differences were considered statistically significant when the probability value was  $< 0.05$ . In diagrams, significance is displayed by a star.

#### **2.2.4. Cell culture**

##### **2.2.4.1. Cell strains and primary cultures**

For culturing postnatal astroglia we followed the procedure described previously by Heins et al. (Heins et al., 2002). After removal of the meninges, grey matter tissue from P1 and P5-P7 cerebral cortex of C57BL/6J mice was dissected and dissociated mechanically. Subsequently, cells were centrifuged for 5 min at 1000 RPM, re-suspended, and plated in astrocytes proliferation medium. Contaminating oligodendrocyte precursor cells were removed by brusquely shaking the culture flasks several times. Cells were passaged after one week using trypsin/EDTA and plated on poly-D-lysine glass coated coverslips at a density of 60.000 cells per coverslip in the same medium. The vast majority of the cells ( $> 90\%$ ) in these cultures were positive for GFAP as previously described (Berninger et al., 2007).

HEK293T cells display a widely used laboratory cell strain. They were cultured in HEK medium and splitted using trypsin to 750.000 cells per well (6-well-plate) or 50.000 cells per well (24-well- plate), respectively.

Astrocyte-enriched culture of lesioned mouse cortices was generated by basically applying the protocol used for postnatal astroglia. Another centrifugation mode was used (1400 RPM, 5 minutes) and in addition to mechanical dissection, hyaluronidase and trypsin were used for dissociation.

#### **2.2.4.2. Transfection**

Transfection via DNA-liposome complexes was performed in cortical astroglia and HEK293T cells.

Passaged cortical astroglia were plated on poly-D-lysine coated 24 well tissue plates. DNA-liposome complexes were prepared in Optimem medium using the plasmids pCAG-Mash1-IRES-DsRed, pCMV-STAT3C, pCAG-EmGFP-2miRNA-STAT3, pCAG-EmGFP-2miRNA-STAT1, pCAG-EmGFP-2miRNA-STAT1/3, pCAG-STAT3-IRES-GFP and pCAG-STAT1-IRES-GFP or the control plasmids pCAG-IRES-DsRed, pCMV-GFP and Lipofectamine 2000 as cationic liposome formulation. Two hours after plating, astrocyte cultures were exposed to DNA-liposome complexes at a concentration of 0.5 µg DNA per 400 µL of Optimem medium for 4 hours. Subsequently, the medium was replaced by astrocyte differentiation medium and the 24 well tissue plates were kept in an incubating chamber for either 2 or 9 days.

For HEK293T cells nearly the same method was applied. Here, we used 6 well tissue plates and 4 µg DNA per 1200 µL of Optimem medium. Cells were kept for two days before they were collected for western blot (see 2.2.4.4.).

#### **2.2.4.3. Immunocytochemistry**

For immunocytochemistry, cultures were fixed in 4 % paraformaldehyde (PFA) in phosphate buffered saline (PBS) for 15 min at room temperature. For pSTAT3 staining we applied methanol pretreatment (10 minutes at -20 °C). Cells were then incubated in blocking solution for 60 minutes. As already described for immunohistochemistry, staining procedures for phosphorylated proteins were conducted with TBS instead of PBS. Primary antibodies were incubated on specimen overnight at 4°C in 2 % BSA, 0,5 % Triton X-100 in PBS (TBS). The following primary antibodies were used:

- Anti-GFP (green fluorescent protein, chicken, 1:2000, Aves Labs, Tigard, OR, USA)
- Anti-GFAP (rabbit, 1:4000, DakoCytomation, Hamburg, D)
- Anti-RFP (red fluorescent protein, rabbit, 1:500, Merck Millipore, Billerica, MA, USA)
- Anti-RFP (rabbit, 1:2000, Rockland, Gilbertsville, PA, USA)
- Anti- $\beta$ III-tubulin (mouse IgG2b, 1:500, Sigma-Aldrich, St. Louis, MO, USA)
- Anti-pSTAT3 (rabbit, 1:250, Cell Signaling, Beverly, MA, USA)
- Anti-STAT3 (mouse, 1:1000, Cell Signaling, Beverly, MA, USA)
- Anti-O4 (mouse IgM, 1:200, Sigma-Aldrich, St. Louis, MO, USA).

After extensive washing in PBS, cells were incubated with appropriate species- or subclass-specific secondary antibodies conjugated to:

- Cy<sup>TM</sup>3 (1:500, Dianova, Hamburg, D)
- Cy<sup>TM</sup>5 (1:500, Dianova, Hamburg, D)
- DyLight 649 (1:500, Dianova, Hamburg, D)
- Alexa Fluor 488 (1:500, Life Technologies, Carlsbad, CA, USA)
- FITC (fluorescein isothiocyanate, 1:500, Dianova, Hamburg, D)
- TRITC (tetramethyl rhodamine isothiocyanate, 1:500, Dianova, Hamburg, D)

for 2h in the dark at room temperature, followed by extensive washing in PBS and incubation with DAPI (5 minutes, 1:1000). Coverslips were finally mounted onto a glass slide with an anti-fading mounting medium.

#### **2.2.4.4. Western blot**

To collect cells for western blot experiments, cells were rinsed with PBS and incubated with RIPA buffer for 2 minutes. Subsequently, cells were scratched intensively, transferred to an Eppendorf and centrifuged at 14000 RPM at 4 °C for 30 minutes. Eventually, the pellet was discarded and the sample kept until further processing at -80 °C. Protein concentration was measured according to the aforementioned protocol (2.2.2.2.) and western blot technique conducted (2.2.2.).

#### 2.2.4.5. Neurosphere assay

For evaluation of the stem cell capacity *in vitro* a neurosphere assay of reactive tissue after cortical injury was applied (for scientific explanation see subchapter 1.4.2.1.). Therefore, after removal of meninges, cerebral cortices of MCAo mice were dissected in HBSS containing 10 mM Hepes. Forceps were used to cut off the white matter. Tissue of interest was collected in Solution 1, mechanically triturated and subsequently incubated for 30 minutes at 37 °C in a mix with dissociation medium. After stopping the enzyme reaction with Solution 3, cells were passed through a 70 µm-strainer. The resulting mix was centrifuged at 1500 RPM for 5 minutes. Afterwards, the pellet was resuspended in solution 2 and again centrifuged at 2000 RPM for 10 minutes. The suspension of the pellet in Solution 3 was gently applied on top of Solution 3 and afterwards centrifuged at 1500 RPM for 7 minutes. The pellet was resuspended in Neurosphere medium and kept in a flask. First, small neurospheres were picked and transferred to PDL-coated coverslips in a 24-well-plate in differentiation medium. After approx. 8 days, neurospheres were fixed with 4 % PFA for 15 minutes. Immunostaining was conducted as described above (2.2.4.3.).

#### 2.2.5. Molecular cloning

##### 2.2.5.1. Restriction digestion of DNA

According to the manufacturer's protocol (Life Technologies, Carlsbad, CA, USA) a typical reaction was conducted as follows:

1 µg or 6 µg	DNA of MaxiPrep or MiniPrep
1,5 µl	10x reaction buffer
0,15 µl	100x BSA
1 µl	Restriction enzyme mix
Ad 15 µl	H <sub>2</sub> O

The resulting mix was incubated at 37 °C for 1 hour. Analysis of DNA fragments was performed using agarose gels (see 2.2.5.4.).

### 2.2.5.2. Analysis of DNA fragments

Analysis of DNA fragments was performed according to (Meyers et al., 1976). An agarose gel was prepared by solubilizing agarose in 1x TAE at a percentage of 1-2 %, depending on DNA size. Dissolving was performed by boiling in a microwave. After administration of ethidium bromide (final concentration approx. 1 µg/ml), the solution was poured into a gel chamber and cooled down with a ridge. Samples were supplemented with DNA sample buffer and together with 1 kb DNA ladder loaded. An approximate voltage of 80-90 V was applied. When separated, the samples were photographed with the Gel imaging system GelDoc™ XR.

When separation was performed for further ligation of fragments, fragments were cut out using a fluorescent table (UV light at 254 nm) and purified with the NucleoSpin Extract II kit. According to the manufacturer's protocol, weight-adapted NT buffer was added, the sample heated to 50 °C for approx. 5 minutes and centrifuged. After a washing step the DNA was diluted in 30 µl H<sub>2</sub>Odd.

### 2.2.5.3. Ligation

According to the manufacturer's protocol (Life Technologies, Carlsbad, CA, USA) a typical ligation reaction was prepared as follows:

7 µl	Insert DNA
2 µl	Vector DNA
1 µl	T4 DNA Ligase (1 U/µl)
1,5 µl	10x T4 DNA Ligation Buffer
ad 15 µl	H <sub>2</sub> Odd

Generally, insert DNA amount exceeded vector DNA by 3-10 fold. The mix incubated at room temperature for 1 hour.

#### **2.2.5.4. Preparation of bacterial agar plates**

For agar plates, 7,5 g of Bacto-Agar were mixed in 500 ml LB. After autoclaving and a cooling step, the appropriate antibiotic was added in a prudential concentration. The resulting mix was poured in 10 cm culture dishes, cooled down to room temperature and stored at 4 °C.

#### **2.2.5.5. Transformation of chemo-competent E.coli**

Transformation of chemo-competent TOP10 E.coli was performed according to (Hanahan, 1983). Shortly, 100 ng of DNA were added to 50 µl of bacteria and left for 30 minutes on ice. Consecutively, bacteria were heated to 42 °C for 40 seconds and afterwards again kept on ice for another 2 minutes. 250 µl of SOC-medium (including 100 µl 1 M Glucose, 125 µl 1 M MgSO<sub>4</sub> and 125 µl 1 M MgCl<sub>2</sub>) were added and the sample incubated at 37 °C for 1 hour in a shaker. Finally, different amounts (50 µl or 250 µl) were plated on bacterial agar plates and incubated overnight at 37 °C.

#### **2.2.5.6. Bacterial liquid cultures**

A single colony was inoculated in 2-3 ml LB medium or 200 ml LB medium (including the appropriate antibiotic) for small scale DNA preparation (MiniPrep) or large scale DNA preparation (MaxiPrep), respectively and incubated overnight at 37 °C under vigorous shaking.

#### **2.2.5.7. Small scale DNA preparation (MiniPrep)**

Small scale DNA preparation (1-5 µg DNA) was conducted using the Nucleospin Plasmid, Plasmid DNA purification kit. 2 ml of small scale bacterial liquid cultures were centrifuged at 6000 RPM for 10 minutes. According to the manufacturer's protocol, the pellet was resuspended in 250 µl of Buffer A1. After lysis of bacteria, DNA was separated by centrifugation and washed repeatedly until resuspension in 30 µl of H<sub>2</sub>Odd. Correctness of the plasmid was examined with restriction digestion and subsequent analysis on agarose gels.

#### **2.2.5.8. Large scale DNA preparation (MaxiPrep)**

Large scale DNA preparation (200-500 µg DNA) was conducted using the PureLink HiPure Plasmid MaxiPrep kit (Life technologies, Carlsbad, CA, USA). Accordingly, the large scale bacterial liquid culture was centrifuged at 6000 g for 10 minutes. Then, cells and DNA were further processed according to the manufacturer's protocol.

#### **2.2.5.9. Sequencing of DNA**

DNA of interest was sequenced by Eurofins MWG Operon, Ebersberg, D.

#### **2.2.5.10. Design of miRNAs against STAT3 and STAT1**

As used before in our laboratory and proved to be efficient, we designed miRNAs against STAT3 and STAT1 using the Invitrogen BLOCK-iT™ RNAi Designer (<http://rnaidesigner.invitrogen.com/rnaiexpress/>). The manufacturer guaranteed that of two ordered oligonucleotides at least one will give greater than 70 % knockdown of the target RNA given a transfection rate of at least 80 % (<http://rnaidesigner.invitrogen.com/rnaiexpress/setOption.do?designOption=mirna&pid=-8000760282235669486>). The strategy for the selection of the appropriate miRNAs is presented in subchapter 3.3.1.1.

#### **2.2.5.11. Virus production**

As described in subchapter 3.3.1.3., we first produced a plasmid containing the retroviral backbone using the Gateway Technology (Life Technologies, Carlsbad, CA, USA). For all steps we followed exclusively the protocol described by the company. Subsequently, we performed the viral production by first preparing the DNA using the Caesium chloride gradient method, then transfecting HEK293T cells with the designated viral packaging vector and expression plasmid and finally using ultracentrifugation in order to separate cells and viral particles and to remove debris and aggregates.



### 3. Results

The results obtained during this medical thesis work have been published or are under way to be submitted. The following paragraphs shortly indicate my contributions to these different studies.

First, the results addressing the overall goal of this dissertation (see subchapter 1.7.) will be submitted for publication in the foreseeable future with the title “Role of STAT3 signaling in the inhibition of neuronal reprogramming of reactive astrocytes” by Tiedt S, Gascón S, Haffner C, Dichgans M, Götz M\* and Heinrich C\* (\* These authors contributed equally to this work.).

Parts of this thesis work have already been published. Recently, our laboratory was able to show that invasive brain injuries elicit a higher stem cell response of reactive astrocytes, triggered by elevated levels of Shh, compared to non-invasive injuries (Sirko et al., 2013). I was involved in the experiments of neurosphere generation after MCAo (see Sirko et al., 2013, Fig. 3b) and determination of the activation of STAT3 signaling after different injury conditions (see Sirko et al., 2013, Suppl. Fig. 4a and b; or this thesis Fig. 33).

Next, I contributed to a study of our laboratory showing that cortical astroglia are able to undergo conversion into synapse-forming functional neurons induced by forced expression of neurogenic fate determinants (Heinrich et al., 2010). In particular, I was involved in showing that fate-mapped astroglia from the postnatal cortex transduced with control retrovirus exhibit glial morphology (see Heinrich et al., 2010 Fig. 3b). Due to stringency reasons, this work has not been included in this thesis.

#### 3.1. Expression of STAT3 and activation of STAT3 signaling in the injured cerebral cortex

The main aim of this work was to investigate whether STAT signaling influences reprogramming of reactive astrocytes into neurons. Therefore, as a first step, we examined whether STAT signaling, in particular STAT3 signaling, is activated over time in reactive astrocytes in different injury models, such as MCAo and stab wound.

### 3.1.1. Expression analysis of GFAP and STAT3 over a time course of seven days after stab wound injury

As reviewed in subchapter 1.6.3.2. the characteristics of STAT3 expression remain controversial after experimental stroke conditions and have not been described yet in the stab wound model. Therefore, we first aimed at studying the pattern of STAT3 and GFAP expression, the latter being an indicator of reactive astrogliosis, over a time course of seven days following a stab wound injury. In this initial set of experiments we performed a western blot analysis at one, three, five and seven days post stab wound (dpSW) ( $n = 1$  mouse for each time point, Fig. 16). We compared the cortical hemisphere where the stab wound was inflicted (ipsilateral site) with the contralateral, non-injured cortical hemisphere. As no overt differences could be observed between the contralateral hemispheres, they were pooled for this analysis and loaded in one lane (lane: contra).

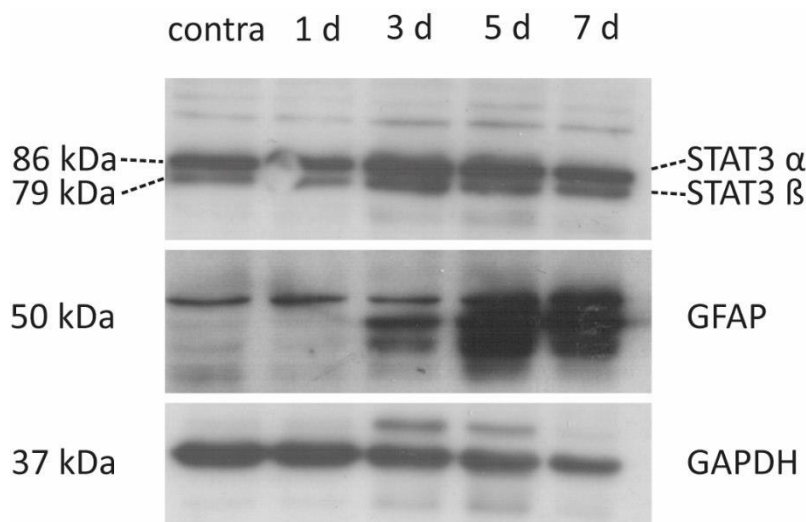


**Fig. 16: Expression pattern of STAT3 and GFAP over seven days after stab wound**

Representative western blot is shown. Independent tissues of the ipsilateral cortices of stab wounded mice at 1, 3, 5 and 7 dpSW were loaded ( $n = 1$  for each time point). Contralateral cortices were mixed and loaded in one lane. Expression levels of STAT3 and GFAP were determined. GAPDH signals were used as loading controls.

The expression levels of both isoforms,  $\alpha$  and  $\beta$ , of STAT3 showed an increase at 3 and 5 dpSW compared to contralateral levels while no difference was observed at 1 dpSW. This was accompanied by an increase in expression of different GFAP isoforms already detectable at 3 dpSW and massive at 5 dpSW, in agreement with previous observations (Robel et al., 2011,

Hozumi et al., 1990). While STAT3 decreased thereafter and returned to control expression levels by 7 dpSW, GFAP expression remained very high at 7 dpSW.

Taken together, although using one mouse per time point, these data suggested that the protein levels of both STAT3 and GFAP increased concomitantly in the injured cortex at 3 and 5 days following a stab wound lesion. Based on these data we mainly focused on the 3 and 5 dpSW time points for further analysis.

### **3.1.2. Analysis of STAT3 expression and activation after stab wound using subcellular fractionated cortical extracts**

As reviewed in subchapter 1.6.2. the JAK/STAT signaling is mediated by the translocation of phosphorylated STAT dimers into the nucleus to exert their function as transcriptional activators. Whole cell extracts, which were used so far, would not be sufficient to follow this process as nuclear and cytoplasmic fractions cannot be separated. In order to demonstrate changes in protein levels between nuclear and cytoplasmic fractions, subcellular fractionation had to be applied to separate the nuclei and the cytoplasms.

#### **3.1.2.1. Protocol for subcellular fractionation**

Here we adjusted a protocol that was previously described by Na et al. (Na et al., 2007). In brief we changed the buffers that were used and adopted centrifugation steps to our needs. Furthermore, we added another cleaning step in order to get correctly separated fractions (see subchapter 2.2.2.1.). We used Enolase, a phosphopyruvate hydratase involved in glycolysis, and Nucleoporin p62, a nuclear pore complex protein, as loading controls for the cytoplasmic and nuclear fraction, respectively, as previously described (Na et al., 2007).

#### **3.1.2.2. Expression pattern of STAT3 after stab wound**

Applying subcellular fractionation would now make it feasible for us to demonstrate not only possible changes of STAT3 protein levels in the cytoplasmic and nuclear fractions, but also allow us to following the process of nuclear translocation of STAT3. Therefore, a western blot analysis of subcellular fractionated brain extracts collected at 3, 5 and 7 dpSW was conducted

(n = 3 mice for each time point, Table 4, Fig. 17). First, immunoblotting for enolase revealed the presence of this protein only in the cytoplasmic fraction of the brain extracts and its virtual absence in the nuclear fraction. Nucleoporin opposed this pattern by being only present in the nuclear fraction. This shows that these two fractions were properly separated by our subcellular fractionation technique.

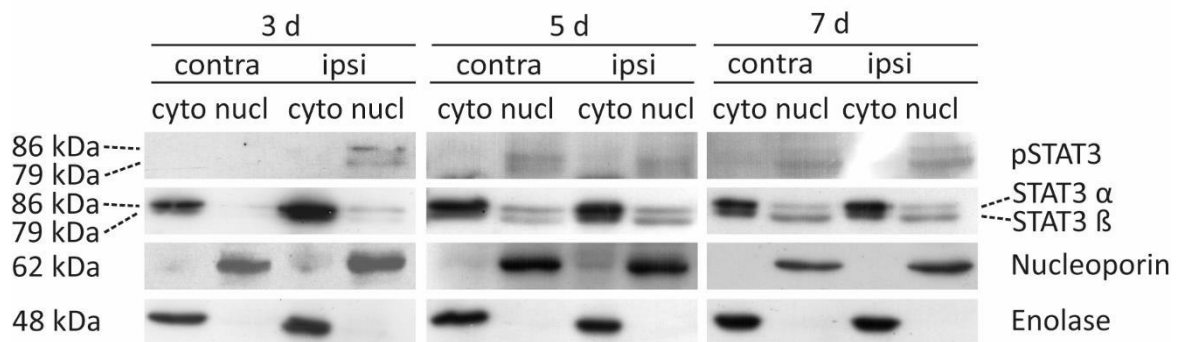


**Fig. 17: Expression of STAT3 and pSTAT3 in cytoplasmic and nuclear fractions at 3, 5 and 7 dpSW**

For each time point a representative western blot from one mouse is shown. Tissues of the contra- and ipsilateral cortices of stab wounded mice at three, five or seven days were loaded. Expression levels of STAT3 and pSTAT3 were determined. Enolase and nucleoporin signals were used as cytoplasmic and nuclear loading controls, respectively.

Second, we found that at all time points investigated and independent of the hemisphere, the expression levels of STAT3 were significantly higher in the cytoplasmic fractions compared to the corresponding nuclear fractions (Fig. 17).

Next, we compared the side ipsilateral to the lesion with the contralateral side and analyzed cytoplasmic and nuclear fractions as well as the total samples (cytoplasmic plus nuclear fractions) (Table 4). For each analysis we first normalized contra- and ipsilateral STAT3 signals to nucleoporin and/or enolase signals, then set the STAT3 expression level in the contralateral fraction as 100 % and calculated the expression level in the ipsilateral fraction in relation to the contralateral fraction (see legend of Table 4 and subchapter 2.2.2.8. for more detailed description of western blot quantification).

Fractions:		Contralateral	Ipsilateral	P-value	Significance
3 dpSW	Cytoplasmic:	100,0 ± 0,0 %	174,2 ± 15,7 %	0,009	**
	Nuclear:	100,0 ± 0,0 %	178,9 ± 22,2 %	0,023	*
	Total:	100,0 ± 0,0 %	170,3 ± 15,9 %	0,011	*

5 dpSW	Cytoplasmic:	100,0 ± 0,0 %	163,7 ± 31,3 %	0,111	-
	Nuclear:	100,0 ± 0,0 %	131,8 ± 8,9 %	0,023	*
	Total:	100,0 ± 0,0 %	151,7 ± 20,2 %	0,063	-
7 dpSW	Cytoplasmic:	100,0 ± 0,0 %	105,0 ± 7,6 %	0,546	-
	Nuclear:	100,0 ± 0,0 %	54,8 ± 17,1 %	0,057	-
	Total:	100,0 ± 0,0 %	94,2 ± 9,0 %	0,554	-

**Table 4: Expression of STAT3 at 3, 5 and 7 dpSW in contralateral versus ipsilateral cortical hemispheres**

Relative densities of western blot bands (antibody against STAT3) of cytoplasmic and nuclear fractions are shown as mean ± SEM for the contra- and ipsilateral hemispheres at 3, 5 and 7 dpSW (n = 3 for each time point) after quantification with Image J 1.42q by using densitometric analysis (see subchapter 2.2.2.8. for more detailed description of western blot quantification). P-values for the determination of significant differences between cytoplasmic and nuclear fractions were calculated using a 2-tailed t-test. Different levels of significance are indicated (\*\* p < 0,01, \* p < 0,05).

Here we found that STAT3 levels were significantly higher in the total ipsilateral fraction at three days compared to the contralateral fraction ( $170,3 \pm 15,9$  % versus  $100,0 \pm 0,0$  %,  $p = 0,011$ , n = 3 animals, Fig. 18A), but not anymore at five days ( $151,7 \pm 20,2$  % versus  $100,0 \pm 0,0$  %,  $p = 0,063$ ) and seven days after stab wound ( $94,2 \pm 9,0$  % versus  $100,0 \pm 0,0$  %,  $p = 0,554$ , n = 3 animals for each time point, Table 4, Fig. 18A). In the cytoplasmic ipsilateral fractions STAT3 levels were significantly elevated compared to the cytoplasmic contralateral fractions at three days after stab wound ( $174,2 \pm 15,7$  % versus  $100,0 \pm 0,0$  %,  $p = 0,009$ ) but again not anymore at 5 dpSW ( $163,7 \pm 31,3$  % versus  $100,0 \pm 0,0$  %,  $p = 0,111$ ) and 7 dpSW ( $105,0 \pm 7,6$  % versus  $100,0 \pm 0,0$  %,  $p = 0,546$ ; n = 3 for each time point, Table 4, Fig. 18B). More importantly, at three and five days after stab wound, the ipsilateral nuclear fractions contained significantly more STAT3 than the contralateral nuclear fractions (3 dpSW:  $178,9 \pm 22,2$  % versus  $100,0 \pm 0,0$  %,  $p = 0,011$ ; 5 dpSW:  $131,8 \pm 8,9$  % versus  $100,0 \pm 0,0$  %,  $p = 0,023$ , n = 3 for each time point, Table 4, Fig. 18C). This demonstrates an overall increase in STAT3 protein levels, including the nuclear fraction, after injury (Table 4).

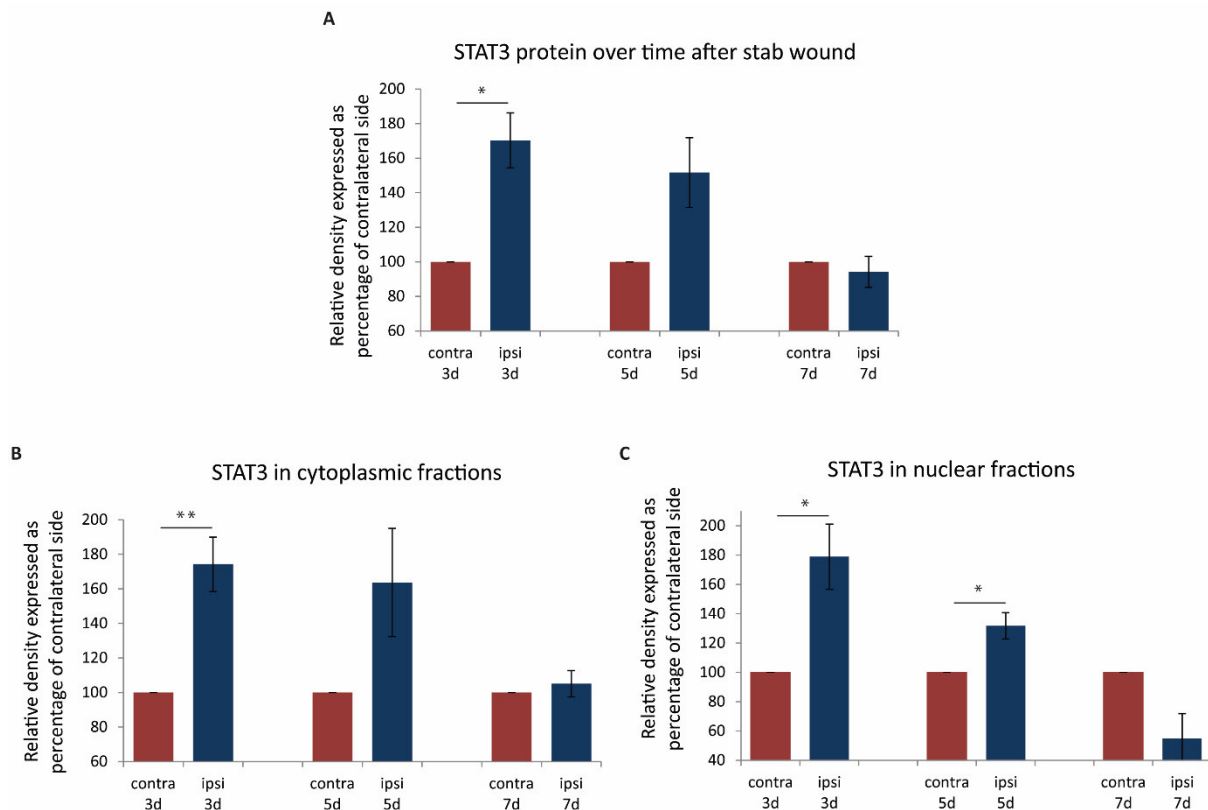


**Fig. 18: Protein levels of STAT3 in ipsilateral versus contralateral fractions at 3, 5 and 7 dpSW**

Quantification of the western blot bands (as shown in Fig. 17) with Image J 1.42q by using densitometric analysis. (A) Total ipsilateral versus contralateral fractions (cytoplasmic plus nuclear fraction) at 3, 5 and 7 dpSW ( $n = 3$  for each time point). (B) Ipsilateral cytoplasmic versus contralateral cytoplasmic fractions at 3, 5 and 7 dpSW ( $n = 3$  for each time point). (C) Ipsilateral nuclear versus contralateral nuclear fractions at 3, 5 and 7 dpSW ( $n = 3$  for each time point). \*\*  $p < 0,01$ , \*  $p < 0,05$ .

Taken together, these data showed that STAT3 is highly upregulated at 3 dpSW in the injured cerebral cortex after stab wound lesion. In particular, our subcellular fractionation revealed a prominent increase in STAT3 protein in the cytoplasmic but also in the nuclear fractions at this time point, thus suggesting a nuclear translocation of STAT3 protein and an increased activation of STAT3 signaling.

### 3.1.2.3. Analysis of STAT3 signaling activation after stab wound by studying the phosphorylation status of STAT3 at Tyr705

As reviewed in subchapter 1.6.2. STAT3 undergoes phosphorylation at Tyr705 by JAKs when associated to the cytokine receptor. Thereafter it is able to homo- or heterodimerize which in turn is necessary for nuclear translocation. Accordingly, the Tyr705 phosphorylation is a critical step in the activation of STAT3 signaling. In order to study the phosphorylated STAT3

protein, we used phosphorylation site specific antibodies (see subchapter 2.2.2. and 2.2.3.). Here we conducted a western blot analysis of the subcellular fractionated cerebral cortex extracts at 3, 5 and 7 dpSW (n = 3 animals for each time point, Fig. 17).

First, we found that, in contrast to STAT3, pSTAT3 expression was virtually restricted to the nuclear fractions compared to the cytoplasmic fractions at all time points investigated and in both hemispheres (Fig. 17). This is in agreement with the literature, describing that phosphorylated STAT proteins are translocated into the nucleus (see subchapter 1.6.2.).

For the following quantitative analysis we first normalized pSTAT3 signals to the corresponding nucleoporin signal, then set the nuclear fraction contralateral to the lesion as 100 % and calculated the pSTAT3 expression level in the ipsilateral side relative to this value. Most importantly, we observed a significant upregulation of pSTAT3 in the nuclear fraction ipsilateral to the lesion compared with the contralateral nuclear fraction at 3 dpSW ( $411,5 \pm 147,3$  % versus  $100,0 \pm 0,0$  %,  $p = 0,022$ ,  $n = 3$ , Fig. 19) but not anymore at 5 and 7 dpSW (5 dpSW:  $209,2 \pm 83,1$  % versus  $100,0 \pm 0,0$  %,  $p = 0,259$ ,  $n = 3$ ; 7 dpSW:  $71,6 \pm 36,3$  % versus  $100,0 \pm 0,0$  %,  $p = 0,478$ ,  $n = 3$ , Fig. 19).

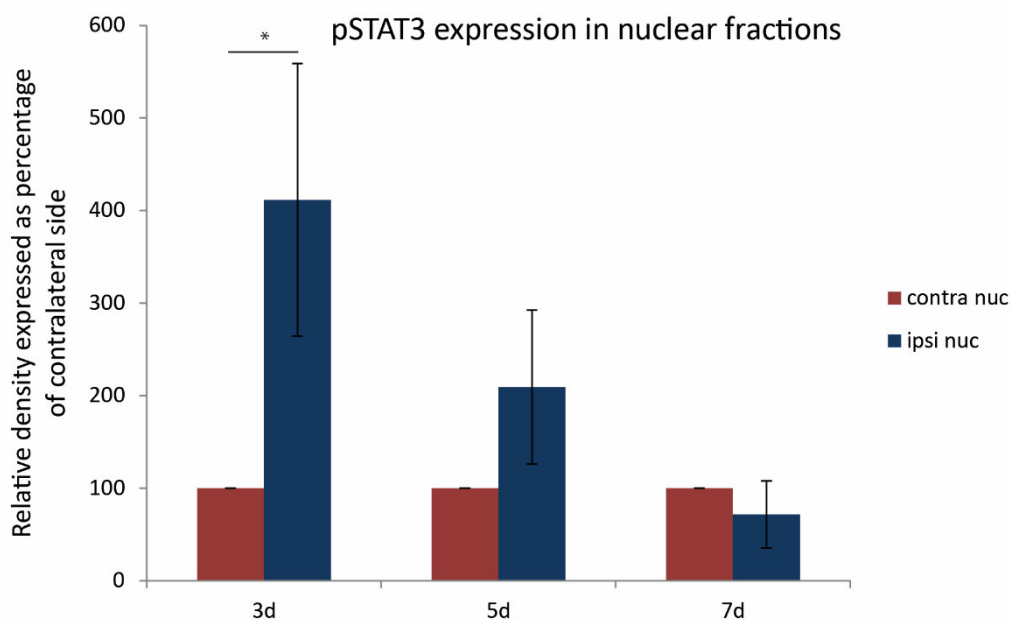


**Fig. 19: Expression of pSTAT3 in ipsilateral versus contralateral nuclear fractions at 3, 5 and 7 dpSW**

Quantification of the western blot bands (as shown in Fig. 17) with Image J 1.42q by using densitometric analysis. Ipsilateral nuclear versus contralateral nuclear fractions at 3, 5 and 7 dpSW (n = 3 for each time point). \*  $p < 0,05$ .

Overall, these data showed that pSTAT3 is upregulated specifically in the nuclear fraction of the ipsilateral side at 3 dpSW, thus indicating an early activation of STAT3 signaling pathways following injury in the cerebral cortex.

### **3.1.3. Expression and activation pattern of STAT3 after MCAo**

In the next set of experiments, we investigated whether the upregulation of STAT3 and the activation of STAT3 signaling that we evidenced in the stab wound model would also be observed in other acute injury models. To this aim, we used an experimental stroke model (MCAo), which is also clinically more relevant (see subchapter 2.2.1.6. for detailed description). We applied the same western blot analysis of subcellular fractionated cerebral cortex extracts obtained from mice sacrificed at 3-4 days after MCAo. We studied the levels and activation of STAT3 as described above (n = 3 animals for STAT3 and pSTAT3, Fig. 20). First, as after stab wound, immunoblotting for enolase and nucleoporin revealed that these proteins were only present in the cytoplasmic and nuclear fraction, respectively, ensuring that our samples were properly fractionated. Next, we observed that independent of the hemisphere, the expression levels of STAT3 were significantly increased in the cytoplasmic compared to the corresponding nuclear fractions (Fig. 20A).

In order to compare the side ipsilateral to the lesion with the contralateral side we again first normalized STAT3 and pSTAT3 signals to enolase and/or nucleoporin signals, then set the STAT3/pSTAT3 expression level in the contralateral fraction as 100 % and calculated the protein level in the ipsilateral in relation to the contralateral fraction.



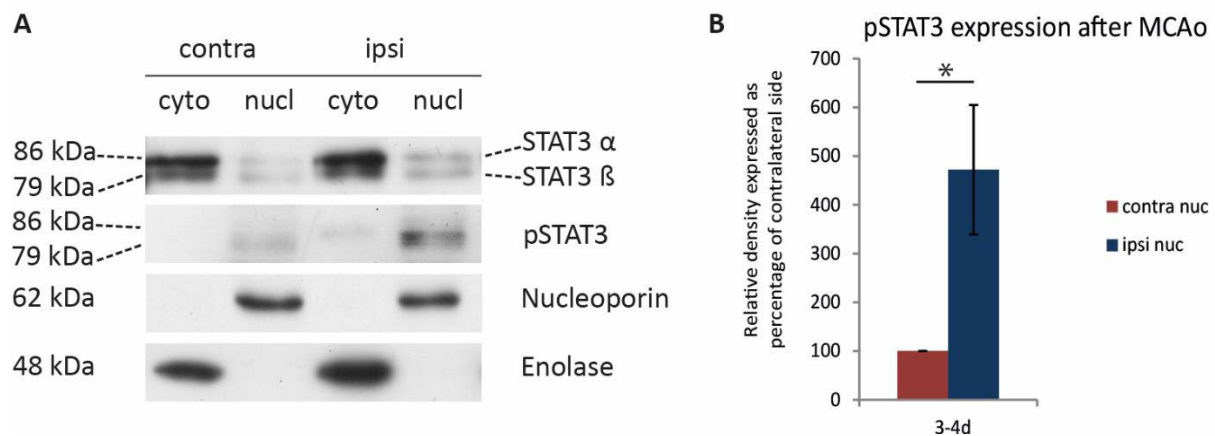


**Fig. 20: Expression and activation of STAT3 at 3-4 days after MCAo**

(A) Representative western blots are shown. Independent tissues of the contra- and ipsilateral cortices of mice, that underwent MCAo and were kept for 3-4 days, were loaded ( $n = 3$  for STAT3 and pSTAT3). Expression levels of STAT3 and pSTAT3 were determined. Nucleoporin and enolase signals served as nuclear and cytoplasmic loading controls, respectively. (B) Quantification of the western blot bands (as shown in Fig. 20A) with Image J 1.42q by using densitometric analysis. Ipsilateral nuclear versus contralateral nuclear fractions at 3-4 days after MCAo ( $n = 3$  for each time point). \*  $p < 0,05$ .

Here we did not observe a significant difference in STAT3 protein levels in the total ipsilateral versus contralateral fraction ( $162,5 \pm 32,8$  % versus  $100,0 \pm 0,0$  %,  $p = 0,129$ ,  $n = 3$ ) or in the cytoplasmic (ipsilateral  $95,5 \pm 17,2$  % versus contralateral  $100,0 \pm 0,0$  %,  $p = 0,808$ ,  $n = 3$ ) or nuclear fractions (ipsilateral  $718,5 \pm 375,8$  % versus contralateral  $100,0 \pm 0,0$  %,  $p = 0,175$ ,  $n = 3$ ).

The activation of STAT3 signaling was analyzed by studying the phosphorylation status at Tyr705 of STAT3. In agreement with our stab wound model data, pSTAT3 was mostly localized in the nucleus. Importantly, we demonstrated a significant upregulation in pSTAT3 expression in the nuclear fraction in the lesioned side compared to the contralateral nuclear fraction ( $472,1 \pm 133,0$  % versus contralateral  $100,0 \pm 0,0$  %,  $p = 0,049$ ,  $n = 3$ , Fig. 20B), i.e. to comparable levels as observed after stab wound.

Taken together, these data revealed an early activation of STAT3 signaling in the injured cerebral cortex following a stroke episode. While no significant differences in STAT3 expression could be detected between the ipsilateral and contralateral fractions at 3-4 days after MCAo, pSTAT3 displayed a significant upregulation in the ipsilateral nuclear fractions compared to the contralateral side. This indicated an activation of STAT3 signaling at 3-4 days after MCAo, as it was found in the stab wound model after 3 days, thus suggesting that

activation of STAT3 in the cerebral cortex is a general response induced by an acute invasive injury.

### 3.1.4. Expression analysis of STAT1 and STAT5

As written in subchapter 1.6.3.2., also other proteins of the STAT family have been suggested to be expressed after CNS injury. Here we examined if especially STAT1 and STAT5 are upregulated after stab wound injury.

First, we investigated the STAT5a protein levels in our initial series of experiments over a time course of seven days after stab wound ( $n = 1$  animal for each time point, Fig. 21A). Different STAT5a antibodies were tested but they all resulted in poor signals in western blot. In contrast to STAT3, the overall level of STAT5a protein was lower and no obvious upregulation could be observed. Unfortunately, subsequent experiments with other STAT5 antibodies to detect STAT5b and pSTAT5 failed to disclose the protein in western blot due to poor specificity of these antibodies.

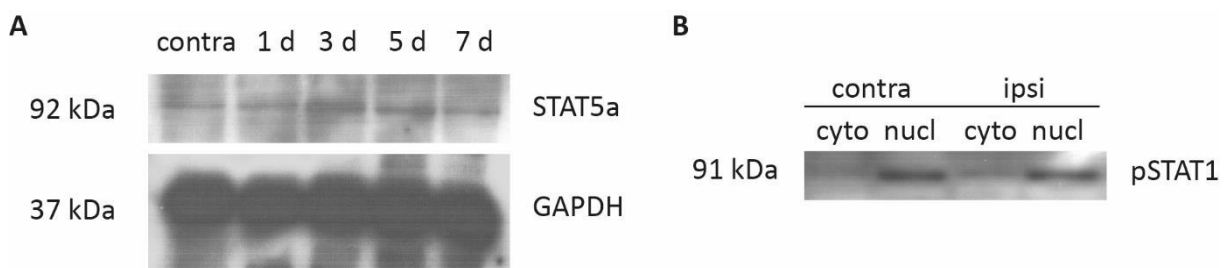


**Fig. 21: Expression of STAT5a and pSTAT1 after stab wound**

(A) Representative western blot is shown. Independent tissues of the ipsilateral cortices of stab wounded mice at 1, 3, 5 and 7 dpSW were loaded ( $n = 1$  for each time point). Contralateral cortices were mixed and loaded in one lane. Expression levels of STAT5a were determined. GAPDH signals served as loading controls. (B) Representative western blot is shown. Contra- and ipsilateral cortex of a stab wounded mice, that was kept for 3 d, were loaded ( $n = 1$ ). Expression levels of pSTAT1 were determined.

Second, we studied the activation of STAT1 at 3 dpSW in subcellular fractionated cortical brain extracts ( $n = 1$  animal) by using a phosphorylation site (Tyr701) specific antibody (see subchapter 2.2.2., Fig. 21B). In this experiment we found that pSTAT1 is rather high in the nucleus. However, no difference between the nuclear contralateral and ipsilateral fractions was detectable. Nevertheless, given the fact that a loading control is missing in this experiment, no final conclusions can be drawn.

Given the lower levels of STAT5a protein and the lack of an injury-dependent pSTAT1 regulation, we mainly focused on STAT3 signaling in the next set of experiments.

### **3.2. Which cell types express and activate STAT3 signaling in the injured cerebral cortex?**

Our western blot experiments revealed that STAT3 is upregulated and activated at three days after stab wound and also activated at three days after MCAo. However, our western blot analysis could not answer the question in which cell types this process of STAT3 activation occurs after cerebral injury. Additionally, a review of the recent literature revealed that regarding the expression of STAT3 in different cell types, so far only contradictory results had been published after experimental stroke and no results after stab wound (see subchapter 1.6.3.2.). Therefore, a detailed immunohistochemical analysis of STAT3 expression was required at different time points in acute invasive injury models, such as the stab wound injury and MCAo. In addition, we also examined STAT3 expression in non-invasive injury models, such as Alzheimer's disease models.

#### **3.2.1. Cellular localization of STAT3 at three days after stab wound**

Our western blot findings indicated that STAT3 expression and activation have their peaks at three days after stab wound. Therefore, we first investigated which cell types expressed STAT3 at three days after stab wound injury by immunohistochemistry. Accordingly, we stained 30  $\mu\text{m}$  Cryostat sections from mouse brains collected at 3 dpSW, for STAT3 and GFAP, which is a marker for reactive astrocytes, and compared the injured cortex with the contralateral hemisphere.

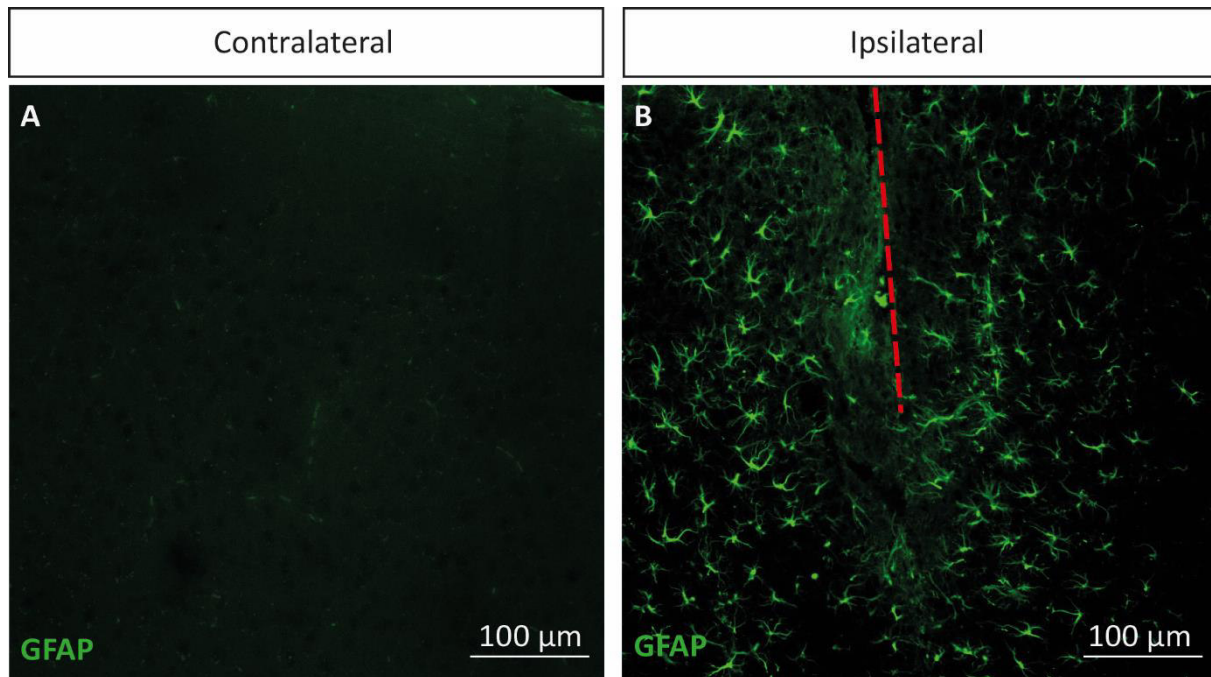


**Fig. 22: GFAP immunohistochemistry at 3 dpSW in the contra- versus ipsilateral hemisphere**

Representative micrographs are shown. Contra- (A) and ipsilateral (B) example belong to the same mouse. Stainings against GFAP were performed with brain sections from mice that were perfused at 3 dpSW. The stab wound is indicated by a red dashed line.

Whereas the ipsilateral cortical hemisphere displayed a massive upregulation of GFAP around the stab wound area, virtually no GFAP+ cell was observed in the contralateral hemisphere (Fig. 22) as described before (Hozumi et al., 1990, Buffo et al., 2005, Buffo et al., 2008, Robel et al., 2011, Bardehle et al., 2013).

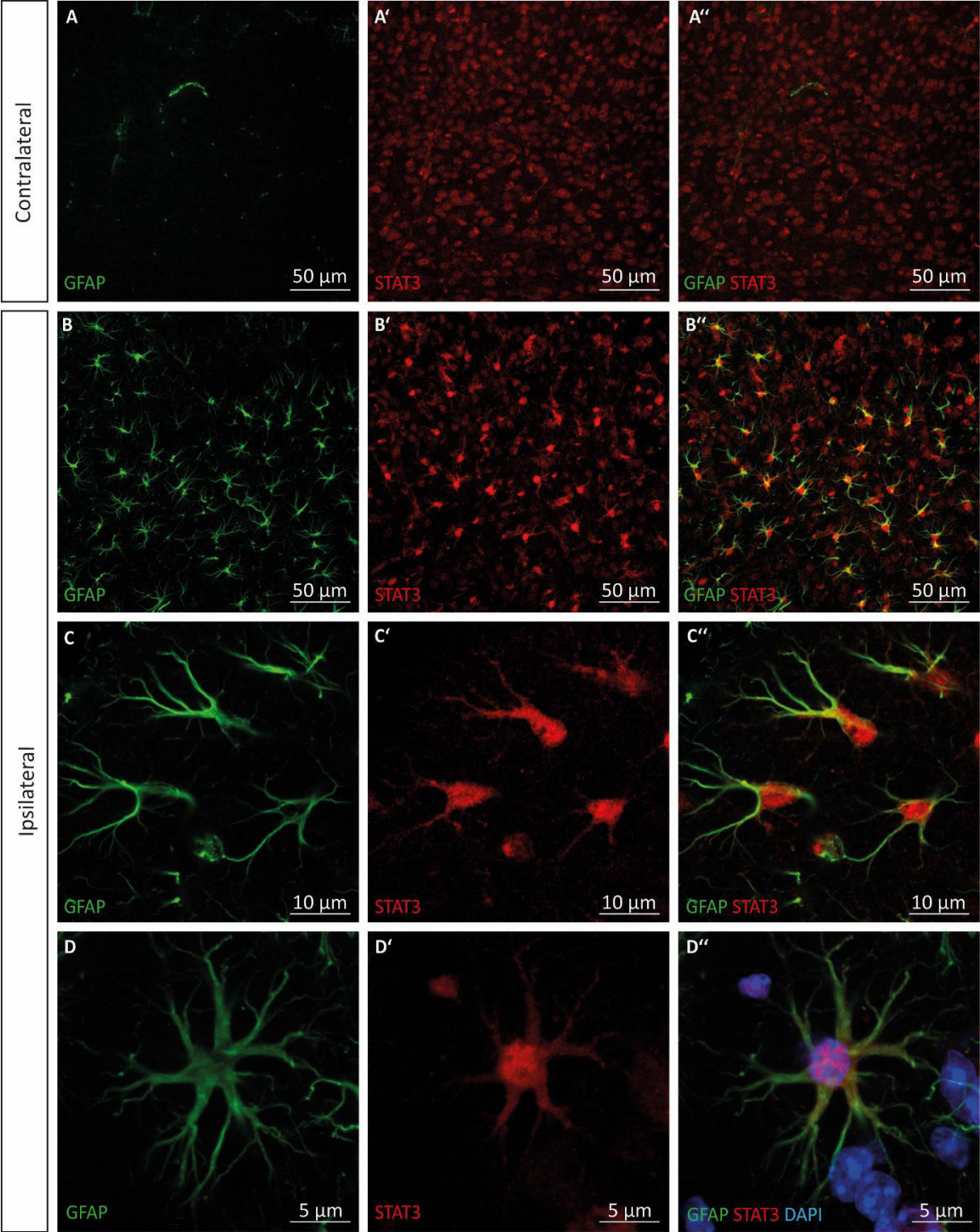


**Fig. 23: GFAP and STAT3 costaining at 3 dpSW in contra- and ipsilateral cortices**  
Representative micrographs are shown. Contra- and ipsilateral examples belong to the same mouse. Stainings against GFAP and STAT3 were performed with brain sections from mice that were perfused at 3 dpSW. (A-A'') Overview of the contralateral hemisphere. (B-B'') Overview of the ipsilateral hemisphere. (C-C'') Higher magnification of reactive astrocytes in the ipsilateral hemisphere. (D-D'') Costaining with DAPI, GFAP and STAT3 of a reactive astrocyte in the vicinity of the lesion.

Furthermore, our staining showed that STAT3 protein is expressed in both, the contra- and ipsilateral hemisphere (Fig. 23A' and B') in agreement with our western blot data. Moreover, we detected an overall upregulation of STAT3 expression in some cells in the ipsilateral injured cortex compared to the control side (Fig. 23A' and B'). In addition, this upregulation was particularly visible in the nuclei of the injured cortex compared to the contralateral side, thus confirming and extending our western blot results. The costaining with GFAP revealed that virtually all these strongly STAT3-immunoreactive cells in the ipsilateral side were also GFAP positive (Fig. 23B''). Together with their typical morphology showing long star-shaped processes, this population most likely represented reactive astrocytes. Moreover, pictures acquired at higher magnification in the ipsilateral side unraveled that STAT3 is expressed in both, the nuclear and cytoplasmic compartment – the latter best seen in the long processes (Fig. 23C') – in agreement with our western blot data. To provide further evidence of the nuclear localization of STAT3, a costaining with the nuclear marker DAPI was performed (Fig. 23D-D'') and showed that STAT3 is indeed present in the nucleus but absent in nucleoli. Taken together, these experiments revealed an upregulation of STAT3 in the injured cortex in some cells, which virtually all costained with GFAP, thus indicating an increased expression of STAT3 in reactive astrocytes.

Next, in order to further examine which cell population expressed STAT3 in the contralateral cortical hemisphere, we performed a costaining with NeuN, a marker of mature neurons, with brain sections from mice that were perfused at 3 dpSW (Fig. 24). Again, we observed that STAT3 is expressed contra- and ipsilaterally but is upregulated in some nuclei ipsilaterally (Fig. 24A' and B'). In the ipsilateral cortical hemisphere virtually no STAT3+ cell colocalized with NeuN as previously suggested by the abundant colocalisation of STAT3 with GFAP (Fig. 24A'' and 23B''). In contrast, we could observe that virtually all weakly STAT3+ cells in the contralateral cortical hemisphere were NeuN+ neurons (Fig. 24B''). The magnified pictures demonstrated STAT3 to be expressed in the nuclei and the surrounding cytoplasm of NeuN+ cells (Fig. 24C-C'). The STAT3 protein level in the contralateral cortical hemisphere was consistently above background levels (immunohistochemistry without primary antibody, data not shown).



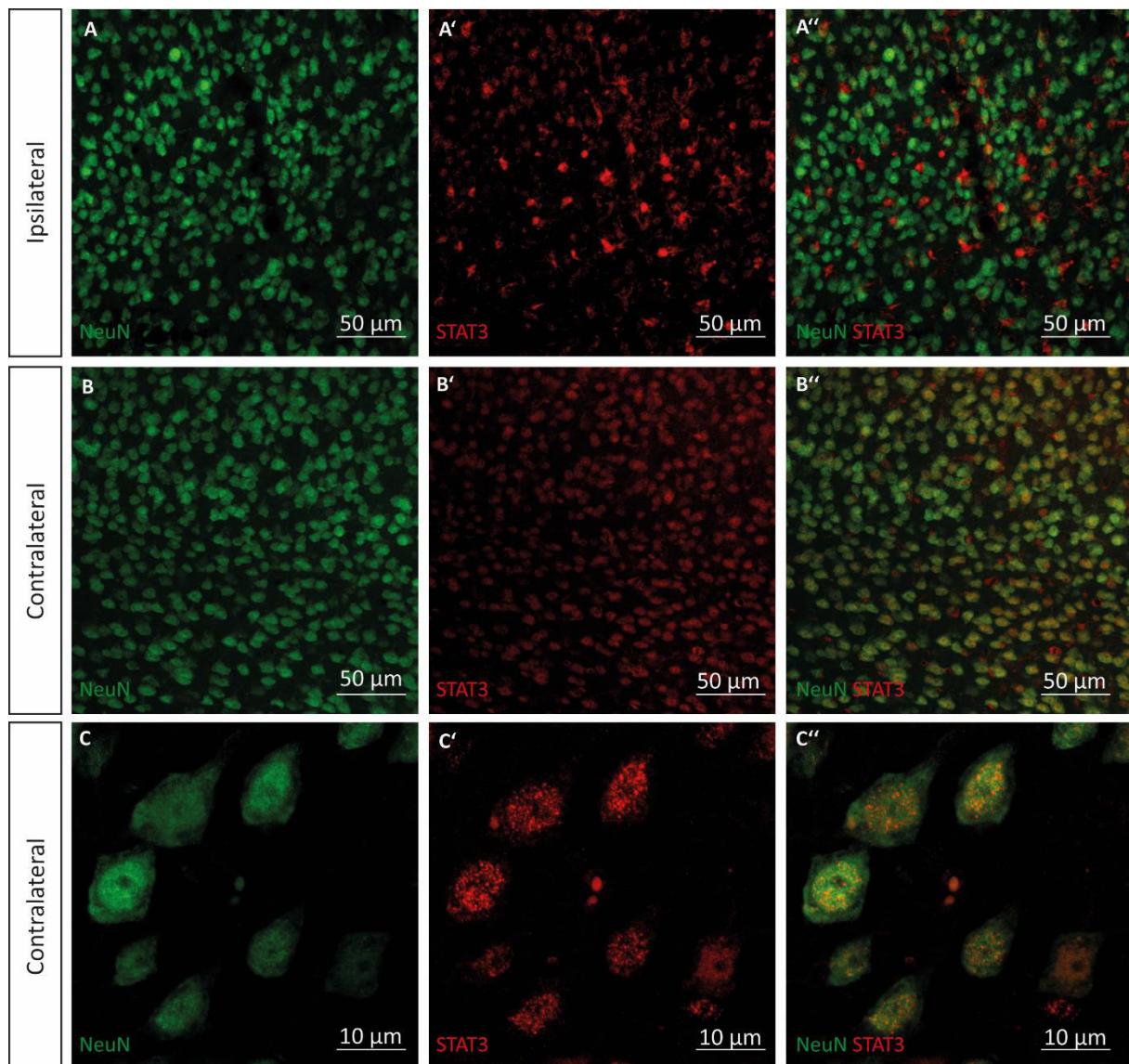


**Fig. 24: NeuN and STAT3 costaining at 3 dpSW in contra- and ipsilateral cortices**

Representative micrographs are shown. Contra- and ipsilateral example belong to the same mouse. Stainings against NeuN and STAT3 were performed with brain sections from mice that were perfused at 3 dpSW. (A-A'') Overview of the ipsilateral hemisphere. (B-B'') Overview of the contralateral hemisphere. (C-C'') Higher magnification of neurons in the contralateral hemisphere.

These stainings clearly demonstrated a STAT3 colocalization with GFAP at 3 dpSW, i.e. an expression in reactive astrocytes, in the ipsilateral side and with NeuN, i.e. an expression in mature neurons, in the contralateral cortical hemisphere.

### 3.2.2. Activation pattern of STAT3 signaling after stab wound by investigating STAT3 phosphorylation status

As described in 3.1.2.3., the investigation of the phosphorylation status of STAT3 is crucial to demonstrate activation of STAT3 signaling. In order to study if STAT3 is not only expressed but

also activated in reactive astrocytes at 3 dpSW, we performed immunohistochemical analysis of pSTAT3 and GFAP expression (Fig. 25).

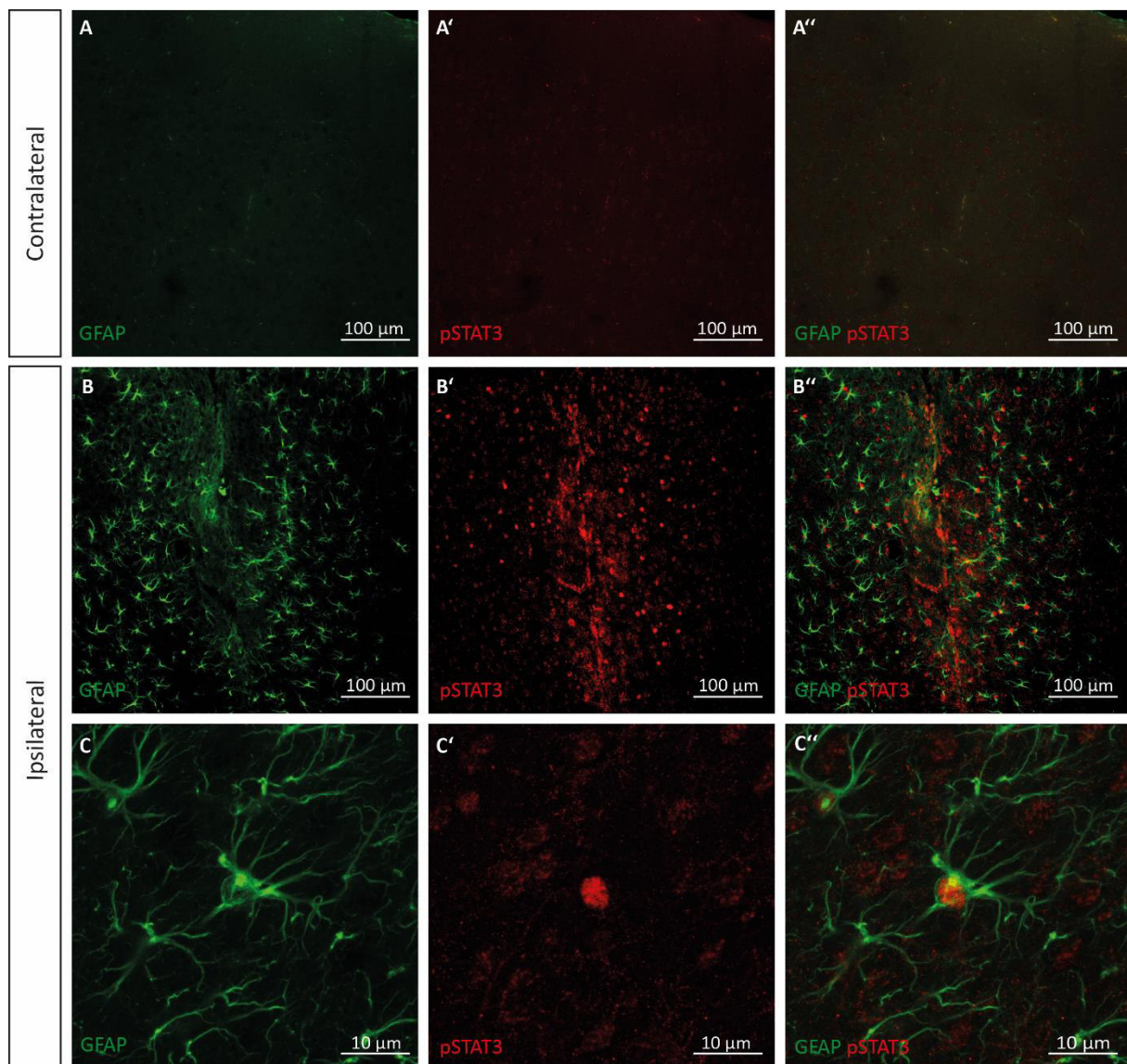


**Fig. 25: pSTAT3 and GFAP costaining at 3 dpSW in contra- and ipsilateral cortices**

Representative micrographs are shown. Contra- and ipsilateral example belong to the same mouse. Stainings against GFAP and pSTAT3 were performed with brain sections from mice that were perfused at 3 dpSW. (A-A'') Overview of the contralateral hemisphere. (B-B'') Overview of the ipsilateral hemisphere. (C-C'') Higher magnification of reactive astrocytes in the ipsilateral hemisphere.

First of all, we observed round and bright pSTAT3+ nuclei that were localized in the vicinity of the stab wound lesion in the ipsilateral side, while virtually no pSTAT3+ cells could be observed in the contralateral cortical hemisphere (Fig. 25A' and B'). Higher magnification revealed its exclusive nuclear localization (Fig. 25C'') thus confirming our western blot data. Virtually all of these pSTAT3+ nuclei were surrounded by GFAP, i.e. were contained in reactive astrocytes (Fig. 25B'' and C'').  $20,0 \pm 2,3$  % of GFAP+ cells showed pSTAT3 expression in the stab wound



lesion area ( $\pm 400 \mu\text{m}$ ; see below for details of quantification). The specificity of our pSTAT3 antibody was confirmed by the previously known pSTAT3 expression in neuronal nuclei of the periventricular hypothalamic nucleus (Hakansson and Meister, 1998) (data not shown).

In the laboratory, a new *in vitro* culture system was recently characterized that allows to culturing reactive glial cells isolated from the stab wound injured cortex. We took the opportunity to use this *in vitro* model to confirm our pSTAT3 data. We found that pSTAT3 was exclusively expressed in the nucleus of GFAP+ reactive astrocytes, thus confirming our *in vivo* findings (Fig. 26A and B). The nuclear staining was proven by colocalization with DAPI (Fig. 26C and D).

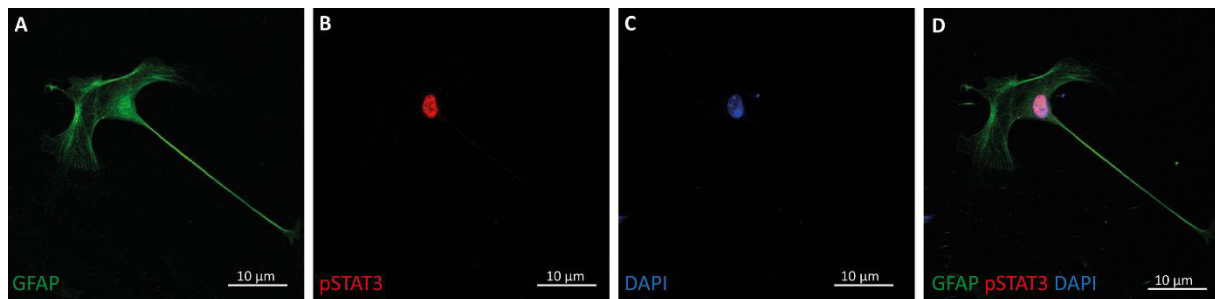


**Fig. 26: pSTAT3 and GFAP costaining of reactive astrocytes isolated in culture**

Three days after stab wound mouse cortices were dissected and mechanically dissociated with hyaluronidase and trypsin. Cells were stained for GFAP (A), pSTAT3 (B) and DAPI (C) at 3 days after plating. D shows the merge picture.

Next, we examined the expression of pSTAT3 over time after stab wound, as our western blot findings showed that STAT3 signaling was mainly activated at 3 dpSW (see subchapter 3.1.2.2. and 3.1.2.3.). Here we compared pSTAT3 immunohistochemistry of brain sections from mice perfused at 3, 5 and 7 dpSW (n = 3 animals per time point, Fig. 27).

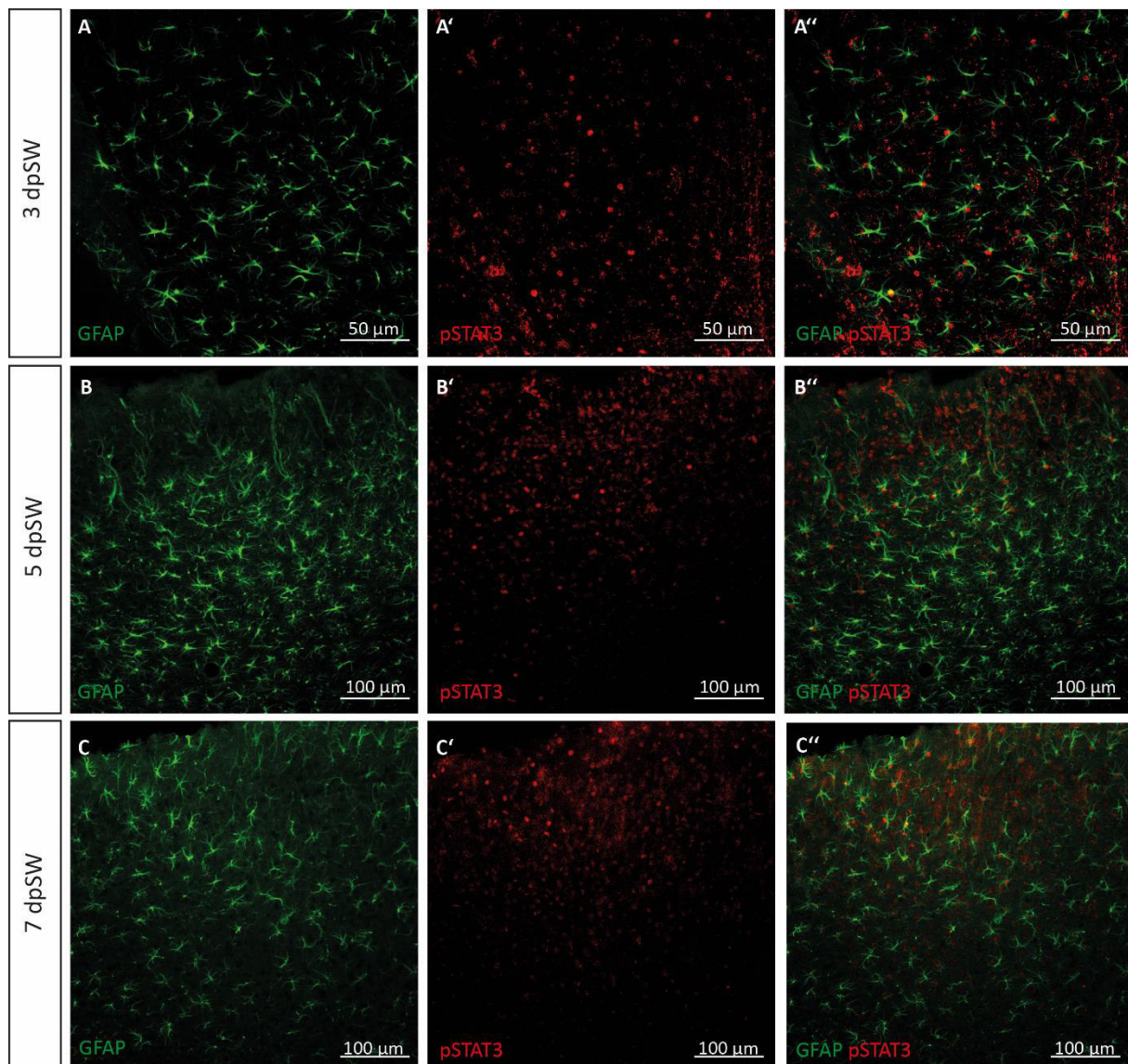


**Fig. 27: pSTAT3 and GFAP costaining at 3, 5 and 7 dpSW**

Representative micrographs are shown. Stainings against GFAP and pSTAT3 were performed with brain sections from mice that were perfused at 3, 5 or 7 dpSW ( $n = 3$  animals per time point). (A-A'') Overview of the ipsilateral hemisphere at 3 dpSW. (B-B'') Overview of the ipsilateral hemisphere at 5 dpSW. (C-C'') Overview of the ipsilateral hemisphere at 7 dpSW.

When we quantified cell numbers using Image J 1.42q we found that the percentage of pSTAT3+ cells among GFAP+ cells decreased significantly from 3 dpSW to 5 and 7 dpSW ( $20,0 \pm 2,3$  % (3 dpSW) versus  $6,5 \pm 3,8$  % (5 dpSW),  $p = 0,038$ ; and versus  $8,7 \pm 1,4$  % (7 dpSW),  $p = 0,014$ ,  $n = 3$  animals per time point, Fig. 28A). Moreover, the percentage of GFAP+ cells among pSTAT3+ cells also decreased, although not significantly, from 3 dpSW to 5 and 7 dpSW ( $100,0 \pm 0,0$  % versus  $78,9 \pm 9,7$  % (5 dpSW),  $p = 0,096$ ; and versus  $65,9 \pm 13,9$  % (7 dpSW),  $p = 0,069$ ,  $n = 3$  animals per time point, Fig. 28B), and between 5 and 7 dpSW ( $p = 0,483$ ). These data suggest that other cell types may express pSTAT3 at 5 and 7 dpSW. Further analysis is required to investigate which other cell types contain pSTAT3 at these later time points.

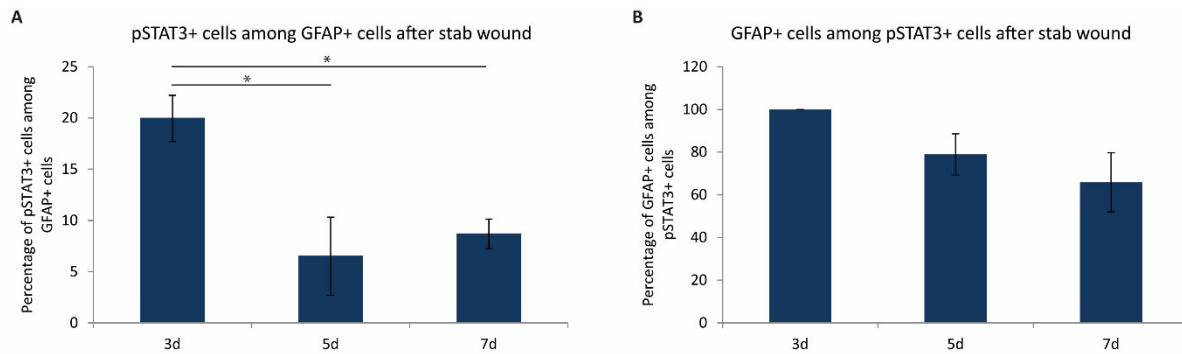


**Fig. 28: Quantification of pSTAT3+ cells at 3, 5 and 7 dpSW**

Analysis of the percentage of pSTAT3+ cells among GFAP+ cells (A) and GFAP+ cells among pSTAT3+ cells (B) by using Image J 1.42q (n = 3 animals for each time point). Values are given as mean  $\pm$  SEM. \* p < 0,05.

Overall, these data indicated an upregulation of pSTAT3 in GFAP+ cells in the vicinity of the stab wound, thus indicating a specific activation of STAT3 signaling in reactive astrocytes. In addition, the number of pSTAT3+ cells among GFAP+ cells was maximal at 3 dpSW and decreased thereafter. Nevertheless, it is likely that this number of pSTAT3+ cells is underestimated due to the high turn over and transitory feature of the phosphorylation status of a transcription factor at a given time point.

### 3.2.3. Activation pattern of STAT3 signaling after MCAo by studying STAT3 phosphorylation status

The results of our western blot experiments indicated that STAT3 is also activated after MCAo (see subchapter 3.1.3.). Moreover, the reviewed literature exhibited contradictory results regarding the STAT3 expression in different cell types after MCAo (see subchapter 1.6.3.2.). Therefore, we asked which cell types activate STAT3 signaling after MCAo and performed immunohistochemistry for GFAP and pSTAT3 on brain sections from mice that were perfused at 3-4 days after MCAo (n = 3 mice).

While virtually no GFAP+ cell was detected in the contralateral cortical hemisphere we observed a massive astrogliosis, as revealed by upregulation of GFAP, in the side ipsilateral to the ischemic infarct. In addition, we observed a large necrotic core, devoid of any GFAP+ cell, that had a clear-cut border to the surrounding astrogliosis (Fig. 29).



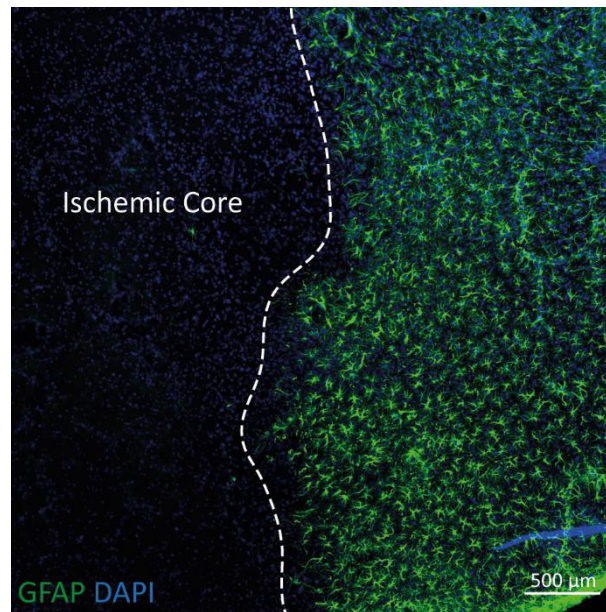


**Fig. 29: GFAP-immunostaining at 3-4 days after MCAO**

Representative micrograph is shown. Stainings against GFAP and DAPI were performed with brain sections from mice that were perfused at 3-4 days after MCAO.

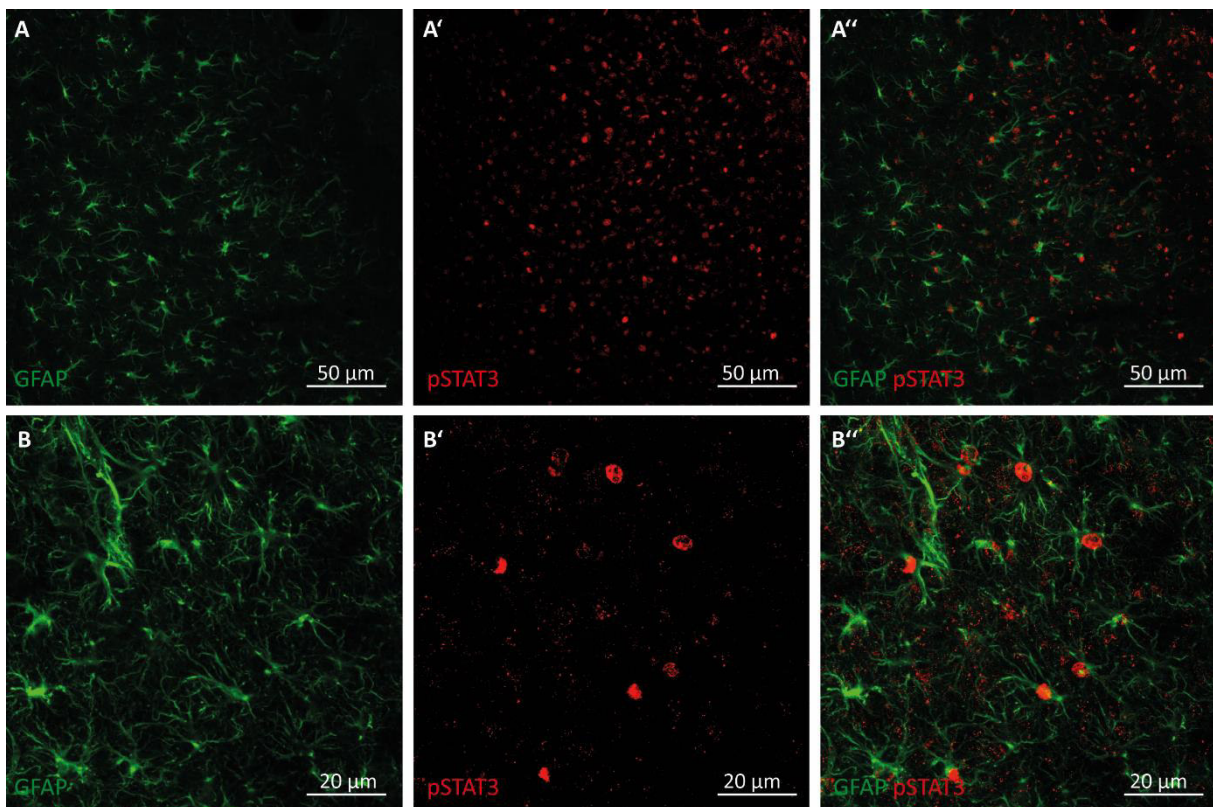


**Fig. 30: Costaining of GFAP and pSTAT3 at 3-4 days after MCAO**

Representative micrographs are shown. Stainings against GFAP and pSTAT3 were performed with brain sections from mice that were perfused at 3-4 days after MCAO ( $n = 3$  animals). (A-A'') Overview of the ipsilateral hemisphere. (B-B'') Higher magnification of reactive astrocytes in the ipsilateral hemisphere.

Round and bright pSTAT3+ nuclei were localized in the ipsilateral ischemic cortex (Fig. 30), while no pSTAT3+ cells could be observed in the contralateral side. More importantly, our

double immunostaining revealed that pSTAT3 was virtually only contained in the nuclei of GFAP+ reactive astrocytes (Fig. 30A'', B'') as previously observed for the stab wound injury. Quantification revealed that the percentage of pSTAT3+ cells among GFAP+ cells at 3-4 days after MCAo did not differ significantly from 3 dpSW ( $18,8 \pm 6,4$  % versus  $20,0 \pm 2,3$  %,  $p = 0,867$ ,  $n = 3$  animals for each condition, Fig. 31A). However, the number of GFAP+ cells among pSTAT3+ cells differed significantly between 3-4 d after MCAo and 3 dpSW ( $58,9 \pm 6,5$  % versus  $100,0 \pm 0,0$ ,  $p = 0,003$ ,  $n = 3$  animals for each condition, Fig. 31B), suggesting that STAT3 is also activated in other cell types 3-4 days after MCAo.

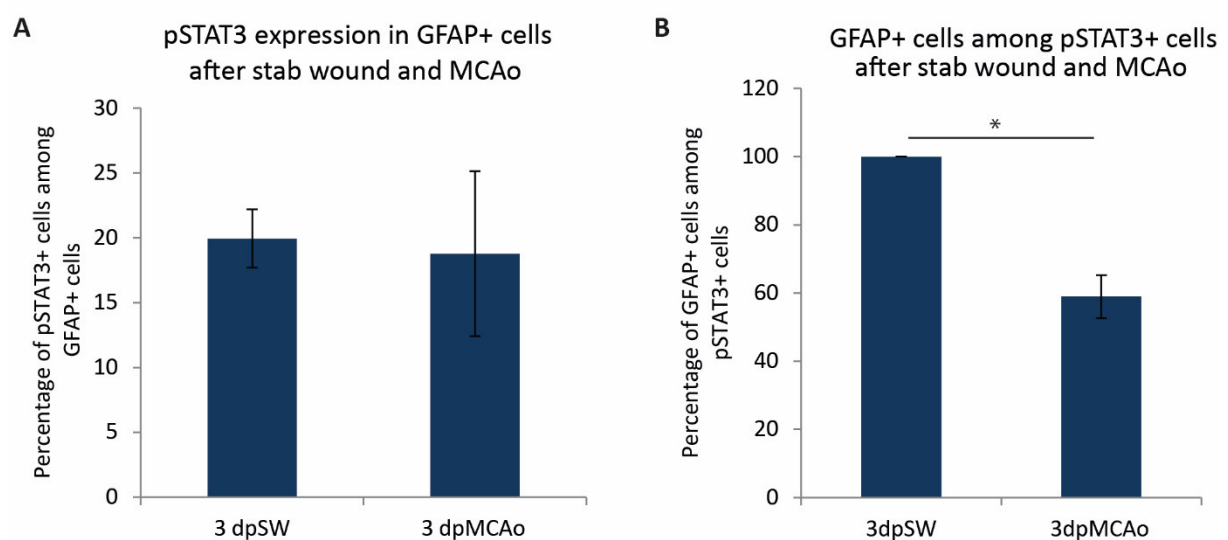


**Fig. 31: Quantification of pSTAT3+ cells at 3 days after MCAo and stab wound**

Analysis of the percentage of pSTAT3+ cells among GFAP+ cells (A) and GFAP+ cells among pSTAT3+ cells (B) by using Image J 1.42q ( $n = 3$  animals for each time point and condition). Values are given as mean  $\pm$  SEM. \*  $p < 0,05$ .

Taken together, these data indicate that at 3-4 days after MCAo, STAT3 signaling is activated in reactive astrocytes to a similar extent as observed at 3 dpSW. This suggested that the activation of STAT3 signaling in reactive astrocytes could be a general response to an acute invasive injury.

### 3.2.4. Activation pattern of STAT3 signaling in non-invasive injury models like APP/PS1 and CKp25

The brain injury models examined so far, stab wound and experimental stroke, represent acute invasive brain injuries. In order to investigate whether STAT3 signaling may be restricted to invasive injury, we examined its activation also in non-invasive injury models. Especially

Alzheimer's disease (AD), a highly prevalent brain disorder in elderly people which leads to cognitive impairment, has caught our attention. Here, we investigated STAT3 expression and activation in two different mouse models: one showing a progressive (chronic) amyloid plaque deposition and the other showing a non-invasive, widespread neuronal death.

#### **3.2.4.1. Mouse model of amyloidosis: the APP/PS1 mouse**

To model amyloidosis many mouse models have been generated. I will here shortly introduce the APP/PS1 mouse, which expresses mutant forms of both APP and PS1 in neurons (Radde et al., 2006).

When generating mouse models for diseases, it has always been useful to check familial forms for genetic mutations. For AD a genetic variance of APP was found in a Swedish family leading to the generation of the KM670/671NL mutated mouse line (Hsiao et al., 1996). Recently, another mutation (PS1-L166P), which in humans presents as very aggressive familial form of AD, has been added (Radde et al., 2006), leading to the generation of a mouse line expressing human APP with the Swedish double mutation together with PS1 L166P under the Thy1 neuronal promoter and showing stable early onset amyloid plaque deposition in the cortical grey matter and no gender differences. However, in contrast to human pathology, this mouse model does not display tau pathology and fails to show substantial neuronal loss (Rupp et al., 2011).

#### **3.2.4.2. Mouse model of non-invasive neuronal death: the CK/p25 mouse**

Therefore, we aimed at also examining another mouse model better reflecting the widespread neuronal loss observed in AD. To this end, we used the CK/p25 mouse, in which neuronal death can be induced by targeted activation of p25 expression in neurons of the cerebral cortex. Mice expressing p25 under the promoter of the tetracycline operator (tetO) were crossed with mice expressing the tetracycline controlled transactivator (tTA) (Gossen and Bujard, 1992) under the neuronal forebrain promoter CAM kinase II (CK) (Mayford et al., 1996) (Fig. 32). The resulting mouse line expresses p25 in neurons when withdrawing a tetracyclic drug (here we used Doxycyclin) and represses p25 when administrating doxycycline (Cruz et al., 2003) (Fig. 32).

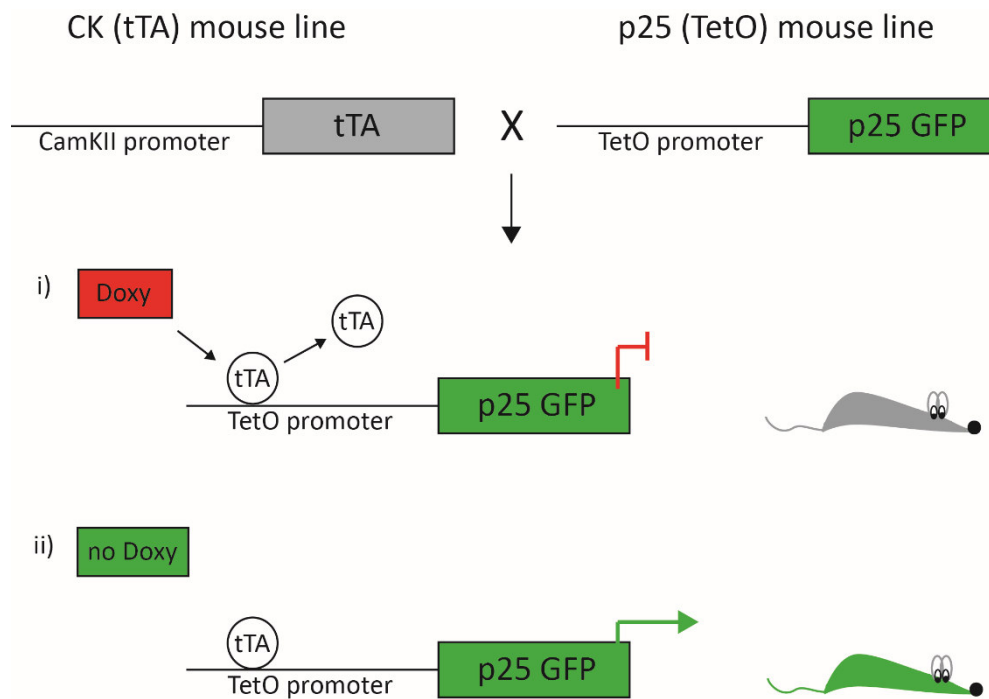


**Fig. 32: Scheme of the CK/p25 mouse model**

The CK (tTA) mouse line and the p25 (TetO) mouse line are crossed and generate a mouse line that expresses p25 in neurons, as the neuronal promoter CamKII drives the expression of tTA, which is required for TetO-linked p25 GFP activation, when doxycycline (Doxy) is withdrawn (ii). If doxycycline is administered, the transcription will be blocked (i). Modified from Mayford et al., 1996.

P25 is a truncated and more stable form of p35, which interacts with cyclin-dependent kinase 5 (Cdk5). In neurodegenerative diseases like AD, Cdk5 activity is enhanced by p25 (Bu et al., 2002, Lee et al., 2000, Nguyen et al., 2001) thus leading to tau phosphorylation, neurotoxic effects by beta-amyloid accumulation in neurons, apoptotic cell death and therefore extensive loss of neurons. Accordingly, these mice recapitulate many hallmark features of AD like amyloidosis, tauopathy, substantial neuronal loss and impaired synaptic plasticity (Cruz et al., 2003).

### 3.2.4.3. Activation of STAT3 signaling in mouse models of non-invasive brain injury

Although it was already suggested that reactive astrocytes upregulate GFAP expression in mouse models of AD (Kamphuis et al., 2012), we were not able to identify studies that investigated the expression and activation of STAT3 in the above described mouse models (see subchapter 1.6.3.2.). To analyze the activation of STAT3 signaling in these mouse models, we performed immunohistochemistry for pSTAT3 and GFAP in six months old APP/PS1 mice and CK/p25 mice that were off doxycycline for five weeks (Fig. 33).



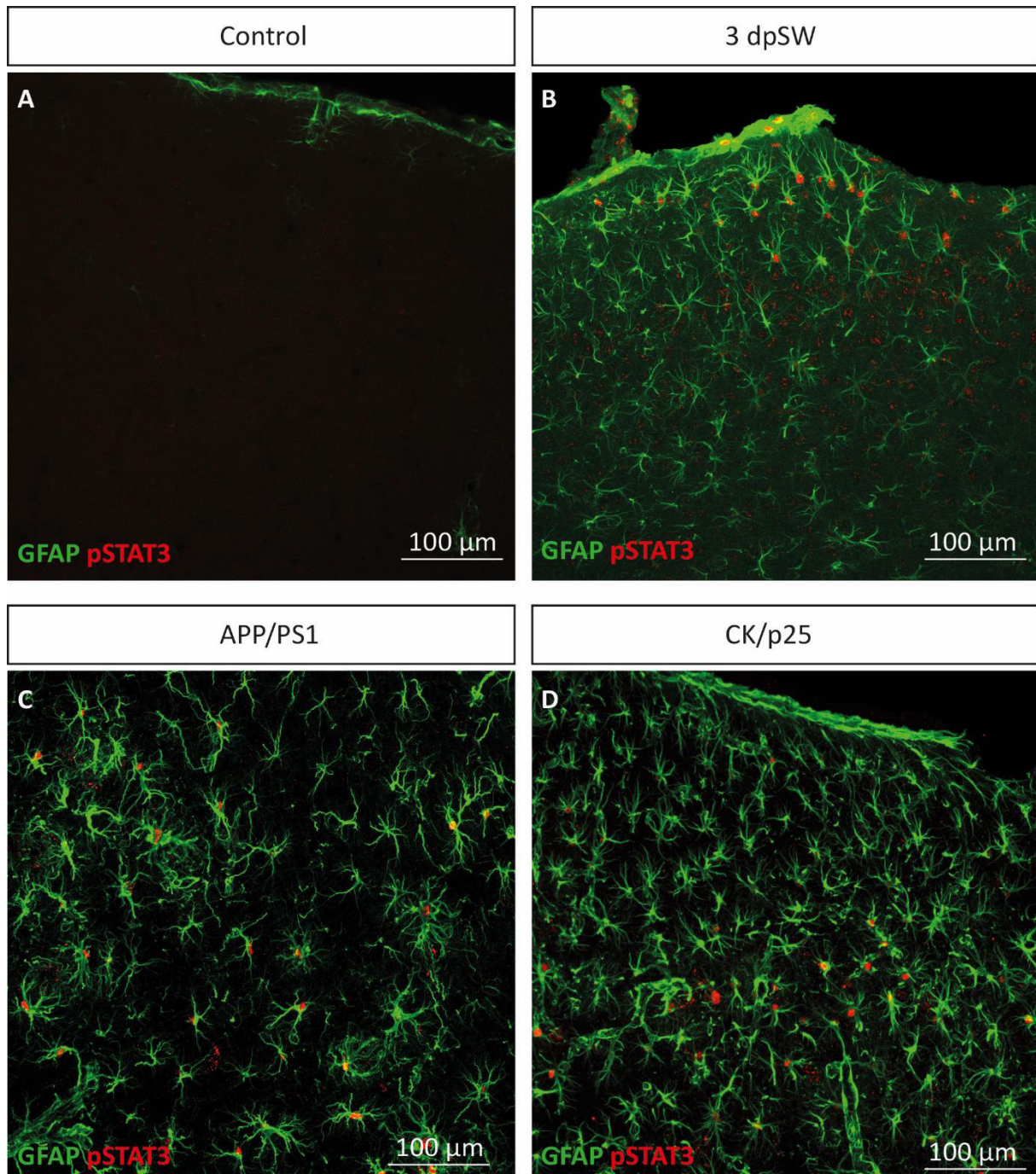


**Fig. 33: Costaining of GFAP and pSTAT3 in CK/p25 and APP/PS1 mice**

Representative micrographs are shown. Stainings against GFAP and pSTAT3 were performed with brain sections from CK/p25 (D) (that were perfused at five weeks after withdrawal of Doxycyclin) and APP/PS1 mice (six months old) (C) in comparison with stab wound (B) and control mice (A).

In both models we observed a strong reactive gliosis in the cerebral cortex as evidenced by GFAP expression spreading through all cortical layers (Fig. 33C and D). APP/PS1 mice exhibited a more pronounced expression of GFAP in the close vicinity of amyloid plaques (data not shown). In both models we observed pSTAT3+ nuclei that were scattered through the different cortical layers (Fig. 33C and D). As described above in the stab wound model, also here the vast majority of these pSTAT3+ nuclei colocalized with GFAP (Fig. 33C and D) and no



significant differences in the percentage of GFAP+ cells among pSTAT3+ cells could be evidenced between the stab wound and APP/PS1 or CK/p25 mice (Fig. 33B, C and D; Fig. 34B). However, we observed a significantly lower percentage of pSTAT3+ cells among GFAP+ cells in six months old APP/PS1 mice compared to mice analyzed 3 dpSW ( $7,4 \pm 2,9$  % (APP/PS1) versus  $20,0 \pm 2,3$  % (3 dpSW),  $p = 0,026$ ,  $n = 3$  animals for each condition, Fig. 34A).

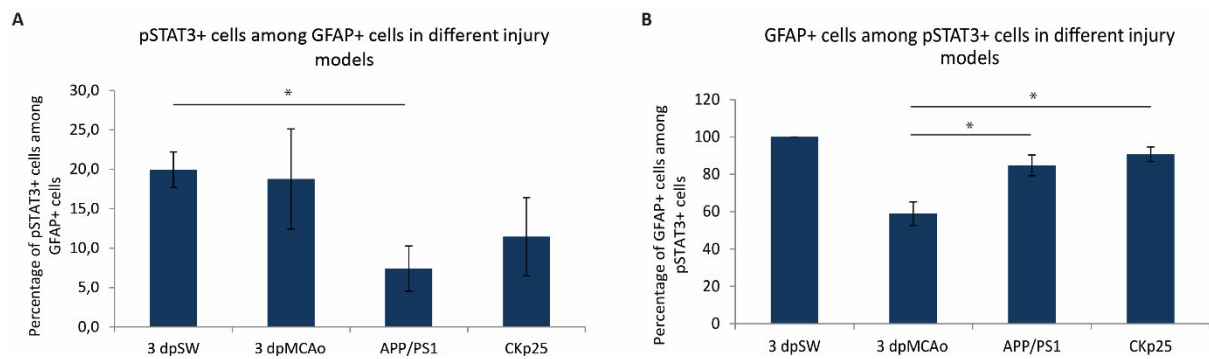


**Fig. 34: Quantification of pSTAT3+ cells at 3 dpSW, 3-4 days after MCAo and in APP/PS1 and CK/p25 mice**

Analysis of the percentage of pSTAT3+ cells among GFAP+ cells (A) and GFAP+ cells among pSTAT3+ cells (B) by using Image J 1.42q ( $n = 3$  animals for each time point and condition). Values are given as mean  $\pm$  SEM. \*  $p < 0,05$ .

Taken together, these data clearly showed that STAT3 signaling is also activated in reactive astrocytes in APP/PS1 and CK/p25 mice, however, to a lower extent compared to the stab wound and MCAo models (approximately half). Thus, these results suggested that STAT3 activation is less prominent in non-invasive injury compared to acute invasive injury conditions.

### 3.2.5. Activation of STAT3 signaling in the adult neurogenic niches – SVZ and SGZ

Until now we analyzed the expression and activation of STAT3 in different injury models and found STAT3 signaling to be activated in reactive astrocytes mostly at 3 dpSW and 3-4 days after MCAo and to a lesser extent also in APP/PS1 and CK/p25 mice. Astrocytes are remarkable as in addition to their diverse functions in the brain parenchyma, they also serve as neural stem/progenitor cells in the adult neurogenic niches. As reviewed in subchapter 1.6.3.2., STAT3 signaling was shown to inhibit embryonic neurogenesis (Bonni et al., 1997, Gu et al., 2005). Thus, we hypothesized that STAT3 signaling would not be activated in the SVZ astrocytes and SGZ radial astrocytes that give rise to neurons in the adult neurogenic niches. We performed immunohistochemistry for GFAP to identify SVZ and SGZ astrocytes, and pSTAT3 on brain sections from adult eight weeks old mice (Fig. 35A-D).

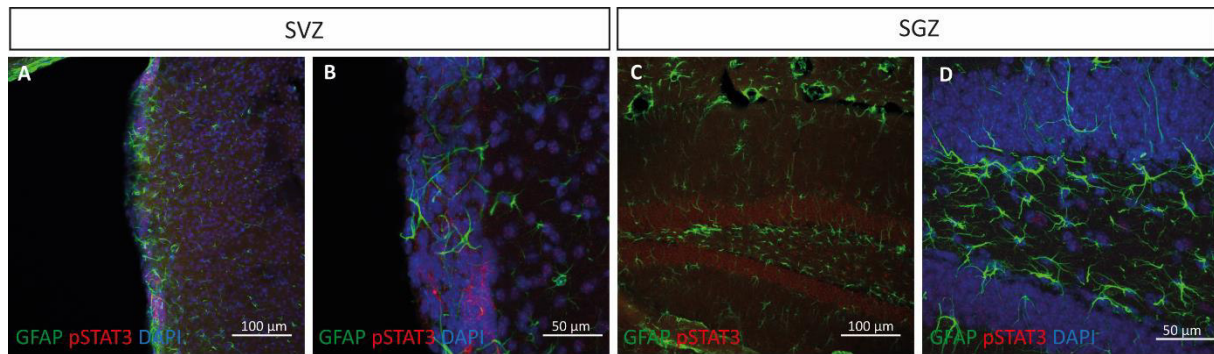


**Fig. 35: Expression of GFAP and pSTAT3 in the adult neurogenic niches**

Representative micrographs are shown. Stainings against GFAP, pSTAT3 and DAPI were performed with brain sections from adult eight weeks old mice. Displayed are (A) an overview about the SVZ at the lateral site of the lateral ventricles, (B) a higher magnification of the SVZ, (C) an overview of the hippocampal SGZ and (D) a higher magnification of the SGZ.

In agreement with our hypothesis virtually no pSTAT3+ cell could be detected in the population of GFAP+ cells in both neurogenic niches. Thus, it seems that a lack of STAT3 activation in the SGZ and SVZ radial astrocytes correlates with their ability to generate neurons. This further supports our hypothesis that activation of STAT3 signaling in non-neurogenic reactive astrocytes in the lesioned cortex could exert anti-neurogenic effects, and maintain them in their glial lineage.

### 3.2.6. Cellular localization and activation pattern of STAT1 and STAT5 following stab wound injury

As mentioned in subchapter 1.6.3.2. and 3.1.4., also STAT1 and STAT5 have been suggested to be upregulated after CNS injury. Our western blot results suggested virtually no upregulation of STAT5a or activation of STAT1 signaling after injury. However, as discussed above, the western blots for STAT5a and pSTAT1 did not give the most conclusive data. Therefore, we investigated these proteins also by immunohistochemistry at 3 dpSW by applying costainings for (i) STAT5a and either GFAP or NeuN (Fig. 36A-C) and (ii) pSTAT1 and GFAP (Fig. 37A-B) (n = 1 animal per each condition).

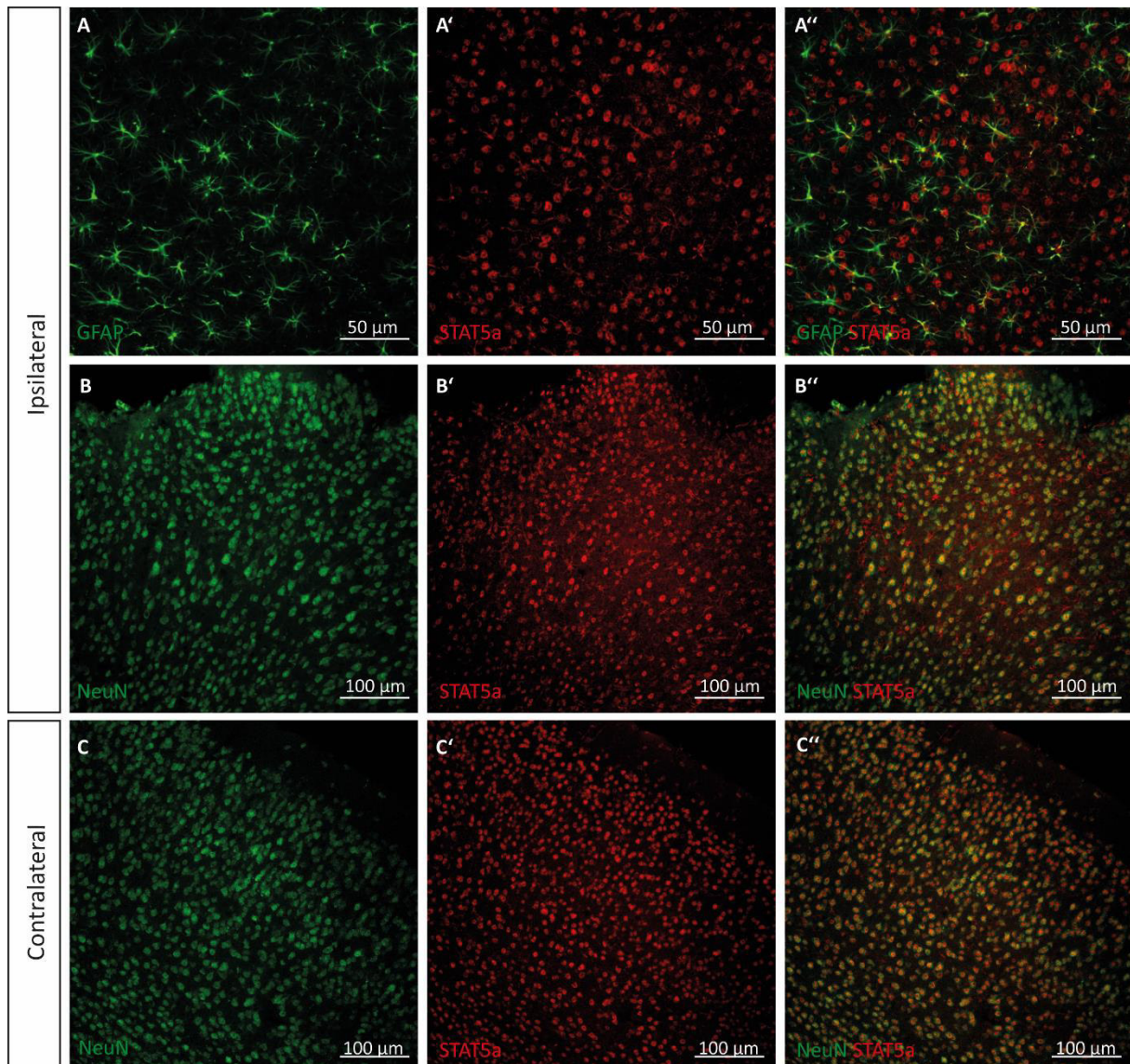


**Fig. 36: Costaining with STAT5a and GFAP or NeuN at 3 dpSW in contra- versus ipsilateral cortices**

Representative micrographs are shown. Contra- and ipsilateral example belong to the same mouse. Stainings against GFAP, NeuN and STAT5a were performed with brain sections from mice that were perfused at 3 dpSW. (A-A'') Overview of the ipsilateral hemisphere stained with GFAP and STAT5a. (B-B'') Overview of the ipsilateral hemisphere stained with NeuN and STAT5a. (C-C'') Overview of the contralateral hemisphere stained with NeuN and STAT5a.

At 3 dpSW we found that STAT5a-immunostaining was present throughout all layers of the injured cortex and mainly colocalized with NeuN (Fig. 36B'') and not with GFAP (Fig. 36A''), in contrast to STAT3. In addition, this localization and the overall signals of STAT5a-immunostaining in the injured cortex were not different from the ones observed in the contralateral cortical hemisphere where STAT5a also colocalized largely with NeuN+ neurons (Fig. 36B'' and C''). Importantly, these data confirmed our impression in western blot analysis that STAT5a was not upregulated after injury compared to the control non-injured cortex.



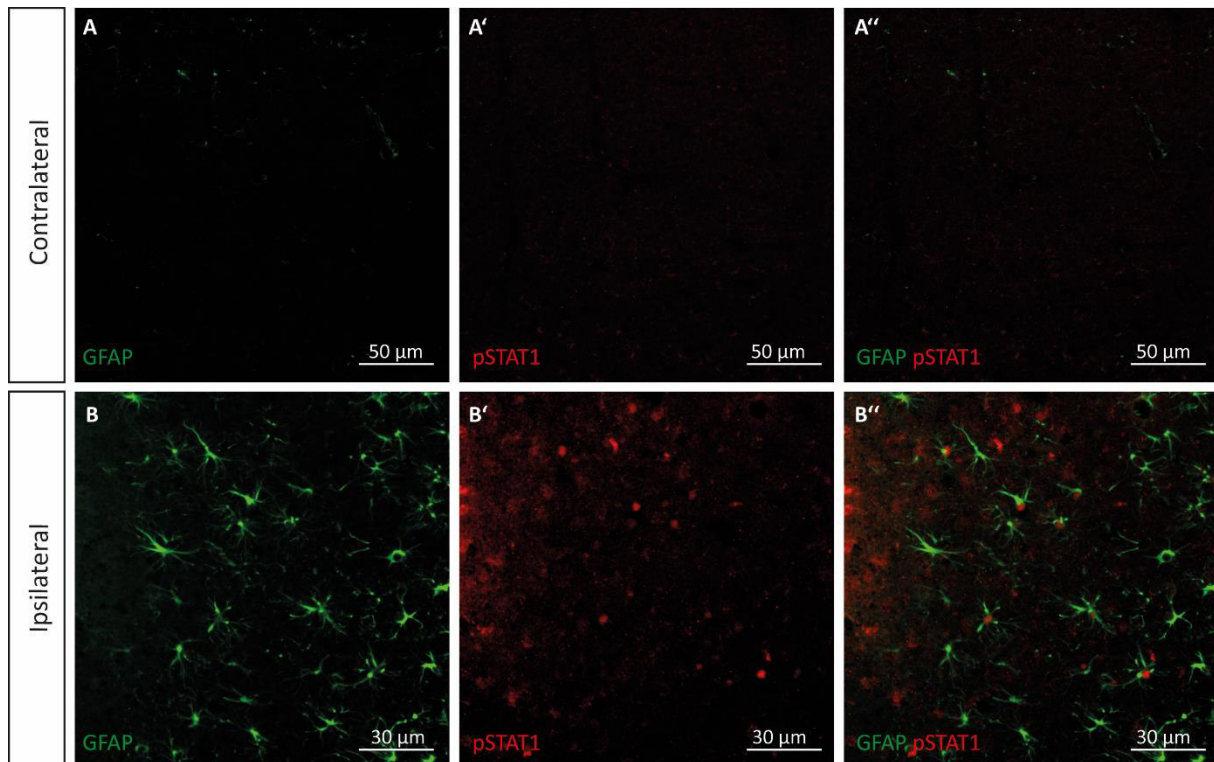


**Fig. 37: Costaining with pSTAT1 and GFAP at 3 dpSW in contra- versus ipsilateral cortices**

Representative micrographs are shown. Contra- and ipsilateral example belong to the same mouse. Stainings against GFAP and pSTAT1 were performed with brain sections from mice that were perfused at 3 dpSW. (A-A'') Overview of the contralateral hemisphere. (B-B'') Ipsilateral hemisphere.

Virtually no pSTAT1+ cells were detected in the contralateral non-injured cortex (Fig. 37A'). In contrast, we could see very few pSTAT1+ nuclei in GFAP+ cells in the injured cortex (Fig. 37B' and B'').

Taken together, these data showed that STAT1 is activated only in very few reactive astrocytes in the injured cortex at 3 dpSW. Furthermore, STAT5a, which is bilaterally expressed in neurons, does not appear to be expressed in reactive astrocytes after stab wound injury.

### 3.3. Does STAT3 signaling inhibit reprogramming of reactive and postnatal astrocytes into neurons?

So far, we showed that STAT3 signaling is activated in a subset of reactive astrocytes early after cortical injury, while no STAT3 activation could be detected in the neurogenic astrocytes in the neurogenic niches. During embryonic development, the activation of STAT3 signaling was shown to inhibit neurogenesis and to promote the differentiation of cerebral cortical precursor cells into astrocytes (Bonni et al., 1997). In addition, forced activation of STAT3

signaling could lead to precocious astrogliogenesis (He et al., 2005). Cellular reprogramming of astroglia into functional neurons emerges as an innovative approach to regenerate lost neurons for brain repair (Berninger et al., 2007, Buffo et al., 2005, Heins et al., 2002, Robel et al., 2011, Amamoto and Arlotta, 2014). Recent literature suggests that it can be enhanced in specific regions and depends on the type of injury as well as on the factors that were provided (Grande et al., 2013). Moreover, it has been shown that astroglia-to-neuron conversion rates can be increased by applying specific neurogenic fate determinants *in vivo* (Guo et al., 2014). However, in many brain regions the astroglia-to-neuron conversion is still limited *in vivo* after injury. Therefore, we hypothesized that the STAT3 activation that we observed to be upregulated in reactive astrocytes in the injured cerebral cortex may contribute to restrict astrocytes in their glial lineage and prevent them to generate neurons when provided with the appropriate neurogenic fate determinants. In order to perform gain- and loss-of-function experiments, we first aimed at finding ways to overactivate and to inhibit STAT3 signaling. Next, we decided to test our hypothesis on the well-established neuronal reprogramming of postnatal cortical astrocytes *in vitro* (as reviewed in subchapter 1.5.3.1.) by activating and inhibiting STAT3 signaling pathways. Indeed, this model was easy to use in the framework of this thesis in order to validate our hypothesis before going on with the *in vivo* condition.

### **3.3.1. Molecular cloning of constructs containing miRNAs against STAT3 and STAT1**

In order to inhibit STAT signaling we took advantage of a well established biological method to reduce protein levels. miRNAs direct translational repression or degradation of messenger RNAs (mRNAs) of protein-coding genes and comprise approx. 20 to 23 nucleotides (Bartel, 2009). The following paragraph will describe the molecular cloning of constructs containing newly designed miRNAs against STAT1 and STAT3. Although the activation of STAT1 was much less pronounced after brain injury compared to STAT3, we decided to also inhibit STAT1 signaling as we postulated that STAT1 may take over the gliogenesis-promoting function of STAT3 when the latter would be downregulated. This was endorsed by the detection of binding sites for STAT1 and 3 in the promoters of STAT1, STAT3, gp130, Jak1, GFAP and S100 $\beta$  (He et al., 2005).

### 3.3.1.1. Design of effective miRNAs against STAT3 and STAT1

miRNAs against STAT3 and STAT1 were designed using the Invitrogen BLOCK-iT™ RNAi Designer (<http://rnaidesigner.invitrogen.com/rnaiexpress/>). Nucleotide sequences of STAT3 and STAT1, respectively, were provided and subsequent resulting highest-ranked suggestions were accepted in a way that miRNAs were distributed over the respective nucleotide sequence (see table 1 and 2 in subchapter 2.1.6.1.). Thus, four miRNAs against STAT1 and three miRNAs against STAT3 with Top and Bottom Strand, each containing linker, mature miR RNAi sequence, a loop sequence and nucleotides 1-8 and 11-21 of the target sequence, were ordered from Life Technologies (Carlsbad, CA, USA). The double-stranded oligo was produced by annealing Top and Bottom Strand according to the manufacturer's protocol. Shortly, equal amounts of Top and Bottom Strand were mixed and heated to 95 °C for 4 minutes.

Subsequently, each double strand miRNA was ligated into a linearized form of pcDNA™6.2-GW/EmGFP-miR. In order to select the most efficient miRNAs to impair STAT3 and STAT1 signaling, western blot of transfected HEK293T cells was performed. Shortly, plated HEK293T cells were exposed to either a vector overexpressing STAT3 (OE STAT3, plasmid IRAVp968E059D from Source BioScience containing complementary DNA (cDNA) encoding for STAT3) and one of the three miRNAs against STAT3 (Fig. 38A) or a vector overexpressing STAT1 (OE STAT1, plasmid IRAVp968D078D from Source BioScience containing cDNA encoding for STAT1) and one of the four miRNAs against STAT1 (Fig. 38B). Each overexpressing vector was also tested with a control-miRNA (prior testing in our laboratory revealed no effect on protein level).

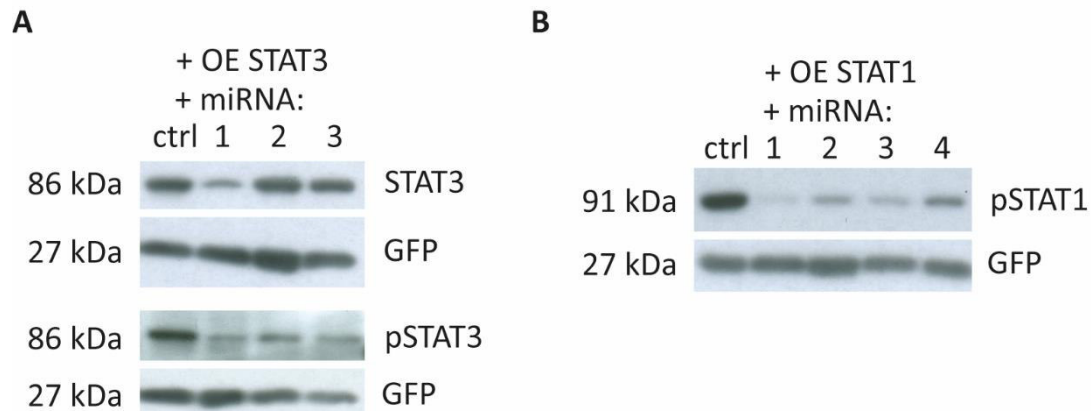


**Fig. 38: Effect of miRNAs against STAT3 and STAT1 in HEK293T cells**

Representative western blots are shown. After plating, HEK293T cells were transfected with the designated miRNAs against STAT1 (B) or STAT3 (A) (each 3  $\mu$ g) and vectors overexpressing STAT1 (B) or STAT3 (A) (1  $\mu$ g). Cells were collected at two days after transfection. Each condition was loaded in a single lane and western blot analysis was performed. Signals for pSTAT1 (B), STAT3 and pSTAT3 (A) were detected. GFP signals served as loading controls.

Two days after transfection the greatest downregulation of STAT3 expression was achieved by the miRNA-STAT3-1. Importantly, the levels of pSTAT3 were also decreased, thus indicating a reduction of the activation of STAT3 signaling (Fig. 38A). The miRNA-STAT1-1 and miRNA-STAT1-3 drastically reduced the levels of pSTAT1 (Fig. 38B). As a consequence, these miRNAs were selected for further analysis.

In order to further investigate the efficiency of the miRNA-STAT3-1, we performed immunostaining for STAT3 in HEK293T cells after transfection (Fig. 39). Shortly, three days after plating HEK293T cells were transfected with OE STAT3 alone (Fig. 39A) or miRNA-STAT3-1 and OE STAT3 (Fig. 39B) and fixed two days after transfection.

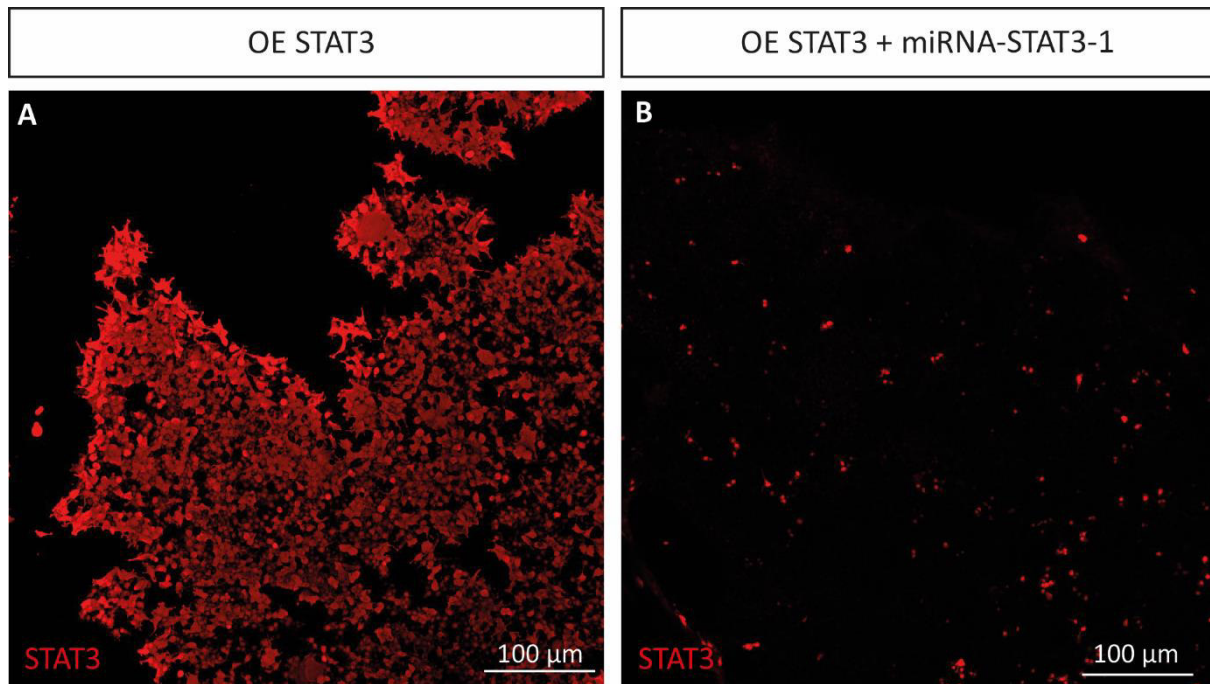


**Fig. 39: Effect of miRNA-STAT3-1 in HEK293T cells**

Representative micrographs are shown. Staining against STAT3 was performed at two days after transfection. Transfection with OE STAT3 alone (A) or with OE STAT3 and miRNA-STAT3-1 (B).

A strong downregulation of STAT3 expression in HEK293T cells transfected with miRNA-STAT3-1 and OE STAT3 (Fig. 39B) compared to OE STAT3 alone (Fig. 39A) was observed. The vast majority of cells showed virtually no expression of STAT3 anymore after transfection with miRNA-STAT3-1. Only sparse cells showed a comparable level of STAT3 expression to cells transfected with OE STAT3 only (Fig. 39B).

Taken together, these data indicated that miRNA-STAT3-1 as well as miRNA-STAT1-1 and miRNA-STAT1-3 strongly impair STAT3- and STAT1 signaling, respectively, and thus were selected for further analysis.

### 3.3.1.2. Cloning of constructs containing several miRNAs against STAT3 and STAT1

In order to increase the expression level of one miRNA and/or to combine different miRNAs to further suppress the STAT3 or STAT1 signaling, we cloned different miRNAs together in one plasmid. Toward this aim, the following constructs were synthesized using restriction enzymes and ligation of DNA fragments:

1. pcDNA<sup>TM</sup>6.2-GW/EmGFP including twice the miRNA-STAT3-1 (called **pcDNA<sup>TM</sup>6.2-GW/EmGFP-2miRNA-STAT3**) by inserting the BamHI/XhoI fragment of pcDNA<sup>TM</sup>6.2-



GW/EmGFP-miRNA-STAT3-1 into the BglII/XhoI digested pcDNA<sup>TM</sup>6.2-GW/EmGFP-miRNA-STAT3-1 vector (Fig. 40A)

2. pcDNA<sup>TM</sup>6.2-GW/EmGFP including miRNA-STAT1-1 and miRNA-STAT1-3 (called **pcDNA<sup>TM</sup>6.2-GW/EmGFP-2miRNA-STAT1**) by inserting the BamHI/XhoI fragment of pcDNA<sup>TM</sup>6.2-GW/EmGFP-miRNA-STAT1-3 into the BglII/XhoI digested pcDNA<sup>TM</sup>6.2-GW/EmGFP-miRNA-STAT1-1 vector (Fig. 40B)
3. pcDNA<sup>TM</sup>6.2-GW/EmGFP including miRNA-STAT1-1, miRNA-STAT1-3 and twice the miRNA-STAT3-1 (called **pcDNA<sup>TM</sup>6.2-GW/EmGFP-2miRNA-STAT1/3**) in a four fragment ligation by:
  - a. inserting the BamHI/XhoI fragment of pcDNA<sup>TM</sup>6.2-GW/EmGFP-miRNA-STAT1-1 into the BglII/XhoI fragment of pcDNA<sup>TM</sup>6.2-GW/EmGFP-miRNA-STAT3-1 (Fig. 40C, 1),
  - b. the Sall/BglII fragment of pcDNA<sup>TM</sup>6.2-GW/EmGFP-miRNA-STAT3-1 into the Sall/BamHI fragment of the prior to this produced pcDNA<sup>TM</sup>6.2-GW/EmGFP-2miRNA-STAT3/1 (Fig. 40C, 2)
  - c. and the BamHI/XhoI fragment of pcDNA<sup>TM</sup>6.2-GW/EmGFP-miRNA-STAT1-3 into the BglII/XhoI fragment of pcDNA<sup>TM</sup>6.2-GW/EmGFP-3miRNA-STAT3/1 (Fig. 40C, 3).

Each fragment ligation step was performed by first fragmenting the plasmids by using restriction digestion. Subsequently, DNA fragments were separated using agarose gel electrophoresis and desired fragments were cut out and purified. DNA ligation of these designated fragments was followed by transformation of chemo-competent E.coli and small scale DNA preparation (MiniPrep) including extraction of the DNA and final analysis of DNA fragments. Large scale DNA preparations (MaxiPrep) were then used to increase the amount of DNA.

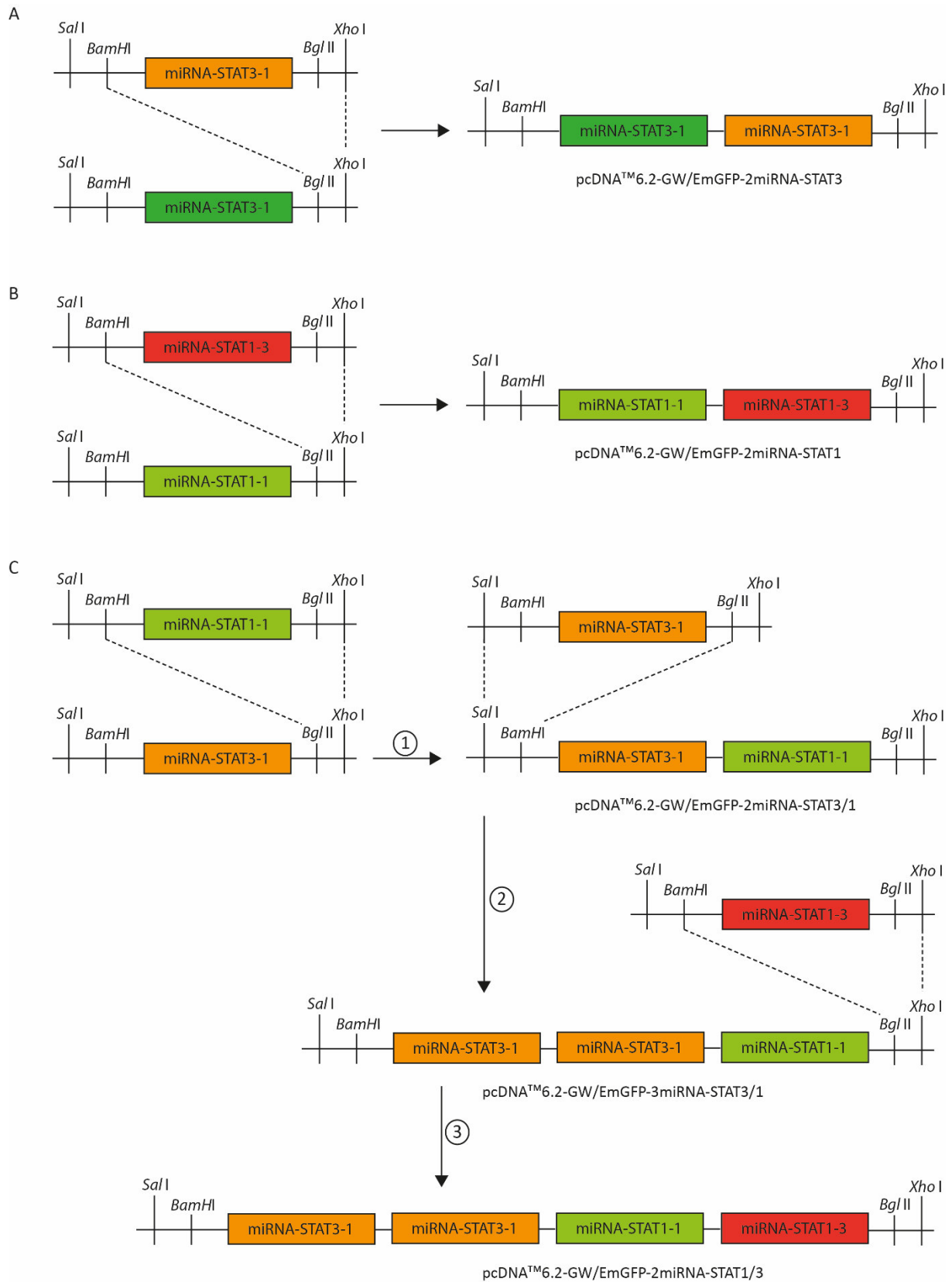


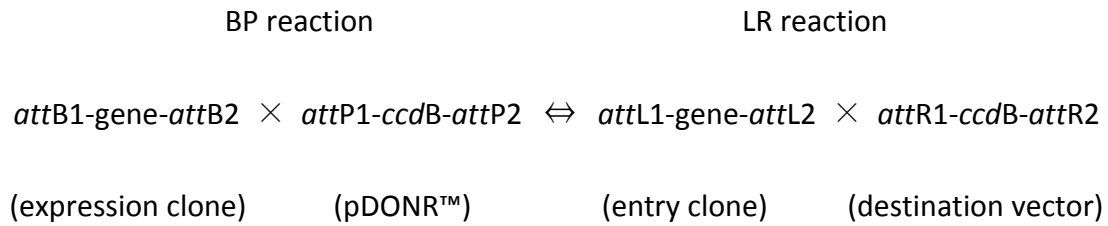
**Fig. 40: Cloning of constructs containing several miRNA against STAT3 and/or STAT1**

Three constructs were synthesized using restriction enzymes and ligation of DNA fragments. (A) **pcDNA<sup>TM</sup>6.2-GW/EmGFP-2miRNA-STAT3** by inserting the BamHI/XhoI fragment of pcDNA<sup>TM</sup>6.2-GW/EmGFP-miRNA-STAT3-1 into the BglII/XhoI digested pcDNA<sup>TM</sup>6.2-GW/EmGFP-miRNA-STAT3-1 vector, (B) **pcDNA<sup>TM</sup>6.2-GW/EmGFP-2miRNA-STAT1** by inserting the BamHI/XhoI fragment of pcDNA<sup>TM</sup>6.2-GW/EmGFP-miRNA-STAT1-3 into the BglII/XhoI digested pcDNA<sup>TM</sup>6.2-GW/EmGFP-miRNA-STAT1-1 vector, (C) **pcDNA<sup>TM</sup>6.2-GW/EmGFP-2miRNA-STAT1/3** in a four fragment ligation by inserting the BamHI/XhoI fragment of pcDNA<sup>TM</sup>6.2-GW/EmGFP-miRNA-STAT1-1 into the BglII/XhoI fragment of pcDNA<sup>TM</sup>6.2-GW/EmGFP-miRNA-STAT3-1 (1), the Sall/BglII fragment of pcDNA<sup>TM</sup>6.2-GW/EmGFP-miRNA-STAT3-1 into the Sall/BamHI fragment of the prior to this produced pcDNA<sup>TM</sup>6.2-GW/EmGFP-2miRNA-STAT3/1 (2) and the BamHI/XhoI fragment of pcDNA<sup>TM</sup>6.2-GW/EmGFP-miRNA-STAT1-3 into the BglII/XhoI fragment of pcDNA<sup>TM</sup>6.2-GW/EmGFP-3miRNA-STAT3/1 (3).

**3.3.1.3. Cloning of the miRNAs against STAT3 and STAT1 into retroviral vectors**

We hypothesized that strong and persistent expression of the miRNAs directed against STAT3 and STAT1 expression would be helpful to evaluate their effects on neuronal reprogramming of astrocytes. Previously used long terminal repeat (LTR)-driven Moloney Murine Leukemia Virus (MMLV)-derived retroviral constructs were shown to be only 2-3 fold higher than endogenous expression (Heins et al., 2002, Heins et al., 2001) and even more important prone to silencing (Gaiano et al., 1999). To avoid these constraints we decided to subclone the miRNAs into a self-inactivating retroviral vector driving gene expression under the control of a chicken beta-actin promoter (pCAG) that was shown to sustain long-term expression over months in the adult mouse brain (Zhao et al., 2006) and to more efficiently convert astroglia into neurons (Heinrich et al., 2010).

First, we changed the backbone from our so far used pcDNA<sup>TM</sup>6.2-GW/EmGF (for miRNAs) and pCMV-SPORT6 (for OE STAT3 and OE STAT1) to the retroviral pCAG backbone. To be able to perform this change we used the Gateway Technology (Life Technologies, Carlsbad, CA, USA). This cloning method uses site-specific recombination properties of bacteriophage lambda (Landy, 1989) to be able to efficiently move DNA sequences into different vector systems. It uses two reactions, the BP and LR reaction (named after respective flanking *att* sites, see reaction below), to move from expression clone and pDONR to entry clone and destination vector (BP reaction) or vice versa (LR reaction):



The BP reaction was conducted using the respective vector encoding the different miRNA combinations (pcDNA™6.2-GW/EmGFP-2miRNA-STAT3, pcDNA™6.2-GW/EmGFP-2miRNA-STAT1 or pcDNA™6.2-GW/EmGFP-2miRNA-STAT1/3) and the pDONR™221 vector (Life Technologies, Carlsbad, CA, USA). The resulting entry clone was then reacted to the retroviral destination vector pCAG.

The same method was applied to OE STAT3 and OE STAT1 as well as the retroviral destination vector pCAG-IRES-GFP.

First, in order to control our molecular cloning, we aimed at showing that pCAG-EmGFP-2miRNA-STAT3, pCAG-EmGFP-2miRNA-STAT1 and pCAG-EmGFP-2miRNA-STAT1/3 indeed comprise the respective miRNA sequence and sequenced the appropriate part of these vectors (for confirming results see section 2.1.7.2., for sequencing method see section 2.2.5.9.). Their correspondent effects on the expression levels of STAT3 and STAT1 were further analyzed by western blot of transfected HEK293T cells (Fig. 41A and B). Shortly, HEK293T cells were transfected with the retroviral vector plasmids: pCAG-STAT3-IRES-GFP (OE STAT3, Fig. 41A) or pCAG-STAT1-IRES-GFP (OE STAT1, Fig. 41B) plus a miRNA-control (ctrl) or pCAG-EmGFP-2miRNA-STAT3 (mi3, Fig. 41A), pCAG-EmGFP-2miRNA-STAT1 (mi1, Fig. 41B) or pCAG-EmGFP-2miRNA-STAT1/3 (miAll, Fig. 41A/B).

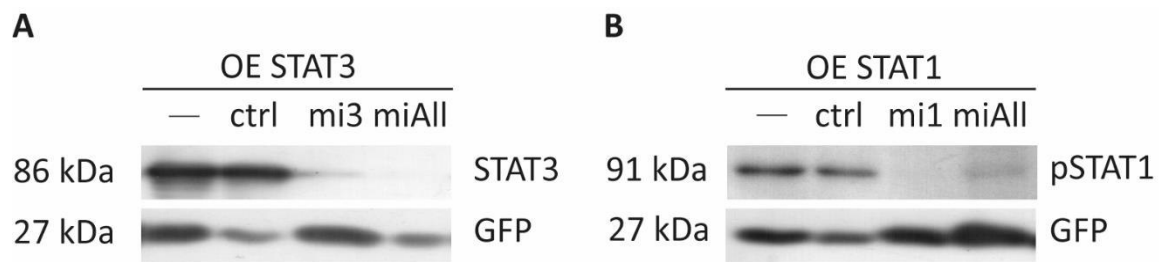


**Fig. 41: Effects of retroviral backbone plasmids expressing STAT3, STAT1, 2miRNA3, 2miRNA1 or 2miRNA3/1**

Representative western blots are shown. After plating, HEK293T cells were transfected with the final plasmids containing retroviral backbone encoding STAT3 (A) or STAT1 (B) (1  $\mu$ g) and either the designated miRNAs against STAT3 or STAT1 or a control-miRNA (each 3  $\mu$ g). Cells were collected at two days after transfection. Each condition was loaded in a single lane. Signals for pSTAT1 and STAT3 were detected. GFP signals served as loading controls. mi3: 2miRNA1-STAT3, mi1: 2miRNA1/3-STAT1, miAll: 2miRNA-STAT1/3, ctrl: control-miRNA.

The vectors pCAG-EmGFP-2miRNA-STAT3 encoding miRNAs against STAT3 (Fig. 41A) and pCAG-EmGFP-2miRNA-STAT1 encoding miRNAs against STAT1 (Fig. 41B) were able to decrease the expression level of STAT3 and pSTAT1, respectively, to a level that was not detectable anymore. In addition, the vector pCAG-EmGFP-2miRNA-STAT1/3 encoding miRNAs against both STAT3 and STAT1 decreased the expression of both STAT3 and pSTAT1 equally well. Subsequently, viral preparations were performed (see subchapter 2.2.5.10.).

Overall, we were able to produce retroviral vectors that encode either the different combinations of miRNAs, STAT3 or STAT1 under the control of a strong and silencing-resistant promoter.

### 3.3.2. Expression analysis of STAT3 and pSTAT3 in postnatal astrocytes

As reviewed above, our lab has previously shown that astrocytes isolated *in vitro* from the postnatal cortex can be directly reprogrammed into fully functional neurons by forced expression of neurogenic fate determinants (Heinrich et al., 2010, Heinrich et al., 2011, Berninger et al., 2007). In addition, the neurotransmitter identity of the reprogrammed neurons could be achieved by overexpressing selective transcription factors. In particular, the transcription factor Neurog2, known to instruct the generation of glutamatergic neurons during embryonic development was shown to drive astroglia-derived neurons toward a glutamatergic identity. Conversely, forced expression of Mash1 and/or Dlx2, known to instruct a GABAergic neuronal phenotype, was converting postnatal astrocytes into inhibitory neurons. We decided to assess in this model, whether (i) activation of STAT3 signaling would impair

neuronal reprogramming of postnatal astrocytes, and conversely (ii) downregulation of STAT3 signaling would enhance the efficiency of such a reprogramming. Indeed, this experiment represented the first step to assess the effects of STAT-signaling on reprogramming of astrocytes, before moving *in vivo* after brain injury, which was clearly beyond the scope of this MD thesis. First, we assessed whether postnatal astrocytes could partially mimic adult reactive astrocytes, i.e. if they express STAT3 and show STAT3 signaling activation. This step was important for the assessment whether it is reasonable to perform gain- and loss-of-function experiments of STAT3 signaling in postnatal astrocytes. We investigated the expression and activation level of pSTAT3 in postnatal astrocytes under control conditions by performing western blot analysis of cultured astrocytes of mouse cortices that were dissected at postnatal day 1 and 6 and expanded in culture for seven days (Fig. 42). We observed that STAT3 was expressed and activated in astrocytes in both conditions. In addition, to further confirm the specificity of STAT3 expression and activation of STAT3 signaling, we investigated the expression levels in liver extracts, known to express both STAT3 forms (Alonzi et al., 2001), as positive controls. We indeed found STAT3 expression in the cytoplasmic liver extract fraction and pSTAT3 in the nuclear liver extract fraction (Fig. 42).

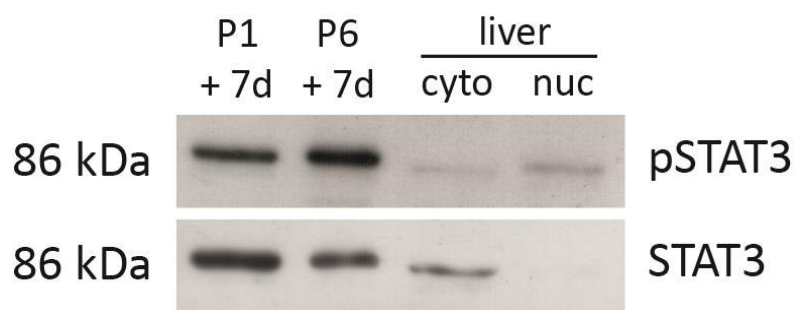


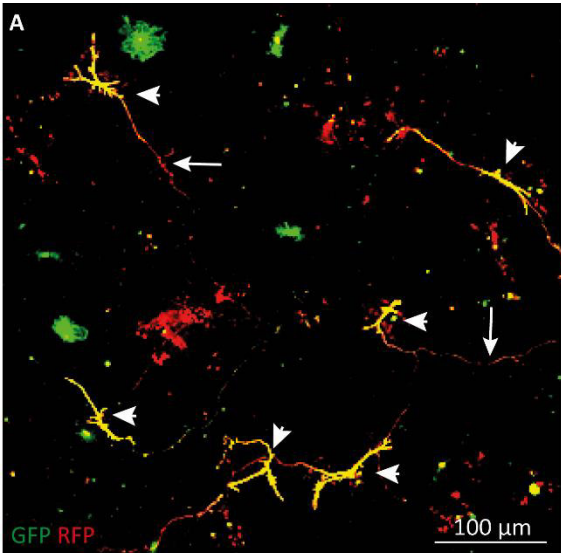
**Fig. 42: Expression of STAT3 and pSTAT3 in astrocytes**

Representative western blots are shown. Postnatal astrocytes were collected seven days after plating. Nuclear and cytoplasmic extracts of liver tissue were loaded as controls. Antibodies against STAT3 and pSTAT3 were then applied.

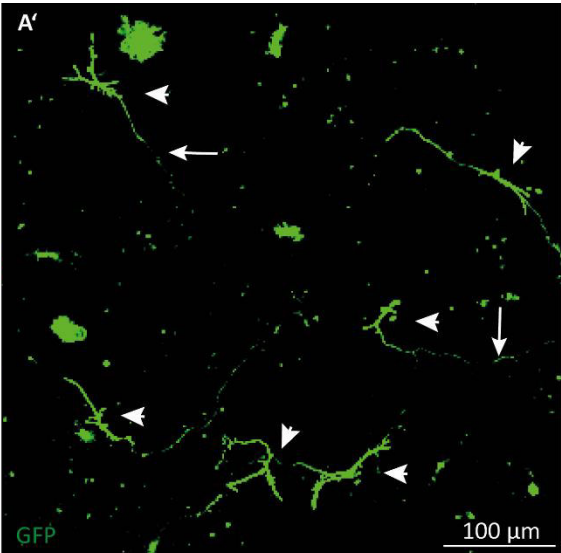
These results showed that STAT3 is expressed and activated in postnatal astrocytes, similarly to what we found before for adult reactive astrocytes. This indicated that *in vitro* cultured postnatal astrocytes can be used as a model for investigating the role of STAT3 signaling on glia-to-neuron conversion.

### **3.3.3. Effects of STAT3 signaling activation on neuronal reprogramming of postnatal astrocytes**

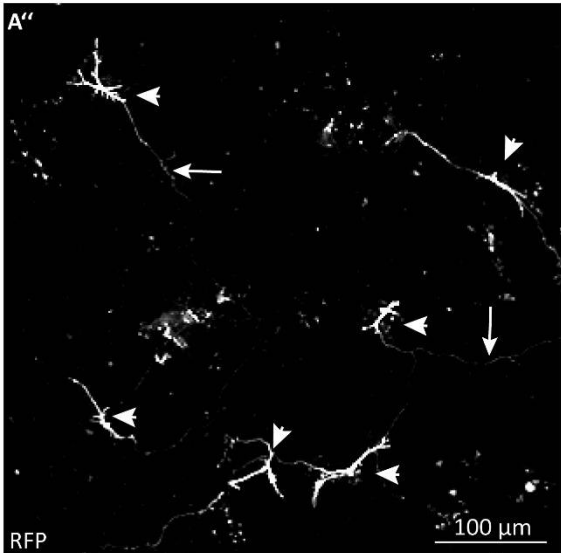
To examine the effects of STAT3 signaling on neuronal reprogramming of postnatal astrocytes, we aimed at further increasing STAT3 signaling activation compared to the endogenous physiological activation and therefore used in the first set of experiments a constitutively active form of STAT3, STAT3C, that by substitution of two cysteine residues within the C-terminal loop of the SH2 domain of STAT3 can spontaneously dimerize, bind to DNA and activate transcription independently of the phosphorylation status (Bromberg et al., 1999) (see 2.1.7. or <http://www.addgene.org/8722/#>). Reprogramming of postnatal astrocytes into neurons was induced as described before by forced expression of Mash1 (Berninger et al., 2007, Heinrich et al., 2010). Shortly, cortices of P6 mice were dissected, the cells dissociated, plated and passaged after seven days. One day later these postnatal astrocytes were either transfected with (i) pCAG-Mash1-IRES-DsRed and pCMV-STAT3C, with (ii) pCAG-Mash1-IRES-DsRed and pCMV-GFP or with (iii) pCAG-IRES-DsRed and pCMV-STAT3C and fixed nine days after transfection (Fig. 43). I counted the number of Mash1-induced neurons amongst cotransfected cells in these different conditions.



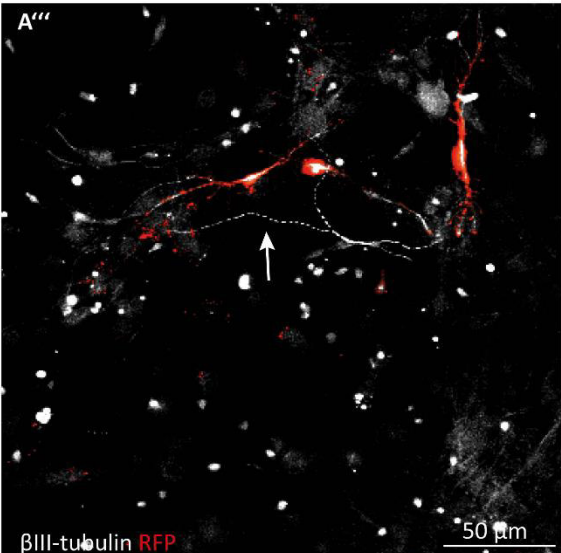
pCMV-GFP  
pCAG-Mash1-IRES-DsRed



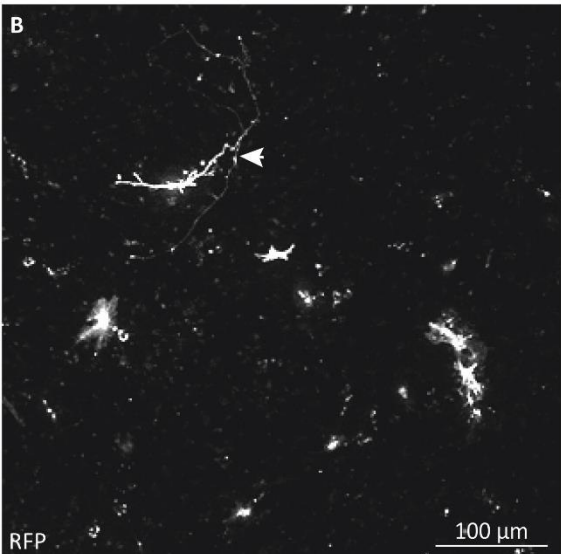
pCMV-GFP  
pCAG-Mash1-IRES-DsRed



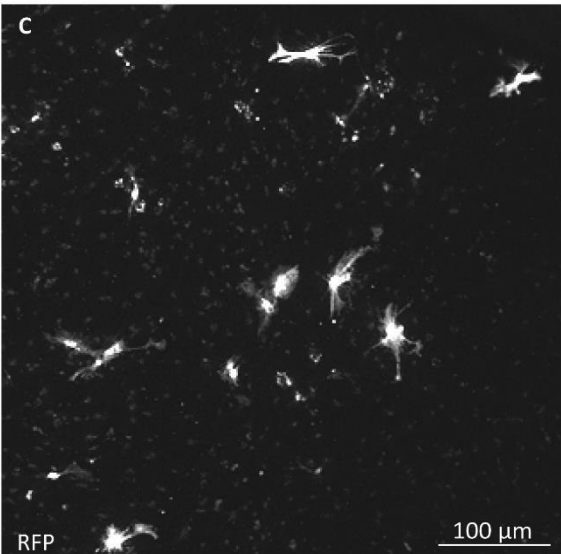
RFP  
pCMV-GFP  
pCAG-Mash1-IRES-DsRed



βIII-tubulin RFP  
pCMV-GFP  
pCAG-Mash1-IRES-DsRed



RFP  
pCMV-STAT3C  
pCAG-Mash1-IRES-DsRed



RFP  
pCMV-STAT3C  
pCAG-IRES-DsRed



**Fig. 43: Astrocytes isolated from the cerebral cortex at postnatal day 6 at 9 days after transfection with Mash1 and GFP or Mash1 and STAT3C or STAT3C and DsRed**

P6 astrocytes that were fixed at nine days after transfection with either Mash1 and GFP (A-A'') or Mash1 and STAT3C (B) or STAT3C and DsRed (C). Staining with RFP, GFP,  $\beta$ III-tubulin and DAPI was applied. Representative micrographs are shown. Short arrowheads in A-A'' and B indicate RFP- and GFP-positive cells or RFP-positive cells, respectively. Longer arrows in A-A'' indicate neuronal processes of RFP- and GFP-positive cells.

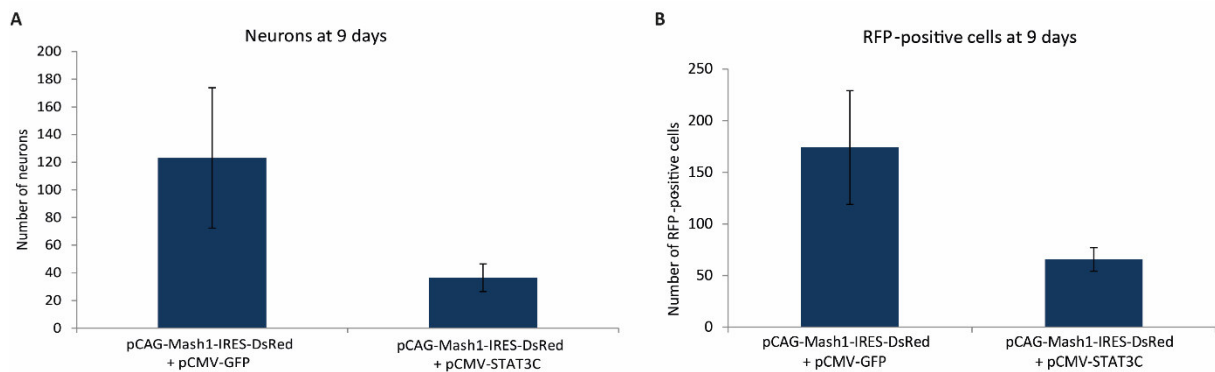


**Fig. 44: Statistical analysis of P6 astrocytes at 9 days after transfection with Mash1 and GFP or Mash1 and STAT3C**

(A) Quantification of neurons at nine days after transfection with either Mash1 and GFP or Mash1 and STAT3C. Values are given as mean  $\pm$  SEM, n = 5 independent experiments. (B) Quantification of RFP-positive cells at nine days after transfection with either Mash1 and GFP or Mash1 and STAT3C. Values are given as mean  $\pm$  SEM, n = 5 independent experiments.

Several reporter+ cells exhibited a neuronal morphology following transfection with pCAG-Mash1-IRES-DsRed and pCMV-GFP and stained positively for RFP and  $\beta$ III-tubulin, indicating that these cells were induced neurons reprogrammed by Mash1 (Fig. 43A-A''). In contrast, when astrocytes were transfected with pCAG-Mash1-IRES-DsRed and pCMV-STAT3C, we could observe some induced neuronal cells, but they were strongly reduced in number (Fig. 43B) (here our co-transfection rate was virtually 100 % as seen with GFP and RFP encoding constructs, data not shown). As expected, we could not detect any reprogrammed neurons following transfection with pCMV-STAT3C and pCAG-IRES-DsRed (Fig. 43C). When we analyzed these experiments quantitatively, we indeed observed a much lower number of neurons nine days after transfection with Mash1 and STAT3C compared to Mash1 and GFP ( $36 \pm 10$  versus  $123 \pm 51$   $\beta$ III-tubulin+ cells, n = 5 independent experiments, Fig. 44A). The percentage of neurons per RFP-positive cells was slightly decreased after transfection with Mash1 and STAT3C compared to Mash1 and GFP ( $54,1 \% \pm 11,7 \%$  versus  $65,5 \% \pm 10,4 \%$ ). This suggested that activation of STAT3 signaling in postnatal astrocytes impaired Mash1-induced neuronal reprogramming.

In parallel the number of Mash1-transfected cells (RFP-positive cells) observed at nine days after transfection was also decreased with Mash1 and STAT3C compared to Mash1 and GFP ( $66 \pm 11$  versus  $174 \pm 55$  Mash1-transfected cells,  $n = 5$  independent experiments, Fig. 44B).

This raised the hypothesis that forced expression of STAT3C itself or in combination with Mash1 may lead to a reduced number of astrocytes or astrocyte-derived neurons. First, in order to rule out that the number of transfected cells would have been initially lower with Mash1 and STAT3C versus Mash1 and GFP, we counted the number of transfected cells based on their RFP fluorescence at two days post transfection (Fig. 45).

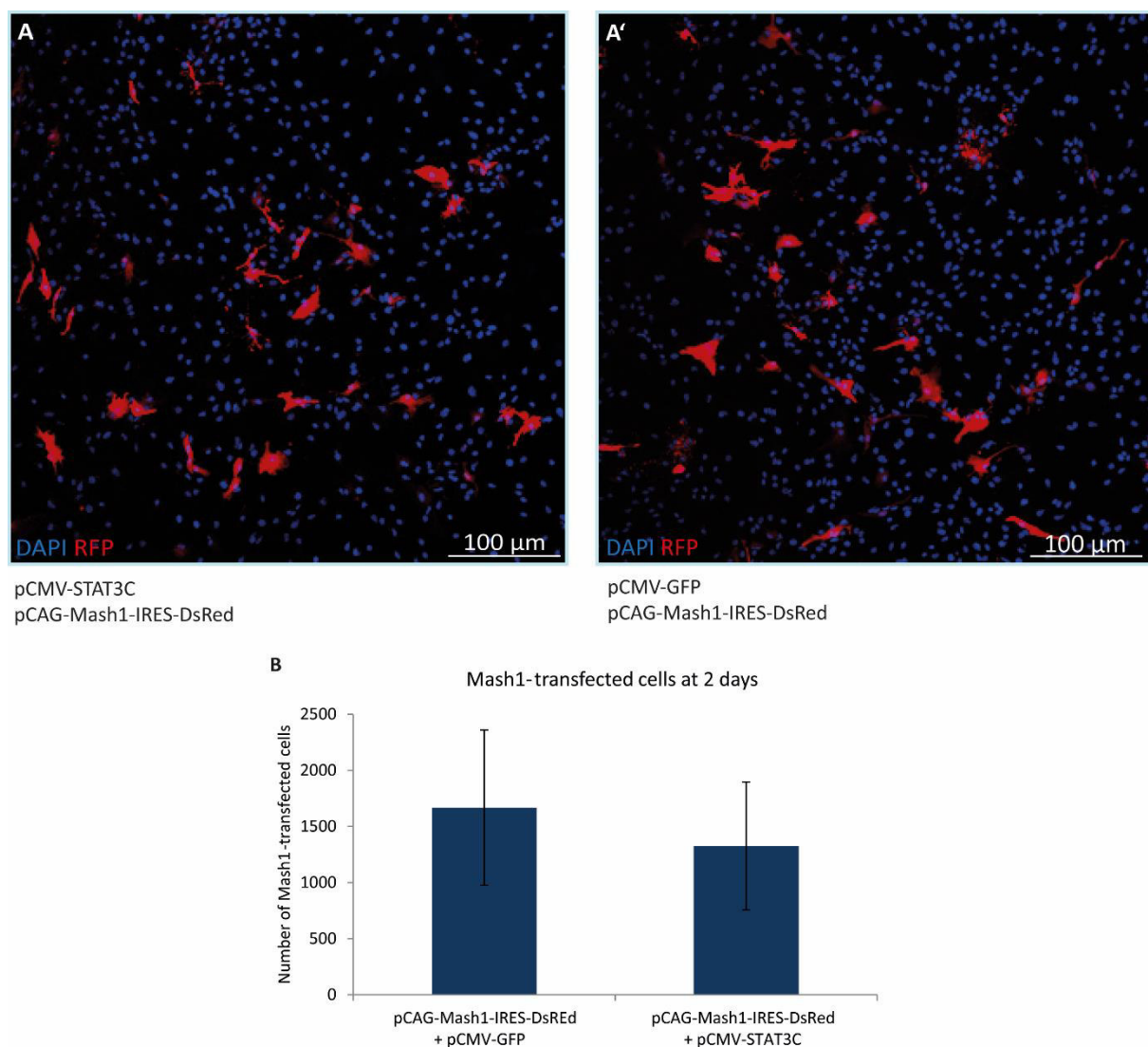


**Fig. 45: Analysis of P6 astrocytes at 2 days after transfection with Mash1 and GFP or Mash1 and STAT3C**

(A and A') P6 astrocytes that were fixed at two days after transfection with either Mash1 and GFP (A') or Mash1 and STAT3C (A). Stainings with RFP and DAPI were applied. Representative micrographs are shown. (B) Quantification of RFP+ cells at two days after transfection with either Mash1 and GFP or Mash1 and STAT3C per well. Values are given as mean  $\pm$  SEM,  $n = 3$  independent experiments.

There was no significant difference in the number of Mash1-transfected cells between the P6 astrocytes that were transfected with Mash1 and GFP and the ones that were transfected with Mash1 and STAT3C ( $1668 \pm 692$  versus  $1325 \pm 570$  RFP+ cells,  $n = 3$  independent experiments, Fig. 45B). Moreover, we observed that the transfected cells exhibited a star-shaped morphology indicating their astrocytic nature (Fig. 45A and A'). Thus, we could rule out that the numbers of transfected cells were initially different between the different conditions.

Next, we investigated whether forced expression of STAT3C alone would induce cell death of postnatal astrocytes at nine days post transfection. We found that the number of cells transfected with pCMV-STAT3C and pCAG-IRES-DsRed (Fig. 43C) was not different from the cells transfected with pCMV-GFP and pCAG-IRES-DsRed in control conditions ( $180,7 \pm 49,7$  versus  $154,9 \pm 16,5$ ,  $n = 5$  independent experiments,  $p = 0,634$ ). These data showed that forced expression of STAT3C per se did not induce cell death of postnatal astrocytes.

Taken together, these data strongly suggested that forced expression of Mash1 in combination with STAT3C could lead to cell death of astrocytes or astrocyte-derived neurons, as compared to forced expression of either Mash1 or STAT3C alone. This could be a consequence from the activation of two conflictive differentiation pathways, Mash1 inducing a neurogenic conversion of astrocytes, and STAT3 protein driving genes that could possibly lead to maintain these cells in their glial lineage and/or induce their proliferation.

#### **3.3.4. Effects of STAT3 level reduction on reprogramming of postnatal astrocytes into neurons**

Next, we investigated the impact of STAT3 signaling inhibition on neuronal reprogramming of postnatal astrocytes and therefore used our newly designed miRNA plasmid against STAT3 (see subchapter 3.3.1.). Cortices of P6 mice were dissected, plated and passaged after seven days. One day later these postnatal astrocytes were transfected with pCAG-EmGFP-2miRNA-STAT3. We applied immunocytochemistry for pSTAT3 and GFP two days after transfection and found virtually no STAT3 signaling activation in cells transfected with the plasmid containing the miRNAs against STAT3 (Fig. 46A). Subsequently, we transfected postnatal astrocytes with either (i) pCAG-Mash1-IRES-DsRed and pCMV-GFP or with (ii) pCAG-Mash1-IRES-DsRed and pCAG-EmGFP-2miRNA-STAT3, and fixed nine days after transfection (Fig. 46B

and C). While the number of transfected cells did not differ significantly between Mash1 and GFP compared to Mash1 and miRNAs against STAT3 at nine days post transfection ( $68 \pm 53$  RFP+ cells in Mash1 and GFP versus  $50 \pm 22$  RFP+ cells in Mash1 and pCAG-2miRNA-STAT3,  $p = 0,763$ ,  $n = 3$  independent experiments, Fig. 46D), the proportion of neurons per transfected cells was higher after transfection with Mash1 and miRNAs against STAT3 than after Mash1 and GFP transfection ( $57,5 \pm 6,9$  % of neurons per transfected cells in Mash1 and pCAG-EmGFP-2miRNA-STAT3 versus  $39,4 \pm 10,8$  % in Mash1 and GFP,  $n = 3$  independent experiments, Fig. 46E). This difference did not reach significance due to high variations observed in the survival of the cells. Additional experiments should be performed to enable a reliable statistical analysis.

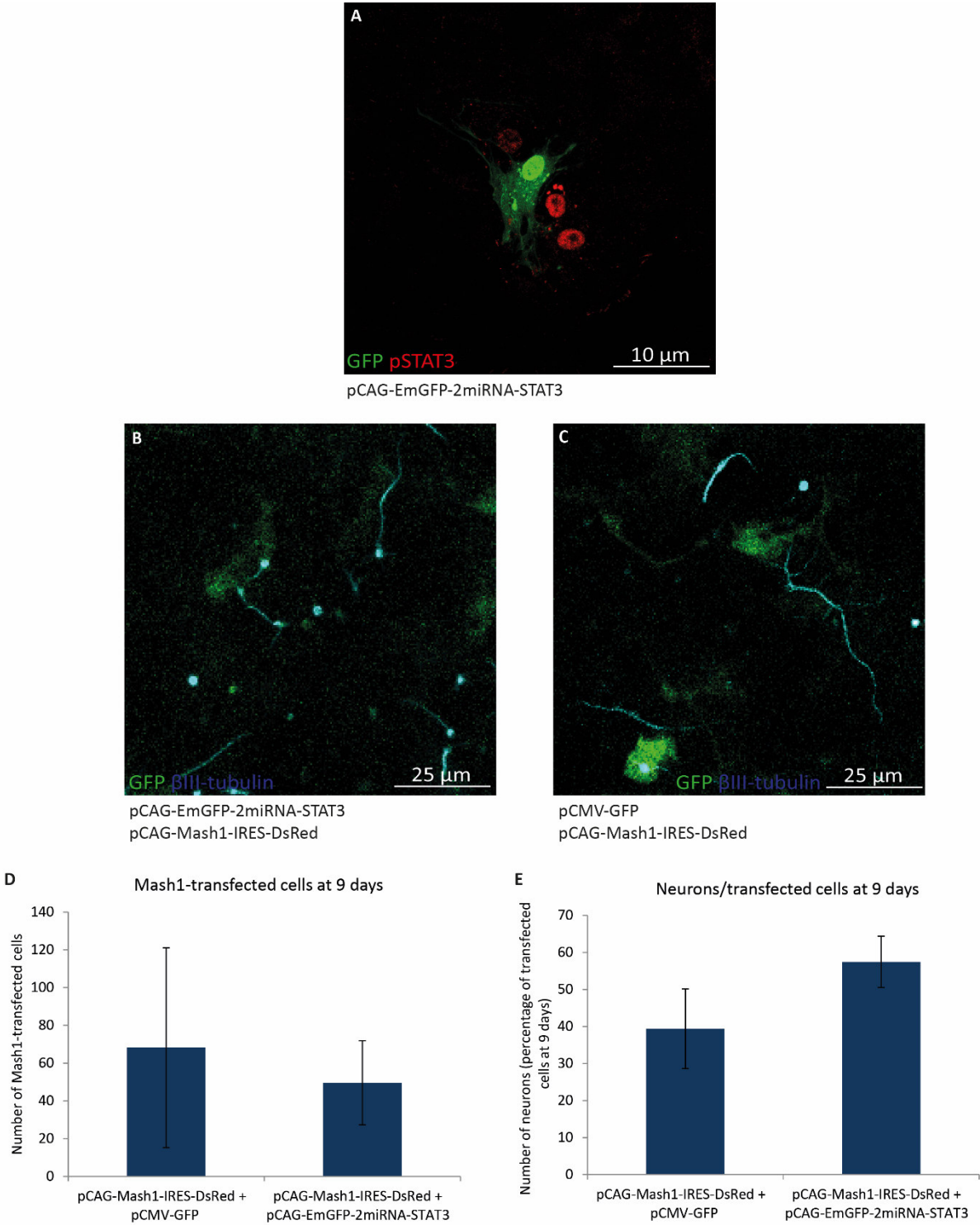


**Fig. 46: Analysis of P6 astrocytes at 2 and 9 days after transfection with Mash1 and GFP or Mash1 and miRNAs against STAT3**

(A) P6 astrocytes that were fixed at two days after transfection with miRNAs against STAT3. Staining with GFP and pSTAT3 was applied. Representative micrograph is shown. (B) and (C) P6 astrocytes that were fixed at nine days after transfection with Mash1 and miRNAs against STAT3 (B) or Mash1 and GFP (C). Staining with GFP and  $\beta$ III-tubulin was applied. Representative micrographs are shown. (D) and (E) Quantification of transfected cells at nine days (D), and number of neurons per transfected cells at nine days (E), with either Mash1 and GFP or Mash1 and miRNAs against STAT3. Values are given as mean  $\pm$  SEM, n = 3 independent experiments.

Nevertheless, these data suggested that antagonizing STAT3 signaling by the addition of a miRNA against STAT3 improved the neuronal reprogramming efficiency induced by Mash1 compared to Mash1 alone. Furthermore, antagonizing STAT3 signaling in cells transfected with Mash1 did not reduce cell numbers, in contrast to our previous results showing that instead forced expression of STAT3 and Mash1 led to reduced numbers of postnatal astrocytes.

Taken together, our data revealed that endogenous STAT3 signaling impairs the neuronal reprogramming of postnatal astrocytes induced by Mash1.

In addition to pCAG-EmGFP-2miRNA-STAT3, we also generated pCAG-EmGFP-2miRNA-STAT1 and pCAG-EmGFP-2miRNA-STAT1/3 (see subchapter 3.3.1.). These constructs remain to be tested in order to further examine the possible effect that in the case of STAT3 suppression STAT1 would overtake parts of the gliogenic function of STAT3 as suggested by He et al. (He et al., 2005).

### **3.4. Do reactive astrocytes acquire stem cell properties after acute invasive injury?**

Reactive astrocytes at the site of injury appear as potential candidates for *in vivo* reprogramming, in order to generate new neurons from an endogenous cellular source. Our data showed that activation of STAT3 signaling in postnatal astrocytes may impair their conversion into neurons. This suggests that the activation of STAT3 signaling that we evidenced in reactive astrocytes in the adult brain following injury may also exert inhibiting effects on the neuronal reprogramming when these astrocytes are provided with neurogenic transcription factors. This hypothesis remains to be tested. In addition the lab of Magdalena Götz could recently show that reactive astrocytes acquire neural stem cell-like properties in response to stab wound injury in the cerebral cortex (Buffo et al., 2008), as revealed by their ability to generate self-renewing and multipotent neurospheres *in vitro*. This also suggests that reactive astrocytes would be amenable to reprogramming into neurons when provided with the appropriate neurogenic fate determinants.

During my MD thesis, I was also involved in a larger project aiming at comparing the properties of reactive glia in the injured brain in response to different injury paradigms. In particular, we investigated whether the stem cell response of reactive astrocytes is a general feature

observed after acute invasive injury inducing a high rate of astrocyte proliferation. To this aim, we used again the experimental stroke model (MCAo), and examined whether reactive astrocytes isolated from the ischemic cortex, would generate neurospheres *in vitro*. Shortly, injured cortices of mice that underwent MCAo were dissected 3-4 days after injury and dissociated for subsequent neurosphere cultures (see subchapter 2.2.4.5). We observed the formation of neurospheres to a similar level as for the stab wound-injured tissue. These neurospheres showed the typical hallmarks of stem cells: they could be passaged and were capable of self-renewal as indicated by the formation of secondary neurospheres (Fig. 47). This figure includes additional work by Gwendolyn Behrendt and Lana Sirko, I was only involved in the generation of neurospheres from the MCAo group.

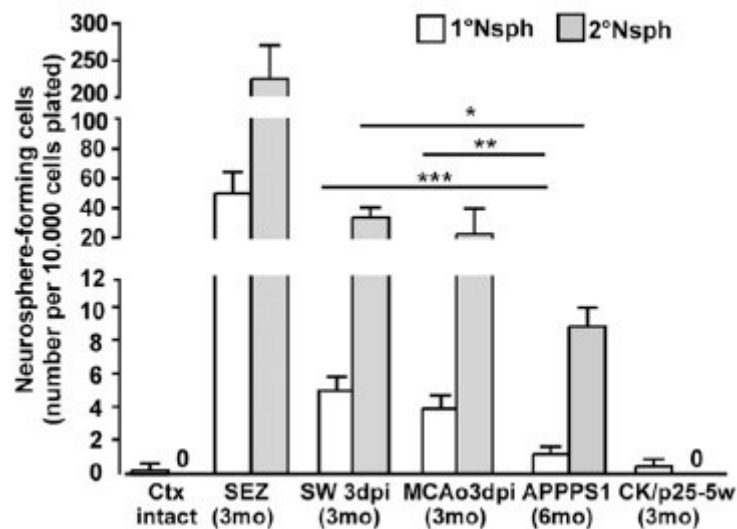


**Fig. 47: Formation of neurospheres from cells from different injury models**

Comparison of the generation of neurospheres from cells from different injury models (stab wound, MCAo, APP/PS1 and CK/p25). White bars indicate primary neurospheres, grey bars indicate secondary neurospheres. \* $p < 0.05$ , \*\* $p < 0.01$ , and \*\*\* $p < 0.001$ . From Sirko et al., 2013.

In order to assess the multipotency of the neurospheres, we exposed the cells to differentiation conditions for seven days and applied immunocytochemistry with antibodies against GFAP (to label astrocytes),  $\beta$ III-tubulin (to label neurons) and O4 (to label cells of the oligodendrocyte lineage). We found that all three cell types were generated by some neurosphere cells derived from the ischemia-injured cortex (Fig. 48A-A'''). This showed the multipotency of these neurosphere cells that constituted about one third of all neurospheres.



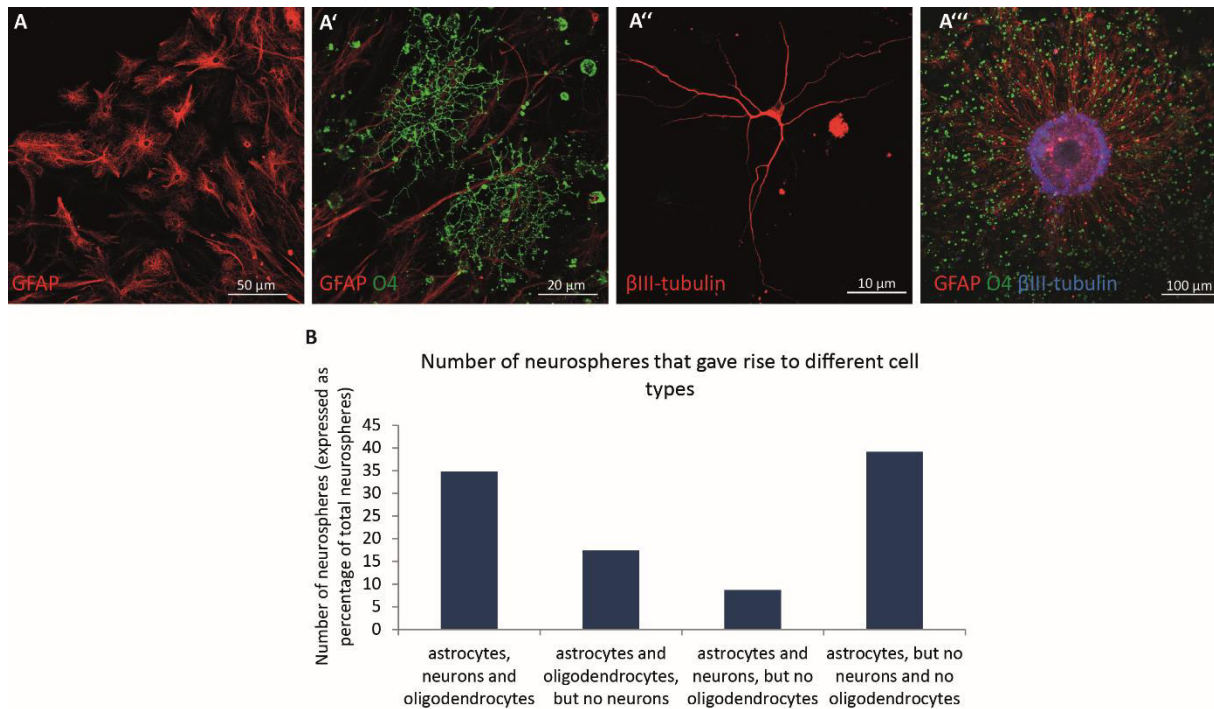


**Fig. 48: Neurosphere assay at 3-4 days after MCAO**

(A) When neurospheres were exposed to differentiation conditions, they generated  $\beta$ III-tubulin+ neurons ((A'') and (A''')), GFAP+ astrocytes ((A), (A') and (A''')) and O4+ oligodendrocytes ((A') and (A''')). Representative micrographs are shown. (B) Quantification showing the differentiation of single plated neurospheres (n = 1 experiment).

Next, we further analyzed the multipotency potentials of single plated neurospheres and found that all of them gave rise to astrocytes. In addition, approximately one third (8/23) of these neurospheres also generated neurons and oligodendrocytes. Nevertheless, approximately 40 % (9/23) generated only astrocytes, four of 23 generated astrocytes and oligodendrocytes and two of 23 generated astrocytes and neurons (Fig. 48B). Thus, almost half (10 of 23) of the neurospheres derived from reactive glia after MCAO showed the potential of generating neurons.

Taken together, these results showed that self-renewing and bipotent neurospheres can be obtained from the MCAO injured cortex. In addition, their degree of neuron generation is comparable to that of neurospheres generated from the stab wound-injured cortex.



## 4. Discussion

### 4.1. Comprehensive summary of the results

In the present work I examined the expression and activation of STAT signaling after brain injury and investigated the impact of STAT3 signaling on the reprogramming of astrocytes into neurons.

We first aimed at performing a thorough analysis of the pattern of expression and activation of STAT signaling after various types of brain lesion. Here we showed with western blot and immunohistochemistry that STAT3 expression is upregulated in the injured cortex after acute invasive injury such as stab wound and ischemia. Furthermore, we demonstrated that ipsilateral to the lesion STAT3 is virtually only expressed in reactive astrocytes, while contralateral it is mainly expressed in mature neurons. In order to determine the activation of STAT3 signaling we examined the expression of the phosphorylated form of STAT3, pSTAT3, and could show its expression exclusively in reactive astrocytes in the injured cortex. By demonstrating this pattern of STAT3 expression and activation not only after stab wound but also in an experimental stroke model, MCAo, we were able to increase the clinical significance of our findings. Compared with these acute invasive brain injury models the activation of STAT3 signaling was lower in mouse models mimicking non-invasive brain injury by exhibiting hallmarks of Alzheimer's disease, APP/PS1 and CK/p25. In contrast to STAT3, we were not able to reveal an unambiguous upregulation of expression and activation of STAT5 and STAT1 signaling after cortical injury.

Together with the susceptibility of reactive astrocytes to be reprogrammed into neurons when provided with the appropriate neurogenic fate determinants and the gliogenic function of STAT3 signaling during embryonic development, these results, showing the activation of STAT3 after acute brain injury, led to the investigation of the potential role of STAT3 signaling on neuronal reprogramming of astrocytes. In order to be able to perform gain- and loss-of-function experiments, we first designed new vector constructs containing STAT3C, a constitutively active form of STAT3, or miRNAs against STAT3, with the purpose to decrease STAT3 expression. Next, we showed both the expression and activation of STAT3 signaling in postnatal astrocytes, which were then used as an established culture system for astrocyte-to-

neuron conversion. We were afterwards able to provide evidence that the combination of Mash1 and STAT3C impairs neuronal reprogramming of postnatal astrocytes *in vitro* compared to Mash1 alone. Of note, we demonstrated by cotransfection of these postnatal astrocytes with Mash1 and miRNAs against STAT3 that reprogramming into neurons could be slightly enhanced *in vitro* compared to transfection with Mash1 alone. Future experiments will be required to study whether such an effect of STAT3 signaling also holds true *in vivo*, by investigating the effects of the delivery of neurogenic genes such as Mash1 and miRNAs to block STAT3 signaling in reactive astrocytes in the injured cortex after stab wound or MCAo.

Moreover, we demonstrated that after MCAo, reactive astrocytes can give rise to neurospheres *in vitro* meaning that they acquire stem cell-like properties after MCAo, as described after stab wound (Buffo et al., 2008). The molecular pathway responsible for this apparently general effect after acute invasive injury is part of ongoing discussion. Shh was already shown to be involved (Sirko et al., 2013), but whether STAT3 signaling plays a role in this context remains to be investigated. Our expression analysis after brain injury showed a correlation between the number of generated neurospheres and the level of STAT3 signaling activation. Indeed, in acute invasive brain injury models (like stab wound and MCAo) reactive astrocytes expressed high levels of pSTAT3 and gave rise to high numbers of neurospheres, while they showed lower levels of pSTAT3 in non-invasive brain injury models (like APP/PS1 and CK/p25) and produced much less neurospheres. Further studies are required to investigate whether activation of STAT3 signaling in reactive astrocytes plays a role in their capacity to acquire stem cell-like properties. Given the described roles of STAT3 signaling for proliferation (Brantley and Benveniste, 2008) and the acquisition of pluripotency (Yang et al., 2010), it is conceivable that the activation of STAT3-signaling supports the formation of neurospheres.

Taken together, we first provided evidence for the activation of STAT3 signaling in reactive astrocytes in different brain injury models. By inhibiting STAT3 signaling we were then able to increase the neuronal reprogramming of astrocytes in culture, suggesting that activation of STAT3 signaling impairs the conversion of astrocytes into neurons. On the other hand, we showed that the formation of neurospheres, indicative for the stem cell potential of astrocytes, correlates positively with the level of STAT3 signaling activation. From our data, one may speculate a dual function of STAT3 signaling over time in reactive astrocytes: it may participate

in their dedifferentiation, acquisition of stem cell properties and scar formation at early time points following injury, which might be beneficial for brain repair. However, at later time points the decrease of STAT3 signaling activation may be required to promote the conversion of these reactive astrocytes into neurons. Future investigations are required to unravel the potential benefit for brain regeneration of either activating or inhibiting STAT3 signaling at defined time points.

## **4.2. Expression and activation of STAT3 in the adult injured cerebral cortex**

So far the STAT3 expression and activation pattern have not been described after stab wound injury to the adult cerebral cortex and in the two mouse models APP/PS1 and CK/p25. Additionally, published data about the expression of STAT after MCAo have been contradictory. Here we investigated the expression and activation of STAT3 signaling in these brain lesion models with western blot and immunohistochemistry in order to be able to evaluate subsequent gain- and loss-of-function experiments for investigating the effects of STAT signaling on reprogramming of reactive astrocytes into neurons.

### **4.2.1. Expression of STAT3 and pSTAT3 within the different subcellular compartments**

Our western blots of subcellular fractionated extracts of brain tissue and our immunohistochemistry data demonstrated that STAT3 is expressed in the cytoplasm and the nucleus, independently of the hemisphere (contra- and ipsilateral), the time and the lesion model. This finding is strongly supported by the theory of the canonical STAT signaling pathway (for review see (Aaronson and Horvath, 2002)), which assumes that STAT monomers are usually existent in the cytoplasm and upon activation by cytokines, translocated into the nucleus after dimerization and phosphorylation. It therefore suggests that virtually no non-phosphorylated STAT proteins should be located in the nucleus. Thus, one may ask why a fraction of STAT3 was detected in the nuclear compartments in our experiments. Here, we need to keep in mind that the antibody used against STAT3 for western blot and immunohistochemistry did not differentiate between non-phosphorylated or phosphorylated STAT3 proteins suggesting that the detected nuclear STAT3 fraction also represents phosphorylated STAT3 proteins. Taking this into consideration, the very low level of STAT3

expression in the nuclear fraction of the contralateral hemisphere that was detected with western blot could display a baseline activation level of the STAT3 signaling pathway.

Fitting with the described canonical STAT signaling cascade and our data on STAT3, we demonstrated that pSTAT3, detected by a phosphorylation site specific antibody in western blot and immunohistochemistry, was mainly localized in the ipsilateral nuclear compartment. Here it is important to note that in general within activated STAT signaling pathways the turnover of the phosphorylation status is very high. Phosphorylated STAT proteins that are translocated into the nucleus will then be dephosphorylated and return to the cytoplasm where they again can be phosphorylated (Haspel et al., 1996). So when evaluating the activation of the STAT signaling cascade by only measuring the nuclear expression levels of pSTAT3, we may underestimate the full dynamics of this activation.

#### **4.2.2. Upregulation and activation of STAT3 signaling over time after stab wound**

In order to thoroughly describe the expression and activation pattern of STAT3 after stab wound we performed western blot with whole cell and subcellular fractionated extracts and immunohistochemistry over the first seven days. We observed with western blot of whole brain extracts that the expression of STAT3 starts to increase at 3 dpSW, in parallel with GFAP, a marker for reactive astrocytes (Robel et al., 2011), as already shown before (Hozumi et al., 1990). Next, by investigating separated nuclear and cytoplasmic fractions by subcellular fractionation, we could show a significant upregulation in both fractions in the ipsilateral compared to the contralateral cortex at 3 dpSW. This suggests that STAT3 proteins in the ipsilateral hemisphere are produced upon STAT3 promoter activation, possibly by STAT3 itself (He et al., 2005), and subsequently translocated into the nucleus in order to exert its transcriptional activation function. We reinforced these data by showing that also pSTAT3 displays a significant upregulation in the nuclear fraction of the lesioned hemisphere compared to the contralateral side at 3 dpSW. Both, STAT3 and pSTAT3, decreased nearly completely to baseline levels at 5 and 7 dpSW.

Our western blot results can be correlated with our results from immunohistochemistry after stab wound. We showed that virtually all of the cells that upregulated and activated STAT3 at 3 dpSW were GFAP+. Thus the ipsilateral expression of STAT3 and pSTAT3 detected at 3 dpSW

in western blots represents the expression and activation of STAT3 signaling in reactive astrocytes. We next observed that instead the contralateral expression of STAT3 in western blot corresponds to the STAT3 expression in mature neurons. On the lesioned site, in contrast to 3 dpSW, we observed at 5 and 7 dpSW only 78,9 % and 65,9 %, respectively, of pSTAT3+ cells to be GFAP+. Additionally, while approximately 20 % of reactive astrocytes, mainly in the close vicinity of the stab wound, were pSTAT3+ at 3 dpSW, this value significantly decreased at 5 and 7 dpSW. Overall, this observed pattern of pSTAT3 argues for a lower relative number of GFAP+ cells that activated STAT3 signaling at 5 and 7 dpSW compared to 3 dpSW and suggests that other cell types must have upregulated STAT3 signaling at 5 and 7 dpSW. Although no published data exist on STAT3 signaling in the different cell types after stab wound, investigations in other CNS lesion models, mainly SCI, have been performed. Yamauchi and colleagues found that pSTAT3 is significantly upregulated in neurons as well as reactive astrocytes at 12 hours and microglia at 48 hours after SCI (Yamauchi et al., 2006). However, this study did not evaluate the pSTAT3 expression in different cell types beyond 48 hours. More recent studies on the activation of STAT3 signaling after SCI focused only on reactive astrocytes and did not investigate other cell populations (Herrmann et al., 2008, Wanner et al., 2013, O'Callaghan et al., 2014). In contrast, Planas and colleagues used a MCAo model to induce transient focal cerebral ischemia and found STAT3 upregulated in microglial cells at 4, 7 and 15 days after MCAo. However, they did not provide any quantifications or immunohistochemistry investigating the expression in astrocytes or neurons (Planas et al., 1996). A study from our laboratory investigated the proliferative reaction of glial cells after stab wound injury (Simon et al., 2011) and showed that at 7 dpSW most proliferating cells were positive for Iba1, a marker for microglia, CD45, that is expressed on many hematopoietic cells, or S100 $\beta$ , an astroglial marker. Taken together, these data suggest that CD45+ cells, microglia or neurons could constitute the cell populations that, in addition to reactive astrocytes, upregulate pSTAT3 at 5 and 7 dpSW.

Very recently, our laboratory was able to further discriminate different populations of reactive astrocytes after stab wound (Bardehle et al., 2013). For up to 28 days after injury single astrocytes were followed with *in vivo* two-photon laser-scanning microscopy. Thereby, at least three different subpopulations could be distinguished: one population of astrocytes keeping their original morphologic shape, another population navigating their processes toward the lesion and a third subset, proliferating, at a juxtavascular location. Independently of the subset,

no single astrocyte migrated toward the lesion site. It will be very interesting to examine the STAT3 expression and activation of these three subsets given the role of STAT3 in proliferation.

#### **4.2.3. Upregulation and activation of STAT3 signaling after MCAo**

As mentioned before, no results have been published yet on the expression and activation pattern of STAT signaling after stab wound injury to the adult cerebral cortex. Therefore, we aimed to rule out stab wound model-related effects by conducting the same analysis in MCAo mice. 3-4 days after MCAo cortices were dissected and subsequently western blots of subcellular fractionated extracts were performed. Here we found no upregulation of STAT3 expression in the ipsilateral hemisphere. In contrast, pSTAT3 was significantly higher in the ipsilateral compared to the contralateral nuclear fraction. This pattern was in contrast to the changes that we evidenced in the stab wound model where we observed a significant upregulation of both, pSTAT3 and STAT3 in the ipsilateral cortex. Different reasons can be found for this different level of activation of the signaling cascade. First, the different pathophysiologies of the two models lead to the activation of different additional pathways that can influence the STAT3 signaling pathway. As a consequence, some promoters, e.g. the STAT3 promoter itself, may be blocked and can't be activated by pSTAT3 dimers while other promoters can be accessed now. Additionally, the faster or more effective onset of inhibitory regulators of the STAT signaling cascade, in particular of PIAS, which would inhibit the DNA recognition of phosphorylated STAT dimers in the nucleus (Shuai, 2000), could lead to less increased expression of STAT proteins overall in the ipsilateral cortex. Second, these two models also display totally different neuropathological features. For example the necrotic core and the area affected by the ischemia are manifold larger after MCAo than after stab wound. Given the fact that the dissection of the cortices were performed in the same way (namely cutting the brain frontally in three or four sections and afterwards dissecting cortices of contra- and ipsilateral hemispheres), we may have taken proportionally more parts of the necrotic core in the MCAo animals compared to the SW animals. As this dead tissue could not show increased STAT3 signaling, it may have had a dilutional effect on the whole sample. Although displaying different pathophysiologies and neuropathologies, both, stab wound and MCAo are models of acute invasive brain injuries. The activation of STAT3 signaling therefore

does not only seem to be an effect, which would be specific for the stab wound model, but instead a more general phenomenon after acute invasive brain injury.

Again, in order to investigate the cell types activating STAT3 after MCAo, we performed immunohistochemistry with pSTAT3. As after SW, we observed that most pSTAT3+ cells were GFAP+. We could therefore argue that the significant difference that was observed in the ipsilateral compared to the contralateral nuclear fraction in the western blot represents the changes of pSTAT3 expression in these reactive astrocytes. As at 3 dpSW, the percentage of GFAP+ cells expressing pSTAT3 at 3-4 days after MCAo was approx. 20 %. In contrast, the percentage of pSTAT3+ cells that were also GFAP+ at 3-4 days after MCAo was significantly lower than at 3 dpSW. This suggests that other cell types do activate STAT3 signaling at 3-4 days after MCAo. This difference may again be explained by the different pathophysiology underlying these two brain lesions. While the stab wound may lead to focal disruption of blood vessels with subsequent intraparenchymal hemorrhage, disruption of neuronal projections as well as local cell death of neurons and glial cells, the experimental stroke model MCAo leads to an ischemia that covers much larger parts of the brain and subsequently results in cell death by excitotoxicity, peri-infarct depolarizations, inflammation and apoptosis. Furthermore, after MCA occlusion for 1-2 hours, the proportion of neurons, which are affected by the pathophysiology but not immediately dead after insults (the so-called penumbra), may be much larger than after stab wound in which some cells may die immediately but the majority of the surrounding cells may not be affected. As it is known that STAT3 promotes neuronal survival by upregulating neuroprotective genes (for review see (Dziennis and Alkayed, 2008)), the neurons in the ischemic penumbra may represent a group of cells that could upregulate STAT3 signaling and therefore represent a population of cells that in addition to reactive astrocytes upregulated STAT3 signaling. A previous study by Suzuki and colleagues indeed found pSTAT3 to be expressed in neurons at 3,5 and 24 hours after MCAo but not in GFAP+ cells at four days after MCAo (Suzuki et al., 2001). As mentioned above Planas and colleagues found even another pattern of STAT3 signaling activation after MCAo as they reported only microglia and not neurons or other glial cells to express STAT3 at 4, 7 and 15 days after MCAo (Planas et al., 1996). The same group reported four years later that STAT3, in contrast to their first study, is also upregulated in layer V neurons and astrocytes at several days after MCAo (Justicia et al., 2000). Together, this supports the idea that neurons may be an additional

population of cells that upregulate STAT3 signaling after MCAo and therefore explain the decrease of the proportion of pSTAT3+ cells being GFAP+.

Another not significant but remarkable difference of the percentage of GFAP+ cells expressing pSTAT3 was observed between the conditions three days after stab wound and MCAo on the one hand (20,0 and 18,8 %) and 5 and 7 days after stab wound on the other hand (6,5 and 8,7 %). Apparently, reactive astrocytes activate STAT3 signaling more at earlier (three days after insult) than at later time points (five and seven days after insult) independent of the brain lesion. This is consistent with Yamauchi and colleagues which showed with western blot of whole cell extracts, that pSTAT3 decreases from three to seven days after SCI. Additionally, they found STAT3 signaling to be upregulated from 6 hours on after insult (Yamauchi et al., 2006). In contrast, Zamanian and colleagues demonstrated a sustained upregulation of STAT3 gene expression up to one week after MCAo (Zamanian et al., 2012), indicating that STAT3 may be translationally repressed at five and seven days. The role of STAT3 in reactive astrocytes may be important to understand in order to explain the designated difference between earlier and later time points. Mainly three studies investigated the function of STAT3 in reactive astrocytes and found it to be highly important for the glial scar formation after brain lesion (Okada et al., 2006, Herrmann et al., 2008, Wanner et al., 2013). Possible links were provided as first, a STAT3 binding site was found in the promoter of GFAP (Bonni et al., 1997), which is one of the structural hallmarks of reactive astrogliosis, second, mice with a conditional STAT3 knockout lacked astrocytic hypertrophy (Herrmann et al., 2008) and third, STAT3 led to a decrease of E-cadherin, a cell adhesion molecule (Okada et al., 2006). Furthermore, Okada and colleagues showed with an *in vitro* migration assay that STAT3 is crucial for the migration of astrocytes (it will be interesting to see if injection of our miRNA expressing plasmids *in vivo* also leads to reduced migration of reactive astrocytes to the lesion site). The glial scar is especially important early after brain lesion as it inhibits the spread of inflammatory cells via STAT3-dependent mechanisms (Wanner et al., 2013) and helps to repair the blood brain barrier, which consecutively leads to smaller lesion size and less neuronal loss (Bush et al., 1999, Faulkner et al., 2004, Voskuhl et al., 2009). Thus, we hypothesized here that the STAT3 signaling activation that we evidenced in acute brain injuries at early time points is likely related to the role of STAT3 in the formation of the glial scar that is particularly valuable at early time points after brain injury.



#### **4.2.4. Upregulation and activation of STAT3 signaling in mouse models of non-invasive brain injury**

For the purpose of extending the spectrum from acute/invasive to non-acute/non-invasive injuries and additionally to increase the clinical significance of our findings regarding the expression and activation of STAT3 signaling after brain lesion, we investigated the pattern of STAT3 signaling also in two mouse models mimicking AD - APP/PS1 and CK/p25, which have not been examined yet in this context. With immunohistochemistry we found that in both models the percentage of reactive astrocytes that were pSTAT3+ was lower compared to 3 dpSW and 3-4 days after MCAo. This fits with our beforehand described hypothesis that STAT3 activation is important for the initial formation of the glial scar within days after injury. The still existent but lower activation of STAT3 signaling at late time points (six months old APP/PS1 mice and CK/p25 mice that were off doxycycline for five weeks) suggests that activation of STAT3 at a baseline level promotes the ongoing process of reactive astrogliosis. Nevertheless, we need to keep in mind that this baseline expression level is based on some pSTAT3+ cells as a subset of the total GFAP+ cell population and does not display a general average expression of pSTAT3 in every GFAP+ cell. Also the percentage of GFAP+/pSTAT3+ cells did not differ between both models indicating that the chronicity of the lesion could play a role. Interestingly, this percentage value was in both models lower than at 3 dpSW and significantly higher than after MCAo. Again, these differences may be explained by the pathophysiology. After MCAo we identified neurons within the penumbra and microglia as potential cell populations to activate STAT3 signaling. Here, these two non-invasive brain injury models lack a penumbra. In addition, their vascular integrity is not affected and consequently, immune cells (e.g. CD45+ cells) can invade the affected brain areas only to a much lower extent than after invasive brain injury models where blood vessels are disrupted. Therefore, these models display much less immunological response than after MCAo. Moreover, in the CK/p25 mice, neurons overexpress p25 which interacts with Cdk5 which in turn associates to and subsequently phosphorylates STAT3 at the Ser727 residue (Fu et al., 2004). This phosphorylation step appears to be important for full transcriptional activation (Decker and Kovarik, 2000). This could indicate that given the higher transcriptional capacity of single STAT dimers in p25 expressing neurons either lower pSTAT3 expression levels are needed for the

necessary STAT3 transcriptional function or negative regulators as SOCS and SHP2 are upregulated and therefore pSTAT3 expression levels decreased.

*Overall, we here provided evidence for the first time that STAT3 signaling is activated in reactive astrocytes after stab wound and in two mouse models mimicking AD – APP/PS1 and CK/p25. Additionally, we were able to add further experimental evidence that STAT3 is activated in reactive astrocytes after MCAo. Future studies will have to clarify which other cell types may activate STAT3 after these brain lesions.*

### **4.3. STAT5 and STAT1 signaling in the injured cerebral cortex**

Besides STAT3 also other members of the family of STAT proteins have been suggested to be expressed after CNS lesion, mainly STAT1 and STAT5. Here we investigated with western blot and immunohistochemistry if these proteins are expressed or activated after stab wound.

#### **4.3.1. Expression of STAT5a after stab wound**

With western blot of whole cell extracts and immunohistochemistry we first showed that STAT5a was not upregulated in the ipsilateral cortex at several days after stab wound (1, 3, 5 and 7 dpSW with western blot and 3 dpSW with immunohistochemistry). Second, we showed that, in contrast to STAT3 and pSTAT3 after injury, STAT5a is mostly expressed by mature neurons, as shown by colocalization with NeuN. No obvious difference in colocalization between contra- and ipsilateral hemisphere was observed. Regrettably, antibodies that were meant to detect STAT5b and pSTAT5 did not work in our hands. Therefore, we were not able to pursue further analysis of STAT5b and pSTAT5 expression.

Previously published studies regarding the expression and activation of STAT5 signaling after brain injury focused so far on models of cerebral ischemia. The mRNA for both proteins, STAT5a and STAT5b, were shown to be upregulated at 24 hours after MCAo in the ipsilateral hippocampus by using microarray analysis (Sun et al., 2007). Unfortunately, no protein levels were measured in this study. Another study used a model of transient global ischemia. Here, Zhang and colleagues focused on the CA1 area of the rat hippocampus (as short global ischemia leads to a selective and delayed neuronal cell death in this area) and showed that while total STAT5 expression levels do not change, the level of pSTAT5 is increased at 1 and 3

hours after reperfusion with an earlier increase of pSTAT5a than pSTAT5b (Zhang et al., 2007). Given first, the different model of a transient global ischemia, which is performed by a twelve minutes long four-vessel occlusion, second, the usage of an antibody against STAT5, which detects STAT5a and STAT5b and third, the investigation of only the CA1 area of the hippocampus, these results can hardly be compared to ours. In addition, this study did not address the role of STAT5 signaling in ischemia. Furthermore, Yamaura and colleagues observed STAT5a to be an integral player against the myocardial ischemia-reperfusion injury (Yamaura et al., 2003), indicating that STAT5 signaling in ischemia is not brain-specific.

*Overall, our data suggest that STAT5a is not upregulated at 3 dpSW, but bilaterally expressed in neurons. Future studies are required to check if this expression pattern changes over time at 5 and 7 dpSW or in different injury models. Furthermore, it will be interesting to see if STAT5b and pSTAT5 show a distinct pattern of expression as indicated by previous studies.*

#### **4.3.2. Activation of STAT1 after stab wound**

By applying western blot of subcellular fractionated extracts that were collected from mice at 3 dpSW we observed no obvious upregulation of pSTAT1 in the ipsilateral versus the contralateral hemisphere. As expected from our results with pSTAT3 and suggested by the canonical STAT signaling pathway, pSTAT1 was mainly found in the nuclear fractions. But as the loading control was missing in this experiment, no solid conclusions can be drawn. With immunohistochemistry we demonstrated that pSTAT1 is only expressed in the ipsilateral hemisphere and here virtually always by GFAP+ cells. In contrast to pSTAT3, these cells represented only a very minor fraction of reactive astrocytes in the vicinity of the lesion. Although these cells in the ipsilateral cortex exhibited pSTAT1 staining only in the nucleus, the lack of pSTAT1+ cells in the contralateral hemisphere was in clear contrast to our western blot findings. As we succeeded in detecting a single band matching the presumed molecular weight of the phosphorylated form of STAT1 as well as only nuclei of single cells, the specificity of the antibody was apparently not questionable. However, the sensitivity of this antibody for immunohistochemistry might have been low. In that case we may have only detected the cells that expressed pSTAT1 at highest levels. Alternatively, the missing nuclear loading control for our western blot could have lead to false interpretation of this western blot data.

So far no data have been published on the upregulation of STAT1 signaling after stab wound and little is known about its expression after MCAo and SCI. While Planas and colleagues found STAT1 expression in western blot of brain tissue from four days on after MCAo until 15 days (Planas et al., 1997), Takagi and his team found pSTAT1 to be expressed in neurons even within several hours after MCAo and proposed a role in cell death, as STAT1 knockout mice showed reduced infarct volume and less neurological deficits (Takagi et al., 2002). Osuka and colleagues found that pSTAT1 is upregulated around 6 hours after SCI in neurons but not translocated into the nuclear compartment, in strong disagreement with the canonical signaling pathway (Osuka et al., 2011). STAT1 activation in reactive astrocytes after injury was reported in the hippocampus after kainic acid-induced seizures (Choi et al., 2003).

*Our data suggest that the activated form of STAT1, pSTAT1, is expressed in a subset of reactive astrocytes at three days after stab wound. Other studies will unravel how this pattern develops over time and in other injury models.*

#### **4.4. Impact of STAT3 signaling on reprogramming of postnatal astrocytes into neurons**

The long-term goal of the whole study is to investigate if STAT-mediated pathways could hamper the reprogramming of reactive astrocytes into neurons after injury of the cerebral cortex. In order to evaluate whether a strategy aiming at decreasing or increasing STAT signaling would make sense we first conducted a thorough analysis of the pattern of expression and activation of STAT signaling after various brain lesions, which was presented and discussed above. For the purpose of evaluating the impact of STAT signaling on neuronal reprogramming we used the neuronal reprogramming of postnatal astrocytes *in vitro*, a system, which has been established by our laboratory. Indeed, our lab was previously able to show that cortical postnatal astrocytes can be directly reprogrammed into fully functional neurons by forced expression of neurogenic fate determinants (Berninger et al., 2007, Heinrich et al., 2010, Heinrich et al., 2011). Therefore, this controlled *in vitro* system represented the ideal setting to evaluate the effect of STAT signaling on neuronal reprogramming. Very recent data on the reprogramming of brain-resident cells into neurons *in vivo* (as introduced in subchapter 1.5.3.3.) will allow us to investigate this pathway in this *in*

*in vivo* setting in future experiments. Here we first investigated if postnatal astrocytes would indeed mimic reactive astrocytes regarding the expression and activation of STAT signaling.

#### **4.4.1. Expression and activation of STAT3 in postnatal astrocytes**

We chose to study the expression and activation of STAT3 in postnatal astrocytes mainly for two reasons: to see whether they can be used as a model for reactive astrocytes and second to assess if it is reasonable to perform gain- or loss-of-function experiments of STAT3 signaling in postnatal astrocytes. By using western blot we found STAT3 to be expressed and activated in cortical astrocytes that were cultured from mouse pups sacrificed at postnatal day one or six and subsequently expanded for seven days *in vitro*. At these postnatal days astrogliogenesis is indeed at its peak. As reviewed in detail in subchapter 1.6.3.2. STAT3 is at the centre of astrogliogenesis regulation and becomes robustly elevated from E11.5 on (He et al., 2005). It was even suggested that STAT3 expression increases before from E7.5 on (Foshay and Gallicano, 2008). Then during postnatal development, Gautron and colleagues observed by using immunohistochemistry that STAT3 expression increases from P3 to P21 (Gautron et al., 2006). Fourth, it was demonstrated that JAK/STAT signaling was among the 20 enriched signaling pathways in astrocytes from the forebrain of mice that were one to thirty days old (Cahoy et al., 2008). Overall, our finding that STAT3 is expressed and activated in our culture of cortical astrocytes is in line with previously published data. With regard to STAT signaling, postnatal astrocytes can therefore be used as a model for reactive astrocytes and it was reasonable to perform subsequent gain- and loss-of-function experiments in postnatal astrocytes.

#### **4.4.2. Inhibition of STAT signaling: several possible approaches**

Here we took advantage of a widely used method to reduce protein expression – miRNAs. Although we observed a much more pronounced STAT3 activation in reactive astrocytes after injury and data on the impact on neuro- vs. astrogliogenesis have been much more intriguing for STAT3 than for STAT1, we decided to also create miRNAs against STAT1 as binding sequences of STAT1 in astroglial promoters (GFAP and S100 $\beta$ ) have been found (He et al., 2005) and we hypothesized that STAT1 could thus overtake the gliogenesis-promoting

function of STAT3. For the purpose of higher efficiency and GFP labeling the newly designed miRNAs were subjected to different cloning steps that led to three different constructs, one containing two miRNAs against STAT3, one with two miRNAs against STAT1 and one with two miRNAs against STAT3 and two against STAT1. During this process their sequence was tested repeatedly (by Eurofins MWG Operon, Ebersberg, D) and at all times found to be correct. Subsequently, we decided to subclone each of the miRNA constructs and overexpressing vectors into a retroviral vector under the control of the pCAG promoter. That would allow long-term expression by avoiding silencing (Gaiano et al., 1999, Zhao et al., 2006, Heinrich et al., 2010). Unfortunately, the time that was available for the present work was not sufficient to test the viruses' transduction efficiency and to perform further experiments with them. Future studies will reveal if the application of these viruses leads to better inhibition of STAT signaling and therefore allow more pronounced effects on the reprogramming of reactive astrocytes into neurons.

miRNAs represent not only tools that can be exogenously delivered to target mRNAs but are also endogenously available, exert a plethora of effects by targeting approximately 30 % of all mRNAs and thereby modify many different signaling pathways (Bartel, 2004). These endogenous miRNAs affect also processes like oligodendrocyte proliferation and differentiation as well as myelin formation (Barca-Mayo and Lu, 2012). Investigating the role of endogenous miRNAs in astrocytes, especially after brain injury, displays an interesting approach on its own, which warrants future studies.

Many different ways to inhibit proteins in general have been proposed as well. miRNAs are part of the RNA interference system, with another component of this system being small interfering RNAs (siRNAs). Exogenously delivered small hairpin RNAs (shRNAs) are cytoplasmically processed into siRNAs (Bernstein et al., 2001), which then target mRNAs to degrade them or to inhibit their translation (as miRNAs do), but compared to miRNAs they target only one mRNA specifically. We here chose to work with miRNAs as the manufacturer of the RNAi expression vector kit (Life Technologies, Carlsbad, CA, USA), that was established in our laboratory, reported that the knockdown success rates of miRNAs in reducing mRNA expression are higher than that of shRNAs (> 70 % versus 50 %; <http://de-de.invitrogen.com/site/de/de/home/Products-and-Services/Applications/rnai/Vector-based-RNAi/Pol-II-miR-RNAi-Vectors.html>).

In addition to the mRNA level, other levels of the protein synthesis or elements of the STAT signaling pathway could be targeted to reduce STAT signaling. For example a dominant negative form of STAT3 has recently been used to inhibit STAT3 signaling – STAT3F (Bonni et al., 1997). STAT3F can bind to phosphorylated cytokine receptors but cannot be phosphorylated itself as Tyr705 was substituted by phenylalanine. Subsequently, it cannot dissociate from the receptor and thus inhibits the recruitment of endogenous STATs to the cytokine receptor (He et al., 2005). Ultimately, it is therefore thought to prevent the activation of endogenous STATs (originally developed by Nakajima and colleagues (Nakajima et al., 1996)). We tested STAT3F by transfecting cultured astrocytes isolated from postnatal day six cerebral cortex, but unfortunately, in our hands the molecule was not able to decrease the intensity of pSTAT3 in the nucleus significantly (data not shown), as the designed miRNAs did. Other STAT-mediated pathway inhibitors as Stattic (Schust et al., 2006), a STAT3-specific inhibitor or AG490 (Meydan et al., 1996), a Jak2 inhibitor, have been described. We instead decided to use vectors encoding the respective miRNAs because only with them we would be able to track successfully transfected cells by GFP labeling (by the use of vectors that at the same time encode GFP).

In parallel to exogenously delivered molecules, genetically modified mice have also proven to be a valuable tool for the alteration of signaling pathways. While STAT3 knockout mice per se die at embryonic ages (Takeda et al., 1997), conditional knockouts, in order to be able to induce the knockout at a specific time point and only in a selected cell type, have been generated recently (e.g. see (Herrmann et al., 2008)). Such a mouse line, e.g. GLAST<sup>creERT2</sup>STAT3<sup>flox/flox</sup>, would allow for astrocyte-specific STAT3 deletion by inducing cre expression under control of the astrocyte-specific glutamate transporter GLAST and by inducing its translocation to the nucleus upon delivery of tamoxifen at any given time point (Mori et al., 2006). Future experiments will reveal the effects of such an *in vivo* deletion of STAT3 specifically in astrocytes.

Due to their simple experimental use and easy tracking of expression by following GFP we decided to use miRNAs instead of other inhibitors. Here, we developed miRNAs against STAT3 and STAT1 and proved them to lower the respective STAT protein remarkably.

#### 4.4.3. Impact of STAT3 signaling on reprogramming of postnatal astrocytes into neurons

As STAT3 was shown to promote astrogliogenesis during embryonic development we here aimed at investigating its function on the neuronal reprogramming of postnatal astrocytes induced by a well-known neurogenic fate determinant, Mash1 (also named Ascl1, achaete-scute homolog 1). Therefore, we first cotransfected P6 astrocytes with STAT3C and Mash1. At nine days after transfection, the number of neurons was lower in Mash1/STAT3C-transfected cells than in Mash1/GFP-transfected cells. Concomitantly, at this time point the number of RFP+ cells was lower in Mash1/STAT3C-transfected cells than in Mash1/GFP-transfected cells. To rule out transfection related cell death we studied the number of Mash1-transfected cells shortly after transfection, at two days, and found no difference between the conditions Mash1/GFP and Mash1/STAT3C. In addition, STAT3C-related cell death could be excluded as the number of RFP+ cells at nine days after cotransfection with STAT3C/DsRed was not lower than the number of RFP+ cells in GFP/DsRed-transfected cells. These results indicate that STAT3C impairs the reprogramming of postnatal astrocytes into neurons, possibly by inducing cell death of the cells cotransfected with both, STAT3 and Mash1, which exert opposite effects: while STAT3 would maintain the astrocytes in their glial lineage or induce their proliferation, Mash1 would force them to become neurons, thus inducing a cell fate conflict resulting in cell death.

Next, in order to block STAT3 signaling we cotransfected cells with Mash1 and GFP-2miRNA3 and observed that the number of neurons per transfected cells was higher than with Mash1 alone. Interestingly, the number of Mash1-transfected cells did not change between Mash1/GFP-2miRNA3- and Mash1/STAT3C-transfected cells. Conditions like these that led to equal cell numbers do not exclude the possibility of cell death because compensatory proliferation can occur. However, the withdrawal of proliferation factors in these cultures after transfection leads to very little proliferation. In general, we interpreted reduced cell numbers as netto cell death (more cell death than proliferation). Future studies will investigate the cell death in these conditions in more details, e.g. with live imaging, immunostaining of caspases or TUNEL assay (terminal deoxynucleotidyl transferase dUTP nick end labeling).



Regarding the combined forced expression of Mash1, a neurogenic fate determinant, and STAT3, a gliogenic fate determinant, it is necessary to discuss the pivotal molecular process that underlies the transition from neurogenesis to astrogliogenesis. Several mechanisms have been suggested to suppress STAT signaling during the neurogenic phase. First Neurog1, which is highly expressed during cortical neurogenesis and low during gliogenesis, sequesters the CBP/p300/Smad1 complex away from STAT3, which subsequently cannot bind to glial promoters and directly suppresses JAK/STAT signaling (Sun et al., 2001). Second, STAT proteins are not able to access astrocytic genes due to histone H3K9 or DNA methylation (Takizawa et al., 2001, Fan et al., 2005). And third, during the neurogenic phase astrogliogenesis is inhibited by the erbB4-NCoR signaling (Sardi et al., 2006). In contrast, at the transition between neurogenic and astrogenic phase Neurog1 and Neurog2 loci are epigenetically silenced by the polycomb group complex (Hirabayashi et al., 2009) leading to negligible Neurog2 expression in postnatal astroglia (Heinrich et al., 2010). Consecutively, the CBP/p300/Smad1 complex can bind to STAT3 and subsequently activate glial promoters. The neurogenic phase ends in the mouse cortex at approx. E18.5 (Levers et al., 2001) while STAT starts to regulate the onset of gliogenesis (Bonni et al., 1997). At P6 then these astrocytes still express STAT3 and do not have any intrinsic neurogenic capacity (Ge et al., 2012). The forced expression of Mash1 and Dlx2, which is a direct downstream target of the ventral telencephalic transcription factor Mash1, was shown to reprogram these postnatal astrocytes into GABAergic neurons *in vitro* (Heinrich et al., 2010). However, we show now that the forced expression of STAT3 by administrating STAT3C can indeed robustly inhibit this process. The activation of two opposed differentiation pathways, Mash1 for the neurogenic and STAT3 for the gliogenic pathways, leads to cell death. Alternatively, as the blockade of STAT3 signaling tends to increase neuronal reprogramming, the endogenous activation of STAT3 signaling could also inhibit the neuronal reprogramming process itself.

*Here we suggest that cell death due to the activation of two opposed differentiation pathways but also the inhibition of the process of neuronal reprogramming itself, led to decreased numbers of neurons after cotransfection with Mash1/STAT3C compared to Mash1 alone. In contrast, the blockade of STAT3 signaling partially increases the neuronal reprogramming of postnatal astrocytes induced by Mash1.*

#### **4.5. Acquisition of stem cell properties by reactive astrocytes after brain injury**

Recently, our group was able to demonstrate that acute/invasive injuries (MCAo and SW) significantly differ from non-invasive injuries (APP/PS1 and CK/p25) concerning proliferation and stem cell properties of responding astrocytes (Sirko et al., 2013). While invasive models elicited a large degree of proliferation and capacity to form multipotent and self-renewing neurospheres among astrocytes, non-invasive models showed an astrocytic response with virtually no potential to form neurospheres and only low levels of proliferation. Strikingly, our group could identify Shh as participating pathway responsible for the astrocytic reaction after invasive injury. Notably, the STAT3 signaling pathway may have an important effect in this context – independent or interacting with the Shh signaling pathway as both pathways can lead to transcriptional activation (Yang et al., 2012). Here, our expression analysis showed higher levels of pSTAT3 in reactive astrocytes after acute brain injury models like stab wound and MCAo, that also show a higher capacity to form multipotent and self-renewing neurospheres, compared to lower expression levels of pSTAT3 in reactive astrocytes after non-acute and non-invasive brain injury models like APP/PS1 and CK/p25, that also show lower potential to generate neurospheres. Various causative links can be found for this apparent correlation between the number of generated neurospheres and the level of STAT3 signaling activation. First, it is suggested that insufficient activation of JAK/STAT3 is a limiting condition for the acquisition of pluripotency in heterogenous embryonic stem cell lines (Yang et al., 2010). While pluripotency refers to the ability of a stem cell to differentiate into derivatives of any of the three embryonic germ layers, multipotency is a more restricted competence, which indicates the capacity of a progenitor cell to develop into more than one cell type. Consequently, it is conceivable that STAT3 signaling may also play a role in the acquisition of multipotency. Second, STAT signaling is linked to cellular proliferation - a critical process in the development of neurospheres - in different contexts, e.g. of embryonic CNS cells (Cattaneo et al., 1996) and in various tumors like gliomas (Brantley and Benveniste, 2008).

*Further studies are required to determine whether STAT3 signaling plays a key role in the potential of reactive astrocytes to generate neurospheres. Given the described roles of STAT3*

*signaling for proliferation and pluripotency, it is conceivable that the activation of STAT3 signaling indeed supports the formation of neurospheres.*

#### **4.6. Effect of STAT signaling on reprogramming of reactive astrocytes into neurons in the adult injured brain**

The final goal of the present work will be to investigate the impact of STAT signaling inhibition on reprogramming of reactive astrocytes into neurons. Here it will be particularly interesting to see if neuronal reprogramming of reactive astrocytes *in vivo* can be enhanced after injection of our newly produced virus containing miRNAs against STAT3, in combination with forced expression of neurogenic transcription factors like Neurog2, NeuroD1 or Sox2 as recently described (Grande et al., 2013, Guo et al., 2014, Niu et al., 2013).

Reactive astrocytes derive from mature protoplasmic astrocytes from the grey matter that reenter cell cycle after injury to the CNS (Buffo et al., 2008) and thereby contribute to a process called reactive gliosis. Amongst others, they upregulate GFAP, Vimentin, Nestin and BLBP (for review see (Robel et al., 2011)). They also activate STAT3 *in vivo* (see our own findings and e.g. (Herrmann et al., 2008)) as postnatal astrocytes do. This is in sharp contrast to SGZ and SVZ astrocytes in the adult neurogenic zones, which are able to generate neurons and do not activate STAT3 signaling. This is supported by our own data and the previous work of Bauer and Patterson which also found virtually no STAT3 activation in the SVZ using immunohistochemistry (Bauer and Patterson, 2006). Overall, this provides further support for the link between STAT3 signaling activation and inhibition of neurogenesis. Indeed both, reactive and postnatal astrocytes, while showing strong STAT3 signaling activation, lack the intrinsic neurogenic capacity, which SGZ and SVZ astrocytes exhibit.

In our experiments with postnatal astrocytes the blockade of STAT3 in combination with forced expression of Mash1 led to increased neuronal reprogramming compared to forced expression of Mash1 alone. Given that STAT3 is activated in reactive astrocytes as well, it will be interesting to see, if future studies can reveal the same effect for reactive astrocytes, possibly *in vivo*. Although STAT1 signaling has been suggested to be more expressed in neurons after CNS lesion (Osuka et al., 2011, Takagi et al., 2002), we found STAT1 also to be activated in reactive astrocytes after stab wound. Future studies will unravel if STAT1 is further

activated when STAT3 is blocked in reactive astrocytes *in vivo* and therefore whether additional blockade of STAT1 may be necessary to promote neuronal reprogramming *in vivo*.

In addition to their potential to be possibly reprogrammed into neurons after CNS injury, reactive astrocytes exhibit another important function by forming a scar. The role of this process has been described in detail in subchapters 1.4.2.2. and 4.1.3., but shortly, during early times after injury it is essential for improving recovery by impairing the spread of inflammatory cells and repairing the BBB among other mechanisms (e.g. (Bush et al., 1999)). At later times the detrimental inhibition of axon regeneration by scar formation outweighs the positive role as also inflammation has disappeared and the BBB has recovered. It has been shown that STAT3 is a key regulator of this mechanism (Herrmann et al., 2008, Okada et al., 2006). Therefore, the blockade of STAT3 signaling to induce neuronal reprogramming of reactive astrocytes should occur when the initial scar was formed. Otherwise resulting adverse effects of the missing scar at early times may outweigh the potential positive effects of newly generated neurons. It will be a key question to find the optimal time point when to inhibit STAT3 signaling to allow both, scar formation early after injury when STAT3 is still expressed (and therefore can exert its influence on processes like proliferation and acquisition of multipotency) and later to allow reactive astrocytes to be reprogrammed into neurons by ablating STAT3 signaling and possibly also facilitate axon regeneration due to less glial scar. Recent studies on the *in vivo* reprogramming of brain-resident cells into neurons reported also low survival rate of these newly generated neurons (Guo et al., 2014, Grande et al., 2013). It would be exciting to investigate if a decrease of STAT3 signaling activation at these later time points could prolong these neurons' lives. Future experiments will reveal at what time after brain injury STAT3 would need to be inhibited as it was here found to be a potential target for inducing reprogramming of reactive astrocytes into neurons *in vivo*.

*In summary, we first demonstrated the activation of STAT3 signaling in reactive astrocytes in different brain injury models. We suggest that this activation of STAT3 signaling impairs the conversion of astrocytes into neurons as we were able to increase the neuronal reprogramming of astrocytes in culture by inhibiting STAT3 signaling with miRNAs. However, we showed that the level of STAT3 signaling activation correlates positively with the formation of neurospheres, indicative for multipotency and self-renewal. Therefore, we suggest a dual function of STAT3 signaling over time in reactive astrocytes: it may be involved in their dedifferentiation,*

---

*acquisition of stem cell properties and scar formation at early time points following injury, which might be beneficial for brain repair. On the other hand, at later time points the decrease of STAT3 signaling activation may be necessary to promote the reprogramming of these reactive astrocytes into neurons and allow long-term survival of these neurons. Future investigations will unravel the potential benefit for brain regeneration of either activating or inhibiting STAT3 signaling at defined time points.*

## 5. Summary

Currently, no curative therapies for many neurological disorders, e.g. stroke and Alzheimer's disease, exist as the neuronal loss cannot be substituted. Unfortunately, the survival and functional integration of newly generated neurons from the two adult neurogenic niches into existing neuronal circuits in the damaged area remains negligible. In order to overcome the major ethical and immunological obstacles, that are associated with cellular transplantation, a new concept has been invented by our laboratory: endogenous glial cells, which proliferate in the proximity of CNS lesions, could be reprogrammed into neurons. Using forced expression of neurogenic fate determinants our laboratory was able to show that reactive astrocytes can be reprogrammed into functional subtype specific neurons in a highly sufficient manner *in vitro*. Recently, it was even demonstrated that this reprogramming process can be triggered *in vivo*. Unfortunately, long-term survival and functional circuitry integration remain very limited so far. Therefore, it is crucial to look not only for factors that enhance neurogenesis but also to search for hampering factors. Of note, the STAT signaling pathway is known to promote gliogenesis and inhibit neurogenesis during embryonic development.

The goal of the present work was to investigate if first the STAT signaling pathways are activated in reactive astrocytes after different cerebral cortical injury models and second to determine if these STAT-mediated pathways could inhibit the reprogramming of astrocytes into neurons.

First we showed with western blot and immunohistochemistry that STAT3 expression is upregulated at three days after stab wound in the mouse cerebral cortex. Moreover, we demonstrated that ipsilateral to the lesion STAT3 is virtually only expressed in reactive astrocytes, while contralateral it is mainly expressed in mature neurons. Furthermore, we could evidence that the activated, phosphorylated form of STAT3, pSTAT3, is also expressed in reactive astrocytes in the injured cortex after stab wound. We were able to increase the clinical significance of our findings by demonstrating principally the same pattern of STAT3 activation in an experimental stroke model, MCAo. Compared with these invasive brain injury models the activation of STAT3 signaling in non-invasive brain injury models, APP/PS1 and CK/p25, was decreased. In contrast to STAT3, we could not reveal an unambiguous upregulation of expression and activation of STAT5 and STAT1 signaling after stab wound.

Second, we investigated the role of STAT3 signaling on the reprogramming of astrocytes into neurons. In order to be able to perform gain- and loss-of-function experiments, we designed new vector constructs containing miRNAs against STAT3, with the purpose to decrease STAT3 expression, or STAT3C, a constitutively active form of STAT3. After we had shown the expression and activation of STAT3 signaling in postnatal astrocytes, we were able to provide evidence that the combination of Mash1 and STAT3C impairs neuronal reprogramming of postnatal astrocytes *in vitro* compared to Mash1 alone. Of note, we demonstrated by cotransfection of these postnatal astrocytes with Mash1 and newly designed miRNAs against STAT3, compared to transfection with Mash1 alone, that neuronal reprogramming could be enhanced *in vitro*.

Moreover, we demonstrated that after MCAo, reactive astrocytes can give rise to neurospheres meaning that they acquire stem cell-like properties after MCAo, as described after stab wound. The apparent correlation between the number of generated neurospheres and the level of STAT3 signaling activation - higher levels of pSTAT3 in acute brain injury models like stab wound and MCAo, which also show higher numbers of neurospheres, compared to lower levels of pSTAT3 in non-invasive brain injury models like APP/PS1 and CK/p25, which also show lower numbers of neurospheres – needs further analysis.

Taken together, we first demonstrated the activation of STAT3 signaling in reactive astrocytes after different brain injury models. By inhibiting STAT3 signaling we were then able to increase the conversion of postnatal astrocytes into neurons *in vitro*. However, the formation of neurospheres, indicative for the stem cell potential of astrocytes, correlates positively with the level of activation of STAT3 signaling in our study. Future investigations will further determine the optimal time point of modulating STAT3 signaling and its benefit for brain regeneration after injury as STAT3 was here found to be a potential target for inducing reprogramming of reactive astrocytes into neurons *in vivo*.

## 6. Zusammenfassung

Für viele neurologische Krankheitsbilder, wie z.B. Schlaganfall oder die Alzheimer-Erkrankung, existieren momentan keine kurativen Therapien, da der Verlust von Neuronen nicht ausgeglichen werden kann. Zwei adulte neurogene Zonen produzieren zwar Neurone. Ihr Überleben und funktionelle Integration in existierende neuronale Kreise in der geschädigten Gehirnregion bleibt aber leider vernachlässigbar. Um nun die hauptsächlich ethischen und immunologischen Hürden, die mit zellulärer Transplantation verbunden sind, zu umgehen, ist in unserem Labor ein neuer Ansatz entwickelt worden: endogene Gliazellen, die in der unmittelbaren Umgebung des verletzten Gehirnareals proliferieren, könnten zu Neuronen reprogrammiert werden. Mithilfe von forcierter Expression von neurogenen Schicksalsdeterminanten war es unserem Labor möglich zu zeigen, dass reaktive Astrozyten *in vitro* in funktionelle subtypspezifische Neurone reprogrammiert werden können. Dieser Prozess konnte kürzlich sogar *in vivo* nachvollzogen werden. Das Langzeitüberleben sowie die Integration in neuronale Schaltkreise sind bisher jedoch sehr limitiert. Es ist daher notwendig nicht nur nach Faktoren zu suchen, die die Neurogenese aktivieren, sondern auch nach hemmenden Faktoren. Interessanterweise ist bekannt, dass der STAT-Signalweg die Gliogenese aktiviert und die Neurogenese während der embryonalen Entwicklung inhibiert.

Das Ziel der vorliegenden Arbeit war es zu untersuchen, ob STAT-Signalwege in reaktiven Astrozyten nach verschiedenen Verletzungsmodellen des zerebralen Kortex aktiviert sind. Anschließend sollte analysiert werden, ob diese STAT-Signalwege die Reprogrammierung von Astrozyten in Neurone hemmen.

Zunächst konnten wir mithilfe von Western Blot und Immunhistochemie zeigen, dass die kortikale Expression von STAT3 drei Tage nach Stichwundenverletzung erhöht ist. Während STAT3 auf der ipsilateral zur Läsion gelegenen Seite fast ausschließlich in reaktiven Astrozyten exprimiert wurde, war es kontralateral hauptsächlich in vollständig ausgebildeten Neuronen zu finden. Zusätzlich konnten wir dann zeigen, dass auch die aktivierte, phosphorylierte Form von STAT3, pSTAT3, in reaktiven Astrozyten im verletzten kortikalen Areal nach Stichwundenverletzung aufreguliert war. Durch den Nachweis des gleichen Expressionsmuster in einem experimentellen Schlaganfallmodell, MCAo, konnten wir die klinische Relevanz unserer Ergebnisse steigern. Im Vergleich zu diesen invasiven



Gehirnverletzungsmodellen war die Aktivierung des STAT3-Signalweges in nicht-invasiven Gehirnverletzungsmodellen, APP/PS1 and CK/p25, verringert. Im Gegensatz zu STAT3 konnten wir jedoch keine zweifelsfreie Aufregulierung der Expression und Aktivierung des STAT5- und STAT1-Signalweges nach Stichwundenverletzung demonstrieren.

Um nachfolgend den Einfluss der STAT-Signalwege auf die neuronale Reprogrammierung von Astrozyten zu untersuchen, konstruierten wir Plasmide, die z.B. miRNAs gegen STAT3, um das Expressionslevel von STAT3 zu senken, oder STAT3C, eine konstitutiv aktive Form von STAT3, enthielten. Nachdem wir die Expression und Aktivierung des STAT3-Signalweges in postnatalen Astrozyten gezeigt hatten, konnten wir demonstrieren, dass die Kombination von Mash1 und STAT3C die neuronale Reprogrammierung von postnatalen Astrozyten *in vitro* im Vergleich zu Mash1 alleine hemmt. Interessanterweise konnten wir dann zeigen, dass die Kotransfektion dieser postnatalen Astrozyten mit Mash1 und neu designten miRNAs gegen STAT3, verglichen mit der Transfektion mit Mash1 alleine, die neuronale Reprogrammierung *in vitro* erhöhte.

In einem nächsten Schritt konnten wir darlegen, dass reaktive Astrozyten nach MCAo, wie schon für die Stichwundenverletzung gezeigt, dazu fähig sind Eigenschaften von Stammzellen anzunehmen indem sie Neurosphären bildeten. Die scheinbare Korrelation zwischen der Zahl der generierten Neurosphären und dem Level der Aktivierung des STAT3-Signalweges – höhere Level von pSTAT3 in invasiven Gehirnverletzungsmodellen wie der Stichwundenverletzung und MCAo, die auch mehr Neurosphären bilden verglichen mit niedrigeren Level von pSTAT3 in nicht-invasiven Gehirnverletzungsmodellen wie APP/PS1 und CK/p25, die auch weniger Neurosphären bilden – bedarf weiterer Analyse.

Zusammengefasst konnten wir demonstrieren, dass der STAT3-Signalweg in reaktiven Astrozyten nach verschiedenen Gehirnverletzungsmodellen aktiviert ist. Durch die Inhibierung des STAT3-Signalweges konnten wir die Reprogrammierung von postnatalen Astrozyten in Neurone *in vitro* steigern. Im Gegensatz dazu korrelierte die Generierung von Neurosphären, bezeichnend für die Stammzeleigenschaften der Astrozyten, positiv mit dem Level der Aktivierung des STAT3-Signalweges in unserer Studie. STAT3 wurde hier als potentiell Target zur Induzierung der Reprogrammierung von reaktiven Astrozyten in Neurone *in vivo* identifiziert. Zukünftige Studien werden den optimalen Zeitpunkt für die Modulation des STAT3-Signalweges, gemäß seiner unterschiedlichen Funktionen, finden.

## 7. References

- AARONSON, D. S. & HORVATH, C. M. 2002. A road map for those who don't know JAK-STAT. *Science*, 296, 1653-5.
- AHN, S. & JOYNER, A. L. 2005. In vivo analysis of quiescent adult neural stem cells responding to Sonic hedgehog. *Nature*, 437, 894-7.
- AKIRA, S., NISHIO, Y., INOUE, M., WANG, X. J., WEI, S., MATSUSAKA, T., YOSHIDA, K., SUDO, T., NARUTO, M. & KISHIMOTO, T. 1994. Molecular cloning of APRF, a novel IFN-stimulated gene factor 3 p91-related transcription factor involved in the gp130-mediated signaling pathway. *Cell*, 77, 63-71.
- ALLEN, C. L. & BAYRAKTUTAN, U. 2008. Risk factors for ischaemic stroke. *Int J Stroke*, 3, 105-16.
- ALONZI, T., MARITANO, D., GORGONI, B., RIZZUTO, G., LIBERT, C. & POLI, V. 2001. Essential role of STAT3 in the control of the acute-phase response as revealed by inducible gene inactivation [correction of activation] in the liver. *Mol Cell Biol*, 21, 1621-32.
- ALTMAN, J. 1962. Are new neurons formed in the brains of adult mammals? *Science*, 135, 1127-8.
- ALTMAN, J. & BAYER, S. A. 1990. Mosaic organization of the hippocampal neuroepithelium and the multiple germinal sources of dentate granule cells. *J Comp Neurol*, 301, 325-42.
- ALVES, J. A., BARONE, P., ENGELENDER, S., FROES, M. M. & MENEZES, J. R. 2002. Initial stages of radial glia astrocytic transformation in the early postnatal anterior subventricular zone. *J Neurobiol*, 52, 251-65.
- AMAMOTO, R. & ARLOTTA, P. 2014. Development-inspired reprogramming of the mammalian central nervous system. *Science*, 343, 1239882.
- AMARENCO, P., BOGOUSLAVSKY, J., CALLAHAN, A., 3RD, GOLDSTEIN, L. B., HENNERICI, M., RUDOLPH, A. E., SILLESEN, H., SIMUNOVIC, L., SZAREK, M., WELCH, K. M. & ZIVIN, J. A. 2006. High-dose atorvastatin after stroke or transient ischemic attack. *N Engl J Med*, 355, 549-59.
- AMBASUDHAN, R., TALANTOVA, M., COLEMAN, R., YUAN, X., ZHU, S., LIPTON, S. A. & DING, S. 2011. Direct reprogramming of adult human fibroblasts to functional neurons under defined conditions. *Cell Stem Cell*, 9, 113-8.
- ANDERSON, S. A., KAZNOWSKI, C. E., HORN, C., RUBENSTEIN, J. L. & MCCONNELL, S. K. 2002. Distinct origins of neocortical projection neurons and interneurons in vivo. *Cereb Cortex*, 12, 702-9.
- ANDROUTSELLIS-THEOTOKIS, A., LEKER, R. R., SOLDNER, F., HOEPPNER, D. J., RAVIN, R., POSER, S. W., RUEGER, M. A., BAE, S. K., KITTAPPA, R. & MCKAY, R. D. 2006. Notch signalling regulates stem cell numbers in vitro and in vivo. *Nature*, 442, 823-6.
- ANKARCRONA, M., DYPBUKT, J. M., BONFOCO, E., ZHIVOTOVSKY, B., ORRENIUS, S., LIPTON, S. A. & NICOTERA, P. 1995. Glutamate-induced neuronal death: a succession of necrosis or apoptosis depending on mitochondrial function. *Neuron*, 15, 961-73.

- ANTHONY, T. E., KLEIN, C., FISHELL, G. & HEINTZ, N. 2004. Radial glia serve as neuronal progenitors in all regions of the central nervous system. *Neuron*, 41, 881-90.
- ARLOTTA, P. & BERNINGER, B. 2014. Brains in metamorphosis: reprogramming cell identity within the central nervous system. *Curr Opin Neurobiol*, 27C, 208-214.
- ARVIDSSON, A., COLLIN, T., KIRIK, D., KOKAIA, Z. & LINDVALL, O. 2002. Neuronal replacement from endogenous precursors in the adult brain after stroke. *Nat Med*, 8, 963-70.
- ARVIDSSON, A., KOKAIA, Z. & LINDVALL, O. 2001. N-methyl-D-aspartate receptor-mediated increase of neurogenesis in adult rat dentate gyrus following stroke. *Eur J Neurosci*, 14, 10-8.
- ASANO, H., AONUMA, M., SANOSAKA, T., KOHYAMA, J., NAMIHIRA, M. & NAKASHIMA, K. 2009. Astrocyte differentiation of neural precursor cells is enhanced by retinoic acid through a change in epigenetic modification. *Stem Cells*, 27, 2744-52.
- ASTRUP, J., SIESJO, B. K. & SYMON, L. 1981. Thresholds in cerebral ischemia - the ischemic penumbra. *Stroke*, 12, 723-5.
- AZAM, M., ERDJUMENT-BROMAGE, H., KREIDER, B. L., XIA, M., QUELLE, F., BASU, R., SARIS, C., TEMPST, P., IHLE, J. N. & SCHINDLER, C. 1995. Interleukin-3 signals through multiple isoforms of Stat5. *EMBO J*, 14, 1402-11.
- BANERJEE, S., WILLIAMSON, D., HABIB, N., GORDON, M. & CHATAWAY, J. 2011. Human stem cell therapy in ischaemic stroke: a review. *Age Ageing*, 40, 7-13.
- BARCA-MAYO, O. & LU, Q. R. 2012. Fine-Tuning Oligodendrocyte Development by microRNAs. *Front Neurosci*, 6, 13.
- BARDEHLE, S., KRUGER, M., BUGGENTHIN, F., SCHWAUSCH, J., NINKOVIC, J., CLEVERS, H., SNIPPERT, H. J., THEIS, F. J., MEYER-LUEHMANN, M., BECHMANN, I., DIMOU, L. & GOTZ, M. 2013. Live imaging of astrocyte responses to acute injury reveals selective juxtavascular proliferation. *Nat Neurosci*, 16, 580-6.
- BARTEL, D. P. 2004. MicroRNAs: genomics, biogenesis, mechanism, and function. *Cell*, 116, 281-97.
- BARTEL, D. P. 2009. MicroRNAs: target recognition and regulatory functions. *Cell*, 136, 215-33.
- BATTISTE, J., HELMS, A. W., KIM, E. J., SAVAGE, T. K., LAGACE, D. C., MANDYAM, C. D., EISCH, A. J., MIYOSHI, G. & JOHNSON, J. E. 2007. *Ascl1* defines sequentially generated lineage-restricted neuronal and oligodendrocyte precursor cells in the spinal cord. *Development*, 134, 285-93.
- BAUER, S. 2009. Cytokine control of adult neural stem cells. *Ann N Y Acad Sci*, 1153, 48-56.
- BAUER, S. & PATTERSON, P. H. 2006. Leukemia inhibitory factor promotes neural stem cell self-renewal in the adult brain. *J Neurosci*, 26, 12089-99.
- BECKERVORDERSANDFORTH, R., TRIPATHI, P., NINKOVIC, J., BAYAM, E., LEPIER, A., STEMPFHUBER, B., KIRCHHOFF, F., HIRRLINGER, J., HASLINGER, A., LIE, D. C., BECKERS, J., YODER, B., IRMLER, M. & GOTZ, M. 2010. In vivo fate mapping and expression analysis reveals molecular hallmarks of prospectively isolated adult neural stem cells. *Cell Stem Cell*, 7, 744-58.

- BEGITT, A., MEYER, T., VAN ROSSUM, M. & VINKEMEIER, U. 2000. Nucleocytoplasmic translocation of Stat1 is regulated by a leucine-rich export signal in the coiled-coil domain. *Proc Natl Acad Sci U S A*, 97, 10418-23.
- BEKAR, L. K., HE, W. & NEDERGAARD, M. 2008. Locus coeruleus alpha-adrenergic-mediated activation of cortical astrocytes in vivo. *Cereb Cortex*, 18, 2789-95.
- BENJELLOUN-TOUIMI, S., JACQUE, C. M., DERER, P., DE VITRY, F., MAUNOURY, R. & DUPOUEY, P. 1985. Evidence that mouse astrocytes may be derived from the radial glia. An immunohistochemical study of the cerebellum in the normal and reeler mouse. *J Neuroimmunol*, 9, 87-97.
- BENTIVOGLIO, M. & MAZZARELLO, P. 1999. The history of radial glia. *Brain Res Bull*, 49, 305-15.
- BERGMANN, O., LIEBL, J., BERNARD, S., ALKASS, K., YEUNG, M. S., STEIER, P., KUTSCHERA, W., JOHNSON, L., LANDEN, M., DRUID, H., SPALDING, K. L. & FRISEN, J. 2012. The age of olfactory bulb neurons in humans. *Neuron*, 74, 634-9.
- BERNINGER, B. 2010. Making neurons from mature glia: a far-fetched dream? *Neuropharmacology*, 58, 894-902.
- BERNINGER, B., COSTA, M. R., KOCH, U., SCHROEDER, T., SUTOR, B., GROTHE, B. & GOTZ, M. 2007. Functional properties of neurons derived from in vitro reprogrammed postnatal astroglia. *J Neurosci*, 27, 8654-64.
- BERNSTEIN, E., CAUDY, A. A., HAMMOND, S. M. & HANNON, G. J. 2001. Role for a bidentate ribonuclease in the initiation step of RNA interference. *Nature*, 409, 363-6.
- BETZ, A. & DARNELL, J. E., JR. 2006. A Hopscotch-chromatin connection. *Nat Genet*, 38, 977-9.
- BIGNAMI, A. & DAHL, D. 1974. Astrocyte-specific protein and radial glia in the cerebral cortex of newborn rat. *Nature*, 252, 55-6.
- BIRNER, P., TOUMANGELOVA-UZEIR, K., NATCHEV, S. & GUENTCHEV, M. 2010. STAT3 tyrosine phosphorylation influences survival in glioblastoma. *J Neurooncol*, 100, 339-43.
- BLISS, T., GUZMAN, R., DAADI, M. & STEINBERG, G. K. 2007. Cell transplantation therapy for stroke. *Stroke*, 38, 817-26.
- BLISS, T. M., ANDRES, R. H. & STEINBERG, G. K. 2010. Optimizing the success of cell transplantation therapy for stroke. *Neurobiol Dis*, 37, 275-83.
- BLISS, T. M., KELLY, S., SHAH, A. K., FOO, W. C., KOHLI, P., STOKES, C., SUN, G. H., MA, M., MASEL, J., KLEPPNER, S. R., SCHALLERT, T., PALMER, T. & STEINBERG, G. K. 2006. Transplantation of hNT neurons into the ischemic cortex: cell survival and effect on sensorimotor behavior. *J Neurosci Res*, 83, 1004-14.
- BONAGUIDI, M. A., PENG, C. Y., MCGUIRE, T., FALCIGLIA, G., GOBESKE, K. T., CZEISLER, C. & KESSLER, J. A. 2008. Noggin expands neural stem cells in the adult hippocampus. *J Neurosci*, 28, 9194-204.
- BONFANTI, L. & PERETTO, P. 2007. Radial glial origin of the adult neural stem cells in the subventricular zone. *Prog Neurobiol*, 83, 24-36.
- BONITA, R., DUNCAN, J., TRUELSEN, T., JACKSON, R. T. & BEAGLEHOLE, R. 1999. Passive smoking as well as active smoking increases the risk of acute stroke. *Tob Control*, 8, 156-60.

- BONNI, A., SUN, Y., NADAL-VICENS, M., BHATT, A., FRANK, D. A., ROZOVSKY, I., STAHL, N., YANCOPOULOS, G. D. & GREENBERG, M. E. 1997. Regulation of gliogenesis in the central nervous system by the JAK-STAT signaling pathway. *Science*, 278, 477-83.
- BORLONGAN, C. V., TAJIMA, Y., TROJANOWSKI, J. Q., LEE, V. M. & SANBERG, P. R. 1998. Transplantation of cryopreserved human embryonal carcinoma-derived neurons (NT2N cells) promotes functional recovery in ischemic rats. *Exp Neurol*, 149, 310-21.
- BOWMAN, T. & JOVE, R. 1999. STAT Proteins and Cancer. *Cancer Control*, 6, 615-619.
- BRAMBILLA, R., BRACCHI-RICARD, V., HU, W. H., FRYDEL, B., BRAMWELL, A., KARMALLY, S., GREEN, E. J. & BETHEA, J. R. 2005. Inhibition of astroglial nuclear factor kappaB reduces inflammation and improves functional recovery after spinal cord injury. *J Exp Med*, 202, 145-56.
- BRANTLEY, E. C. & BENVENISTE, E. N. 2008. Signal transducer and activator of transcription-3: a molecular hub for signaling pathways in gliomas. *Mol Cancer Res*, 6, 675-84.
- BREUNIG, J. J., SARKISIAN, M. R., ARELLANO, J. I., MOROZOV, Y. M., AYOUB, A. E., SOJITRA, S., WANG, B., FLAVELL, R. A., RAKIC, P. & TOWN, T. 2008. Primary cilia regulate hippocampal neurogenesis by mediating sonic hedgehog signaling. *Proc Natl Acad Sci U S A*, 105, 13127-32.
- BRILL, M. S., NINKOVIC, J., WINPENNY, E., HODGE, R. D., OZEN, I., YANG, R., LEPIER, A., GASCON, S., ERDELYI, F., SZABO, G., PARRAS, C., GUILLEMOT, F., FROTSCHER, M., BERNINGER, B., HEVNER, R. F., RAINETEAU, O. & GOTZ, M. 2009. Adult generation of glutamatergic olfactory bulb interneurons. *Nat Neurosci*, 12, 1524-33.
- BRILL, M. S., SNAPYAN, M., WOHLFROM, H., NINKOVIC, J., JAWERKA, M., MASTICK, G. S., ASHERY-PADAN, R., SAGHATELYAN, A., BERNINGER, B. & GOTZ, M. 2008. A *dlx2*- and *pax6*-dependent transcriptional code for periglomerular neuron specification in the adult olfactory bulb. *J Neurosci*, 28, 6439-52.
- BROMBERG, J. 2002. Stat proteins and oncogenesis. *J Clin Invest*, 109, 1139-42.
- BROMBERG, J. F., WRZESZCZYNSKA, M. H., DEVGAN, G., ZHAO, Y., PESTELL, R. G., ALBANESE, C. & DARNELL, J. E., JR. 1999. Stat3 as an oncogene. *Cell*, 98, 295-303.
- BU, B., LI, J., DAVIES, P. & VINCENT, I. 2002. Deregulation of *cdk5*, hyperphosphorylation, and cytoskeletal pathology in the Niemann-Pick type C murine model. *J Neurosci*, 22, 6515-25.
- BUFFO, A., RITE, I., TRIPATHI, P., LEPIER, A., COLAK, D., HORN, A. P., MORI, T. & GOTZ, M. 2008. Origin and progeny of reactive gliosis: A source of multipotent cells in the injured brain. *Proc Natl Acad Sci U S A*, 105, 3581-6.
- BUFFO, A., VOSKO, M. R., ERTURK, D., HAMANN, G. F., JUCKER, M., ROWITCH, D. & GOTZ, M. 2005. Expression pattern of the transcription factor *Olig2* in response to brain injuries: implications for neuronal repair. *Proc Natl Acad Sci U S A*, 102, 18183-8.
- BURDON, T. G., DEMMER, J., CLARK, A. J. & WATSON, C. J. 1994. The mammary factor MPBF is a prolactin-induced transcriptional regulator which binds to STAT factor recognition sites. *FEBS Lett*, 350, 177-82.
- BUSH, T. G., PUVANACHANDRA, N., HORNER, C. H., POLITO, A., OSTENFELD, T., SVENDSEN, C. N., MUCKE, L., JOHNSON, M. H. & SOFRONIEW, M. V. 1999. Leukocyte infiltration,

- neuronal degeneration, and neurite outgrowth after ablation of scar-forming, reactive astrocytes in adult transgenic mice. *Neuron*, 23, 297-308.
- CAHOY, J. D., EMERY, B., KAUSHAL, A., FOO, L. C., ZAMANIAN, J. L., CHRISTOPHERSON, K. S., XING, Y., LUBISCHER, J. L., KRIEG, P. A., KRUPENKO, S. A., THOMPSON, W. J. & BARRES, B. A. 2008. A transcriptome database for astrocytes, neurons, and oligodendrocytes: a new resource for understanding brain development and function. *J Neurosci*, 28, 264-78.
- CAIAZZO, M., DELL'ANNO, M. T., DVORETSKOVA, E., LAZAREVIC, D., TAVERNA, S., LEO, D., SOTNIKOVA, T. D., MENEGON, A., RONCAGLIA, P., COLCIAGO, G., RUSSO, G., CARNINCI, P., PEZZOLI, G., GAINETDINOV, R. R., GUSTINCICH, S., DITYATEV, A. & BROCCOLI, V. 2011. Direct generation of functional dopaminergic neurons from mouse and human fibroblasts. *Nature*, 476, 224-7.
- CAJAL, S. R. Y. 1913-14. Estudios sobre la degeneración y regeneración del sistema nervioso. Madrid, Moya.
- CALDENHOVEN, E., VAN DIJK, T. B., SOLARI, R., ARMSTRONG, J., RAAIJMAKERS, J. A., LAMMERS, J. W., KOENDERMAN, L. & DE GROOT, R. P. 1996. STAT3beta, a splice variant of transcription factor STAT3, is a dominant negative regulator of transcription. *J Biol Chem*, 271, 13221-7.
- CAMPBELL, K. 2005. Cortical neuron specification: it has its time and place. *Neuron*, 46, 373-6.
- CAMPBELL, K. & GOTZ, M. 2002. Radial glia: multi-purpose cells for vertebrate brain development. *Trends Neurosci*, 25, 235-8.
- CARLEN, M., MELETIS, K., GORITZ, C., DARSALIA, V., EVERGREN, E., TANIGAKI, K., AMENDOLA, M., BARNABE-HEIDER, F., YEUNG, M. S., NALDINI, L., HONJO, T., KOKAIA, Z., SHUPLIAKOV, O., CASSIDY, R. M., LINDVALL, O. & FRISEN, J. 2009. Forebrain ependymal cells are Notch-dependent and generate neuroblasts and astrocytes after stroke. *Nat Neurosci*, 12, 259-67.
- CARLETON, A., PETREANU, L. T., LANSFORD, R., ALVAREZ-BUYLLA, A. & LLEDO, P. M. 2003. Becoming a new neuron in the adult olfactory bulb. *Nat Neurosci*, 6, 507-18.
- CASAROSA, S., FODE, C. & GUILLEMOT, F. 1999. Mash1 regulates neurogenesis in the ventral telencephalon. *Development*, 126, 525-34.
- CATTANEO, E., DE FRAJA, C., CONTI, L., REINACH, B., BOLIS, L., GOVONI, S. & LIBOI, E. 1996. Activation of the JAK/STAT pathway leads to proliferation of ST14A central nervous system progenitor cells. *J Biol Chem*, 271, 23374-9.
- CHAPMAN, R. S., LOURENCO, P. C., TONNER, E., FLINT, D. J., SELBERT, S., TAKEDA, K., AKIRA, S., CLARKE, A. R. & WATSON, C. J. 1999. Suppression of epithelial apoptosis and delayed mammary gland involution in mice with a conditional knockout of Stat3. *Genes Dev*, 13, 2604-16.
- CHEN, X., VINKEMEIER, U., ZHAO, Y., JERUZALMI, D., DARNELL, J. E., JR. & KURIYAN, J. 1998. Crystal structure of a tyrosine phosphorylated STAT-1 dimer bound to DNA. *Cell*, 93, 827-39.
- CHOI, B. H. 1988. Prenatal gliogenesis in the developing cerebrum of the mouse. *Glia*, 1, 308-16.

- CHOI, B. H. & LAPHAM, L. W. 1978. Radial glia in the human fetal cerebrum: a combined Golgi, immunofluorescent and electron microscopic study. *Brain Res*, 148, 295-311.
- CHOI, D. W. 1992. Excitotoxic cell death. *J Neurobiol*, 23, 1261-76.
- CHOI, D. W. & ROTHMAN, S. M. 1990. The role of glutamate neurotoxicity in hypoxic-ischemic neuronal death. *Annu Rev Neurosci*, 13, 171-82.
- CHOI, J. S., KIM, S. Y., PARK, H. J., CHA, J. H., CHOI, Y. S., KANG, J. E., CHUNG, J. W., CHUN, M. H. & LEE, M. Y. 2003. Upregulation of gp130 and differential activation of STAT and p42/44 MAPK in the rat hippocampus following kainic acid-induced seizures. *Brain Res Mol Brain Res*, 119, 10-8.
- COLAK, D., MORI, T., BRILL, M. S., PFEIFER, A., FALK, S., DENG, C., MONTEIRO, R., MUMMERY, C., SOMMER, L. & GOTZ, M. 2008. Adult neurogenesis requires Smad4-mediated bone morphogenic protein signaling in stem cells. *J Neurosci*, 28, 434-46.
- COLUCCI-D'AMATO, L., BONAVIDA, V. & DI PORZIO, U. 2006. The end of the central dogma of neurobiology: stem cells and neurogenesis in adult CNS. *Neurol Sci*, 27, 266-70.
- CONWAY, G. 2006. STAT3-dependent pathfinding and control of axonal branching and target selection. *Dev Biol*, 296, 119-36.
- CRUZ, J. C., TSENG, H. C., GOLDMAN, J. A., SHIH, H. & TSAI, L. H. 2003. Aberrant Cdk5 activation by p25 triggers pathological events leading to neurodegeneration and neurofibrillary tangles. *Neuron*, 40, 471-83.
- CURTIS, M. A., KAM, M., NANNMARK, U., ANDERSON, M. F., AXELL, M. Z., WIKKELSO, C., HOLTAS, S., VAN ROON-MOM, W. M., BJORK-ERIKSSON, T., NORDBORG, C., FRISEN, J., DRAGUNOW, M., FAULL, R. L. & ERIKSSON, P. S. 2007. Human neuroblasts migrate to the olfactory bulb via a lateral ventricular extension. *Science*, 315, 1243-9.
- DE-FRAJA, C., CONTI, L., GOVONI, S., BATTAINI, F. & CATTANEO, E. 2000. STAT signalling in the mature and aging brain. *Int J Dev Neurosci*, 18, 439-46.
- DECKER, T. & KOVARIK, P. 2000. Serine phosphorylation of STATs. *Oncogene*, 19, 2628-37.
- DESAI, A. R. & MCCONNELL, S. K. 2000. Progressive restriction in fate potential by neural progenitors during cerebral cortical development. *Development*, 127, 2863-72.
- DIRNAGL, U., IADECOLA, C. & MOSKOWITZ, M. A. 1999. Pathobiology of ischaemic stroke: an integrated view. *Trends Neurosci*, 22, 391-7.
- DOETSCH, F., CAILLE, I., LIM, D. A., GARCIA-VERDUGO, J. M. & ALVAREZ-BUYLLA, A. 1999. Subventricular zone astrocytes are neural stem cells in the adult mammalian brain. *Cell*, 97, 703-16.
- DOETSCH, F., GARCIA-VERDUGO, J. M. & ALVAREZ-BUYLLA, A. 1997. Cellular composition and three-dimensional organization of the subventricular germinal zone in the adult mammalian brain. *J Neurosci*, 17, 5046-61.
- DRANOVSKY, A. & HEN, R. 2006. Hippocampal neurogenesis: regulation by stress and antidepressants. *Biol Psychiatry*, 59, 1136-43.
- DROGEMULLER, K., HELMUTH, U., BRUNN, A., SAKOWICZ-BURKIEWICZ, M., GUTMANN, D. H., MUELLER, W., DECKERT, M. & SCHLUTER, D. 2008. Astrocyte gp130 expression is critical for the control of Toxoplasma encephalitis. *J Immunol*, 181, 2683-93.

- DZIENNIS, S. & ALKAYED, N. J. 2008. Role of signal transducer and activator of transcription 3 in neuronal survival and regeneration. *Rev Neurosci*, 19, 341-61.
- ECKENHOFF, M. F. & RAKIC, P. 1984. Radial organization of the hippocampal dentate gyrus: a Golgi, ultrastructural, and immunocytochemical analysis in the developing rhesus monkey. *J Comp Neurol*, 223, 1-21.
- EDDLESTON, M. & MUCKE, L. 1993. Molecular profile of reactive astrocytes--implications for their role in neurologic disease. *Neuroscience*, 54, 15-36.
- EDWARDS, M. A., YAMAMOTO, M. & CAVINESS, V. S., JR. 1990. Organization of radial glia and related cells in the developing murine CNS. An analysis based upon a new monoclonal antibody marker. *Neuroscience*, 36, 121-44.
- EKDAHL, C. T., MOHAPEL, P., WEBER, E., BAHR, B., BLOMGREN, K. & LINDVALL, O. 2002. Caspase-mediated death of newly formed neurons in the adult rat dentate gyrus following status epilepticus. *Eur J Neurosci*, 16, 1463-71.
- ENG, L. F. 1985. Glial fibrillary acidic protein (GFAP): the major protein of glial intermediate filaments in differentiated astrocytes. *J Neuroimmunol*, 8, 203-14.
- FAN, G., MARTINOWICH, K., CHIN, M. H., HE, F., FOUSE, S. D., HUTNICK, L., HATTORI, D., GE, W., SHEN, Y., WU, H., TEN HOEVE, J., SHUAI, K. & SUN, Y. E. 2005. DNA methylation controls the timing of astroglialogenesis through regulation of JAK-STAT signaling. *Development*, 132, 3345-56.
- FAULKNER, J. R., HERRMANN, J. E., WOO, M. J., TANSEY, K. E., DOAN, N. B. & SOFRONIEW, M. V. 2004. Reactive astrocytes protect tissue and preserve function after spinal cord injury. *J Neurosci*, 24, 2143-55.
- FILIPPOV, V., KRONENBERG, G., PIVNEVA, T., REUTER, K., STEINER, B., WANG, L. P., YAMAGUCHI, M., KETTENMANN, H. & KEMPERMANN, G. 2003. Subpopulation of nestin-expressing progenitor cells in the adult murine hippocampus shows electrophysiological and morphological characteristics of astrocytes. *Mol Cell Neurosci*, 23, 373-82.
- FLETCHER, L., KOHLI, S., SPRAGUE, S. M., SCRANTON, R. A., LIPTON, S. A., PARRA, A., JIMENEZ, D. F. & DIGICAYLIOGLU, M. 2009. Intranasal delivery of erythropoietin plus insulin-like growth factor-I for acute neuroprotection in stroke. Laboratory investigation. *J Neurosurg*, 111, 164-70.
- FODE, C., MA, Q., CASAROSA, S., ANG, S. L., ANDERSON, D. J. & GUILLEMOT, F. 2000. A role for neural determination genes in specifying the dorsoventral identity of telencephalic neurons. *Genes Dev*, 14, 67-80.
- FOGARTY, M., RICHARDSON, W. D. & KESSARIS, N. 2005. A subset of oligodendrocytes generated from radial glia in the dorsal spinal cord. *Development*, 132, 1951-9.
- FOSHAY, K. M. & GALLICANO, G. I. 2008. Regulation of Sox2 by STAT3 initiates commitment to the neural precursor cell fate. *Stem Cells Dev*, 17, 269-78.
- FU, A. K., FU, W. Y., NG, A. K., CHIEN, W. W., NG, Y. P., WANG, J. H. & IP, N. Y. 2004. Cyclin-dependent kinase 5 phosphorylates signal transducer and activator of transcription 3 and regulates its transcriptional activity. *Proc Natl Acad Sci U S A*, 101, 6728-33.



- FUKUDA, S., KATO, F., TOZUKA, Y., YAMAGUCHI, M., MIYAMOTO, Y. & HISATSUNE, T. 2003. Two distinct subpopulations of nestin-positive cells in adult mouse dentate gyrus. *J Neurosci*, 23, 9357-66.
- GAIANO, N., KOHTZ, J. D., TURNBULL, D. H. & FISHELL, G. 1999. A method for rapid gain-of-function studies in the mouse embryonic nervous system. *Nat Neurosci*, 2, 812-9.
- GAUTRON, L., DE SMEDT-PEYRUSSE, V. & LAYE, S. 2006. Characterization of STAT3-expressing cells in the postnatal rat brain. *Brain Res*, 1098, 26-32.
- GE, W. P., MIYAWAKI, A., GAGE, F. H., JAN, Y. N. & JAN, L. Y. 2012. Local generation of glia is a major astrocyte source in postnatal cortex. *Nature*, 484, 376-80.
- GOSEN, M. & BUJARD, H. 1992. Tight control of gene expression in mammalian cells by tetracycline-responsive promoters. *Proc Natl Acad Sci U S A*, 89, 5547-51.
- GOTZ, M. & HUTTNER, W. B. 2005. The cell biology of neurogenesis. *Nat Rev Mol Cell Biol*, 6, 777-88.
- GOULD, E. & CAMERON, H. A. 1996. Regulation of neuronal birth, migration and death in the rat dentate gyrus. *Dev Neurosci*, 18, 22-35.
- GRANDE, A., SUMIYOSHI, K., LOPEZ-JUAREZ, A., HOWARD, J., SAKTHIVEL, B., ARONOW, B., CAMPBELL, K. & NAKAFUKU, M. 2013. Environmental impact on direct neuronal reprogramming in vivo in the adult brain. *Nat Commun*, 4, 2373.
- GROSS, R. E., MEHLER, M. F., MABIE, P. C., ZANG, Z., SANTSCHI, L. & KESSLER, J. A. 1996. Bone morphogenetic proteins promote astroglial lineage commitment by mammalian subventricular zone progenitor cells. *Neuron*, 17, 595-606.
- GU, F., HATA, R., MA, Y. J., TANAKA, J., MITSUDA, N., KUMON, Y., HANAKAWA, Y., HASHIMOTO, K., NAKAJIMA, K. & SAKANAKA, M. 2005. Suppression of Stat3 promotes neurogenesis in cultured neural stem cells. *J Neurosci Res*, 81, 163-71.
- GUILLEMOT, F. 2005. Cellular and molecular control of neurogenesis in the mammalian telencephalon. *Curr Opin Cell Biol*, 17, 639-47.
- GUILLEMOT, F. 2007. Spatial and temporal specification of neural fates by transcription factor codes. *Development*, 134, 3771-80.
- GUO, Z., ZHANG, L., WU, Z., CHEN, Y., WANG, F. & CHEN, G. 2014. In Vivo direct reprogramming of reactive glial cells into functional neurons after brain injury and in an Alzheimer's disease model. *Cell Stem Cell*, 14, 188-202.
- GUPTA, S., YAN, H., WONG, L. H., RALPH, S., KROLEWSKI, J. & SCHINDLER, C. 1996. The SH2 domains of Stat1 and Stat2 mediate multiple interactions in the transduction of IFN-alpha signals. *EMBO J*, 15, 1075-84.
- GURDON, J. B. 1962. The developmental capacity of nuclei taken from intestinal epithelium cells of feeding tadpoles. *J Embryol Exp Morphol*, 10, 622-40.
- GUSTAFSSON, E., ANDSBERG, G., DARSALIA, V., MOHAPEL, P., MANDEL, R. J., KIRIK, D., LINDVALL, O. & KOKAIA, Z. 2003. Anterograde delivery of brain-derived neurotrophic factor to striatum via nigral transduction of recombinant adeno-associated virus increases neuronal death but promotes neurogenic response following stroke. *Eur J Neurosci*, 17, 2667-78.

- HACK, M. A., SAGHATELYAN, A., DE CHEVIGNY, A., PFEIFER, A., ASHERY-PADAN, R., LLEDO, P. M. & GOTZ, M. 2005. Neuronal fate determinants of adult olfactory bulb neurogenesis. *Nat Neurosci*, 8, 865-72.
- HACKE, W., KASTE, M., BLUHMKI, E., BROZMAN, M., DAVALOS, A., GUIDETTI, D., LARRUE, V., LEES, K. R., MEDEGHRI, Z., MACHNIG, T., SCHNEIDER, D., VON KUMMER, R., WAHLGREN, N. & TONI, D. 2008. Thrombolysis with alteplase 3 to 4.5 hours after acute ischemic stroke. *N Engl J Med*, 359, 1317-29.
- HAJOS, F., WOODHAMS, P. L., BASCO, E., CSILLAG, A. & BALAZS, R. 1981. Proliferation of astroglia in the embryonic mouse forebrain as revealed by simultaneous immunocytochemistry and autoradiography. *Acta Morphol Acad Sci Hung*, 29, 361-4.
- HAKANSSON, M. L. & MEISTER, B. 1998. Transcription factor STAT3 in leptin target neurons of the rat hypothalamus. *Neuroendocrinology*, 68, 420-7.
- HANAHAHAN, D. 1983. Studies on transformation of *Escherichia coli* with plasmids. *J Mol Biol*, 166, 557-80.
- HANISCH, U. K. & KETTENMANN, H. 2007. Microglia: active sensor and versatile effector cells in the normal and pathologic brain. *Nat Neurosci*, 10, 1387-94.
- HANKEY, G. J. 2006. Potential new risk factors for ischemic stroke: what is their potential? *Stroke*, 37, 2181-8.
- HART, R. G., BENAVENTE, O., MCBRIDE, R. & PEARCE, L. A. 1999. Antithrombotic therapy to prevent stroke in patients with atrial fibrillation: a meta-analysis. *Ann Intern Med*, 131, 492-501.
- HARTFUSS, E., GALLI, R., HEINS, N. & GOTZ, M. 2001. Characterization of CNS precursor subtypes and radial glia. *Dev Biol*, 229, 15-30.
- HASHIOKA, S., KLEGERIS, A., SCHWAB, C. & MCGEER, P. L. 2009. Interferon-gamma-dependent cytotoxic activation of human astrocytes and astrocytoma cells. *Neurobiol Aging*, 30, 1924-35.
- HASPEL, R. L. & DARNELL, J. E., JR. 1999. A nuclear protein tyrosine phosphatase is required for the inactivation of Stat1. *Proc Natl Acad Sci U S A*, 96, 10188-93.
- HASPEL, R. L., SALDITT-GEORGIEFF, M. & DARNELL, J. E., JR. 1996. The rapid inactivation of nuclear tyrosine phosphorylated Stat1 depends upon a protein tyrosine phosphatase. *EMBO J*, 15, 6262-8.
- HATA, R., MIES, G., WIESSNER, C., FRITZE, K., HESSELBARTH, D., BRINKER, G. & HOSSMANN, K. A. 1998. A reproducible model of middle cerebral artery occlusion in mice: hemodynamic, biochemical, and magnetic resonance imaging. *J Cereb Blood Flow Metab*, 18, 367-75.
- HAUBENSAK, W., ATTARDO, A., DENK, W. & HUTTNER, W. B. 2004. Neurons arise in the basal neuroepithelium of the early mammalian telencephalon: a major site of neurogenesis. *Proc Natl Acad Sci U S A*, 101, 3196-201.
- HE, F., GE, W., MARTINOWICH, K., BECKER-CATANIA, S., COSKUN, V., ZHU, W., WU, H., CASTRO, D., GUILLEMOT, F., FAN, G., DE VELLIS, J. & SUN, Y. E. 2005. A positive autoregulatory loop of Jak-STAT signaling controls the onset of astroglialogenesis. *Nat Neurosci*, 8, 616-25.

- HE, W., INGRAHAM, C., RISING, L., GODERIE, S. & TEMPLE, S. 2001. Multipotent stem cells from the mouse basal forebrain contribute GABAergic neurons and oligodendrocytes to the cerebral cortex during embryogenesis. *J Neurosci*, 21, 8854-62.
- HEINRICH, C., BLUM, R., GASCON, S., MASSERDOTTI, G., TRIPATHI, P., SANCHEZ, R., TIEDT, S., SCHROEDER, T., GOTZ, M. & BERNINGER, B. 2010. Directing astroglia from the cerebral cortex into subtype specific functional neurons. *PLoS Biol*, 8, e1000373.
- HEINRICH, C., GASCON, S., MASSERDOTTI, G., LEPIER, A., SANCHEZ, R., SIMON-EBERT, T., SCHROEDER, T., GOTZ, M. & BERNINGER, B. 2011. Generation of subtype-specific neurons from postnatal astroglia of the mouse cerebral cortex. *Nat Protoc*, 6, 214-28.
- HEINRICH, P. C., BEHRMANN, I., HAAN, S., HERMANN, H. M., MULLER-NEWEN, G. & SCHAPER, F. 2003. Principles of interleukin (IL)-6-type cytokine signalling and its regulation. *Biochem J*, 374, 1-20.
- HEINRICH, P. C., BEHRMANN, I., MULLER-NEWEN, G., SCHAPER, F. & GRAEVE, L. 1998. Interleukin-6-type cytokine signalling through the gp130/Jak/STAT pathway. *Biochem J*, 334 ( Pt 2), 297-314.
- HEINS, N., CREMISI, F., MALATESTA, P., GANGEMI, R. M., CORTE, G., PRICE, J., GOUDREAU, G., GRUSS, P. & GOTZ, M. 2001. Emx2 promotes symmetric cell divisions and a multipotential fate in precursors from the cerebral cortex. *Mol Cell Neurosci*, 18, 485-502.
- HEINS, N., MALATESTA, P., CECCONI, F., NAKAFUKU, M., TUCKER, K. L., HACK, M. A., CHAPOUTON, P., BARDE, Y. A. & GOTZ, M. 2002. Glial cells generate neurons: the role of the transcription factor Pax6. *Nat Neurosci*, 5, 308-15.
- HERRMANN, J. E., IMURA, T., SONG, B., QI, J., AO, Y., NGUYEN, T. K., KORSACK, R. A., TAKEDA, K., AKIRA, S. & SOFRONIEW, M. V. 2008. STAT3 is a critical regulator of astrogliosis and scar formation after spinal cord injury. *J Neurosci*, 28, 7231-43.
- HICKS, A. & JOLKKONEN, J. 2009. Challenges and possibilities of intravascular cell therapy in stroke. *Acta Neurobiol Exp (Wars)*, 69, 1-11.
- HIRABAYASHI, Y., SUZKI, N., TSUBOI, M., ENDO, T. A., TOYODA, T., SHINGA, J., KOSEKI, H., VIDAL, M. & GOTOH, Y. 2009. Polycomb limits the neurogenic competence of neural precursor cells to promote astrogenic fate transition. *Neuron*, 63, 600-13.
- HONG, H. S., HWANG, E. M., SIM, H. J., CHO, H. J., BOO, J. H., OH, S. S., KIM, S. U. & MOOK-JUNG, I. 2003. Interferon gamma stimulates beta-secretase expression and sAPPbeta production in astrocytes. *Biochem Biophys Res Commun*, 307, 922-7.
- HORVATH, C. M., STARK, G. R., KERR, I. M. & DARNELL, J. E., JR. 1996. Interactions between STAT and non-STAT proteins in the interferon-stimulated gene factor 3 transcription complex. *Mol Cell Biol*, 16, 6957-64.
- HOZUMI, I., CHIU, F. C. & NORTON, W. T. 1990. Biochemical and immunocytochemical changes in glial fibrillary acidic protein after stab wounds. *Brain Res*, 524, 64-71.
- HSIAO, K., CHAPMAN, P., NILSEN, S., ECKMAN, C., HARIGAYA, Y., YOUNKIN, S., YANG, F. & COLE, G. 1996. Correlative memory deficits, Abeta elevation, and amyloid plaques in transgenic mice. *Science*, 274, 99-102.
- IMAYOSHI, I., SAKAMOTO, M., OHTSUKA, T., TAKAO, K., MIYAKAWA, T., YAMAGUCHI, M., MORI, K., IKEDA, T., ITOHARA, S. & KAGEYAMA, R. 2008. Roles of continuous

- neurogenesis in the structural and functional integrity of the adult forebrain. *Nat Neurosci*, 11, 1153-61.
- IVANOV, V. N., BHOUMIK, A., KRASILNIKOV, M., RAZ, R., OWEN-SCHAUB, L. B., LEVY, D., HORVATH, C. M. & RONAI, Z. 2001. Cooperation between STAT3 and c-jun suppresses Fas transcription. *Mol Cell*, 7, 517-28.
- JIN, K., MAO, X. O., SUN, Y., XIE, L. & GREENBERG, D. A. 2002. Stem cell factor stimulates neurogenesis in vitro and in vivo. *J Clin Invest*, 110, 311-9.
- JIN, K., MINAMI, M., LAN, J. Q., MAO, X. O., BATTEUR, S., SIMON, R. P. & GREENBERG, D. A. 2001. Neurogenesis in dentate subgranular zone and rostral subventricular zone after focal cerebral ischemia in the rat. *Proc Natl Acad Sci U S A*, 98, 4710-5.
- JIN, K., WANG, X., XIE, L., MAO, X. O. & GREENBERG, D. A. 2010. Transgenic ablation of doublecortin-expressing cells suppresses adult neurogenesis and worsens stroke outcome in mice. *Proc Natl Acad Sci U S A*, 107, 7993-8.
- JOHANSSON, C. B., MOMMA, S., CLARKE, D. L., RISLING, M., LENDAHL, U. & FRISEN, J. 1999. Identification of a neural stem cell in the adult mammalian central nervous system. *Cell*, 96, 25-34.
- JOHN, G. R., LEE, S. C. & BROSINAN, C. F. 2003. Cytokines: powerful regulators of glial cell activation. *Neuroscientist*, 9, 10-22.
- JONES, K. J., KORB, E., KUNDEL, M. A., KOCHANNEK, A. R., KABRAJI, S., MCEVOY, M., SHIN, C. Y. & WELLS, D. G. 2008. CPEB1 regulates beta-catenin mRNA translation and cell migration in astrocytes. *Glia*, 56, 1401-13.
- JUSTICIA, C., GABRIEL, C. & PLANAS, A. M. 2000. Activation of the JAK/STAT pathway following transient focal cerebral ischemia: signaling through Jak1 and Stat3 in astrocytes. *Glia*, 30, 253-70.
- KAMAKURA, S., OISHI, K., YOSHIMATSU, T., NAKAFUKU, M., MASUYAMA, N. & GOTOH, Y. 2004. Hes binding to STAT3 mediates crosstalk between Notch and JAK-STAT signalling. *Nat Cell Biol*, 6, 547-54.
- KAMPHUIS, W., MAMBER, C., MOETON, M., KOOIJMAN, L., SLUIJS, J. A., JANSEN, A. H., VERVEER, M., DE GROOT, L. R., SMITH, V. D., RANGARAJAN, S., RODRIGUEZ, J. J., ORRE, M. & HOL, E. M. 2012. GFAP isoforms in adult mouse brain with a focus on neurogenic astrocytes and reactive astrogliosis in mouse models of Alzheimer disease. *PLoS One*, 7, e42823.
- KANG, S. H., FUKAYA, M., YANG, J. K., ROTHSTEIN, J. D. & BERGLES, D. E. 2010. NG2+ CNS glial progenitors remain committed to the oligodendrocyte lineage in postnatal life and following neurodegeneration. *Neuron*, 68, 668-81.
- KAPLAN, M. S. & HINDS, J. W. 1977. Neurogenesis in the adult rat: electron microscopic analysis of light radioautographs. *Science*, 197, 1092-4.
- KAROW, M., SANCHEZ, R., SCHICHOR, C., MASSERDOTTI, G., ORTEGA, F., HEINRICH, C., GASCON, S., KHAN, M. A., LIE, D. C., DELLAVALLE, A., COSSU, G., GOLDBRUNNER, R., GOTZ, M. & BERNINGER, B. 2012. Reprogramming of pericyte-derived cells of the adult human brain into induced neuronal cells. *Cell Stem Cell*, 11, 471-6.

- KEMPERMANN, G., GAST, D., KRONENBERG, G., YAMAGUCHI, M. & GAGE, F. H. 2003. Early determination and long-term persistence of adult-generated new neurons in the hippocampus of mice. *Development*, 130, 391-9.
- KEMPERMANN, G., KUHN, H. G. & GAGE, F. H. 1997. More hippocampal neurons in adult mice living in an enriched environment. *Nature*, 386, 493-5.
- KESSARIS, N., FOGARTY, M., IANNARELLI, P., GRIST, M., WEGNER, M. & RICHARDSON, W. D. 2006. Competing waves of oligodendrocytes in the forebrain and postnatal elimination of an embryonic lineage. *Nat Neurosci*, 9, 173-9.
- KIM, J., SU, S. C., WANG, H., CHENG, A. W., CASSADY, J. P., LODATO, M. A., LENGNER, C. J., CHUNG, C. Y., DAWLATY, M. M., TSAI, L. H. & JAENISCH, R. 2011. Functional integration of dopaminergic neurons directly converted from mouse fibroblasts. *Cell Stem Cell*, 9, 413-9.
- KISSELEVA, T., BHATTACHARYA, S., BRAUNSTEIN, J. & SCHINDLER, C. W. 2002. Signaling through the JAK/STAT pathway, recent advances and future challenges. *Gene*, 285, 1-24.
- KIZER, J. R., WIEBERS, D. O., WHISNANT, J. P., GALLOWAY, J. M., WELTY, T. K., LEE, E. T., BEST, L. G., RESNICK, H. E., ROMAN, M. J. & DEVEREUX, R. B. 2005. Mitral annular calcification, aortic valve sclerosis, and incident stroke in adults free of clinical cardiovascular disease: the Strong Heart Study. *Stroke*, 36, 2533-7.
- KOCH, P., OPITZ, T., STEINBECK, J. A., LADEWIG, J. & BRUSTLE, O. 2009. A rosette-type, self-renewing human ES cell-derived neural stem cell with potential for in vitro instruction and synaptic integration. *Proc Natl Acad Sci U S A*, 106, 3225-30.
- KOKAIA, Z. & LINDVALL, O. 2003. Neurogenesis after ischaemic brain insults. *Curr Opin Neurobiol*, 13, 127-32.
- KREBS, D. L. & HILTON, D. J. 2001. SOCS proteins: negative regulators of cytokine signaling. *Stem Cells*, 19, 378-87.
- KRIEGSTEIN, A. & ALVAREZ-BUYLLA, A. 2009. The glial nature of embryonic and adult neural stem cells. *Annu Rev Neurosci*, 32, 149-84.
- LANDY, A. 1989. Dynamic, structural, and regulatory aspects of lambda site-specific recombination. *Annu Rev Biochem*, 58, 913-49.
- LANG, B., LIU, H. L., LIU, R., FENG, G. D., JIAO, X. Y. & JU, G. 2004. Astrocytes in injured adult rat spinal cord may acquire the potential of neural stem cells. *Neuroscience*, 128, 775-83.
- LAWES, C. M., BENNETT, D. A., FEIGIN, V. L. & RODGERS, A. 2004a. Blood pressure and stroke: an overview of published reviews. *Stroke*, 35, 1024.
- LAWES, C. M., PARAG, V., BENNETT, D. A., SUH, I., LAM, T. H., WHITLOCK, G., BARZI, F. & WOODWARD, M. 2004b. Blood glucose and risk of cardiovascular disease in the Asia Pacific region. *Diabetes Care*, 27, 2836-42.
- LAYWELL, E. D., RAKIC, P., KUKKOV, V. G., HOLLAND, E. C. & STEINDLER, D. A. 2000. Identification of a multipotent astrocytic stem cell in the immature and adult mouse brain. *Proc Natl Acad Sci U S A*, 97, 13883-8.

- LAZARINI, F. & LLEDO, P. M. 2011. Is adult neurogenesis essential for olfaction? *Trends Neurosci*, 34, 20-30.
- LEE, C. K., RAZ, R., GIMENO, R., GERTNER, R., WISTINGHAUSEN, B., TAKESHITA, K., DEPINHO, R. A. & LEVY, D. E. 2002. STAT3 is a negative regulator of granulopoiesis but is not required for G-CSF-dependent differentiation. *Immunity*, 17, 63-72.
- LEE, M. S., KWON, Y. T., LI, M., PENG, J., FRIEDLANDER, R. M. & TSAI, L. H. 2000. Neurotoxicity induces cleavage of p35 to p25 by calpain. *Nature*, 405, 360-4.
- LEHMANN, U., SCHMITZ, J., WEISSENBACH, M., SOBOTA, R. M., HORTNER, M., FRIEDERICH, K., BEHRMANN, I., TSIARIS, W., SASAKI, A., SCHNEIDER-MERGENER, J., YOSHIMURA, A., NEEL, B. G., HEINRICH, P. C. & SCHAPER, F. 2003. SHP2 and SOCS3 contribute to Tyr-759-dependent attenuation of interleukin-6 signaling through gp130. *J Biol Chem*, 278, 661-71.
- LEUNER, B., GOULD, E. & SHORS, T. J. 2006. Is there a link between adult neurogenesis and learning? *Hippocampus*, 16, 216-24.
- LEVERS, T. E., EDGAR, J. M. & PRICE, D. J. 2001. The fates of cells generated at the end of neurogenesis in developing mouse cortex. *J Neurobiol*, 48, 265-77.
- LEVISON, S. W., CHUANG, C., ABRAMSON, B. J. & GOLDMAN, J. E. 1993. The migrational patterns and developmental fates of glial precursors in the rat subventricular zone are temporally regulated. *Development*, 119, 611-22.
- LEVITT, P. & RAKIC, P. 1980. Immunoperoxidase localization of glial fibrillary acidic protein in radial glial cells and astrocytes of the developing rhesus monkey brain. *J Comp Neurol*, 193, 815-40.
- LEVY, D. E. & DARNELL, J. E., JR. 2002. Stats: transcriptional control and biological impact. *Nat Rev Mol Cell Biol*, 3, 651-62.
- LEVY, D. E. & LEE, C. K. 2002. What does Stat3 do? *J Clin Invest*, 109, 1143-8.
- LI, W., COGSWELL, C. A. & LOTURCO, J. J. 1998. Neuronal differentiation of precursors in the neocortical ventricular zone is triggered by BMP. *J Neurosci*, 18, 8853-62.
- LI, W. X. 2008. Canonical and non-canonical JAK-STAT signaling. *Trends Cell Biol*, 18, 545-51.
- LI, Y., CHEN, J., CHEN, X. G., WANG, L., GAUTAM, S. C., XU, Y. X., KATAKOWSKI, M., ZHANG, L. J., LU, M., JANAKIRAMAN, N. & CHOPP, M. 2002. Human marrow stromal cell therapy for stroke in rat: neurotrophins and functional recovery. *Neurology*, 59, 514-23.
- LIE, D. C., COLAMARINO, S. A., SONG, H. J., DESIRE, L., MIRA, H., CONSIGLIO, A., LEIN, E. S., JESSBERGER, S., LANSFORD, H., DEARIE, A. R. & GAGE, F. H. 2005. Wnt signalling regulates adult hippocampal neurogenesis. *Nature*, 437, 1370-5.
- LIE, D. C., SONG, H., COLAMARINO, S. A., MING, G. L. & GAGE, F. H. 2004. Neurogenesis in the adult brain: new strategies for central nervous system diseases. *Annu Rev Pharmacol Toxicol*, 44, 399-421.
- LINDVALL, O. & KOKAIA, Z. 2006. Stem cells for the treatment of neurological disorders. *Nature*, 441, 1094-6.
- LINDVALL, O., KOKAIA, Z. & MARTINEZ-SERRANO, A. 2004. Stem cell therapy for human neurodegenerative disorders-how to make it work. *Nat Med*, 10 Suppl, S42-50.

- LIU, J., SOLWAY, K., MESSING, R. O. & SHARP, F. R. 1998. Increased neurogenesis in the dentate gyrus after transient global ischemia in gerbils. *J Neurosci*, 18, 7768-78.
- LIU, L., MCBRIDE, K. M. & REICH, N. C. 2005. STAT3 nuclear import is independent of tyrosine phosphorylation and mediated by importin- $\alpha$ 3. *Proc Natl Acad Sci U S A*, 102, 8150-5.
- LLOYD-JONES, D., ADAMS, R. J., BROWN, T. M., CARNETHON, M., DAI, S., DE SIMONE, G., FERGUSON, T. B., FORD, E., FURIE, K., GILLESPIE, C., GO, A., GREENLUND, K., HAASE, N., HAILPERN, S., HO, P. M., HOWARD, V., KISSELA, B., KITTNER, S., LACKLAND, D., LISABETH, L., MARELLI, A., MCDERMOTT, M. M., MEIGS, J., MOZAFFARIAN, D., MUSSOLINO, M., NICHOL, G., ROGER, V. L., ROSAMOND, W., SACCO, R., SORLIE, P., THOM, T., WASSERTHIEL-SMOLLER, S., WONG, N. D. & WYLIE-ROSETT, J. 2010. Heart disease and stroke statistics--2010 update: a report from the American Heart Association. *Circulation*, 121, e46-e215.
- LOH, E., SUTTON, M. S., WUN, C. C., ROULEAU, J. L., FLAKER, G. C., GOTTLIEB, S. S., LAMAS, G. A., MOYE, L. A., GOLDBERGER, S. Z. & PFEFFER, M. A. 1997. Ventricular dysfunction and the risk of stroke after myocardial infarction. *N Engl J Med*, 336, 251-7.
- LOIS, C. & ALVAREZ-BUYLLA, A. 1993. Proliferating subventricular zone cells in the adult mammalian forebrain can differentiate into neurons and glia. *Proc Natl Acad Sci U S A*, 90, 2074-7.
- LOIS, C. & ALVAREZ-BUYLLA, A. 1994. Long-distance neuronal migration in the adult mammalian brain. *Science*, 264, 1145-8.
- LUI, J. H., HANSEN, D. V. & KRIEGSTEIN, A. R. 2011. Development and evolution of the human neocortex. *Cell*, 146, 18-36.
- MA, D. K., BONAGUIDI, M. A., MING, G. L. & SONG, H. 2009a. Adult neural stem cells in the mammalian central nervous system. *Cell Res*, 19, 672-82.
- MA, D. K., KIM, W. R., MING, G. L. & SONG, H. 2009b. Activity-dependent extrinsic regulation of adult olfactory bulb and hippocampal neurogenesis. *Ann N Y Acad Sci*, 1170, 664-73.
- MADISON, R. D. & MACKLIS, J. D. 1993. Noninvasively induced degeneration of neocortical pyramidal neurons in vivo: selective targeting by laser activation of retrogradely transported photolytic chromophore. *Exp Neurol*, 121, 153-9.
- MAGAVI, S. S., LEAVITT, B. R. & MACKLIS, J. D. 2000. Induction of neurogenesis in the neocortex of adult mice. *Nature*, 405, 951-5.
- MAGAVI, S. S., MITCHELL, B. D., SZENTIRMAI, O., CARTER, B. S. & MACKLIS, J. D. 2005. Adult-born and preexisting olfactory granule neurons undergo distinct experience-dependent modifications of their olfactory responses in vivo. *J Neurosci*, 25, 10729-39.
- MALATESTA, P., HARTFUSS, E. & GOTZ, M. 2000. Isolation of radial glial cells by fluorescent-activated cell sorting reveals a neuronal lineage. *Development*, 127, 5253-63.
- MANDAIRON, N., SACQUET, J., JOURDAN, F. & DIDIER, A. 2006. Long-term fate and distribution of newborn cells in the adult mouse olfactory bulb: Influences of olfactory deprivation. *Neuroscience*, 141, 443-51.
- MARRO, S., PANG, Z. P., YANG, N., TSAI, M. C., QU, K., CHANG, H. Y., SUDHOF, T. C. & WERNIG, M. 2011. Direct lineage conversion of terminally differentiated hepatocytes to functional neurons. *Cell Stem Cell*, 9, 374-82.

- MASSOUH, M. & SAGHATELYAN, A. 2010. De-routing neuronal precursors in the adult brain to sites of injury: role of the vasculature. *Neuropharmacology*, 58, 877-83.
- MATHERS C, F. D., BOERMA JT, WORLD HEALTH ORGANIZATION 2008. The global burden of disease: 2004 update. Geneva, Switzerland: World Health Organization.
- MAYFORD, M., BACH, M. E., HUANG, Y. Y., WANG, L., HAWKINS, R. D. & KANDEL, E. R. 1996. Control of memory formation through regulated expression of a CaMKII transgene. *Science*, 274, 1678-83.
- MERKLE, F. T., MIRZADEH, Z. & ALVAREZ-BUYLLA, A. 2007. Mosaic organization of neural stem cells in the adult brain. *Science*, 317, 381-4.
- MERKLE, F. T., TRAMONTIN, A. D., GARCIA-VERDUGO, J. M. & ALVAREZ-BUYLLA, A. 2004. Radial glia give rise to adult neural stem cells in the subventricular zone. *Proc Natl Acad Sci U S A*, 101, 17528-32.
- MESHI, D., DREW, M. R., SAXE, M., ANSORGE, M. S., DAVID, D., SANTARELLI, L., MALAPANI, C., MOORE, H. & HEN, R. 2006. Hippocampal neurogenesis is not required for behavioral effects of environmental enrichment. *Nat Neurosci*, 9, 729-31.
- MEYDAN, N., GRUNBERGER, T., DADI, H., SHAHAR, M., ARPAIA, E., LAPIDOT, Z., LEEDER, J. S., FREEDMAN, M., COHEN, A., GAZIT, A., LEVITZKI, A. & ROIFMAN, C. M. 1996. Inhibition of acute lymphoblastic leukaemia by a Jak-2 inhibitor. *Nature*, 379, 645-8.
- MEYERS, J. A., SANCHEZ, D., ELWELL, L. P. & FALKOW, S. 1976. Simple agarose gel electrophoretic method for the identification and characterization of plasmid deoxyribonucleic acid. *J Bacteriol*, 127, 1529-37.
- MIES, G., IJIMA, T. & HOSSMANN, K. A. 1993. Correlation between peri-infarct DC shifts and ischaemic neuronal damage in rat. *Neuroreport*, 4, 709-11.
- MIRESCU, C. & GOULD, E. 2006. Stress and adult neurogenesis. *Hippocampus*, 16, 233-8.
- MIRZADEH, Z., MERKLE, F. T., SORIANO-NAVARRO, M., GARCIA-VERDUGO, J. M. & ALVAREZ-BUYLLA, A. 2008. Neural stem cells confer unique pinwheel architecture to the ventricular surface in neurogenic regions of the adult brain. *Cell Stem Cell*, 3, 265-78.
- MIYATA, T., KAWAGUCHI, A., SAITO, K., KAWANO, M., MUTO, T. & OGAWA, M. 2004. Asymmetric production of surface-dividing and non-surface-dividing cortical progenitor cells. *Development*, 131, 3133-45.
- MIZUGUCHI, R., SUGIMORI, M., TAKEBAYASHI, H., KOSAKO, H., NAGAO, M., YOSHIDA, S., NABESHIMA, Y., SHIMAMURA, K. & NAKAFUKU, M. 2001. Combinatorial roles of olig2 and neurogenin2 in the coordinated induction of pan-neuronal and subtype-specific properties of motoneurons. *Neuron*, 31, 757-71.
- MOLYNEAUX, B. J., ARLOTTA, P., MENEZES, J. R. & MACKLIS, J. D. 2007. Neuronal subtype specification in the cerebral cortex. *Nat Rev Neurosci*, 8, 427-37.
- MONJE, M. L., TODA, H. & PALMER, T. D. 2003. Inflammatory blockade restores adult hippocampal neurogenesis. *Science*, 302, 1760-5.
- MORENO, M. M., LINSTER, C., ESCANILLA, O., SACQUET, J., DIDIER, A. & MANDAIRON, N. 2009. Olfactory perceptual learning requires adult neurogenesis. *Proc Natl Acad Sci U S A*, 106, 17980-5.



- MORI, T., TANAKA, K., BUFFO, A., WURST, W., KUHN, R. & GOTZ, M. 2006. Inducible gene deletion in astroglia and radial glia--a valuable tool for functional and lineage analysis. *Glia*, 54, 21-34.
- MOSKOWITZ, M. A., LO, E. H. & IADECOLA, C. 2010. The science of stroke: mechanisms in search of treatments. *Neuron*, 67, 181-98.
- MOWEN, K. A., TANG, J., ZHU, W., SCHURTER, B. T., SHUAI, K., HERSCHMAN, H. R. & DAVID, M. 2001. Arginine methylation of STAT1 modulates IFNalpha/beta-induced transcription. *Cell*, 104, 731-41.
- MUI, A. L., WAKAO, H., O'FARRELL, A. M., HARADA, N. & MIYAJIMA, A. 1995. Interleukin-3, granulocyte-macrophage colony stimulating factor and interleukin-5 transduce signals through two STAT5 homologs. *EMBO J*, 14, 1166-75.
- MULLER, S., CHAKRAPANI, B. P., SCHWEGLER, H., HOFMANN, H. D. & KIRSCH, M. 2009. Neurogenesis in the dentate gyrus depends on ciliary neurotrophic factor and signal transducer and activator of transcription 3 signaling. *Stem Cells*, 27, 431-41.
- MYER, D. J., GURKOFF, G. G., LEE, S. M., HOVDA, D. A. & SOFRONIEW, M. V. 2006. Essential protective roles of reactive astrocytes in traumatic brain injury. *Brain*, 129, 2761-72.
- NA, Y. J., JIN, J. K., KIM, J. I., CHOI, E. K., CARP, R. I. & KIM, Y. S. 2007. JAK-STAT signaling pathway mediates astrogliosis in brains of scrapie-infected mice. *J Neurochem*, 103, 637-49.
- NAKAJIMA, K., YAMANAKA, Y., NAKAE, K., KOJIMA, H., ICHIBA, M., KIUCHI, N., KITAOKA, T., FUKADA, T., HIBI, M. & HIRANO, T. 1996. A central role for Stat3 in IL-6-induced regulation of growth and differentiation in M1 leukemia cells. *EMBO J*, 15, 3651-8.
- NAKASHIMA, K., YANAGISAWA, M., ARAKAWA, H., KIMURA, N., HISATSUNE, T., KAWABATA, M., MIYAZONO, K. & TAGA, T. 1999. Synergistic signaling in fetal brain by STAT3-Smad1 complex bridged by p300. *Science*, 284, 479-82.
- NAKATOMI, H., KURIU, T., OKABE, S., YAMAMOTO, S., HATANO, O., KAWAHARA, N., TAMURA, A., KIRINO, T. & NAKAFUKU, M. 2002. Regeneration of hippocampal pyramidal neurons after ischemic brain injury by recruitment of endogenous neural progenitors. *Cell*, 110, 429-41.
- NDUBUISI, M. I., GUO, G. G., FRIED, V. A., ETLINGER, J. D. & SEHGAL, P. B. 1999. Cellular physiology of STAT3: Where's the cytoplasmic monomer? *J Biol Chem*, 274, 25499-509.
- NEARY, J. T., KANG, Y., WILLOUGHBY, K. A. & ELLIS, E. F. 2003. Activation of extracellular signal-regulated kinase by stretch-induced injury in astrocytes involves extracellular ATP and P2 purinergic receptors. *J Neurosci*, 23, 2348-56.
- NGUYEN, M. D., LARIVIERE, R. C. & JULIEN, J. P. 2001. Deregulation of Cdk5 in a mouse model of ALS: toxicity alleviated by perikaryal neurofilament inclusions. *Neuron*, 30, 135-47.
- NINKOVIC, J., MORI, T. & GOTZ, M. 2007. Distinct modes of neuron addition in adult mouse neurogenesis. *J Neurosci*, 27, 10906-11.
- NINKOVIC, J., PINTO, L., PETRICCA, S., LEPIER, A., SUN, J., RIEGER, M. A., SCHROEDER, T., CVEKL, A., FAVOR, J. & GOTZ, M. 2010. The transcription factor Pax6 regulates survival of dopaminergic olfactory bulb neurons via crystallin alphaA. *Neuron*, 68, 682-94.

- NIU, W., ZANG, T., ZOU, Y., FANG, S., SMITH, D. K., BACHOO, R. & ZHANG, C. L. 2013. In vivo reprogramming of astrocytes to neuroblasts in the adult brain. *Nat Cell Biol*, 15, 1164-75.
- NOCTOR, S. C., FLINT, A. C., WEISSMAN, T. A., DAMMERMAN, R. S. & KRIEGSTEIN, A. R. 2001. Neurons derived from radial glial cells establish radial units in neocortex. *Nature*, 409, 714-20.
- NOCTOR, S. C., MARTINEZ-CERDENO, V., IVIC, L. & KRIEGSTEIN, A. R. 2004. Cortical neurons arise in symmetric and asymmetric division zones and migrate through specific phases. *Nat Neurosci*, 7, 136-44.
- NOCTOR, S. C., MARTINEZ-CERDENO, V. & KRIEGSTEIN, A. R. 2007. Contribution of intermediate progenitor cells to cortical histogenesis. *Arch Neurol*, 64, 639-42.
- NOTTEBOHM, F. 1985. Neuronal replacement in adulthood. *Ann N Y Acad Sci*, 457, 143-61.
- O'CALLAGHAN, J. P., KELLY, K. A., VANGILDER, R. L., SOFRONIEW, M. V. & MILLER, D. B. 2014. Early Activation of STAT3 Regulates Reactive Astroglialosis Induced by Diverse Forms of Neurotoxicity. *PLoS One*, 9, e102003.
- OHAB, J. J., FLEMING, S., BLESCH, A. & CARMICHAEL, S. T. 2006. A neurovascular niche for neurogenesis after stroke. *J Neurosci*, 26, 13007-16.
- OHIRA, K., FURUTA, T., HIOKI, H., NAKAMURA, K. C., KURAMOTO, E., TANAKA, Y., FUNATSU, N., SHIMIZU, K., OISHI, T., HAYASHI, M., MIYAKAWA, T., KANEKO, T. & NAKAMURA, S. 2010. Ischemia-induced neurogenesis of neocortical layer 1 progenitor cells. *Nat Neurosci*, 13, 173-9.
- OKADA, S., NAKAMURA, M., KATOH, H., MIYAO, T., SHIMAZAKI, T., ISHII, K., YAMANE, J., YOSHIMURA, A., IWAMOTO, Y., TOYAMA, Y. & OKANO, H. 2006. Conditional ablation of Stat3 or Socs3 discloses a dual role for reactive astrocytes after spinal cord injury. *Nat Med*, 12, 829-34.
- ONTENIENTE, B., KIMURA, H. & MAEDA, T. 1983. Comparative study of the glial fibrillary acidic protein in vertebrates by PAP immunohistochemistry. *J Comp Neurol*, 215, 427-36.
- ORELLANA, D. I., QUINTANILLA, R. A., GONZALEZ-BILLAULT, C. & MACCIONI, R. B. 2005. Role of the JAKs/STATs pathway in the intracellular calcium changes induced by interleukin-6 in hippocampal neurons. *Neurotox Res*, 8, 295-304.
- OSUKA, K., WATANABE, Y., USUDA, N., ATSUZAWA, K., YASUDA, M., AOSHIMA, C., WAKABAYASHI, T. & TAKAYASU, M. 2011. Activation of STAT1 in neurons following spinal cord injury in mice. *Neurochem Res*, 36, 2236-43.
- PANG, Z. P., YANG, N., VIERBUCHEN, T., OSTERMEIER, A., FUENTES, D. R., YANG, T. Q., CITRI, A., SEBASTIANO, V., MARRO, S., SUDHOF, T. C. & WERNIG, M. 2011. Induction of human neuronal cells by defined transcription factors. *Nature*, 476, 220-3.
- PARENT, J. M., ELLIOTT, R. C., PLEASURE, S. J., BARBARO, N. M. & LOWENSTEIN, D. H. 2006. Aberrant seizure-induced neurogenesis in experimental temporal lobe epilepsy. *Ann Neurol*, 59, 81-91.
- PARENT, J. M., VEXLER, Z. S., GONG, C., DERUGIN, N. & FERRIERO, D. M. 2002. Rat forebrain neurogenesis and striatal neuron replacement after focal stroke. *Ann Neurol*, 52, 802-13.

- PARENT, J. M., YU, T. W., LEIBOWITZ, R. T., GESCHWIND, D. H., SLOVITER, R. S. & LOWENSTEIN, D. H. 1997. Dentate granule cell neurogenesis is increased by seizures and contributes to aberrant network reorganization in the adult rat hippocampus. *J Neurosci*, 17, 3727-38.
- PARK, I. H., ZHAO, R., WEST, J. A., YABUUCHI, A., HUO, H., INCE, T. A., LEROU, P. H., LENSCH, M. W. & DALEY, G. Q. 2008. Reprogramming of human somatic cells to pluripotency with defined factors. *Nature*, 451, 141-6.
- PARNAVELAS, J. G. 1999. Glial cell lineages in the rat cerebral cortex. *Exp Neurol*, 156, 418-29.
- PARNAVELAS, J. G., BARFIELD, J. A., FRANKE, E. & LUSKIN, M. B. 1991. Separate progenitor cells give rise to pyramidal and nonpyramidal neurons in the rat telencephalon. *Cereb Cortex*, 1, 463-8.
- PARRAS, C. M., SCHUURMANS, C., SCARDIGLI, R., KIM, J., ANDERSON, D. J. & GUILLEMOT, F. 2002. Divergent functions of the proneural genes Mash1 and Ngn2 in the specification of neuronal subtype identity. *Genes Dev*, 16, 324-38.
- PEKKNY, M. & NILSSON, M. 2005. Astrocyte activation and reactive gliosis. *Glia*, 50, 427-34.
- PELLERIN, L., BOUZIER-SORE, A. K., AUBERT, A., SERRES, S., MERLE, M., COSTALAT, R. & MAGISTRETTI, P. J. 2007. Activity-dependent regulation of energy metabolism by astrocytes: an update. *Glia*, 55, 1251-62.
- PETRYNIAK, M. A., POTTER, G. B., ROWITCH, D. H. & RUBENSTEIN, J. L. 2007. Dlx1 and Dlx2 control neuronal versus oligodendroglial cell fate acquisition in the developing forebrain. *Neuron*, 55, 417-33.
- PFEFFER, L. M., MULLERSMAN, J. E., PFEFFER, S. R., MURTI, A., SHI, W. & YANG, C. H. 1997. STAT3 as an adapter to couple phosphatidylinositol 3-kinase to the IFNAR1 chain of the type I interferon receptor. *Science*, 276, 1418-20.
- PFISTERER, U., WOOD, J., NIHLBERG, K., HALLGREN, O., BJERMER, L., WESTERGREN-THORSSON, G., LINDVALL, O. & PARMAR, M. 2011. Efficient induction of functional neurons from adult human fibroblasts. *Cell Cycle*, 10, 3311-6.
- PLANAS, A. M., JUSTICIA, C. & FERRER, I. 1997. Stat1 in developing and adult rat brain. Induction after transient focal ischemia. *Neuroreport*, 8, 1359-62.
- PLANAS, A. M., SORIANO, M. A., BERRUEZO, M., JUSTICIA, C., ESTRADA, A., PITARCH, S. & FERRER, I. 1996. Induction of Stat3, a signal transducer and transcription factor, in reactive microglia following transient focal cerebral ischaemia. *Eur J Neurosci*, 8, 2612-8.
- PLESNILA, N., ZHU, C., CULMSEE, C., GROGER, M., MOSKOWITZ, M. A. & BLOMGREN, K. 2004. Nuclear translocation of apoptosis-inducing factor after focal cerebral ischemia. *J Cereb Blood Flow Metab*, 24, 458-66.
- QIANG, L., FUJITA, R., YAMASHITA, T., ANGULO, S., RHINN, H., RHEE, D., DOEGE, C., CHAU, L., AUBRY, L., VANTI, W. B., MORENO, H. & ABELIOVICH, A. 2011. Directed conversion of Alzheimer's disease patient skin fibroblasts into functional neurons. *Cell*, 146, 359-71.
- RABER, J., ROLA, R., LEFEVOUR, A., MORHARDT, D., CURLEY, J., MIZUMATSU, S., VANDENBERG, S. R. & FIKE, J. R. 2004. Radiation-induced cognitive impairments are associated with changes in indicators of hippocampal neurogenesis. *Radiat Res*, 162, 39-47.

- RADDE, R., BOLMONT, T., KAESER, S. A., COOMARASWAMY, J., LINDAU, D., STOLTZE, L., CALHOUN, M. E., JAGGI, F., WOLBURG, H., GENGLER, S., HAASS, C., GHETTI, B., CZECH, C., HOLSCHER, C., MATHEWS, P. M. & JUCKER, M. 2006. Abeta42-driven cerebral amyloidosis in transgenic mice reveals early and robust pathology. *EMBO Rep*, 7, 940-6.
- RAMIREZ-CASTILLEJO, C., SANCHEZ-SANCHEZ, F., ANDREU-AGULLO, C., FERRON, S. R., AROCA-AGUILAR, J. D., SANCHEZ, P., MIRA, H., ESCRIBANO, J. & FARINAS, I. 2006. Pigment epithelium-derived factor is a niche signal for neural stem cell renewal. *Nat Neurosci*, 9, 331-9.
- REICH, N. C. & LIU, L. 2006. Tracking STAT nuclear traffic. *Nat Rev Immunol*, 6, 602-12.
- REYNOLDS, B. A. & WEISS, S. 1992. Generation of neurons and astrocytes from isolated cells of the adult mammalian central nervous system. *Science*, 255, 1707-10.
- RIVERS, L. E., YOUNG, K. M., RIZZI, M., JAMEN, F., PSACHOULIA, K., WADE, A., KESSARIS, N. & RICHARDSON, W. D. 2008. PDGFRA/NG2 glia generate myelinating oligodendrocytes and piriform projection neurons in adult mice. *Nat Neurosci*, 11, 1392-401.
- ROBEL, S., BERNINGER, B. & GOTZ, M. 2011. The stem cell potential of glia: lessons from reactive gliosis. *Nat Rev Neurosci*, 12, 88-104.
- ROCHEFORT, C., GHEUSI, G., VINCENT, J. D. & LLEDO, P. M. 2002. Enriched odor exposure increases the number of newborn neurons in the adult olfactory bulb and improves odor memory. *J Neurosci*, 22, 2679-89.
- ROGER, V. L., GO, A. S., LLOYD-JONES, D. M., ADAMS, R. J., BERRY, J. D., BROWN, T. M., CARNETHON, M. R., DAI, S., DE SIMONE, G., FORD, E. S., FOX, C. S., FULLERTON, H. J., GILLESPIE, C., GREENLUND, K. J., HAILPERN, S. M., HEIT, J. A., HO, P. M., HOWARD, V. J., KISSELA, B. M., KITTNER, S. J., LACKLAND, D. T., LICHTMAN, J. H., LISABETH, L. D., MAKUC, D. M., MARCUS, G. M., MARELLI, A., MATCHAR, D. B., MCDERMOTT, M. M., MEIGS, J. B., MOY, C. S., MOZAFFARIAN, D., MUSSOLINO, M. E., NICHOL, G., PAYNTER, N. P., ROSAMOND, W. D., SORLIE, P. D., STAFFORD, R. S., TURAN, T. N., TURNER, M. B., WONG, N. D. & WYLIE-ROSETT, J. 2011. Heart disease and stroke statistics--2011 update: a report from the American Heart Association. *Circulation*, 123, e18-e209.
- ROTHSTEIN, J. D., DYKES-HOBERG, M., PARDO, C. A., BRISTOL, L. A., JIN, L., KUNCL, R. W., KANAI, Y., HEDIGER, M. A., WANG, Y., SCHIELKE, J. P. & WELTY, D. F. 1996. Knockout of glutamate transporters reveals a major role for astroglial transport in excitotoxicity and clearance of glutamate. *Neuron*, 16, 675-86.
- ROTHWELL, P. M., ELIASZIW, M., GUTNIKOV, S. A., FOX, A. J., TAYLOR, D. W., MAYBERG, M. R., WARLOW, C. P. & BARNETT, H. J. 2003. Analysis of pooled data from the randomised controlled trials of endarterectomy for symptomatic carotid stenosis. *Lancet*, 361, 107-16.
- RUPP, N. J., WEGENAST-BRAUN, B. M., RADDE, R., CALHOUN, M. E. & JUCKER, M. 2011. Early onset amyloid lesions lead to severe neuritic abnormalities and local, but not global neuron loss in APPS1 transgenic mice. *Neurobiol Aging*, 32, 2324 e1-6.
- SANAI, N., BERGER, M. S., GARCIA-VERDUGO, J. M. & ALVAREZ-BUYLLA, A. 2007. Comment on "Human neuroblasts migrate to the olfactory bulb via a lateral ventricular extension". *Science*, 318, 393; author reply 393.

- SANAI, N., NGUYEN, T., IHRIE, R. A., MIRZADEH, Z., TSAI, H. H., WONG, M., GUPTA, N., BERGER, M. S., HUANG, E., GARCIA-VERDUGO, J. M., ROWITCH, D. H. & ALVAREZ-BUYLLA, A. 2011. Corridors of migrating neurons in the human brain and their decline during infancy. *Nature*, 478, 382-6.
- SANO, S., ITAMI, S., TAKEDA, K., TARUTANI, M., YAMAGUCHI, Y., MIURA, H., YOSHIKAWA, K., AKIRA, S. & TAKEDA, J. 1999. Keratinocyte-specific ablation of Stat3 exhibits impaired skin remodeling, but does not affect skin morphogenesis. *EMBO J*, 18, 4657-68.
- SARDI, S. P., MURTIE, J., KOIRALA, S., PATTEN, B. A. & CORFAS, G. 2006. Presenilin-dependent ErbB4 nuclear signaling regulates the timing of astrogenesis in the developing brain. *Cell*, 127, 185-97.
- SAUVAGEOT, C. M. & STILES, C. D. 2002. Molecular mechanisms controlling cortical gliogenesis. *Curr Opin Neurobiol*, 12, 244-9.
- SCHAEFER, T. S., SANDERS, L. K., PARK, O. K. & NATHANS, D. 1997. Functional differences between Stat3alpha and Stat3beta. *Mol Cell Biol*, 17, 5307-16.
- SCHINDLER, C. & STREHLOW, I. 2000. Cytokines and STAT signaling. *Adv Pharmacol*, 47, 113-74.
- SCHUST, J., SPERL, B., HOLLIS, A., MAYER, T. U. & BERG, T. 2006. Stattic: a small-molecule inhibitor of STAT3 activation and dimerization. *Chem Biol*, 13, 1235-42.
- SEKI, T. & ARAI, Y. 1993. Highly polysialylated neural cell adhesion molecule (NCAM-H) is expressed by newly generated granule cells in the dentate gyrus of the adult rat. *J Neurosci*, 13, 2351-8.
- SERI, B., GARCIA-VERDUGO, J. M., COLLADO-MORENTE, L., MCEWEN, B. S. & ALVAREZ-BUYLLA, A. 2004. Cell types, lineage, and architecture of the germinal zone in the adult dentate gyrus. *J Comp Neurol*, 478, 359-78.
- SERI, B., GARCIA-VERDUGO, J. M., MCEWEN, B. S. & ALVAREZ-BUYLLA, A. 2001. Astrocytes give rise to new neurons in the adult mammalian hippocampus. *J Neurosci*, 21, 7153-60.
- SERI, B., HERRERA, D. G., GRITTI, A., FERRON, S., COLLADO, L., VESCOVI, A., GARCIA-VERDUGO, J. M. & ALVAREZ-BUYLLA, A. 2006. Composition and organization of the SCZ: a large germinal layer containing neural stem cells in the adult mammalian brain. *Cereb Cortex*, 16 Suppl 1, i103-11.
- SHANKARANARAYANAN, P., CHAITIDIS, P., KUHN, H. & NIGAM, S. 2001. Acetylation by histone acetyltransferase CREB-binding protein/p300 of STAT6 is required for transcriptional activation of the 15-lipoxygenase-1 gene. *J Biol Chem*, 276, 42753-60.
- SHI, S., CALHOUN, H. C., XIA, F., LI, J., LE, L. & LI, W. X. 2006. JAK signaling globally counteracts heterochromatic gene silencing. *Nat Genet*, 38, 1071-6.
- SHI, S., LARSON, K., GUO, D., LIM, S. J., DUTTA, P., YAN, S. J. & LI, W. X. 2008. Drosophila STAT is required for directly maintaining HP1 localization and heterochromatin stability. *Nat Cell Biol*, 10, 489-96.
- SHIH, A. Y., JOHNSON, D. A., WONG, G., KRAFT, A. D., JIANG, L., ERB, H., JOHNSON, J. A. & MURPHY, T. H. 2003. Coordinate regulation of glutathione biosynthesis and release by Nrf2-expressing glia potently protects neurons from oxidative stress. *J Neurosci*, 23, 3394-406.

- SHINGO, T., SOROKAN, S. T., SHIMAZAKI, T. & WEISS, S. 2001. Erythropoietin regulates the in vitro and in vivo production of neuronal progenitors by mammalian forebrain neural stem cells. *J Neurosci*, 21, 9733-43.
- SHUAI, K. 2000. Modulation of STAT signaling by STAT-interacting proteins. *Oncogene*, 19, 2638-44.
- SHUAI, K., HORVATH, C. M., HUANG, L. H., QURESHI, S. A., COWBURN, D. & DARNELL, J. E., JR. 1994. Interferon activation of the transcription factor Stat91 involves dimerization through SH2-phosphotyrosyl peptide interactions. *Cell*, 76, 821-8.
- SHUAI, K., STARK, G. R., KERR, I. M. & DARNELL, J. E., JR. 1993. A single phosphotyrosine residue of Stat91 required for gene activation by interferon-gamma. *Science*, 261, 1744-6.
- SILVER, J. & MILLER, J. H. 2004. Regeneration beyond the glial scar. *Nat Rev Neurosci*, 5, 146-56.
- SIMON, C., GOTZ, M. & DIMOU, L. 2011. Progenitors in the adult cerebral cortex: cell cycle properties and regulation by physiological stimuli and injury. *Glia*, 59, 869-81.
- SIRKO, S., BEHRENDT, G., JOHANSSON, P. A., TRIPATHI, P., COSTA, M., BEK, S., HEINRICH, C., TIEDT, S., COLAK, D., DICHGANS, M., FISCHER, I. R., PLESNILA, N., STAUFENBIEL, M., HAASS, C., SNAPYAN, M., SAGHATELYAN, A., TSAI, L. H., FISCHER, A., GROBE, K., DIMOU, L. & GOTZ, M. 2013. Reactive glia in the injured brain acquire stem cell properties in response to sonic hedgehog glia. *Cell Stem Cell*, 12, 426-39.
- SMART, I. H., DEHAY, C., GIROUD, P., BERLAND, M. & KENNEDY, H. 2002. Unique morphological features of the proliferative zones and postmitotic compartments of the neural epithelium giving rise to striate and extrastriate cortex in the monkey. *Cereb Cortex*, 12, 37-53.
- SOFRONIEW, M. V. 2005. Reactive astrocytes in neural repair and protection. *Neuroscientist*, 11, 400-7.
- SOFRONIEW, M. V. 2009. Molecular dissection of reactive astrogliosis and glial scar formation. *Trends Neurosci*, 32, 638-47.
- SONG, H. J., STEVENS, C. F. & GAGE, F. H. 2002. Neural stem cells from adult hippocampus develop essential properties of functional CNS neurons. *Nat Neurosci*, 5, 438-45.
- SPASSKY, N., MERKLE, F. T., FLAMES, N., TRAMONTIN, A. D., GARCIA-VERDUGO, J. M. & ALVAREZ-BUYLLA, A. 2005. Adult ependymal cells are postmitotic and are derived from radial glial cells during embryogenesis. *J Neurosci*, 25, 10-8.
- STANCATO, L. F., DAVID, M., CARTER-SU, C., LARNER, A. C. & PRATT, W. B. 1996. Preassociation of STAT1 with STAT2 and STAT3 in separate signalling complexes prior to cytokine stimulation. *J Biol Chem*, 271, 4134-7.
- STREHLOW, I. & SCHINDLER, C. 1998. Amino-terminal signal transducer and activator of transcription (STAT) domains regulate nuclear translocation and STAT deactivation. *J Biol Chem*, 273, 28049-56.
- STROMBERG, H., SVENSSON, S. P. & HERMANSON, O. 2000. Distribution of the transcription factor signal transducer and activator of transcription 3 in the rat central nervous system and dorsal root ganglia. *Brain Res*, 853, 105-14.

- SULTAN, S., MANDAIRON, N., KERMEN, F., GARCIA, S., SACQUET, J. & DIDIER, A. 2010. Learning-dependent neurogenesis in the olfactory bulb determines long-term olfactory memory. *FASEB J*, 24, 2355-63.
- SUN, S. L., LI, T. J., YANG, P. Y., QIU, Y. & RUI, Y. C. 2007. Modulation of signal transducers and activators of transcription (STAT) factor pathways during focal cerebral ischaemia: a gene expression array study in rat hippocampus after middle cerebral artery occlusion. *Clin Exp Pharmacol Physiol*, 34, 1097-101.
- SUN, Y., NADAL-VICENS, M., MISONO, S., LIN, M. Z., ZUBIAGA, A., HUA, X., FAN, G. & GREENBERG, M. E. 2001. Neurogenin promotes neurogenesis and inhibits glial differentiation by independent mechanisms. *Cell*, 104, 365-76.
- SUZUKI, S., TANAKA, K., NOGAWA, S., DEMBO, T., KOSAKAI, A. & FUKUUCHI, Y. 2001. Phosphorylation of signal transducer and activator of transcription-3 (Stat3) after focal cerebral ischemia in rats. *Exp Neurol*, 170, 63-71.
- SWANSON, R. A., YING, W. & KAUPPINEN, T. M. 2004. Astrocyte influences on ischemic neuronal death. *Curr Mol Med*, 4, 193-205.
- TAKAGI, Y., HARADA, J., CHIARUGI, A. & MOSKOWITZ, M. A. 2002. STAT1 is activated in neurons after ischemia and contributes to ischemic brain injury. *J Cereb Blood Flow Metab*, 22, 1311-8.
- TAKAGI, Y., NOZAKI, K., TAKAHASHI, J., YODOI, J., ISHIKAWA, M. & HASHIMOTO, N. 1999. Proliferation of neuronal precursor cells in the dentate gyrus is accelerated after transient forebrain ischemia in mice. *Brain Res*, 831, 283-7.
- TAKAHASHI, K., TANABE, K., OHNUKI, M., NARITA, M., ICHISAKA, T., TOMODA, K. & YAMANAKA, S. 2007. Induction of pluripotent stem cells from adult human fibroblasts by defined factors. *Cell*, 131, 861-72.
- TAKAHASHI, K. & YAMANAKA, S. 2006. Induction of pluripotent stem cells from mouse embryonic and adult fibroblast cultures by defined factors. *Cell*, 126, 663-76.
- TAKAHASHI, T., MISSON, J. P. & CAVINESS, V. S., JR. 1990. Glial process elongation and branching in the developing murine neocortex: a qualitative and quantitative immunohistochemical analysis. *J Comp Neurol*, 302, 15-28.
- TAKEDA, K., CLAUSEN, B. E., KAISHO, T., TSUJIMURA, T., TERADA, N., FORSTER, I. & AKIRA, S. 1999. Enhanced Th1 activity and development of chronic enterocolitis in mice devoid of Stat3 in macrophages and neutrophils. *Immunity*, 10, 39-49.
- TAKEDA, K., KAISHO, T., YOSHIDA, N., TAKEDA, J., KISHIMOTO, T. & AKIRA, S. 1998. Stat3 activation is responsible for IL-6-dependent T cell proliferation through preventing apoptosis: generation and characterization of T cell-specific Stat3-deficient mice. *J Immunol*, 161, 4652-60.
- TAKEDA, K., NOGUCHI, K., SHI, W., TANAKA, T., MATSUMOTO, M., YOSHIDA, N., KISHIMOTO, T. & AKIRA, S. 1997. Targeted disruption of the mouse Stat3 gene leads to early embryonic lethality. *Proc Natl Acad Sci U S A*, 94, 3801-4.
- TAKIZAWA, T., NAKASHIMA, K., NAMIHIRA, M., OCHIAI, W., UEMURA, A., YANAGISAWA, M., FUJITA, N., NAKAO, M. & TAGA, T. 2001. DNA methylation is a critical cell-intrinsic determinant of astrocyte differentiation in the fetal brain. *Dev Cell*, 1, 749-58.

- TATSUMI, K., TAKEBAYASHI, H., MANABE, T., TANAKA, K. F., MAKINODAN, M., YAMAUCHI, T., MAKINODAN, E., MATSUYOSHI, H., OKUDA, H., IKENAKA, K. & WANAKA, A. 2008. Genetic fate mapping of Olig2 progenitors in the injured adult cerebral cortex reveals preferential differentiation into astrocytes. *J Neurosci Res*, 86, 3494-502.
- TAUPIN, P. 2006. HuCNS-SC (StemCells). *Curr Opin Mol Ther*, 8, 156-63.
- TEGLUND, S., MCKAY, C., SCHUETZ, E., VAN DEURSEN, J. M., STRAVOPODIS, D., WANG, D., BROWN, M., BODNER, S., GROSVELD, G. & IHLE, J. N. 1998. Stat5a and Stat5b proteins have essential and nonessential, or redundant, roles in cytokine responses. *Cell*, 93, 841-50.
- TEMPLE, S. 2001. The development of neural stem cells. *Nature*, 414, 112-7.
- TERAMOTO, T., QIU, J., PLUMIER, J. C. & MOSKOWITZ, M. A. 2003. EGF amplifies the replacement of parvalbumin-expressing striatal interneurons after ischemia. *J Clin Invest*, 111, 1125-32.
- THORED, P., WOOD, J., ARVIDSSON, A., CAMMENGA, J., KOKAIA, Z. & LINDVALL, O. 2007. Long-term neuroblast migration along blood vessels in an area with transient angiogenesis and increased vascularization after stroke. *Stroke*, 38, 3032-9.
- TORPER, O., PFISTERER, U., WOLF, D. A., PEREIRA, M., LAU, S., JAKOBSSON, J., BJORKLUND, A., GREALISH, S. & PARMAR, M. 2013. Generation of induced neurons via direct conversion in vivo. *Proc Natl Acad Sci U S A*, 110, 7038-43.
- VALLEY, M. T., MULLEN, T. R., SCHULTZ, L. C., SAGDULLAEV, B. T. & FIRESTEIN, S. 2009. Ablation of mouse adult neurogenesis alters olfactory bulb structure and olfactory fear conditioning. *Front Neurosci*, 3, 51.
- VIERBUCHEN, T., OSTERMEIER, A., PANG, Z. P., KOKUBU, Y., SUDHOF, T. C. & WERNIG, M. 2010. Direct conversion of fibroblasts to functional neurons by defined factors. *Nature*, 463, 1035-41.
- VIERBUCHEN, T. & WERNIG, M. 2011. Direct lineage conversions: unnatural but useful? *Nat Biotechnol*, 29, 892-907.
- VINKEMEIER, U. 2004. Getting the message across, STAT! Design principles of a molecular signaling circuit. *J Cell Biol*, 167, 197-201.
- VINKEMEIER, U., COHEN, S. L., MOAREFI, I., CHAIT, B. T., KURIYAN, J. & DARNELL, J. E., JR. 1996. DNA binding of in vitro activated Stat1 alpha, Stat1 beta and truncated Stat1: interaction between NH2-terminal domains stabilizes binding of two dimers to tandem DNA sites. *EMBO J*, 15, 5616-26.
- VOIGT, T. 1989. Development of glial cells in the cerebral wall of ferrets: direct tracing of their transformation from radial glia into astrocytes. *J Comp Neurol*, 289, 74-88.
- VOSKO, M. R., BURGGRAF, D., LIEBETRAU, M., WUNDERLICH, N., JAGER, G., GROGER, M., PLESNILA, N. & HAMANN, G. F. 2006. Influence of the duration of ischemia and reperfusion on infarct volume and microvascular damage in mice. *Neurol Res*, 28, 200-5.
- VOSKUHL, R. R., PETERSON, R. S., SONG, B., AO, Y., MORALES, L. B., TIWARI-WOODRUFF, S. & SOFRONIEW, M. V. 2009. Reactive astrocytes form scar-like perivascular barriers to leukocytes during adaptive immune inflammation of the CNS. *J Neurosci*, 29, 11511-22.



- WANNER, I. B., ANDERSON, M. A., SONG, B., LEVINE, J., FERNANDEZ, A., GRAY-THOMPSON, Z., AO, Y. & SOFRONIEW, M. V. 2013. Glial scar borders are formed by newly proliferated, elongated astrocytes that interact to corral inflammatory and fibrotic cells via STAT3-dependent mechanisms after spinal cord injury. *J Neurosci*, 33, 12870-86.
- WARNER-SCHMIDT, J. L. & DUMAN, R. S. 2006. Hippocampal neurogenesis: opposing effects of stress and antidepressant treatment. *Hippocampus*, 16, 239-49.
- WILHELMSSON, U., BUSHONG, E. A., PRICE, D. L., SMARR, B. L., PHUNG, V., TERADA, M., ELLISMAN, M. H. & PEKNY, M. 2006. Redefining the concept of reactive astrocytes as cells that remain within their unique domains upon reaction to injury. *Proc Natl Acad Sci U S A*, 103, 17513-8.
- XIA, X. G., HOFMANN, H. D., DELLER, T. & KIRSCH, M. 2002. Induction of STAT3 signaling in activated astrocytes and sprouting septal neurons following entorhinal cortex lesion in adult rats. *Mol Cell Neurosci*, 21, 379-92.
- YAMAUCHI, K., OSUKA, K., TAKAYASU, M., USUDA, N., NAKAZAWA, A., NAKAHARA, N., YOSHIDA, M., AOSHIMA, C., HARA, M. & YOSHIDA, J. 2006. Activation of JAK/STAT signalling in neurons following spinal cord injury in mice. *J Neurochem*, 96, 1060-70.
- YAMAURA, G., TUROCZI, T., YAMAMOTO, F., SIDDIQUI, M. A., MAULIK, N. & DAS, D. K. 2003. STAT signaling in ischemic heart: a role of STAT5A in ischemic preconditioning. *Am J Physiol Heart Circ Physiol*, 285, H476-82.
- YANG, J., LIAO, X., AGARWAL, M. K., BARNES, L., AURON, P. E. & STARK, G. R. 2007. Unphosphorylated STAT3 accumulates in response to IL-6 and activates transcription by binding to NFkappaB. *Genes Dev*, 21, 1396-408.
- YANG, J. & STARK, G. R. 2008. Roles of unphosphorylated STATs in signaling. *Cell Res*, 18, 443-51.
- YANG, J., VAN OOSTEN, A. L., THEUNISSEN, T. W., GUO, G., SILVA, J. C. & SMITH, A. 2010. Stat3 activation is limiting for reprogramming to ground state pluripotency. *Cell Stem Cell*, 7, 319-28.
- YANG, Q., SHEN, S. S., ZHOU, S., NI, J., CHEN, D., WANG, G. & LI, Y. 2012. STAT3 activation and aberrant ligand-dependent sonic hedgehog signaling in human pulmonary adenocarcinoma. *Exp Mol Pathol*, 93, 227-36.
- YOSHIMATSU, T., KAWAGUCHI, D., OISHI, K., TAKEDA, K., AKIRA, S., MASUYAMA, N. & GOTOH, Y. 2006. Non-cell-autonomous action of STAT3 in maintenance of neural precursor cells in the mouse neocortex. *Development*, 133, 2553-63.
- YOSHIMURA, S., TAKAGI, Y., HARADA, J., TERAMOTO, T., THOMAS, S. S., WAEBER, C., BAKOWSKA, J. C., BREAKFIELD, X. O. & MOSKOWITZ, M. A. 2001. FGF-2 regulation of neurogenesis in adult hippocampus after brain injury. *Proc Natl Acad Sci U S A*, 98, 5874-9.
- YUAN, Z. L., GUAN, Y. J., CHATTERJEE, D. & CHIN, Y. E. 2005. Stat3 dimerization regulated by reversible acetylation of a single lysine residue. *Science*, 307, 269-73.
- YUNG, S. Y., GOKHAN, S., JURCSAK, J., MOLERO, A. E., ABRAJANO, J. J. & MEHLER, M. F. 2002. Differential modulation of BMP signaling promotes the elaboration of cerebral cortical GABAergic neurons or oligodendrocytes from a common sonic hedgehog-responsive ventral forebrain progenitor species. *Proc Natl Acad Sci U S A*, 99, 16273-8.

- ZADOR, Z., STIVER, S., WANG, V. & MANLEY, G. T. 2009. Role of aquaporin-4 in cerebral edema and stroke. *Handb Exp Pharmacol*, 159-70.
- ZAMANIAN, J. L., XU, L., FOO, L. C., NOURI, N., ZHOU, L., GIFFARD, R. G. & BARRES, B. A. 2012. Genomic analysis of reactive astrogliosis. *J Neurosci*, 32, 6391-410.
- ZAMBRANO, A., OTTH, C., MACCIONI, R. B. & CONCHA, II 2010. IL-3 controls tau modifications and protects cortical neurons from neurodegeneration. *Curr Alzheimer Res*, 7, 615-24.
- ZERLIN, M., LEVISON, S. W. & GOLDMAN, J. E. 1995. Early patterns of migration, morphogenesis, and intermediate filament expression of subventricular zone cells in the postnatal rat forebrain. *J Neurosci*, 15, 7238-49.
- ZHANG, F., WANG, S., CAO, G., GAO, Y. & CHEN, J. 2007. Signal transducers and activators of transcription 5 contributes to erythropoietin-mediated neuroprotection against hippocampal neuronal death after transient global cerebral ischemia. *Neurobiol Dis*, 25, 45-53.
- ZHANG, J. J., VINKEMEIER, U., GU, W., CHAKRAVARTI, D., HORVATH, C. M. & DARNELL, J. E., JR. 1996. Two contact regions between Stat1 and CBP/p300 in interferon gamma signaling. *Proc Natl Acad Sci U S A*, 93, 15092-6.
- ZHANG, R., CHOPP, M., ZHANG, Z., JIANG, N. & POWERS, C. 1998. The expression of P- and E-selectins in three models of middle cerebral artery occlusion. *Brain Res*, 785, 207-14.
- ZHANG, T., KEE, W. H., SEOW, K. T., FUNG, W. & CAO, X. 2000. The coiled-coil domain of Stat3 is essential for its SH2 domain-mediated receptor binding and subsequent activation induced by epidermal growth factor and interleukin-6. *Mol Cell Biol*, 20, 7132-9.
- ZHAO, C., DENG, W. & GAGE, F. H. 2008. Mechanisms and functional implications of adult neurogenesis. *Cell*, 132, 645-60.
- ZHAO, C., TENG, E. M., SUMMERS, R. G., JR., MING, G. L. & GAGE, F. H. 2006. Distinct morphological stages of dentate granule neuron maturation in the adult mouse hippocampus. *J Neurosci*, 26, 3-11.
- ZIVIN, J. A. 2009. Acute stroke therapy with tissue plasminogen activator (tPA) since it was approved by the U.S. Food and Drug Administration (FDA). *Ann Neurol*, 66, 6-10.

## 8. List of Abbreviations

Aa	Amino acids
AD	Alzheimer's Disease
aIPC	Astrocytic intermediate progenitor cell
AMPA	2-amino-3-(5-methyl-3-oxo-1, 2-oxazol-4-yl)propanoic acid
APP	Amyloid precursor protein
approx.	Approximately
Ascl1	Achaete-scute homolog 1
AT <sub>1</sub>	Angiotensin II receptor
ATP	Adenosine triphosphate
BBB	Blood-brain barrier
Bcl-2	B-cell lymphoma 2
BDNF	Brain-derived neurotrophic factor
BLBP	Brain lipid-binding protein
BMP	Bone morphogenetic protein
BrdU	5-bromo-2'-deoxyuridine
Brn2	Brain-2
BSF-3	B cell-stimulating factor-3
CA1	Cornu ammonis area 1
CAM	Ca <sup>2+</sup> /Calmodulin
CBP	CREB (cAMP responsive element-binding)-binding protein
Cdk5	Cyclin-dependent kinase 5
cDNA	complementary DNA
CGE	Caudal ganglionic eminence
CK	CAM dependent protein kinase II promoter
CK/p25	mouse model with inducible expression of p25 under the CK promoter
CNS	Central nervous system
CNTF	Ciliary neurotrophic factor
CP	Cortical plate
CPEB1	Cytoplasmic polyadenylation element-binding protein 1
CT-1	Cardiotrophin-1

---

DAPI	4',6-diamidino-2-phenylindole dilactate
DCX	Doublecortin
Dlx	Distal-less homeobox
DNA	Deoxyribonucleic acid
dpSW	Day(s) post stab wound
DSD1	Dermatan-sulfate-dependent epitope 1
E12	Embryonic day 12 (adequate for other numbers)
e.g.	Exempli gratia
EGF	Epidermal growth factor
Epo	Erythropoietin
FDA	US agency for Food and Drug Administration
FGF-2	Fibroblast growth factor 2
Fig.	Figure
FITC	Fluorescein isothiocyanate
G	Gravitational constant
GABA	$\gamma$ -aminobutyric acid
GAS	$\gamma$ -interferon activation site
GCSF	Granulocyte colony-stimulating factor
GDNF	Glial cell-derived neurotrophic factor
GFP	Green fluorescent protein
GH	Growth hormone
GLAST	Glutamate Aspartate Transporter
gp130	Glycoprotein 130
hES	Human embryonic stem
HBMC	Human bone marrow cell
HP1	Heterochromatin protein 1
HUCB	Human umbilical cord blood cell
IFN	Interferon
IL	Interleukin
IPS cell	Induced pluripotent stem cell
IRF9	IFN regulatory factor 9
ISVZ	Inner subventricular zone

---

IZ	Intermediate zone
JAK	Janus kinase
kDa	Kilo dalton
LGE	Lateral ganglionic eminence
LIF	Leukemia inhibitory factor
LIFR	LIF-receptor
LTR	long terminal repeat
LV	Lateral ventricle
MA	Mantle
MAP2	Microtubule-associated protein 2
MAPK	Mitogen-activated protein kinase
Mash1	Mammalian achaete-schute homolog 1
MCAo	Medial cerebral artery occlusion
MGE	Medial ganglionic eminence
miRNA	microRNA
MMLV	Moloney Murine Leukemia Virus
mRNA	messenger RNA
MSC	Mesenchymal stem cell
Myt1l	Myelin transcription factor-like 1
MZ	Marginal zone
NE	Neuroepithelium
NeuN	Neuronal nuclear antigen
NeuroD	Neurogenic differentiation
Neurog	Neurogenin
NG2	Neuron-glia antigen 2
nIPC	Neuronal intermediate progenitor cell
NMDA	N-Methyl-D-aspartate
NNT-1	Novel neurotrophin-1
NO	Nitric oxide
NPC	Nuclear pore complex
Nrf2	Nuclear factor (erythroid-derived 2)-like 2
NSC	Neural stem cell

---

NT2	NTera-2
OB	Olfactory bulb
oIPC	Oligodendrocytic intermediate progenitor cell
Olig2	Oligodendrocyte transcription factor 2
OPC	Oligodendrocyte progenitor cell
OSM	Oncostatin M
OSMR	OSM-receptor
OSVZ	Outer subventricular zone
P25	Protein 25
P300	Protein 300
P6	Postnatal day 6 (adequate for other numbers in the low range)
Pax6	Paired box protein 6
PDGF	Platelet derived growth factor
PI3K	Phosphoinositide 3-kinase
PIAS	Protein inhibitors of activated STAT
PRL	Prolactin
PS1	Presenilin 1
PSA-NCAM	Poly-sialated neural cell adhesion molecule
pSTAT	Phosphorylated STAT
RFP	Red fluorescent protein
RG	Radial glia
RMS	Rostral migratory stream
RNA	Ribonucleic acid
RPM	Revolutions per minute
ROS	Reactive oxygen species
S100 $\beta$	S100 calcium binding protein $\beta$
SCI	Spinal cord injury
SCZ	Subcallosal zone
SEZ	Subependymal zone
SGZ	Subgranular zone
SH2	Src homology 2
Shh	Sonic Hedgehog

---

SHP2	SH2-domain-containing tyrosine phosphatase
shRNA	small hairpin RNA
siRNA	small interfering RNA
SOCS	Suppressor of cytokine signaling
Sox2	(Sex determining region Y)-box 2
STAT	Signal transducer and activator of transcription
SVZ	Subventricular zone
Tbr1	T-box brain protein 1
tetO	Tetracycline operator
Thy1	Thymocyte differentiation antigene 1
Thy1-APP/PS1	Mouse model with Swedish double mutation under the Thy1 promoter
TN-C	Tenascin C
tPA	Tissue plasminogen activator
Tpo	Thyroid peroxidase
TRITC	Tetramethyl rhodamine isothiocyanate
tTA	Tetracycline controlled transactivator
TUNEL	Terminal deoxynucleotidyl transferase dUTP nick end labeling
TYK	Tyrosine kinase
VEGF	Vascular endothelial growth factor
VZ	Ventricular zone
Wg	Wingless
Wnt	Hybrid of Int and Wg
w/v	Weight per volume

## 9. List of Figures

Fig. 1: Cortical development	4
Fig. 2: Temporal pattern of generation of neurons, astrocytes and oligodendrocytes in rats	7
Fig. 3: Neurogenic niches in the adult mammalian brain: SVZ and SGZ	9
Fig. 4: Scheme of progenitor cells in the adult brain SVZ	11
Fig. 5: Scheme of progenitor cells in the adult brain SGZ	12
Fig. 6: Regression of functional neurological deficit while structural lesion grows	15
Fig. 7: Detrimental cascade of pathophysiologic events in focal cerebral ischemia	16
Fig. 8: Progressive alterations of reactive astrogliosis after tissue insults	18
Fig. 9: Different roles of the glial cell	20
Fig. 10: Generation of striatal neurons from SVZ stem cells after stroke	22
Fig. 11: Crystal structure of STAT1 molecule	32
Fig. 12: Receptor composition for cytokines from the gp130 family	34
Fig. 13: Canonical JAK/STAT pathway	35
Fig. 14: Inhibitory regulators of STAT signaling	37
Fig. 15: Mechanism of the molecular switch from neurogenesis to astrogliogenesis	40
Table 1: Designed miRNAs against STAT3	59
Table 2: Designed miRNAs against STAT1	59
Table 3: Available plasmids	60
Fig. 16: Expression pattern of STAT3 and GFAP over seven days after stab wound	78
Fig. 17: Expression of STAT3 and pSTAT3 in cytoplasmic and nuclear fractions at 3, 5 and 7 dpSW	80
Table 4: Expression of STAT3 at 3, 5 and 7 dpSW in contralateral versus ipsilateral cortical hemispheres	81



---

Fig. 18: Protein levels of STAT3 in ipsilateral versus contralateral fractions at 3, 5 and 7 dpSW	82
Fig. 19: Expression of pSTAT3 in ipsilateral versus contralateral nuclear fractions at 3, 5 and 7 dpSW	83
Fig. 20: Expression and activation of STAT3 at 3-4 days after MCAo	85
Fig. 21: Expression of STAT5a and pSTAT1 after stab wound	86
Fig. 22: GFAP immunohistochemistry at 3 dpSW in the contra- versus ipsilateral hemisphere	88
Fig. 23: GFAP and STAT3 costaining at 3 dpSW in contra- and ipsilateral cortices	89
Fig. 24: NeuN and STAT3 costaining at 3 dpSW in contra- and ipsilateral cortices	91
Fig. 25: pSTAT3 and GFAP costaining at 3 dpSW in contra- and ipsilateral cortices	92
Fig. 26: pSTAT3 and GFAP costaining of reactive astrocytes isolated in culture	93
Fig. 27: pSTAT3 and GFAP costaining at 3, 5 and 7 dpSW	94
Fig. 28: Quantification of pSTAT3+ cells at 3, 5 and 7 dpSW	95
Fig. 29: GFAP-immunostaining at 3-4 days after MCAo	96
Fig. 30: Costaining of GFAP and pSTAT3 at 3-4 days after MCAo	96
Fig. 31: Quantification of pSTAT3+ cells at 3 days after MCAo and stab wound	97
Fig. 32: Scheme of the CK/p25 mouse model	99
Fig. 33: Costaining of GFAP and pSTAT3 in CK/p25 and APP/PS1 mice	100
Fig. 34: Quantification of pSTAT3+ cells at 3 dpSW, 3-4 days after MCAo and in APP/PS1 and CK/p25 mice	101
Fig. 35: Expression of GFAP and pSTAT3 in the adult neurogenic niches	102
Fig. 36: Costaining with STAT5a and GFAP or NeuN at 3 dpSW in contra- versus ipsilateral cortices	103
Fig. 37: Costaining with pSTAT1 and GFAP at 3 dpSW in contra- versus ipsilateral cortices	104
Fig. 38: Effect of miRNAs against STAT3 and STAT1 in HEK293T cells	107

---

Fig. 39: Effect of miRNA-STAT3-1 in HEK293T cells	108
Fig. 40: Cloning of constructs containing several miRNA against STAT3 and/or STAT1	111
Fig. 41: Effects of retroviral backbone plasmids expressing STAT3, STAT1, 2miRNA3, 2miRNA1 or 2miRNA3/1	113
Fig. 42: Expression of STAT3 and pSTAT3 in astrocytes	114
Fig. 43: Astrocytes isolated from the cerebral cortex at postnatal day 6 at 9 days after transfection with Mash1 and GFP or Mash1 and STAT3C or STAT3C and DsRed	117
Fig. 44: Statistical analysis of P6 astrocytes at 9 days after transfection with Mash1 and GFP or Mash1 and STAT3C	117
Fig. 45: Analysis of P6 astrocytes at 2 days after transfection with Mash1 and GFP or Mash1 and STAT3C	118
Fig. 46: Analysis of P6 astrocytes at 2 and 9 days after transfection with Mash1 and GFP or Mash1 and miRNAs against STAT3	121
Fig. 47: Formation of neurospheres from cells from different injury models	123
Fig. 48: Neurosphere assay at 3-4 days after MCAo	124

## 10. Acknowledgements/Danksagung

Ich möchte diese Gelegenheit zunächst nutzen um meinen beiden Eltern, Kati und Gunter Tiedt, für ihre unermüdliche Unterstützung und Förderung während meiner gesamten Ausbildung und im Speziellen während dieser Doktorarbeit zu danken. Ohne euch wäre es nie so weit gekommen. Allein das Wissen um die Existenz des von euch gebotenen Rückzugsortes gab mir unendlich viel Halt. Meinem Bruder Christian Tiedt gebührt kein geringerer Dank, ich bin froh, dass ich dich habe.

Mein besonderer Dank gilt auch meiner Doktormutter Prof. Dr. Magdalena Götz, deren Tatkraft, Enthusiasmus und Begeisterung für die Forschung ansteckend waren. Die Erfahrungen, die ich im Labor, auf Kongressen und während der Laborbesprechungen sammeln durfte, habe ich größtenteils ihr zu verdanken. Danke auch für das große Verständnis für die Schwierigkeiten, die es mit sich bringt, als Teilzeitkraft Medizinstudent in einem Vollzeitlabor zu arbeiten.

Next I want to thank my personal supervisor, Dr. Christophe Heinrich. I am grateful for every minute I had the possibility to work with you. Your scientific knowledge, passion for science and cleverness have been inspiring. You must have been very scared by the bloody beginner in the first weeks, thanks for the confidence you have had in me! I hope that we stay in contact although being locally separated in the future.

Special thanks also to Sergio for the invaluable knowledge you shared with me regarding molecular cloning. I will always remember you! Thanks also to Gabriela Jäger, Tatiana Simon-Ebert, Ines Mühlhahn, Carmen Meyer, Susanne Schickle and Dethlef Franzen for excellent technical support and a supportive environment in the lab. Furthermore thanks to everybody from the ISD that I had the possibility to work with: especially Prof. Dr. Martin Dichgans, also for mentoring me regarding my medical studies, Dr. Christof Haffner, Rebekka Fischer, Veronika Lellek and Jan Burk for the MCAO mice. Thanks also to Gwen for help with the two AD mouse lines.

Special thanks to the lab folks, especially Ronny for the fun during late-hour-working in the lab, Felipe for his positivity and Sophia for a very good time when we shared the office.

## 11. Publications

### Original Articles

1. Directing Astroglia from the cerebral cortex into subtype specific functional neurons. Heinrich C, Blum R, Gascon S, Masserdotti G, Tripathi P, Sanchez R, **Tiedt S**, Schröder T, Götz M and Berninger B (2010). PLoS Biol May 18; 8(5):e1000373
2. Reactive glia in the injured brain acquire stem cell properties in response to sonic hedgehog. Sirko S, Behrendt G, Johansson PA, Tripathi P, Costa M, Bek S, Heinrich C, **Tiedt S**, Colak D, Dichgans M, Fischer IR, Plesnila N, Staufenbiel M, Haass C, Snapyan M, Saghatelian A, Tsai LH, Fischer A, Grobe K, Dimou L, Götz M. Cell Stem Cell. 2013 Apr 4;12(4):426-39
3. Blogging Medical Students: A Qualitative Analysis. Pinilla S, Weckbach LT, Alig SK, Bauer H, Noerenberg D, Singer K, **Tiedt S**. GMS Z Med Ausbild. 2013;30(1):Doc9
4. Diffuse leukoencephalopathy with spheroids: biopsy findings and a novel mutation. Levin J\*, **Tiedt S\***, Arzberger T, Biskup S, Schuberth M, Stenglein-Krapf G, Kreth FW, Högen T, la Fougère C, Linn J, van der Knaap MS, Giese A, Kretzschmar HA, Danek A. Clin Neurol Neurosurg. 2014 Jul;122:113-5. \* The first two authors contributed equally.

### Poster

1. **Tiedt S**, Heinrich C, Dichgans M und Götz M. Untersuchung des STAT-Signalweges bei der Neurogenese – neue Ansätze, um die Regeneration von Neuronen nach Gehirnverletzung zu ermöglichen. Doktamed 2010, LMU, Munich, Germany
2. Brand V, **Tiedt S**, Kuhm C, Klingbeil J, Störmann S and Hege I. MeCuMMemo – ein neues digitales Lernkartensystem von und für Studenten. Jahrestagung der GMA 2010, Bochum, Germany
3. **Tiedt S**, Heinrich C, Dichgans M and Götz M. Role of STAT-Signaling in reactive gliosis - potential implications for endogenous regenerative neurogenesis following cortical injury in mice. 6th International Symposium on Neurorepair and Neuroprotection 2010, Rostock, Germany

---

4. Brand V, **Tiedt S**, Kuhm C, Woidy M, Klingbeil J, Störmann S, Fischer M. MeCuMMemo, eine harmonische Symbiose: community-based-learning und moderne Lerntechnik für die neue Generation der Studierenden. Jahrestagung der GMA 2011, Munich, Germany

## 12. Curriculum Vitae

Steffen Tiedt, born at the 11<sup>th</sup> of October 1986 in Rostock

### Education and Civil Service

1993 to 1997 Primary School Neubukow, Germany

1997 to 2001 Heinrich-Schliemann-Gymnasium Neubukow, Germany

2001 to 2005 Luise-Gymnasium Hamburg, Germany, Grade: 1.0

2005 to 2006 Civil service as ambulatory officer at G.A.R.D., Hamburg, Germany

### Academic Studies

2006 to 2013 Study of human medicine at Ludwig-Maximilians-Universität (LMU) Munich, Germany

First Step of National Board Examination: good

Second Step of National Board Examination: very good

United States Medical Licensing Examination Step 1: passed

United States Medical Licensing Examination Step 2 CK: passed

### Internships / Practical Year

2011 to 2012 Department of Neurology, University Hospital Munich, Germany

2012 Internal Medicine at Harvard Medical School, Boston, MA, USA  
Rotations: Cardiology, Nephrology, Hematology, Emergency Medicine

2012 General Surgery at Policlinico San Matteo, Università di Pavia

2012 Department of Neurosurgery, University Hospital Munich, Germany

### Scientific Education

Since 2009 Experimental doctoral thesis in the Department of Physiological Genomics (Director: Prof. Dr. Magdalena Götz) at the Institute for Physiology (Managing Directors: Prof. Dr. Magdalena Götz and Prof. Dr. Claudia Veigel) at LMU, Munich, Germany under the supervision of Dr. Christophe Heinrich

Since 2013 Research associate and resident physician at the Institute for Stroke and Dementia Research (Director: Prof. Dr. Martin Dichgans)

### Scholarships and Awards

2009 to 2010 Graduate Program for "Systems biology and Medicine" FöFoLe of LMU

2011 Participant as Young Researcher at the 61<sup>st</sup> Meeting of Nobel Laureates in Lindau

2012 LMU StEP Program for excellent medical students: Scholarship for Practical Year at Harvard Medical School

# Eidesstattliche Versicherung

---

Name, Vorname

Ich erkläre hiermit an Eides statt,  
dass ich die vorliegende Dissertation mit dem Thema

selbständig verfasst, mich außer der angegebenen keiner weiteren Hilfsmittel bedient und alle Erkenntnisse, die aus dem Schrifttum ganz oder annähernd übernommen sind, als solche kenntlich gemacht und nach ihrer Herkunft unter Bezeichnung der Fundstelle einzeln nachgewiesen habe.

Ich erkläre des Weiteren, dass die hier vorgelegte Dissertation nicht in gleicher oder in ähnlicher Form bei einer anderen Stelle zur Erlangung eines akademischen Grades eingereicht wurde.

---

Ort, Datum

---

Unterschrift Doktorandin/Doktorand